

**Development of Advanced Reliability Assessment Models
with Applications in Integrity Management of Onshore
Energy Pipelines**

KONSTANTINOS PESINIS

A thesis submitted in partial fulfilment of the
requirements of the University of Greenwich
for the degree of Doctor of Philosophy

June 2018

DECLARATION

“I certify that the work contained in this thesis, or any part of it, has not been accepted in substance for any previous degree awarded to me, and is not concurrently being submitted for any degree other than that of Doctor of Philosophy being studied at the University of Greenwich. I also declare that this work is the result of my own investigations, except where otherwise identified by references and that the contents are not the outcome of any form of research misconduct.”

Student

Supervisor

Konstantinos Pesinis

Dr Kong Fah Tee

ACKNOWLEDGEMENTS

The kind support received from my supervisor, Dr Kong Fah Tee during the several milestones of my research studies is appreciated. Many thanks go to my family for their support throughout my studies. I would also like to thank Cynthia for the constant encouragement and support in all aspects.

ABSTRACT

This thesis addresses some of the predominant engineering challenges involved in the reliability-based integrity management of energy pipelines. The aim is to conjointly consider realistic safety threats and integrity management strategies, such as in-line inspections, criteria for excavation and direct assessment of energy pipelines. Towards this, advanced algorithmic model-based approaches are developed and proposed, based on fundamental principles of structural reliability analyses, stochastic degradation processes, machine learning through Bayesian statistics, multivariate data analysis, hazard modelling and interval probabilities, in an effort to quantify uncertainties that impose threats and define risks to the integrity of energy pipelines.

First, the quantification of failure probabilities for onshore gas pipelines subjected to external metal-loss corrosion is addressed. The probabilistic methodology proposed is based on a robust integration of stochastic processes within a structural reliability analysis (SRA) framework. It comprehensively accounts for the temporal uncertainty of multiple metal-loss corrosion defects and efficiently predicts long-term time-dependent reliability at the pipe segment level. The application of the methodology is illustrated through two case studies, based on two distinct inspection and maintenance strategies. In specific, an industry-consistent maintenance strategy is considered in one of them, namely External Corrosion Direct Assessment (ECDA). The reliability, originally evaluated at the segment level, is incorporated in an investigation of the influence of imperfect ECDA actions at the system level. The methodology is also applied considering a realistic maintenance and repair strategy based on in-line inspections (ILI). Again, it deals with multiple metal-loss corrosion defects, facilitates the identification of the critical ones and provides expected reliability forecasts for the whole lifecycle of the pipe segment.

Second, two distinct statistical models are proposed that can account for multiple integrity threats, since historical failures form an integral part of informed integrity management strategies. For the implementation actual incidents are employed, derived from the Pipeline and Hazardous Material Safety Administration (PHMSA) database, which contains data of incidents of existing gas transmission pipelines, providing useful insights into their state at the time of the analysis. In both statistical models, a non-repairable system approach is considered, as opposed to the repairable system approach commonly adopted in energy pipeline studies. In the first one, a well-established approach from reliability and survival

analysis is employed, known as nonparametric predictive inference (NPI). This method provides interval probabilities, also known as imprecise reliability, in that probabilities and survival functions are quantified via upper and lower bounds. The focus is on the rupture of a future pipe segment, due to a specific cause among a range of competing risks. The second statistical methodology adopts a parametric hybrid empirical hazard model, complemented with a robust data processing technique, i.e. the non-linear quantile regression, for reliability analysis and prediction. It provides inferences on the complete lifecycle reliability of the average pipe segment of a region under study. For the purpose of cross-verification, the results of the second statistical model are compared with these of the second aforementioned structural reliability model, which is based on the ILI maintenance and repair strategy.

Finally, a robust methodology for estimation of small posterior failure probabilities for gas pipelines based on available inspection data is presented. The analysis of the data is based on the BUS (Bayesian Updating with Structural reliability methods), which sets an analogy between Bayesian updating and a reliability problem. The structural reliability method adopted is Subset Simulation (SuS) and the whole analysis is referred to as BUS-SuS. Two case studies are carried out to illustrate and validate the proposed methodology. In the first case study, hierarchical BUS-SuS is implemented on an existing gas pipeline containing metal-loss corrosion defects and is validated against field data. The reliability of the pipe segment is evaluated in terms of three distinctive failure modes, namely small leak, large leak and rupture. In the second case study, the Bayesian updating is conducted by using BUS-SuS in conjunction with the data augmentation (DA) technique. Simulated data, corresponding to an existing gas pipeline with high-pH stress corrosion cracking (SCC) features and constant internal pressure loading, are employed to illustrate and validate the proposed model. Furthermore, the dependence among the growths of different crack features is taken into account, using the Gaussian copula. At the end, the sensitivity of both the stochastic growth model and pipe segment reliability to different dependence scenarios is investigated. All the aforementioned proposed methodologies aim to assist pipeline operators in decision making and informed implementation of integrity management strategies.

Keywords: Energy pipelines, structural reliability analysis, statistical analysis, stochastic process, metal-loss corrosion, stress corrosion cracking, Bayesian updating, competing risks, historical failure data, non-repairable systems approach.

CONTENTS

Development of Advanced Reliability Assessment Models with Applications in Integrity Management of Onshore Energy Pipelines	
DECLARATION	i
ACKNOWLEDGEMENTS.....	ii
ABSTRACT	iii
CONTENTS	v
LIST OF FIGURES	viii
LIST OF TABLES	xi
LIST OF APPENDICES	xii
LIST OF SYMBOLS	xiii
1. Introduction.....	1
1.1 Background	1
1.2 Objectives and Research Significance	4
1.3 Scope of Study.....	4
1.4 Thesis Format	6
2. Literature Review	7
3. Structural Reliability Analyses for Predictions in Energy Pipelines	18
3.1 Introduction	18
3.2 Physical Model	20
3.2.1 Stochastic Generation of Metal-loss Corrosion Defects	20
3.2.2 Stochastic Growth of Defects	21
3.2.3 Time-dependent Internal Pressure Model.....	24
3.2.4 Time-dependent Reliability Evaluation for Pipe Segment with Multiple Defects ..	25
3.3 Maintenance Plan for the 1st Case Study based on In-line Inspections	27
3.3.1 Uncertainties of ILI Tools	29
3.3.2 Effect of Maintenance on Pipe Segment Reliability	29
3.4 Maintenance Plan for the 2nd Case Study based on ECDA	30
3.4.1 Pipeline System Reliability Prediction based on SSA	30
3.4.2 Linear Approximations.....	36
3.5 Numerical Application for the 1st Case Study based on In-line Inspections.....	36
3.5.1 Results and Discussion	38
3.6 Numerical Application for the 2nd Case Study based on ECDA.....	39
3.6.1. Results and Discussions.....	44

3.7 Conclusions	53
4. Statistical Analyses for Reliability Predictions in Energy Pipelines	56
4.1 Introduction	56
4.2 Competing Risks Analysis of Failures based on the NPI Approach	57
4.2.1 General.....	57
4.2.2 PHMSA Rupture Incidents from 2002-2014.....	58
4.2.3 NPI for Competing Failure Causes	63
4.3 Statistical Analysis based on a Parametric Hybrid Methodology	68
4.3.1 General.....	68
4.3.2 Hazard Functions and Corresponding Reliability	69
4.3.3 Non-linear Quantile Regression.....	72
4.4 Case Study based on the NPI methodology	74
4.4.1 General.....	74
4.4.2 Results and Discussion	76
4.5. Case Study based on the Parametric Hybrid Methodology	85
4.5.1. General.....	85
4.5.2 Results and Discussions.....	88
4.6 Conclusions	94
5. Bayesian Analysis of Pipeline Reliability Based on Imperfect Inspection Data.....	96
5.1 Introduction	96
5.2 Uncertainties Associated with ILI Data.....	98
5.3 Stochastic Models for Corrosion Defect Generation and Growth.....	100
5.3.1 Generation of both Detected and Undetected Corrosion Defects	100
5.3.2 Stochastic Growth of Corrosion Defects	101
5.3.3 Correlations among stochastic degradations through Gaussian copula	102
5.4 Bayesian Updating of the Stochastic Generation and Growth Models	103
5.4.1 Prior Distributions and Hierarchical Representation of the Deterioration Model	103
5.4.2 General Formulation.....	105
5.4.3 Constant c	108
5.4.4 Likelihood Function for the Growth Model of Detected Corrosion Defects.....	109
5.4.5 Likelihood Function for the Generation Model of Corrosion Defects.....	110
5.5 Time-dependent Reliability Analysis	110
5.5.1 Limit State Functions for Metal-Corrosion Defects.....	110
5.5.2 Limit State Functions for High-pH SCC Defects	111
5.5.3 System Reliability Analysis.....	112

5.6 Metal-loss Corrosion Case Study	115
5.6.1 General.....	115
5.6.2 Application and Validation of the Methodology	116
5.6.3 Comparisons of Growth Models and Time-dependent Reliability Analysis	120
5.7 High-pH SCC Case Study.....	129
5.7.1 Model Feasibility Study.....	129
5.7.2 Numerical Application	130
5.7.3 Validation of Bayesian Formulation	132
5.7.4 Parametric and Reliability Analyses	135
5.8 Conclusions	138
6. Conclusions, Research Achievements and Future Works	141
6.1 General Conclusions	141
6.1.1 Structural Reliability Analyses for Predictions in Energy Pipelines.....	141
6.1.2 Statistical Analyses for Reliability Predictions in Energy Pipelines.....	143
6.1.3 Bayesian Analysis of Pipeline Reliability based on Imperfect Inspection Data...	144
6.2 Research Achievements	146
6.3 Recommendations for future study.....	148
REFERENCES	149
Appendix A: Step-by-Step Procedure for Estimating the Posterior Failure Probabilities Conditional on the ILI Data.....	167
Appendix B: List of Publications.....	169

LIST OF FIGURES

Figure 1.1 External metal-loss corrosion on the pipeline body	2
Figure 1.2 Direct Assessment of the pipeline condition in the field	3
Figure 2.1 Dimensions of a typical metal-loss corrosion defect on pipeline (Al-Amin and Zhou, 2013)	8
Figure 3.1 Poisson Square Wave Process model	22
Figure 3.2 Illustration of stochastic Poisson Square Wave Process and time-independent power law defect growth models	22
Figure 3.3 Stochastic Ferry-Borges model for internal pressure of gas pipelines	24
Figure 3.4 Reliability updating based on inspection information	30
Figure 3.5 Example of conditional reliability of a pipeline system with multiple imperfect repairs	32
Figure 3.6 Example of multi-component series system	33
Figure 3.7 Linear approximations to determine the exact time of reliability falling to 0.9	35
Figure 3.8 Results of the structural reliability approach	38
Figure 3.9 Illustration of the NHPP	41
Figure 3.10 Simulated time-dependent internal pressure based on the PSWP model	42
Figure 3.11 Time-dependent reliability prediction for an externally corroded 12m pipe segment	44
Figure 3.12 Comparison of reliability with and without PM	45
Figure 3.13 (a-c) Comparison of reliability predictions in terms of the proportional constant λ_o of the defect generation model	48
Figure 3.14 (a-c) Comparisons of reliability predictions in terms of the generation rate λ of the PSWP internal pressure model	50
Figure 3.15a Comparisons of reliability predictions in terms of the reliability threshold R_{th} .	51
Figure 3.15b Comparisons of reliability predictions in terms of the reliability threshold R_{th} .	52
Figure 4.1 Bath-tub failure pattern	68
Figure 4.2 Bath-tub failure pattern for gas transmission pipelines	69
Figure 4.3 NPI lower and upper survival functions for a future pipeline segment with t in weeks	80
Figure 4.4 NPI conditional (EC, MF) lower and upper survival functions for a future pipeline segment with t in weeks	81

Figure 4.5 NPI conditional (IC, ED, OTHER) lower and upper survival functions for a future pipeline segment with t in weeks	82
Figure 4.6 NPI conditional (PDP, EM) lower and upper survival functions for a future pipeline segment with t in weeks	83
Figure 4.7 Rupture hazard bar chart of the onshore gas transmission pipeline network in 2002-2014.....	86
Figure 4.8 Hazard function curve for $\tau_q = 0.99$ quantile (all failure causes).....	88
Figure 4.9 Reliability function against rupture of the average segment of the onshore gas transmission pipeline network in 2002-2014	89
Figure 4.10 Hazard bar chart for rupture due to external metal-loss corrosion.....	90
Figure 4.11 Comparison of the reliability function curves of the two different methodologies	92
Figure 5.1 Measurement error band and corresponding probability.....	97
Figure 5.2 Hierarchical Bayesian HGP-based model for the j^{th} inspection of the i^{th} defect .	103
Figure 5.3 ILI-reported depths in 2000, 2004, 2007 and field-measured depths in 2010 for each of the seventeen defects.....	114
Figure 5.4 Comparison of the HGP model predictions with the field-measured depths in 2010	115
Figure 5.5 Predicted growth path of defect 4 based on the HGP model.....	116
Figure 5.6 Predicted growth path of defect 9 based on the HGP model.....	117
Figure 5.7 Comparison of the NHGP model predictions with the field measured depths in 2010.....	117
Figure 5.8 ILI-reported depths in 2004, 2007, 2009 and 2011 for each of the ten defects ...	118
Figure 5.9 Initial defect lengths of the 10 defects derived from the ILI in 2011.....	120
Figure 5.10 Comparisons of the growth path predictions of the NHGP- and HGP-based models for four random defects	121
Figure 5.11 Marginal posterior PDFs of depth predictions of four defects in years 2011, 2016 and 2021	123
Figure 5.12(a-c) Comparison of small leak, large leak and rupture probabilities associated with different corrosion growth (NHGP, HGP) and different simulation methods for reliability evaluations (BUS-SuS, MC).....	125
Figure 5.13 Four stages of high-pH SCC.....	127
Figure 5.14 Comparison of predicted and actual number of crack features.....	132
Figure 5.15 Comparison of predicted and actual depths of crack features at year 15	132

Figure 5.16 Comparison of the predicted and actual depths of crack features at year 15 for different correlation coefficients between stochastic growths 134

Figure 5.17 Posterior system reliability at inspection times, based on the proposed methodology and Monte Carlo, for different correlation scenarios among stochastic growths of the crack features 136

LIST OF TABLES

Table 3.1 Input parameters for the models for defect depth.....	24
Table 3.2 Inspection and repair criteria based on ASME B31.8S	28
Table 3.3 Probabilistic characteristics of the random variables	38
Table 3.4 Probabilistic characteristics of the random variables	41
Table 3.5 Scenarios of the parametric analysis	44
Table 4.1 Mapping of the failure causes for the period 2002-2014.....	59
Table 4.2 Mapping of failure modes for the period 2002-2014	61
Table 4.3 179 Rupture failure data with known installation dates	76
Table 4.4 189 Rupture failure data with both known and unknown installation dates.....	76
Table 4.5 Approximation of the onshore gas transmission pipeline network age groups in 2002-2014.....	87
Table 4.6 Parameter estimation results of Eq. (4.17) for all failure causes.....	90
Table 4.7 Parameter estimation results of Eq. (4.17) for external corrosion incidents.....	92
Table 5.1 Probabilistic characteristics of the random variables included in the reliability analysis	122
Table 5.2 Summary of the input simulated inspection data (newly detected crack features in brackets)	133
Table 5.3 Posterior data of the methodology parameters.....	133
Table 5.4 Constant c values for different inspection years	135
Table 5.5 Random variables included in the reliability analysis	137

LIST OF APPENDICES

Appendix A: Step-by-Step Procedure for Estimating the Posterior Failure Probabilities
Conditional on the ILI Data..... 164

Appendix B: List of Publications..... 166

LIST OF SYMBOLS

a_i	= random variable (exponent) of the parameterized stochastic process used to characterise the growth of the i th defect
c	= a positive constant that ensures $cL(\boldsymbol{\theta}) \leq 1$ for all $\boldsymbol{\theta}$
c_{l2}	= constant biases of the ILI tools related to the measured lengths
c_{l2}	= non-constant biases of the ILI tools related to the measured lengths
c_1, \dots, c_{VB}	= right-censored observations
c_{1j}	= constant biases associated with the ILI tool of the j th inspection with regard to the measured depths
c_{2j}	= non-constant biases associated with the ILI tool of the j th inspection with regard to the measured depths
$c_1^\omega, \dots, c_{s_{B\omega}}^\omega$	= right-censored observations in $(n_{B\omega}, n_{B\omega+1})$, $\omega = 0, \dots, u_B$
$c_{\zeta,1}^{\omega_\zeta}, \dots, c_{\zeta,s_{B\zeta,\omega_\zeta}}^{\omega_\zeta}$	= right-censored observations in $(n_{B\zeta,\omega_\zeta}, n_{B\zeta,\omega_{\zeta+1}})$, $\omega_\zeta = 0, \dots, u_{B\zeta}$
d_{ij}	= actual field-measured depth of the i^{th} defect
d_t	= defect depth detection threshold of the ILI tool
$f(\cdot)$	= probability density function of the random variable \cdot
$f(\boldsymbol{\theta})$	= joint prior distribution of the parameters $\boldsymbol{\theta}$
$f(\boldsymbol{\theta} \mathbf{D})$	= posterior probability distribution of the model parameters conditional on the inspection data
$f_p(\cdot)$	= probability mass function of the random variable \cdot
g_1	= limit state function for the corrosion defect penetrating the pipe wall and causing a small leak
g_2	= limit state function for plastic collapse under internal pressure at the defect causing large leak
g_3	= limit state function for unstable defect extension in the axial direction causing rupture of the pipeline
$h(t)$	= hazard function
i	= random defect out of the total s detected defects
iid	= independent and identically distributed
j	= random inspection out of the total l inspections
k_A	= random variable (proportionality factor) of the parameterized stochastic

	process used for defect growth modelling
l	= total number of inspections
n	= input random variables of the pipeline under investigation given ILI data
n_{B1}, \dots, n_{BuB}	= observed failure times
$n_{B\zeta, \omega_\zeta}$	= observed failure time, failure caused by FC_ζ
p	= a standard uniform random variable
p_0	= specific value corresponding to estimates of the conditional probabilities of SuS
q	= inherent ILI tool detection capability
r	= random defect used to enumerate all defects both detected and undetected
$rc-A_{(x)}$	= Coolen and Yan's assumption right-censoring $A_{(x)}$
$S_{B\zeta, \omega_\zeta}$	= number of right-censored observations in $(n_{B\zeta, \omega_\zeta}, n_{B\zeta, \omega_{\zeta+1}})$
t_{i0}	= corrosion initiation time of defect i
t_j	= time of the random inspection j
$t_{\zeta, \omega_\zeta}^{\omega_\zeta}$	= time of observed event in $(n_{B\zeta, \omega_\zeta}, n_{B\zeta, \omega_{\zeta+1}})$, either failure time caused by FC_ζ (or time 0) or right-censoring
t_ψ	= time of observed event, either failure time (or time 0) or right-censoring ($\psi = 1, \dots, x$) and $t_0 = 0$
$t_{\omega^*}^\omega$	= time of observed event in $[n_{B\omega}, n_{B\omega+1})$, either failure time (or time 0) or right-censoring
$u_{B\zeta}$	= number of observed failure times (considering FC_ζ)
\tilde{x}_t	= number of units in the risk set just prior to time t , and $\tilde{x}_{0=x+1}$
y_{ij}	= measured depth by the ILI
$\mathcal{Y}_{B1}, \dots, \mathcal{Y}_{Bx}$	= ordered observations of Y_{B1}, \dots, Y_{Bx}
A_c	= net cross-sectional area of the Charpy impact specimen
$A_{(x)}$	= Hill's inferential assumption
API	= American Petroleum Institute
BUS	= Bayesian Updating with Structural reliability methods
CDF	= cumulative distribution function
CGR	= crack growth rate
C_v	= upper shelf Charpy V-notch (CVN) impact energy

D	= vector containing the inspection data
D	= outside diameter of the pipe
DA	= direct assessment
E	= Young modulus of pipeline steel
ECDA	= External Corrosion Direct Assessment
$F_r(v_r)$	= marginal distribution functions of a multivariate distribution function $F(v_1, v_2, \dots, v_n)$
$F_G^{-1}(\cdot)$	= the inverse function of the gamma distribution function
FC_ζ	= failure cause ζ
G_{fm}	= transformed limit state function in standard Normal space corresponding to g_{fm}
H	= number of samples simulated from \mathbf{V} in Subset Simulation
HGP	= homogenous gamma process
I_G	= indication function of the gamma process
ILI	= inline inspection
I_Z	= indicator function which takes value one if $\{p \leq cL(\boldsymbol{\theta})\}$
K	= stress intensity factor
K_{ISCC}	= threshold stress intensity factor (SIF) for crack growth in high-pH SCC
K_{mat}	= fracture toughness of pipe steel in terms of the stress intensity factor
L_i	= length of the i th defect in the longitudinal direction of the pipeline
L_{Mi}	= measured length by the ILI tool of the i th defect in the longitudinal direction of the pipeline
$L(\mathbf{D} \boldsymbol{\theta})$	= likelihood function that describes the inspection data conditional on the parameters of the model
M	= Folias factor
MC	= Monte Carlo
MFL	= Magnetic Flux Leakage
$M_{Y_B(a_B, b_B)}$	= M function, i.e. probability mass for Y_B assigned to interval (a_B, b_B)
M^ζ	= M function for $N_{B_\zeta, x+1}$
$N_{B_{x+1}}(N_{B_\zeta, x+1})$	= failure time of one future unit (under condition that failure occurs due to FC_ζ)
NHGP	= non-homogeneous gamma process
NHPP	= non-homogeneous Poisson process

N_k	= total number of functional pipe segments of a population at discrete times 1, 2, ..., k
NLQR	= non-linear quantile regression
N_{stp}	= total number of Monte Carlo steps
P_A	= random pulses of the PSWP employed to model the pipeline internal pressure
PDF	= probability density function
PHMSA	= Pipeline and Hazardous Material Safety Administration
PM	= Preventive Maintenance
PMF	= probability mass function
PoD	= probability of detection
\bar{P}, \underline{P}	= lower and upper probability respectively
$\overline{\text{PoD}}_j$	= average PoD corresponding to the S_j^k defects
$\text{Pr}(F_{fmi})$	= probability of failure against $f_m=1,2,3$, i.e. small leak, large leak and rupture failure modes, respectively for the i th defect
P_{Sfi}	= burst pressure capacity of the pipe at a given metal-loss corrosion defect
P_{Sop}	= time-dependent internal pressure of the pipe segment
P_{SR}	= rupture pressure capacity of the pipe at a given metal-loss corrosion defect
PSWP	= Poisson Square Wave Process
P_ζ	= NPI probability for $N_{B\zeta, x+1}$
$Q_{y_B}(\tau_q x_B)$	= conditional quantiles $\tau_q \in [0, 1]$ of the relationship among the response variable y_B and predictor variable x_B in the quantile regression process
RBPM	= Reliability Based Preventive Maintenance
R_{b1}	= burst pressure capacity of the pipe for energy pipelines containing surface cracks, according to the Battelle model
R_{fmi}	= reliability of the pipeline against $f_m=1,2,3$, i.e. small leak, large leak and rupture failure modes respectively for the i th defect
ROCOF	= Rate of Occurrence of Failures
R_s	= overall pipe segment reliability against rupture (survivability)
R_{sc}	= pipe segment conditional reliability against rupture (availability)
R_{sb}	= reliability function of the pipeline subsystem that remains unmaintained

R_{th}	= predefined reliability threshold for the entire pipeline
SCC	= Stress Corrosion Cracking
SMTS	= Specified Minimum Tensile Strength
SMYS	= Specified Minimum Yield Stress
S_j	= total number of defects on the pipe segment at the time of the j th inspection
S_j^0	= number of defects that have initiated prior to the $(j-1)$ th inspection
S_j^k	= number of defects that have initiated between the $(j-1)$ th and j th inspection
S_j^{kde}	= number of detected defects by the ILI tool that form part of the total number S_j^k
S_j^{kun}	= number of undetected defects by the ILI tool that form part of the total number S_j^k
SRA	= Structural Reliability Analysis
SSA	= Split System Approach
$S(t)$	= total number of expected defects on the pipe segment over $[0, t]$
SuS	= Subset Simulation
T_ζ	= unit's random time to failure under condition that failure occurs due to FC_ζ
T_m	= time of the m th PM action
T_{MT}	= given decision horizon for a preventive maintenance strategy
Y_B	= random quantity used in definition of M -function
$Y_{B_1}, \dots, Y_{B_{x+1}}$	= random quantities used in general formulation of $A_{(x)}$
U_{ja}	= random pulse heights of ja duration of the PSWP
U_C	= standard uniformly distributed variable of the Copula functions
UT	= Ultrasonic Thickness device
UTS	= ultimate tensile strength of the pipeline material
\mathbf{V}	= transformed space with independent standard Normal random variables corresponding to the original random variables p and θ
Z_A	= number of pulses of the PSWP process
α_{FT}	= multiplier of the non-linear relationship in the NLQR
$\alpha(t-t_0)^k$	= the time-dependent shape parameter of the gamma process
α_2	= scale parameter of the Weibull distribution

β_{FT}	= exponent of the non-linear relationship in the NLQR
β_i	= rate parameter of the gamma process associated with the i th defect
β_2	= shape parameter of the Weibull distribution
$\gamma(\bullet)$	= the incomplete gamma function
$\gamma_{1-6} (\xi_{1-6})$	= distribution parameters of the prior distributions of model parameters
$\delta_{\omega^*}^{\omega^*}$	= 1 if $t_{\omega^*}^{\omega^*}(t_{\omega^*}^{\omega^*})(t_{\psi^*})$ is a failure time or 0 if a right-censoring time
ε_{ij}	= random scattering error associated with the actual depth of the i th defect reported by the j th inspection
ε_{li}	= random scattering errors related to the measured length of the i th defect
η	= density of corrosion defects
η_A	= safety factor associated with internal pressure-related excavation criteria
θ	= vector of random variables of the physical pipeline model
$\lambda_A(\tau)$	= instantaneous generation rate of corrosion defects
λ	= mean occurrence rate per unit time (or Poisson rate) of the PSWP
μ	= mean of the probability distribution of the random scattering error ε_{ij} associated with the reported defect i in the j th inspection
ξ_A	= safety factor associated with wall thickness-related excavation criteria
ρ_{jq}	= correlation coefficient between the random scattering errors associated with the j th and the q th inspections
σ	= standard deviation of the probability distribution of the random scattering error ε_{ij} associated with the reported defect i in the j th inspection
σ_f	= material flow stress of the pipeline
σ_j	= standard deviation of the random scattering errors associated with the ILI tool used in inspection j
σ_y	= pipe's material ultimate yield strength
$\nu_{B\zeta}$	= number of right-censored observations (considering FC_ζ)
$\Delta\alpha_{ij}$	= the time-dependent shape parameter associated with Δd_{ij}
Δd_{ij}	= the growth of the i th defect among two consecutive ILIs
Z	= observation event $\{p \leq cL(\theta)\}$ in terms of the Bayesian updating
$\Lambda(t)$	= expected number of defects generated over $[0, t]$
Σ_ε	= covariance matrix of the random scattering error
$\Phi^{-1}(\bullet)$	= the inverse of the standard normal distribution function

$\Phi_n(\boldsymbol{\mu}; \mathbf{R})$ = the n -variate standard normal distribution function with $(n \times n)$ matrix of correlation coefficients \mathbf{R}

1. Introduction

1.1 Background

Pipelines are the safest and most economic means of transporting hydrocarbons (e.g. crude oil and natural gas) around the globe. Degradation is considered an inevitable part of the operating lifecycle of pipelines, even for newly built ones, as it typically is for infrastructure. A sudden breakdown can lead to loss of productivity or severe accident with large environmental, economic and social implications. As a result, comprehensive maintenance and rehabilitation plans should be available, as part of a structured reliability-based integrity management program. The success of such programs, depends primarily on how well threats and failure mechanisms are defined. Integrity threats should be considered in conjunction with realistic maintenance strategies including in-line (ILI) inspections, criteria for excavating and repairing defects and direct assessment. Structural reliability analysis (SRA) can have a key role in the reliability-based integrity management. It offers an efficient way of directly assessing the loads and capacity of a pipeline, considering the separate effect of each random variable on the pipeline condition (Barone and Frangopol, 2014). When it comes to SRA models, the uncertainties regarding material and geometrical properties, environmental factors and the models themselves are accounted for probabilistically, towards obtaining realistic forecasts of failure probabilities (Frangopol and Soliman, 2016). The results from the SRA can be used in real industry practice for the development of safe and cost-effective integrity management strategies.

According to incident data from the literature, external corrosion has been identified as the predominant gradual deterioration process (UKOPA, 2014). In addition, stress corrosion cracking (SCC) also poses a major threat to the safe operation and structural integrity of energy pipelines. Bayesian data analysis is a very advantageous way of updating SRA models given corrosion ILI data and has been used considerably in energy pipelines' literature over the past decade (Maes et al., 2009; Pandey and Lu, 2013; Al-Amin and Zhou, 2014; Qin et al., 2015; Zhang and Zhou, 2013; Caleyó et al., 2015). The analytical estimation of the high-dimensional integrals typically involved in Bayesian updating is not feasible in pipeline problems and therefore Markov Chain Monte Carlo (MCMC) sampling techniques are commonly adopted to numerically perform this task (Al-Amin and Zhou, 2014). The limitations of these methods include the uncertainty around ensuring that the

final samples have reached the posterior distribution and also the difficulty in ultimately quantifying small probabilities of rare failure incidents (Straub et al., 2016); particularly rupture due to metal-loss corrosion in the setting of energy pipelines (Zhang and Zhou, 2013). In this case, a more advantageous method is necessary for energy pipelines, one that overcomes the limitations of MCMC.

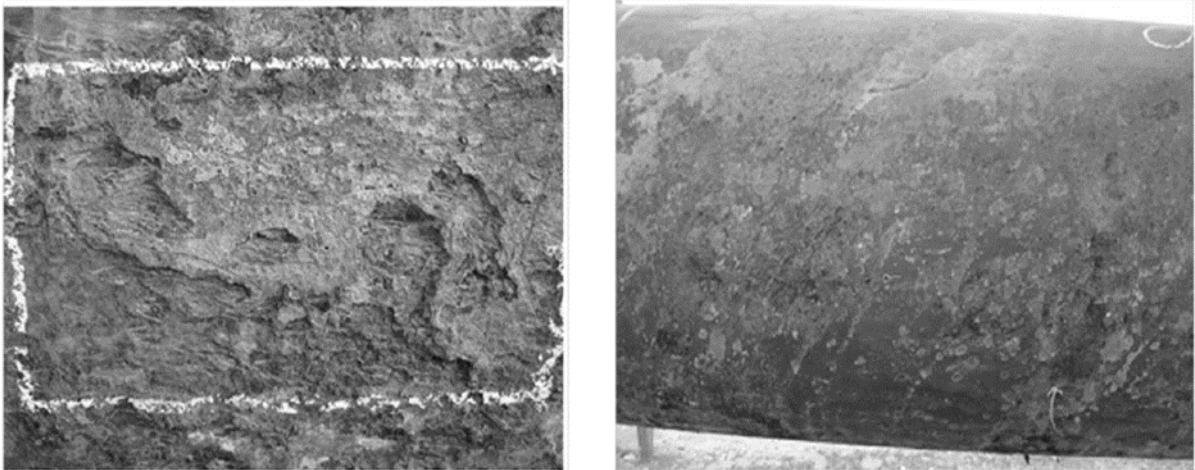


Figure 1.1 External metal-loss corrosion on the pipeline body (Qin et al. 2015).

Even though developments in the technology of ILI tools are constant and at the same time a lot of the older lines are modified to accommodate ILI, for a significant amount of upstream and transmission energy pipelines, ILI will remain inadequate due technical and financial constraints (Kishawy and Gabbar, 2010). Therefore, alternative to ILI inspection and maintenance plans should also be considered. The application of integrity management principles for corroding energy pipelines that cannot be in-line inspected relies mainly on strategies like direct assessment (DA) as specified by the National Association of Corrosion Engineers (NACE) Standard (NACE International, 2010). A DA framework will typically entail indirect inspections and selected direct examinations at bell-hole locations (NACE International, 2010). However, according to the NACE Standard, a DA can be a 100 percent direct examination. Furthermore, oil and gas pipelines span long distances and can be divided into a number of segments with similar functions and conditions. When a pipeline system is preventively maintained though, normally only part of the system gets repaired or replaced, leading to an imperfect repair of the whole system (Sun et al., 2007). As a result, it is of high practical importance to develop an SRA

methodology that includes imperfect DA strategies for a pipeline system that cannot be inspected with ILI tools.



Figure 1.2 Direct Assessment of the pipeline condition in the field (NACE International, 2010).

The validation of SRA based on historical failure data is key to gaining confidence on the results, provided the uncertainties associated with both methods are properly taken into account. Previous studies that employed historical failure data of energy pipelines, evaluated the failure probabilities in the rate of occurrence of failure (ROCOF) sense for repairable systems (Caleyo et al, 2008; Nessim et al, 2009). In brief, the repairable system approach assumes that upon failure, the system is restored to operation by repairing or even replacing some parts of the system, instead of replacing the entire system. Thus, the failure rate refers to a sequence of failure times within a time interval, as opposed to a single time to failure distribution. However, the ROCOF failure rate can be evaluated only for a limited period of time, i.e. for as long as incident data are available. In an alternative approach, the pipeline times to failure can be grouped according to a non-repairable systems approach. The failed pipes are defined as non-repairable segments functioning within a repairable system, which is the entire pipeline network. In other words, the lifetime of a pipe segment is a random variable described by a single time to failure. Such analyses of historical failure data are advantageous in that they can provide a complete

picture of energy pipeline reliability and can be directly comparable to SRA predictions for cross-verification and corroboration of the results.

1.2 Objectives and Research Significance

The aim is to develop technically comprehensive methods that can explicitly define safety threats in the context of realistic pipeline integrity management strategies, in order to accurately evaluate the pipeline remaining life as a function of uncertainties in pipeline operating conditions. The objectives of the study reported in this thesis include: 1) development of model-based methodologies that incorporate stochastic processes within a structural reliability analysis (SRA) framework and predict time-dependent reliability for corroding pipelines, with the consideration of realistic, industry consistent inspection and maintenance techniques, 2) development of methodologies that estimate failure probabilities in a non-repairable approach setting, based on robust statistical analyses of historical incidents, 3) development of methodologies to evaluate small ($<10^{-6}$) failure probabilities for corroding pipelines conditional on ILI data, by employing the developed probabilistic SRA framework, 4) cross-verification of the SRA and statistical methodologies 5) validation of the methodologies conditional on ILI data, based on actual data. It is anticipated that the research outcome of this study will assist energy pipeline operators in implementing informed integrity management plans, based on reliability and safety. This can be of great value not only to the pipeline industry, but also to the communities in the proximity of energy pipelines.

1.3 Scope of Study

This study consists of a relevant literature review in Chapter 2 and three core topics that are presented in Chapters 3 to 5 respectively and form the main body of the thesis. In Chapter 3, a probabilistic methodology for onshore gas pipelines with corrosion defects is proposed, based on a structural reliability analysis (SRA) framework. The application of the SRA methodology is illustrated through two case studies that consider two different maintenance strategies. In the first application, the non-homogeneous Poisson process is used to model the generation of new defects and a parameterized stochastic process (i.e. a non-linear function of two random variables) is used to model the growth of defects. The

internal pressure loading is modelled as a Poisson square wave stochastic process. External Corrosion Direct Assessment (ECDA) is utilised as an industry-consistent maintenance strategy. The second case study implements the SRA methodology with the consideration of a realistic maintenance and repair strategy based on in-line inspections (ILI). The non-homogeneous Poisson process models the generation of new defects and a robust non-linear stochastic process, namely Poisson square wave process, is used to model the growth of defects. The internal pressure loading is modelled as a discrete Ferry-Borges stochastic process. The probability of detection (PoD) and measurement error of the inspection tools are also incorporated in the methodology. The results are validated against a statistical model presented subsequently in Chapter 4. In specific, two statistical models are proposed in Chapter 4, based on historical failure data of onshore gas transmission pipelines from the Pipeline and Hazardous Material Safety Administration (PHMSA) database. The first statistical methodology is based on a well-established non-repairable system approach, namely nonparametric predictive inference (NPI). It provides imprecise probabilities and survival functions via upper and lower bounds, due to a specific cause among a range of competing ones. The second case study concerns the application of a novel statistical methodology, based on a parametric hybrid empirical hazard model and a robust data processing technique (i.e. non-linear quantile regression) with regards to the PHMSA historical failure data. Reliability inferences correspond to the complete lifecycle reliability of the average pipe segment of the respective region under study. The results from the latter are compared with the ILI-based SRA methodology proposed in Chapter 3 for the purpose of cross-verification. Finally, in Chapter 5 a new methodology for estimation of small posterior failure probabilities based on Bayesian analysis of ILI data is presented. Two case studies are conducted to illustrate and validate the proposed methodology. Firstly, the methodology is applied in an existing gas pipeline containing metal-loss corrosion defects and is validated against field data. The reliability conditional on the inspection data is evaluated directly with a single method. In the second case study, Bayesian updating is carried out in conjunction with a data augmentation (DA) technique, for simulated data of high-pH stress corrosion cracking (SCC). The interdependence of crack growths is addressed through the Gaussian copula method. Both numerical applications of Chapter 5 are carried out within a realistic, industry-consistent context.

1.4 Thesis Format

This thesis consists of six chapters in total. Chapter 1 presents a brief introduction of the background, objectives and scope of study. Chapter 2 reviews the literature with respect to the relevant research area of this thesis. Chapters 3 to 5 forms the main body of the thesis, each of which addresses a distinct topic. These constitute the core of the published papers and submitted manuscripts, as listed in Appendix B. The conclusions and main contributions of the research of this thesis, as well as the proposed future works are discussed in Chapter 6.

2. Literature Review

Energy pipeline infrastructure grows about 3-4 percent per year globally. Worldwide, most energy pipelines have been in place for at least 20 years; more than 50 percent of pipelines were installed in the period 1950-1970 (Kiefner and Rosenfeld, 2012). In literature, old pipelines refer to those that were constructed prior to the 1970's (Kishawy and Gabbar, 2010). These are considered of lower standards, in terms of material and external coating, compared to more recent ones. However, gradual deterioration of the pipeline condition is considered inevitable, even for contemporary pipelines, as it typically is for all engineering structures. As a result, comprehensive maintenance and rehabilitation plans should be readily available, as part of a structured integrity management program. The effectiveness of an integrity management program depends on many factors, including how well threats and failure mechanisms have been identified (Kishawy and Gabbar, 2010).

According to statistical analyses and incident data, external corrosion is the predominant gradual deterioration process for onshore energy pipelines (EGIG, 2015; CONCAWE, 2015; UKOPA, 2014; AER, 2013). However, other factors such as third-party activity, material or construction imperfections, geotechnical hazards, incorrect operation and inadequate design, among others, can lead to ultimate failure modes such as leaks and ruptures (Caleyo et al., 2008; El-Abbasy et al., 2014). Nonetheless, the efforts to evaluate pipeline reliability in the literature thus far, either account only for corrosion as a failure mechanism (Li et al., 2009; Zhou, 2010; Lecchi, 2011; Valor et al., 2013; Zhang and Zhou, 2013) or inevitably entail a level of subjectivity due to their prominently conceptual nature (Peng et al., 2009; El-Abbasy et al., 2014). Failures of onshore energy pipelines due to external corrosion can be further distinguished in metal-loss and stress corrosion cracking (SCC) failures (EGIG, 2015; CONCAWE, 2015; UKOPA, 2014; PHMSA, 2015).

Metal-loss corrosion defects typically have an irregular depth profile and extend irregularly in both longitudinal and circumferential directions, as illustrated in Figure 2.1 (Cosham and Hopkins, 2001). Metal-loss corrosion may occur as a single defect or a cluster of adjacent defects, separated by full wall thickness areas and it typically has a length and width less than or equal to three times the full wall thickness (Kiefner and Veith, 1989). The main difference compared to SCC is that metal-loss defects are 'blunt'. That is, the minimum radius equals or exceeds half of the pipe wall thickness and defects that have a width greater than their local depth (Stephens and Leis, 2000; Cosham and

Hopkins, 2001). SCC refers to gradual, environmentally induced crack propagation. This phenomenon is associated with a combination of stress (applied or residual) above some threshold value and specific environment and sometimes metallurgical conditions, which lead to surface cracks with a high aspect ratio (long and shallow) (Manfredi and Otegui, 2002). SCC of pipeline steels can be further categorized into two types: classic or intergranular cracking, which occurs in high-pH solution near cracks in coating disbonded regions and transgranular cracking which occurs in near-neutral pH solution in coating disbonded regions. The high-pH form is by far the most reported form of SCC (Manfredi and Otegui, 2002; Song et al., 2011; Fan et al., 2015; Wenk, 1974).

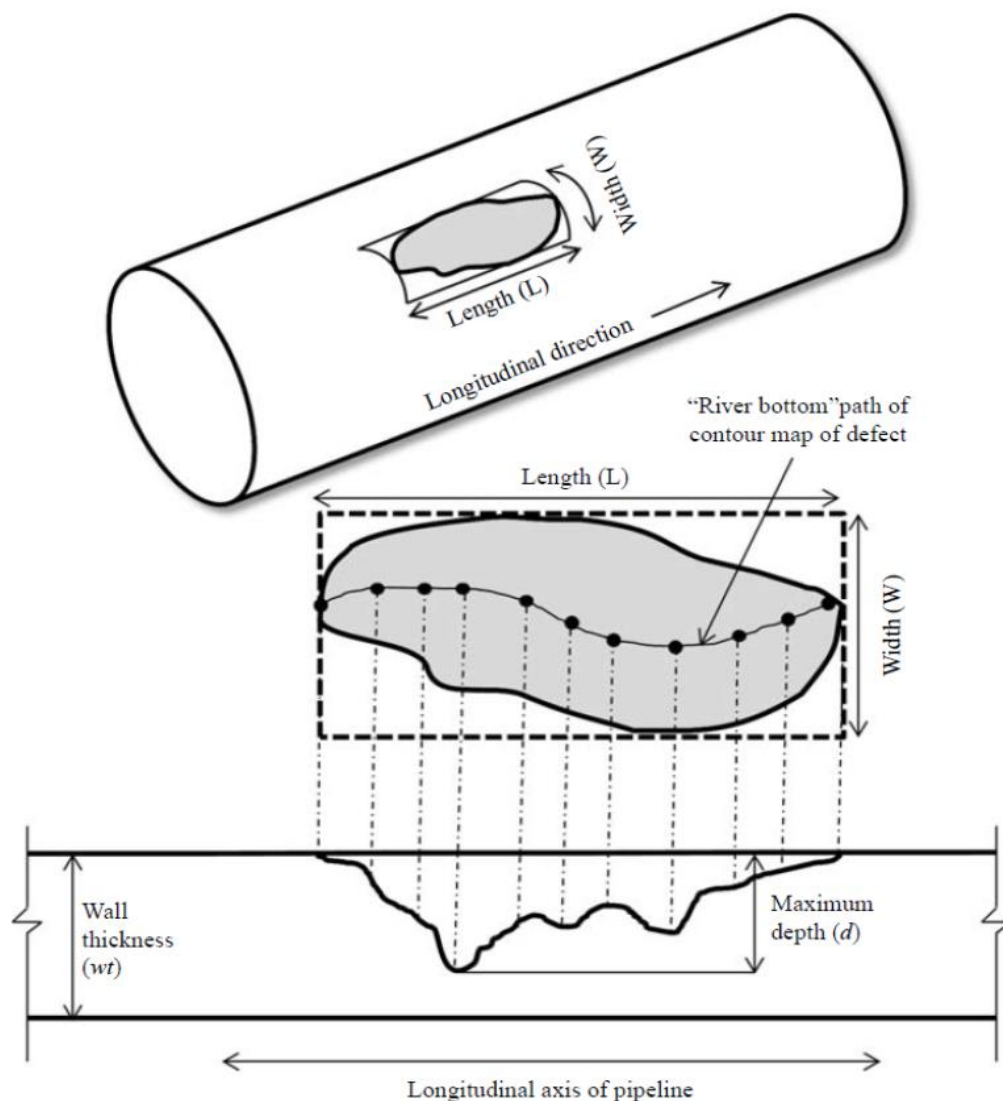


Figure 2.1 Dimensions of a typical metal-loss corrosion defect on pipeline (Al-Amin and Zhou, 2013).

High-pH SCC on high pressure steel pipelines is characterised by the presence of patches or colonies of numerous shallow and longitudinal intergranular cracks, often with little evidence of secondary corrosion (Jaske et al., 1996; Jaske and Beavers, 1998; Kiefner and Veith, 1989). It results from periodic passive film rupture and anodic dissolution and the crack growth rate (CGR) follows Faraday's law (Manfredi and Otegui, 2002; Song et al., 2011). Unlike near-neutral pH SCC, which is often regarded as corrosion fatigue since solely constant (static) loading can rarely cause crack growth, high-pH SCC features commonly initiate and grow in the presence of high-stress conditions, without dynamic loading (Song et al., 2011; Timashev and Bushinskaya, 2016). In general, depending on the type of transported fluid (gas or liquid), the type of loading (constant or cyclic) can be determined. If more precision is required, the variation of hoop stress over time is determined and the stress ratio (R) and loading frequency (f) should be estimated. For gas pipelines, normally $R > 0.8$ and $f < 10^{-5}$, thus high-pH SCC typically develops under constant loading solely (Parkins, 1987).

The current industrial practice for estimating crack growth rates of high-pH SCC is based on empirical approaches mainly relying on linear extrapolations from measured crack depths over a period of time, or is based on using a conservative fixed value. Such CGR models do not account for the uncertain nature of cracking mechanisms and thus may provide non-realistic estimations. A CGR model with embedded crack growth mechanism was developed in Song et al. (2011). However, the updating of the CGR model based on the inspection data did not account for the detecting and sizing uncertainty. Also, the embedded crack growth mechanism yielded a CGR model that is only applicable in the case of increasing CGR over time, which may not always be the case.

Furthermore, different integrity management strategies can be efficiently incorporated in comprehensive condition assessment and prediction studies, by means of structural reliability analyses (SRA), since it offers an efficient and thorough way of directly accounting for the separate effect of each random variable on the pipeline reliability (Barone and Frangopol, 2014). The uncertainties involved in the manufacturing and operation processes are all incorporated in the SRA by means of probabilistic approaches. SRA for corroding energy pipelines has been widely utilised in literature (Ahammed, 1998; Pandey, 1998; Hong, 1999; Caleyó et al., 2002; Texeira et al., 2008; Zhou, 2010; Valor et al., 2013). The corrosion growth modelling is considered critical for the accuracy and the validity of the SRA (Tee et al, 2014; Witek et al, 2018). Generally, most corrosion

growth models reported in literature can be categorised as random-variable based, stochastic process-based models, fuzzy models, interval models and imprecise probability models (Hong, 1999; Timashev, 2008; Caleyó et al., 2009; Maes et al., 2009; Zhang and Zhou, 2013; Senouci et al., 2014; Opeyemi et al., 2015; Fang et al, 2015; Shafiee and Ayudiani, 2015; Chaves et al., 2016; Melchers, 2016; Melchers and Ahammed, 2016; Asadi and Melchers, 2017; Witek, 2018).

Stochastic process-based growth models that have been reported in the literature so far for energy pipelines, mainly concern metal-loss corrosion (Hong, 1999; Timashev, 2008; Caleyó et al., 2009; Maes et al., 2009; Zhang and Zhou, 2013; Dann and Maes, 2018). The Markov chain and gamma process-based models have been used to characterize the growth of corrosion defects in order to evaluate the time-dependent failure probabilities (Shafiee and Finkelstein, 2015). In Maes et al. (2009) and Zhang and Zhou (2013), gamma process was employed to model the growth of corrosion defects on the pipeline. Gamma process represents cumulative temporal variability with stationary increments, while Markov chain models require discretization of the damage states or evaluation of transition probabilities (Bazán and Beck, 2013; Zhang and Zhou, 2014). Another sophisticated model has been proposed in Bazán and Beck (2013), namely Poisson Square Wave Process (PSWP), which provides sample paths of deterioration that are continuous in time. In Valor et al. (2007), Zhang and Zhou (2014) and Qin et al. (2015) the generation of new metal-loss corrosion defects was additionally modelled by means of a non-homogeneous Poisson process (NHPP). Finally, the internal pressure varies with time and should also be characterized by a stochastic process.

The next step in an SRA is the application of a predictive model to calculate the probability of failure, by employing a failure mode limit state function (Valor et al, 2013; Zhou, 2011; Melchers, 2004). Reliability evaluations based on historical failures, inherently include maintenance actions that took part throughout the period of study. Hence, a realistic SRA should also account for inspection and repair actions. The uncertainties involved in the reliability prediction, defect initiation and propagation and the effect of maintenance on the performance of the pipeline, should all be taken into account in an accurate reliability-based integrity management program (Melchers, 2004). Therefore, an SRA that models the generation of corrosion defects, the growth of defects and internal pressure as stochastic processes, whilst incorporates multiple long-term

integrity management strategies and quantifies the relevant uncertainties is of great practical importance.

The corrosion defect growth rate is pivotal and must be accurately modelled when the interval for in-line inspection (ILI), pressure testing and direct assessment is to be determined. The corrosion growth model can also be a key parameter in identifying locations along a pipeline that must be given priority for direct assessment. Bayesian data analysis is the most credible way of updating probabilistic models given observation data and has been widely employed in energy pipelines' literature over the past decade (Maes et al., 2009; Pandey and Lu, 2013; Al-Amin and Zhou, 2014; Qin et al., 2015; Zhang and Zhou, 2013; Caleyó et al., 2015). The analytical estimation of the high-dimensional integrals typically involved in Bayesian updating is not feasible in pipeline problems and therefore Markov Chain Monte Carlo (MCMC) sampling techniques are commonly adopted to numerically perform this task (Al-Amin and Zhou, 2014). A crude Monte Carlo simulation typically follows as a post-processing step after the Bayesian analysis, to estimate the conditional on the posterior distribution probability of failure. The limitations of this framework, is first the uncertainty regarding whether the final samples have reached the posterior distribution in MCMC sampling and second the difficulty of the crude Monte Carlo simulation in subsequently quantifying small probabilities of rare failure incidents (Straub et al., 2016; Betz et al, 2018).

Furthermore, only an approximation of the posterior distribution is typically available in pipeline studies, through samples of the posterior (Maes et al., 2009; Al-Amin and Zhou, 2014; Zhang and Zhou, 2013; Caleyó et al., 2015). Other Structural Reliability methods apart from Monte Carlo, have difficulty working with such an approximation, which eventually limits their efficiency in determining the posterior failure probability given the inspection data. One exception is Subset Simulation (SuS), which can be applied starting from samples of the posterior, but as discussed in Papaioannou et al., (2015), SuS is typically applied in the standard Normal space for efficiency reasons, which again necessitates explicit knowledge of the posterior distribution. What is more, in order to acquire the complete picture of time-dependent failure probabilities and determine suitable mitigation strategies, the generation of new corrosion defects (instead of existing ones only), should be part of the analysis (Qin et al., 2015). The dependence (or correlation) of the stochastic growth of corrosion defects should be considered too. This expresses the spatial dependence among different defects, which is typically due to the similar corrosive

environment (e.g. surrounding soils), similar pipe properties (e.g. wall thickness, yield strength and tensile strength) at the defects' location and the fact that defects are subjected to the same internal pressure (Zhou et al., 2012).

Typically, industry-consistent strategies for reliability-based integrity management of energy pipelines include high-resolution in-line inspections (ILI) to measure defects on the pipeline body and estimate failure probabilities based on the inspection results (Witek et al, 2018). However, according to Kishawy and Gabbar (2010), more than 50% of existing pipelines worldwide are non-detectable by ILI tools, a term referred to in literature as 'unpiggable'. According to the Interstate Natural Gas Association of America (INGAA), which operates approximately two thirds of the US natural gas transmission pipeline system, only 60 percent of the total miles can accommodate ILI tools (PHMSA, 2015). Even though developments in the technology of ILI tools are constant and at the same time a lot of older lines are modified to accommodate ILI tools, it is considered certain that for a significant number of energy pipelines, ILI will remain inadequate. This is usually the case for remote, rural area pipelines that do not pose a threat to the public safety and also for pipelines that present significant technical challenges due to a number of factors (e.g., small-diameter lines, multi-diameter lines and lines with low flow rates, complex geometry or that serve as a single source feed to customers) (PHMSA, 2015; Leewis, 2012). As a result, alternative to ILI maintenance plans should also be available (Haladuick and Dann, 2018). These rely mostly on the use of historical failure data and on methodologies based on direct assessment (NACE International, 2010). A direct assessment framework usually includes indirect inspections and selected direct examinations at bell-hole locations (NACE International, 2010).

Energy pipelines can be characterised as linear assets that span long distances and consist of individual segments with the same function but relatively differing operating and loading features (Haladuick and Dann, 2018). As a result, maintenance decisions based on reliability should be made on the system level (Animah et al, 2018). In practice, conventional engineering asset management systems or decision support tools are not considered adequate for linear assets like energy pipelines (Sun et al., 2014). Usually, in order to maintain the overall reliability of a system in a long period of time, decisions for preventive maintenance should be made, based on extensive inspection and/or condition monitoring of the system (Guo et al, 2013; Shafiee et al., 2015; Gong and Zhou, 2018; Haladuick and Dann, 2018). However, when a pipeline system is preventively maintained,

normally only part of the system is repaired or replaced, leading to an imperfect actions when it comes to the whole system (Sun, et al, 2007; Finkelstein and Shafiee, 2017). For large scale engineering systems like pipelines though, it is not sufficient to estimate the next inspection and preventive maintenance (PM) time, but it is also necessary to define multiple inspection and PM times over a decision horizon, which is normally a long period of time. This enables decision makers to adequately plan various resources such as economic, human and logistic.

Relevant studies of maintenance strategies based on pipeline reliability, either focused only on a single defect to derive the reliability of the pipeline (Gomes, et al, 2013) or required the number of defects to be a priori known from ILI results (Lecchi, 2011; Zhang and Zhou, 2013). Hong (1999) and Zhang and Zhou (2014) employed the homogeneous Poisson process (HPP) and the non-HPP subsequently to generate the number of defects on a single pipeline segment and then find the optimal interval in a periodic inspection plan. Hong (1999) estimated the probability of failure with regard to a defect-based maintenance and repair strategy, as opposed to a segment-based strategy. Zhang and Zhou (2014) did not deal with the overall probability of failure but only estimated the optimal interval based on cost and did not consider multiple segments via system reliability. On the other hand, studies in literature relevant to DA, have so far accounted only for the Bayesian updating of data relevant to uncertainties of inspection tools and of active corrosion defects' characteristics (Van Os, 2006; Francis et al., 2006; Francis et al., 2009; Van Brugel et al., 2011). Recently, Valor et al. (2014) and Caleyó et al. (2015), proposed practical methodologies with regards to the analysis of field data from random sampling for unpiggable underground pipelines. However, according to the NACE Standard, when applying a DA, pipeline operators can adopt a 100 percent direct examination, instead of indirect inspections and selected sampling direct examinations at bell-hole locations.

Previous works that consider a system of pipe segments include De Leon and Macias (2005), Straub and Faber (2005) and Hong et al. (2014). De Leon and Macias (2005) studied the effect of spatial correlation on the failure probability of corroded pipelines. It was found that the correlation degree between failure modes at two pipeline segments, increases with the degree of correlation of the initial corrosion depths of defects of these segments. In addition, for a small number of segments (<5), the correlation was found to be insignificant. Straub and Faber (2005) considered system effects for the inspection planning of steel structures subjected to fatigue deterioration. The system representation

was made by considering a number of 'hot spots' in the structure, which have been chosen as more failure prone or of higher failure consequences. However, it was concluded that for corroded pipelines, in principle 'all spots are hot' and as a result the spatial variability of the deterioration mechanisms should be exhaustively considered. Still though, the number of 'hot spots' is expected to be very large and therefore some level of simplification should be normal. Hong et al. (2014) studied the dependency of the stochastic degradations of multiple components of engineering systems and their effect on the system probability of failure. The result indicated importance solely for parallel systems and not for series systems, like pipelines. In conclusion, system reliability predictions for unpiggable corroding gas pipelines, with the consideration of imperfect repairs, had not been dealt with in the literature, to the best of the author's knowledge.

Furthermore, a comparison between SRA and statistical analyses has always been challenging, for practical reasons. Pipeline historical failure data are scarce and generic, in that they do not account for the wide variety of parameters and conditions associated with different pipelines (Kiefner et al., 2001; Nessim et al., 2009). However, the validation of failure probability calculations (SRA) based on historical failure data is key to gaining confidence on the results, provided the uncertainties associated with both methods are properly considered. Collection of incident data and database development for statistical analyses and probability prediction of future events is a well established practice when it comes to energy pipelines (AER, 2013; UKOPA, 2014; EGIG, 2015; CONCAWE, 2015; PHMSA, 2015). Probabilistic data driven models are complicated, in that they usually require substantial amounts of data for proper development (Dann and Huyse, 2018). In practice, pipeline operators prefer to use quantitative models like these in order to assess risk. However, often there is not enough actual data to yield meaningful results and expert judgment is required to estimate missing data, or to make conservative assumptions. The results of a probabilistic model are generally expressed as the probability of an event being realised. Afterwards, the probability rating can be compared with the overall reliability history of the operator's pipeline, with the level of desired performance and also industry-acceptable thresholds (Kishawy and Gabbar, 2010; Frangopol and Soliman, 2016).

Reliability prediction based on historical failure data, on the other hand, is realised by assuming and defining a direct comparison among the values of each pipe segment with a reference pipeline that summarises the average conditions of the area where the pipeline system operates (Caleyo et al., 2008; Nessim et al., 2009). Other relative reliability ranking

models identify all of the reliability variables that contribute to the likelihood of a failure with respect to a specific threat, such as external corrosion or third-party damage. The models usually provide a system to numerically rank the conditions that could be associated with a model variable, as well as to evaluate the relative contribution of each variable. These could be related to the physical characteristics of the facility, the nature of recurring problems and the root cause of major problems for instance (Caleyo et al., 2015). Most of the information stem from historical failure data or expert knowledge. Thereafter, a numerical weighting factor can be determined. For example, age is a driving variable that must be considered, as many failure causes are time-based damage mechanisms and also because as pipelines grow older, their probability of failure naturally increases. These models are particularly valuable in determining the relative impact of each threat on a particular pipe segment. They allow pipeline operators to assess integrity threats independently or to compare them. In summary, relative risk ranking models provide a consistent approach to assessing the integrity of and assigning a reliability factor to a pipe segment. These models are very valuable in aiding operators to prioritize pipe segments according to the need for assessment but are not considered to be entirely quantitative (Baker, 2008). Therefore, they are not suggested when accurate results are desirable (Valor et al., 2014).

The implementation of probabilistic risk models and subsequent mitigation strategies can be considerably assisted by the pipeline incident and mileage data available at different databases from around the world (Tee et al., 2014). One of the most distinguished is the Pipeline and Hazardous Material Safety Administration (PHMSA) of the United States Department of Transportation (DOT), which collects information on incidents of gas and liquid pipelines that were regulated by PHMSA and met the appropriate criteria. PHMSA pipeline incident database includes information regarding each reported incident and the pipeline involved in the incident, along with annual reports from gas and liquid pipeline operators about the total pipeline mileage, transported commodities and installation dates. Golub et al. (1996) analysed the PHMSA incident data on the gas transmission pipelines between 1970 and 1993 and later Kiefner et al. (2001) also analysed the incidents on the gas transmission and gathering pipelines from 1985 to 1997 as reported in the PHMSA database. Similar analyses have been conducted in the past from data derived from other relevant databases, such as the United Kingdom Onshore Pipeline Operators' Association (UKOPA) or the European Gas pipeline Incident data Group (EGIG) (UKOPA, 2014;

EGIG, 2015; CONCAWE, 2015). It is noted that the principal legislation governing the safety of pipelines is goal setting requiring that pipelines are designed, constructed and operated so that the risks are as low as is reasonably practicable (ALARP) (Papadakis, 2000). In the UK pipeline industry in particular, there are many well established standards, covering design, operations and maintenance of sector major accident hazard pipelines, which can be used to demonstrate risks are ALARP (UKOPA, 2014). For natural gas major accident hazard pipelines the Institution of Gas Engineers and Managers (IGEM) series of recommendation on transmission and distribution practice is advocated by the British Standard Code of Practice for Pipelines, such as IGE/TD/1 and IGE/TD/13 (Goodfellow et al., 2008). Lam and Zhou (2016) analysed the PHMSA database in an effort to derive inferences about the condition of gas transmission pipelines in the US and to develop relevant failure frequencies for assessing the risk of onshore gas transmission pipelines. Also, they proposed a probability of ignition model for ruptures, based on the above-mentioned incidents reported in the PHMSA database for the period from 2002 to 2013.

Additional studies that utilized historical failure data for reliability analysis of energy pipelines, evaluated the failure probabilities in the rate of occurrence of failures (ROCOF) approach for repairable systems (Caleyo et al., 2008; Nessim et al., 2009). This means that upon failure, the system is restored to operation by repairing or even replacing some parts of the system, instead of replacing the entire system. The ROCOF failure rate considers a sequence of failure times within a time interval, as opposed to a single time to failure distribution (Ascher and Feingold, 1984; Leemis, 1995). However, the ROCOF failure rate can be characterised only for a limited period of time, i.e. for as long as incident data are available. In practice, in most databases available incident data that are fairly consistent, usually do not cover operation periods of more than 30 years, while the actual pipeline lifecycle can be significantly more than that. These studies cannot provide a direct estimation of the reliability function for a pipe segment, system or network; instead they can provide rather generic guidelines and inductions that may prove relevant to a risk assessment strategy. As a result, deriving inferences for a complete pipeline lifecycle is not feasible. Moreover, according to the board meeting of the National Transportation Safety Board (NTSB) in January 2015, it was found that the PHMSA database is characterised by a lack of detailed attributes for the gas transmission pipelines and also that there is a discrepancy among the annual report database (that contains the pipeline details and

mileage information) and the incident database, which leads to some level of inaccuracy in the relevant analyses (NTSB, 2015). Therefore, analyses of historical failure data that can provide a complete characterisation of energy pipeline reliability and deal with incomplete and uncertain data efficiently would be of great pertinence.

3. Structural Reliability Analyses for Predictions in Energy Pipelines

3.1 Introduction

In this chapter, two probabilistic methodologies are proposed for onshore gas transmission pipelines subjected to external metal loss corrosion, based on a robust integration of stochastic processes within a structural reliability analysis (SRA) framework. The application of the proposed methodologies is realised through two case studies, based on two different inspection and maintenance strategies. In the first case study, a robust structural reliability model is proposed that provides estimates of rupture probabilities against external corrosion on a reference pipe segment. The reference segment characteristics are derived from historical failure data from PHMSA. In specific, the reported rupture incidents due to external metal loss corrosion for the period 2002-2014 are employed and the reference pipeline is built based on their characteristics. The proposed SRA framework models the mechanical failure of the reference segment by adopting up to date stochastic processes, associated with the segment based loads and resistances. The non-homogeneous Poisson process is used to model the generation of new defects and the Poisson square wave process is used to model the growth of the defects. The internal pressure load is modelled as a discrete Ferry-Borges stochastic process. Then, an inspection and repair program is applied to the reference segment, based on the standardised code of practice (ASME B31.8S) for the in line inspection (ILI) technique, for a service life of 100 years. A realistic characterisation of the probability of detection (PoD) and measurement error, associated with the ILI data is also incorporated in the model.

In the second case study, a different industry consistent maintenance strategy is considered, namely External Corrosion Direct Assessment. In this case, a so called ‘unpiggable’ or ‘non-piggable’ (i.e. that cannot accommodate an ILI tool) corroding onshore gas transmission pipeline system is examined with respect to external metal-loss corrosion. The reliability, first evaluated on the segment level, is subsequently evaluated on the system level and the influence of imperfect ECDA actions is investigated. A heuristic method is adopted, namely Split System Approach (SSA) (Sun et al., 2007; Sun et al., 2009). This method has the ability to link the SRA to long-term preventive maintenance (PM) decision making, so that the decision can be updated by using the latest

inspection and health monitoring information available. In previous works (Sun et al., 2007; Sun et al., 2014), SSA was implemented by adopting the hazard function which belongs to the lifetime functions and was defined based on the probability density function of the time to failure. However, the SRA allows for a clear understanding of the separate contribution of each random variable to either resistance or load, unlike the lifetime functions that summarise the combined effect of all the uncertainties on the pipeline system (Barone and Frangopol, 2014). To the best of the author's knowledge, SSA is applied to a corroded energy pipeline system with the reliability function estimated by an SRA for the first time in this study. The corrosion process is evaluated for a number of defects on a pipe segment of 12m. The non-homogeneous Poisson process (NHPP) is employed to model the uncertainties in the number and generation of defects and a well-established empirical power law model is adopted for the growth of defects over time. The reliability forecast regarding the segment is obtained by the limit state for burst due to internal pressure, with the uncertainties in the pressure incorporated in the analysis through a Poisson square wave process (PSWP) model. Afterwards, the numerical application is carried out on a system of three identical pipe segments that form a series system. The SSA method illustrates the effects of future maintenance actions on the time-dependent reliability of the pipeline system. The impact of some key parameters is examined at the end, in an effort to derive some additional conclusions regarding the proposed methodology.

The contents of this chapter are organised as follows. Section 3.2 presents the physical model, namely generation of new defects, corrosion growth and internal pressure models, as well as the limit state function associated with burst, along with the method for evaluating the time-dependent reliability of a corroding pipe segment that contains multiple defects. Thereinafter, Section 3.3 presents the impact of the ILI inspections and their associated uncertainties on the time-dependent reliability of the pipe segment. Section 3.4 presents the SSA method for long-term system reliability predictions. In Sections 3.5 and 3.6, the numerical applications are illustrated and the results are subsequently discussed. This chapter is completed with concluding remarks in Section 3.7.

3.2 Physical Model

3.2.1 Stochastic Generation of Metal-loss Corrosion Defects

The generation of new defects on a newly built pipe segment (which is approximately 12m long in industry practice), is characterised by means of a non-homogeneous Poisson process (NHPP) (Valor et al., 2007; Kuniewski et al., 2009; Zhang and Zhou, 2014; Shafiee et al., 2015). The defect initiation times are assumed to be produced in a non-uniform way. The total number of defects, $S(t)$, generated over the whole pipeline lifecycle (where $t=0$ is the time of installation of the pipe), follows a Poisson distribution with a probability mass function:

$$f_p(S(t)|\Lambda(t)) = \frac{(\Lambda(t))^{S(t)} e^{-\Lambda(t)}}{S(t)!} \quad (t > 0) \quad (3.1)$$

where $S(t)$ is the total number of defects generated within the time interval $[0, t]$; $\Lambda(t) = \int_0^t \lambda_A(\tau) d\tau = \int_0^t \lambda_0 \tau^\delta d\tau$ represents the expected number of defects generated over the same time interval and $\lambda_A(\tau)$ is the assumed intensity factor corresponding to the pipe segment. It is assumed that $\Lambda(t) = \int_0^t \lambda_0 \tau^\delta d\tau$ where λ_0 and δ are positive quantities that can be determined based on inspection data and/or expert judgement. Considering s generated defects on the pipe segment up to time T , the initiation times of the s defects are denoted by $t_{01}, t_{02}, \dots, t_{0s}$ ($t_{01} \leq t_{02} \leq \dots \leq t_{0s} \leq T$). The joint probability density function (PDF) of $(t_{01}, t_{02}, \dots, t_{0s})$ condition on $S(t) = s$ can be expressed as:

$$f_{t_{01}, \dots, t_{0s} | S(t)}(t_1, \dots, t_s | s) = \frac{s! \prod_{i=1}^s \lambda_A(t_i)}{[\Lambda(t)]^s} \quad (0 < t_1 < t_2 < \dots < t_s \leq T) \quad (3.2)$$

The joint probability density function (PDF) of the initiation times for HPP, conditional on $S(t)=s$ is the same as the joint PDF of the order statistics of samples of $(Y_{A1}, Y_{A2}, \dots, Y_{As})$ where $Y_{A1}, Y_{A2}, \dots, Y_{As}$ are s independent and identically distributed (iid) random variables that are uniformly distributed over $[0, T]$. This conclusion for HPP can be generalised to NHPP, i.e. $Y_{A1}, Y_{A2}, \dots, Y_{As}$ are iid random variables with the distribution (Kulkarni, 2009):

$$P(Y_{A_i} \leq t) = \frac{\Lambda(t)}{\Lambda(T)}, \quad (0 \leq t \leq T) \quad (3.3)$$

It must be noted that, in literature, metal loss corrosion defects are not thought to initiate immediately after the pipeline commissioning time (Peabody, 2001; Velázquez et al., 2009). Instead, initiation time is considered to be directly linked to the total elapsed time from the installation of the pipeline until coating damage occurs, plus the time cathodic protection can provide some level of corrosion prevention, after coating damage. In the study of Velázquez et al. (2009), corrosion field data for buried steel pipelines, indicated different corrosion initiation times depending on the soil conditions, within a range of 2.57 to 3.06 years. To account for this fact in the NHPP model, the initiation time of the first defect t_{01} is selected from a uniform distribution with a lower bound of 2.57 and an upper bound equal to 3.06.

3.2.2 Stochastic Growth of Defects

For buried pipelines, a very comprehensive model in literature is the empirical power law model proposed in Velázquez et al. (2009). This model is based on actual corrosion data from buried energy pipelines that were collected over a period of three years at 250 locations. The model takes into account the corrosion initiation times t_{i0} of the n defects and several properties of the soil that surrounds the pipes. For given values of the parameters k_{Ai} , a_i and t_{i0} , the defect depth at time t is null if $t \leq t_{i0}$, otherwise it is given by

$$d_i(t) = k_{Ai}(t - t_{i0})^{a_i} \quad (3.4)$$

The parameters k_A and a are random variables which can be evaluated from soil properties (Velázquez et al. 2009; Gomes et al. 2013). The distributions adopted herein for k_A and a were selected from a Monte Carlo study conducted by Gomes et al. (2013). The samples were derived from the actual data in the study of Velázquez et al. (2009), by adopting all soil categories. The maximum likelihood function produced each parameter distribution and characteristic value, as presented in Table 3.1. The defect growth model of Eq. (3.4) is a parameterized stochastic process, as it is a function of (two) random variables. This model is thought to be one of the most exhaustive among available empirical models in literature for buried energy pipelines and therefore can provide realistic values of defect depths. This model can be easily calibrated to actual corrosion data or updated by means of Bayesian updating, based on a number of available methods in literature (Bazán and Beck,

2013; Zhang and Zhou, 2013; Qin et al., 2015). However, the updating of actual corrosion data is outside the scope of this chapter and it is dealt with in Chapter 5 of this thesis.

An alternative method for metal-loss corrosion growth modelling is to adopt a stochastic process that accounts for the temporal uncertainty of the defect growth over time. In that respect, a Poisson square wave process (PSWP) is additionally employed in this chapter (Bazán and Beck, 2013). In the PSWP model, the sample paths of deterioration are continuous in time and thus so are the growth of the defects, which is overall a realistic account of metal-loss corrosion (Bazán and Beck, 2013). The proportionality factors k_{Ai} of Eq. (3.4) are characterized by a PSWP with pulse heights (U_{jA}) and durations ($t_{b, jA} = t_{jA+1} - t_{jA}$), which are random variables, as illustrated in Fig. 3.1 (Bazán and Beck, 2013). Pulse durations are adopted as exponential random variables with parameter λ that denotes the mean occurrence rate per unit time (or Poisson rate). The number of pulses Z_A , within a given period of time of ΔT follows a Poisson distribution with a probability mass function:

$$U(Z_A = z_A | \lambda) = (\lambda \Delta T)^{z_A} \exp(-\lambda \Delta T) / z_A! \quad (3.5)$$

with z_A factorial in the denominator.

The magnitudes of different pulses U , are independent and identically distributed random variables and assumed to follow a truncated T-location-scale distribution with distribution parameters μ_{kAi} , σ_{kAi} and ν_{kAi} . Finally, the exponent factors a_i are assumed to follow an Inverse Gaussian distribution with parameters μ_{ai} and λ_{ai} . For each pulse of the proportionality factor k_{Ai} of the defect size in Eq. (3.4), the increment in defect size is as follows:

$$d_i(t_{jA+1}) = d_i(t_{jA}) + U_{jA} [(t_{jA+1} - t_{i0})^{a_i} - (t_{jA} - t_{i0})^{a_i}] \text{ for } j_A = 0, 1, \dots, Z_A \quad (3.6)$$

where Z_A is the number of pulses within a given sample and a_i is a realization of the exponent factor for the i th defect. Fig. 3.2 presents one random realization of defect size sample paths, in comparison to one random realization of the time-independent empirical power law of Eq. (3.4) for the same random defect. The parameters (μ_{kA} , σ_{kAi} , ν_{kAi}) and (μ_a , λ_a) of the random variables k_A and a were assumed to have the values of Table 3.1.

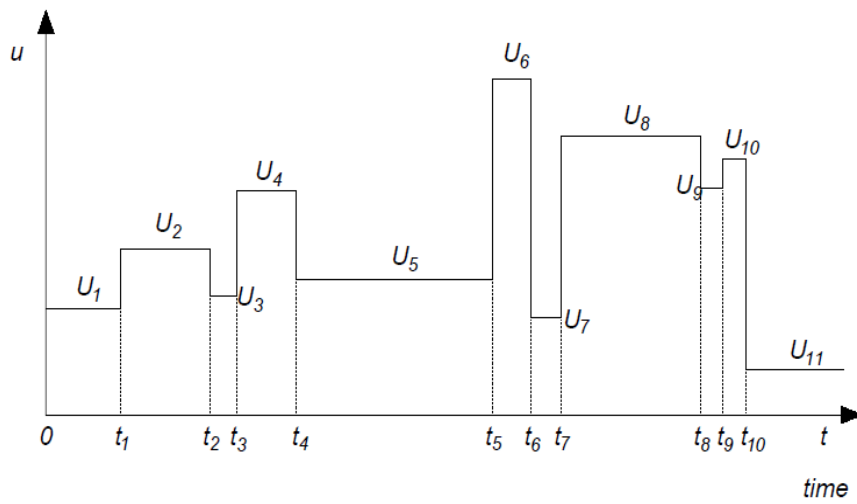


Figure 3.1 Poisson Square Wave Process model

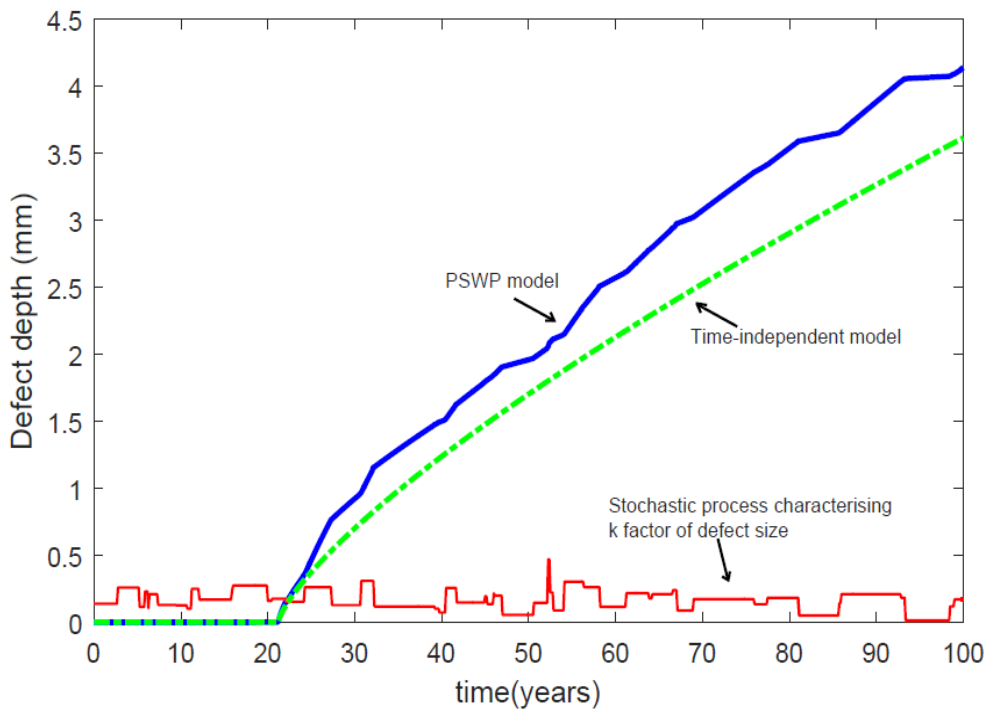


Figure 3.2 Illustration of stochastic Poisson Square Wave Process and time-independent power law defect growth models for a pipeline of 7.09mm wall thickness

Table 3.1 Input parameters for the models for defect depth

Model	Variable	Probability distribution	Parameters	Source
Defect depth	k_A	truncated T-location-scale	Location: $\mu_{k_A}=0.168\text{mm/y}$ Scale: $\sigma_{k_A}=0.063$ Shape: $\nu_{k_A}=4.780$	Gomes et al. (2013)
	a	Inverse Gaussian	Mean: $\mu_a=0.762$ Shape: $\lambda_a=27.016$	
Defect density	η	Deterministic	$\eta=0.321$ def/m for 17 years old pipeline	Valor et al. (2014)

Consistent with the typical assumption in industry practice, the length of the defect is assumed to appear on the pipe, at each defect's initiation time t_{i0} , as a patch with a length and width, due to coating damage. The different defect lengths are assumed to remain unchanged over time and to follow a predefined probability distribution (Stephens and Nessim, 2006; Zhang and Zhou, 2014).

3.2.3 Time-dependent Internal Pressure Model

Many past studies with respect to reliability of high-pressure energy pipelines with active corrosion defects, employed either deterministic or time-independent random variable models for the internal pressure (Hong, 1999; Stephens and Nessim, 2006; Valor et al., 2013, Valor et al., 2014). In practice, pipeline internal pressure fluctuates randomly with time, due to changing operating conditions. Therefore, it is considered realistic to assume internal pressure to be a stochastic process-based load model that varies with time. The reason is that a random variable load would have to represent the maximum loading for the period considered, in order to be consistent with extreme value and structural reliability theories (Melchers, 2004). This type of random variable load models is not considered adequate for problems where resistance is reduced over time, as is due to corrosion herein (Bazán and Beck, 2013). Instead, random periodic fluctuations for the pipeline pressure should be considered, so that it is represented as a continuous process. Thus, combining random periodic extremes with resistance degradation due to corrosion is a reasonable depiction of reality, given that corrosion develops gradually with time. Therefore, in this chapter, sophisticated models are proposed, namely a simple but realistic discrete

stochastic Ferry-Borges process (Melchers, 2004; Zhou, 2010) and a Poisson Square Wave Process (PSWP) (Zhang and Zhou, 2013). Indicative illustrations of both Ferry-Borges and PSWP are presented in Fig. 3.1 and 3.3. The difference of the PSWP application for internal pressure is that unlike the defect growth modelling, there is no need for a strictly positive random variable distribution for pulse heights. In fact, for internal pressure P_{Sop} the magnitudes of different pulses P_A are independent and identically distributed random variables characterized by a PDF of $f_{P_A}(p_A)$. It is assumed that the magnitude of P_A at a given time follows a Gumbel distribution with distribution parameters α_{p_A} and μ_{p_A} , i.e.

$$f_p(p_A | \alpha_{p_A}, \mu_{p_A}) = \alpha_{p_A} \exp\left(-\alpha_{p_A}(p_A - \mu_{p_A})\right) \exp\left(-\exp\left(-\alpha_{p_A}(p_A - \mu_{p_A})\right)\right) \quad (3.7)$$

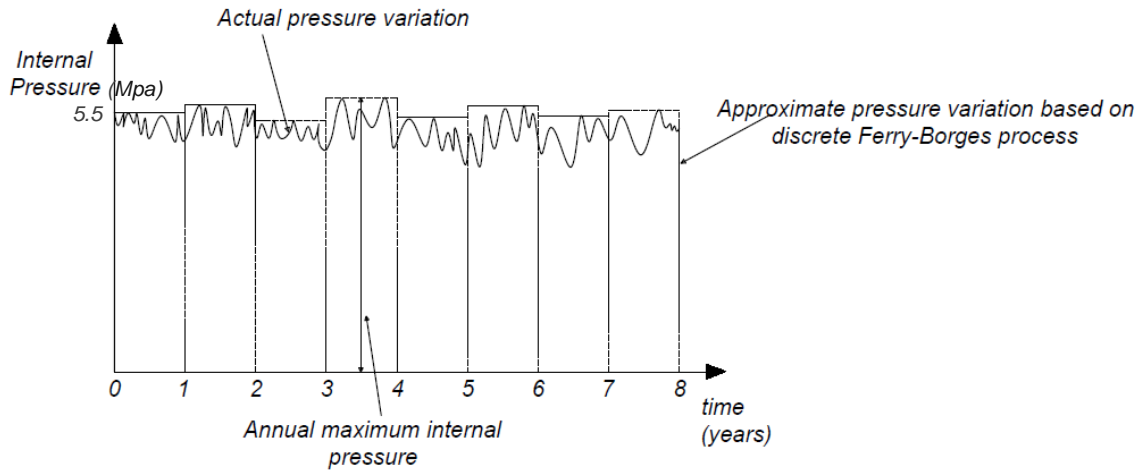


Figure 3.3 Stochastic Ferry-Borges model for internal pressure of gas pipelines with a maximum annual value of 5.5 MPa

3.2.4 Time-dependent Reliability Evaluation for Pipe Segment with Multiple Defects

A corroding gas pipeline that is under internal pressure and contains multiple defects can fail due to three distinct failure modes, namely small leak, large leak and rupture (Zhou, 2010). Small leak is the consequence of a defect penetrating the pipe wall. Large leak and rupture, are together grouped as pipe burst and differ only by the occurrence or not, of an unstable axial propagation of the through wall defect, resulting from plastic collapse of the pipe wall, due to internal pressure at the defect. The reliability assessments in this study were implemented using the pipeline corrosion failure criterion (PCORRC) model to calculate the failure pressure of defects (Leis and Stephens, 1997).

$$P_{S_{f_i}} = 1.33 \frac{2 UTS w_t}{D} \left[1 - \frac{d_i}{w_t} (1 - \exp\left(\frac{-0.157 L_i}{\sqrt{\frac{D(w_t - d_i)}{2}}}\right)) \right] \quad (3.8)$$

where D is the pipe's diameter, w_t is the wall thickness, UTS is the pipe's material ultimate tensile strength and the number 1.33 at the start of the P_f expression is the PCORRC model error factor (Fu et al., 2000; Valor et al., 2014).

The rupture pressure is calculated according to the model developed by Kiefner et al. (1989), as follows:

$$P_{S_R} = \frac{2 UTS w_t}{D M} \quad (3.9a)$$

$$M = \begin{cases} \left[1 + \frac{0.6275 L^2}{D w_t} - 0.003375 \left(\frac{L^2}{D w_t} \right)^2 \right]^{1/2} & L \leq \sqrt{20 D w_t} \\ 3.3 + 0.032 \frac{L^2}{D w_t} & L > \sqrt{20 D w_t} \end{cases} \quad (3.9b)$$

where M is the Folias bulging factor.

Next, a Monte Carlo (MC) framework can be implemented for the estimation of the failure probability (Tee et al, 2014). In each MC step, a vector of the random variables, which are associated with the i th defect and are contained in Eq. (3.8)-(3.9), are randomly generated from their corresponding distributions. Then $P_{S_{f_i}}$ and P_{S_R} are compared with the operating pressure $P_{S_{op}}$, which is also randomly generated based on a Ferry-Borges process realization. If a defect depth is equal or larger than the pipe's wall thickness ($d_i \geq w_t$) then a new failure pressure P_{S_f} is calculated by substituting the defect depth with a delimited value $d_i = 0.0009 w_t$. Then, if $P_{S_{f_i}} \geq P_{S_{op}}$ a small leak is counted. Otherwise, it is examined if $P_{S_{f_i}} > P_{S_R}$ and if it is true, a large leak is considered and if not, a rupture instead. When $d_i < w_t$, the same procedure is followed.

The number of ruptures, for instance, divided by the total number N_{stp} of Monte Carlo steps, constitute an unbiased estimator of the probability of rupture $\Pr(F_{3i})$. For each of the s defects, the above method is repeated N_{stp} times. Therefore, the process is repeated $s \cdot N_{stp}$ in total. It is also repeated for several future times within a set of time intervals. By the end of computations, the probability of rupture for each of the corrosion defects in the pipeline at each time t is evaluated. Considering the definition of reliability (Melchers, 2004):

$$R_{3_i} = 1 - \Pr(F_{3_i}) \quad (3.10)$$

and under the assumption that corrosion defects are independent, an upper bound of the probability of rupture of the pipe segment can be obtained:

$$\Pr(F_3) = 1 - \prod_i [1 - \Pr(F_{3_i})] \quad (3.11)$$

or equivalently of the reliability of the pipe segment against rupture:

$$R_3 = 1 - \Pr(F_3) \quad (3.12)$$

Based on the study of Zhou (2010), the assumption of independent multiple corrosion defect growth rates leads to higher probabilities of failure and thus more conservative results, which is the desired for long term probability of failure predictions, if one considers the detrimental effect of failures of gas transmission pipelines, from the public health perspective.

3.3 Maintenance Plan for the 1st Case Study based on In-line Inspections

An ILI inspection and repair program is implemented on a reference pipe segment based on ASME B31.8S (ASME, 2012), for a considered service life. It is considered that various inspection and maintenance actions take place on pipe segments within a pipeline network during their lifetimes and therefore their overall reliability is consistently maintained within a certain acceptable range. This range varies depending on operators' decision making and the individual maintenance plans. This study assumes that the reference segment's overall reliability is consistent with the implicit reliability considered in ASME B31.8S (Nessim et al., 2009). For the reliability prediction of the reference segment, inspections and subsequent repairs are assumed based on high resolution ILI tools. The repair criteria prescribed in the code of practice in ASME B31.8S are based on the maximum defect depth and the estimated failure pressure at the defect. The proposed inspection intervals are dependent of the pipelines' class location and the second repair criterion (burst pressure at the defect). The above-described prescriptions are summarized in Table 3.2.

Table 3.2 Inspection and repair criteria based on ASME B31.8S

Class	1 st Inspection Year	Repair criteria	
		Remaining wall thickness (% of nominal) (%)	Failure pressure/MAOP
1	10	50	1.39
2	13	50	1.39

After every inspection, the two repair criteria are examined and the pipe segment is excavated and repaired if one of the following is true (Zhang and Zhou, 2014):

$$y_i^{avg} \geq \xi_A w_{tN} \quad (3.13a)$$

$$P_{S_{f_i}} \leq \eta_A P_{opN} \quad (3.13b)$$

where ξ_A and η_A denote the parameters selected based on the above described repair criteria (ASME, 2012), whilst w_{tN} and $P_{S_{opN}}$ are the nominal values of pipe wall thickness and operating pressure, respectively. What is more, y_i^{avg} refers to the measured average defect depth, obtained from Eq. (3.15a) as defined next in Section 3.3.1 and $P_{S_{f_i}}$ to the estimated failure pressure. The latter is estimated by Eq. (3.8), by setting the nominal values of wall thickness and pipe diameter (w_{tN} and D_N) and also the values from Eq. (3.15) for each defect's average depth and length. It should be noted that in Eqs. (3.15a) and (3.15b), the average values from the total number N_{stp} of iterations in the Monte Carlo simulation are used to characterise the defect depths and lengths, for each individual defect.

The repair actions on an excavated pipe segment first involve completely removing the existing coating of the segment. Plain recoating or recoating plus sleeving is applied on the segment, based on the severity of the defects. Regardless of the specific repair action, the segment is considered to be fully restored to pristine condition. This is a realistic assumption, considering that sleeving offers at least a new pipe's resistance capacity, whilst recoating mitigates the existing defects. The likelihood of a repair being of poor quality is considered very low in industry practice and therefore ignored in this study (Zhang and Zhou, 2014).

3.3.1 Uncertainties of ILI Tools

The ability of inspection equipment to locate and size an actual metal-loss corrosion defect is also taken into consideration (Gomes et al, 2013). The probability of detection (PoD) of a defect by a high resolution ILI tool, usually depends on the defect size d_i and the inherent ability of the tools based on their specifications. The PoD adopted in this chapter is of the following exponential form:

$$PoD = 1 - e^{-q d_i} \quad (3.14)$$

where q is a constant that defines the inherent tool detection capability according to vendor specifications (Stephens and Nessim, 2006). Once a defect is detected, then it is assumed that an imperfect measure of its depth and length is obtained. The measured depths and lengths by the ILI tool, y_i and L_{Mi} respectively, are estimated based on the following equations:

$$y_i = c_1 + c_2 d_i + \varepsilon_i \quad (3.15a)$$

$$L_{Mi} = c_{l1} + c_{l2} L_i + \varepsilon_{li} \quad (3.15b)$$

where c_1 (c_{l1}) and c_2 (c_{l2}) are the biases of the ILI tool and are assumed to be deterministic quantities, whilst ε and ε_i are random scattering errors, corresponding to the measured depths and lengths. The latter are assumed to follow a predefined normal distribution, typically with zero mean and known standard deviations, quantified from tool specifications (Zhang and Zhou, 2014).

3.3.2 Effect of Maintenance on Pipe Segment Reliability

The reliability of the pipe segment, derived from Eq. (3.12), is expected to decrease monotonically in time, due to the degradation of the pipeline. Following a repair, the segment reliability is updated, by being restored to its original value at the time of each repair. Thus, it can be described as follows (Okasha and Frangopol, 2010; Barone and Frangopol, 2014):

$$R_{sc}(t_{y_A}) = R_3(t_{y_A} - T_{v_A}) \quad T_{v_A} \leq t_{y_A} < T_{v_{A+1}} \quad (3.16)$$

under the condition that the segment survives (does not fail) up to time T of each repair.

The overall segment reliability, which is equivalent to the segment survival function, considers the survival probability of the segment up to time T_m of regular maintenance intervals and is formulated as:

$$R_s(t_{y_A}) = R_3(t_{y_A} - v_A \cdot T_{v_A}) \cdot R_3(T_m)^{y_A} \quad y_A \cdot T_m \leq t_{y_A} < (y_A + 1) \cdot T_m \quad (3.17)$$

Implicit in the above, is that the overall reliability (survival function) R_s cannot increase throughout the life service, as opposed to the conditional reliability R_{sc} , which is also referred to as availability in literature (Klaassen and Van Peppen, 1989).

3.4 Maintenance Plan for the 2nd Case Study based on ECDA

3.4.1 Pipeline System Reliability Prediction based on SSA

A realistic ECDA maintenance strategy is considered herein that is consistent with industry practice. Initially, the previously-described methodology for reliability prediction regarding a single pipe segment is further incorporated in a methodology that evaluates the overall reliability for a multiple-segment pipeline system. This can be realised by employing the SSA model. The latter models the system reliability with multiple PM actions at the segment level and allows the changes of system reliability due to imperfect repairs to be accurately calculated. Thus, it removes the assumptions regarding the reliability of different states of the system, after the repairs take place (Guo et al., 2013). When a pipeline system is preventively repaired, it is industry-consistent to assume that only part of it is being repaired, due to the human and financial constraints. This method directly links the SRA model with long-term PM decision-making, so that the decision can be updated using the latest inspection information. Fig. 3.4 provides an illustration of the reliability updating based on inspection information (Frangopol and Soliman, 2016). Typically, the reliability updating is carried out by employing the Bayes' theorem (Gomes et al., 2013). In this chapter, only the initial maintenance management plan is considered, before any inspection or repair action actually takes place. Therefore, the information derived from inspections is not known in advance and the probabilistic updating is conducted through the SSA, since it can accurately estimate post-repair reliability changes.

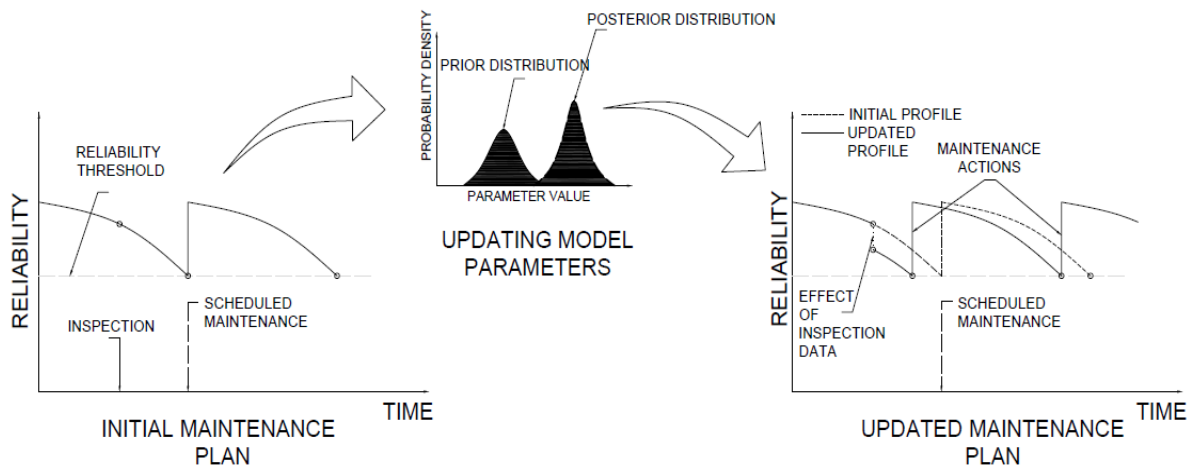


Figure 3.4 Reliability updating based on inspection information

A reliability-based preventive maintenance (RBPM) strategy is adopted and whenever the system reliability falls to a predefined threshold, one pipe segment will be directly excavated and assessed. The selection of the adequate pipe segment for repair each time, can be based on relevant inspection data or expert judgement. In practice, the information obtained either from inspection and direct examination can be used to update the parameters involved in the aforementioned analysis. In other words the defect generation and growth models. The updating based on ECDA of unpiggable pipelines is outside the scope of this thesis. It has been covered in previous studies though, to which the interested reader is referred to (Van Os, 2006; Francis et al., 2006; Francis et al., 2009; Van Burgel et al., 2011; Caleyó et al., 2015; Qin et al., 2015).

After the excavation and examination, repair actions take place as per the selected maintenance strategy. The repair actions on the excavated pipe segment first involve completely removing the existing coating of the segment. Depending on the severity of the condition, recoating or recoating plus sleeving may be applied on the segment. A simple recoating arrests the growth of all the existing defects on the pipe segment, whilst sleeving covers the portion of the segment that contains the critical defect(s). Critical defect(s) can be characterised by the expert judgment of operators. A repaired pipe segment, regardless of the specific repair action is considered to be fully restored to pristine condition. This is a realistic assumption since sleeving offers at least the same resistance capacity as a new pipe segment, whilst recoating mitigates the existing defects. Given that maintenance costs

are not taken into consideration in this methodology, the specific repair action is not of interest and thus specific repair criteria for the different defects are not defined.

According to Sun et al. (2014), industrial practice typically adopts time-based preventive (inspection and) maintenance (TBPM) when it comes to linear assets, like pipeline systems. However, RBPM has also been widely applied and plus it can be useful as a supplementary strategy to compare with a TBPM strategy. When RBPM is applied, some segments of the pipeline system are repaired and this happens whenever the reliability of the entire system falls to a predefined reliability threshold. However, pipe segments scheduled for PM may or may not survive until their individual PM times. The survival probability of a pipeline system, under the condition that its segments have been preventively maintained successfully, is termed as conditional probability. On the other hand, the survival probability of the system that considers the survival probabilities of the individual segments until their scheduled PM times is termed as overall reliability of the system (Guo et al., 2013; Sun et al., 2014). The conditional reliability is more useful for the determination of dynamic PM intervals since it describes the reliability changes between two successive PM actions, while the overall reliability illustrates the reliability changes over the entire lifetime of the system, which typically covers a large number of PM intervals. Thus, it can form a pivotal role in the evaluation of maintenance strategies.

Let $R_s(t)_m$ and $R_{sc}(t)_m$ denote the overall reliability and the conditional reliability of a pipeline after the m^{th} PM action, respectively. As the pipeline is a linear system with serially connected segments, it can be divided into a number of segments. According to Ebeling (1997) and Lewis (1996), the overall reliability and the conditional reliability of the pipeline are linked through the following equation:

$$R_s(t)_m = \prod_{k_c=0}^m R(T_{k_c} - T_{j_c})_{j_c} R_{sc}(t)_m, \quad (3.18)$$

$(0 \leq \tau < (T_{m+1} - T_m), \text{ for } m = 0, 1, 2, \dots, M - 1 \text{ and } 0 \leq \tau < (T_{M_T} - T_M) \text{ when } m = M)$

where M is the number of PM actions during a given decision horizon T_{M_T} and T_m is the m^{th} PM time ($m = 0, 1, 2, \dots, M$). If repair times are assumed negligible, then T_m is also the pipeline operation initiation time after the m^{th} PM action. The value $R(T_m - T_{j_c})_{j_c}$ is the reliability of the preventively repaired segment just before the m^{th} PM action, provided it has been maintained at the j_c^{th} PM action ($0 < j_c < m$). When $m = 0$, $\prod_{k_c=0}^m R(T_{k_c} - T_{k_c-1})_{k_c}$ is set equal to one.

Fig. 3.5 indicates that after an imperfect repair, when only one segment is repaired, the conditional reliability of the system after this PM can be improved but remains lower than the original reliability. What is more, R_{th} is the predefined reliability threshold for the entire pipeline, $R_{sc}(\tau)_m$ is the conditional reliability after the m^{th} PM action in terms of the relative timescale τ , which will be reset to zero after each PM action. Age t is an absolute timescale ranging from 0 to infinity. The relationship between the relative and the absolute timescale is given by

$$\tau = t - T_m \quad (3.19)$$

$$(0 \leq \tau < (T_{m+1} - T_m) \text{ for } m = 0, 1, 2, \dots, M - 1 \text{ and } 0 \leq \tau < (T_{M_T} - T_M) \text{ when } m = M)$$

To calculate the overall reliability according to Eq. (3.18), the conditional reliability should be estimated first. In achieving so, the approach assumes the following (Sun et al., 2007):

- 1) A system with L_C segments is assumed to have l_c ($l_c \leq L_C$) vulnerable segments which are repaired through PM. All l_c repaired components and the unrepaired part of the system (subsystem) are serially connected. Segments are numbered according to their sequence in receiving first repair during the M PM cycles, so that $l_c \leq M$.
- 2) The failures of the repaired segments are independent of the unrepaired segments. That is, when a segment is repaired, the failure distribution of the unrepaired subsystem does not change and the conditions of the subsystem do not affect the reliability characteristics of the repaired segments.
- 3) Repair times are very small compared to the overall pipeline lifetime and can be considered negligible.

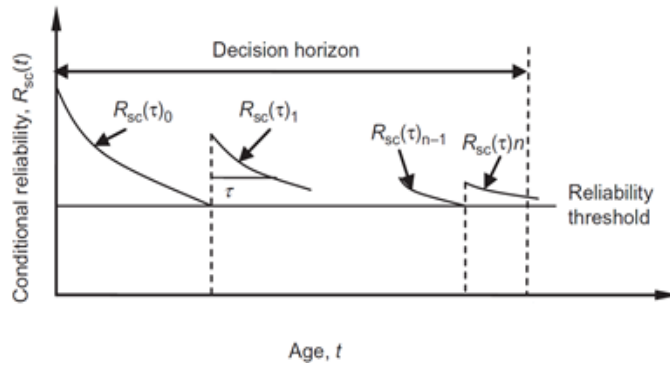


Figure 3.5 Example of conditional reliability of a pipeline system with multiple imperfect repairs

In Fig. 3.6, $R_{rs}(\tau)_{k_c}$, ($k_c=1,2,\dots,l_c$) are the reliability values of the repaired segments. $R_{sb}(\tau)_{k_c}$ and $R_s(\tau)_{k_c}$ are the reliability values of the subsystem that remains unrepaired and of the overall system after the k_c th PM cycle, respectively. After the 1st PM action, the reliability of the system changes (conditional reliability of the system), along with the segment's that was preventively maintained ($R_1(\tau)_1$). In other words, the conditional reliability of the system describes the reliability changes between two PM actions. The conditional reliability of the system $R_{sc}(\tau)_1$ is given by:

$$R_{sc}(\tau)_1 = \frac{R_1(\tau)_1 R_s(\tau + \Delta t_1)_0}{R_1(\tau + \Delta t_1)_0} \quad (3.20)$$

Eq. (3.20) is derived from two other equations:

$$R_{sc}(\tau)_0 = R_s(\tau)_0 \quad (3.21)$$

which means that the initial conditional reliability function of the pipeline is equal to its original overall reliability function and

$$R_{sc}(\tau)_m = R_1(\tau)_m \cdot R_{sb}(\tau)_m \quad (3.22)$$

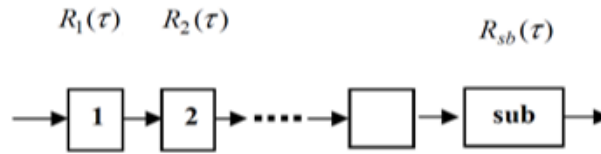


Figure 3.6 Example of multi-component series system

In Eq. (3.20), $\frac{R_1(\Delta t_1)_0 R_1(\tau)_1}{R_1(\tau + \Delta t_1)_0}$ and $R_1(\tau)_1$ are reliability of the subsystem and segment one respectively, after the first PM action. Eq. (3.20) does not include the failure probability of segment 1 before the PM action. Therefore, it represents the conditional reliability of the system only. The reliability of the system considering the first PM action is:

$$R_s(\tau)_1 = R_1(\Delta t_1)_0 R_{sc}(\tau)_1 = \frac{R_1(\Delta t_1)_0 R_1(\tau)_1}{R_1(\tau + \Delta t_1)_0} R_s(\tau + \Delta t_1)_0 \quad (3.23)$$

where $R_s(\tau)_1$ is the reliability of the system after the first PM action. $R_1(\Delta t_1)_0$ is the probability of survival of the first segment up to time one.

The conditional reliability changes in a saw tooth form, whereas the reliability of the system decreases monotonically. From Eq. (3.23), it can be observed that for the system reliability to improve, i.e. to let $R_s(\tau)_1 > R_1(\Delta t_1)_0$, the following inequality must hold:

$$\frac{R_1(\Delta t_1)_0 R_1(\tau)_1}{R_1(\tau + \Delta t_1)_0} > 1 \quad (3.24)$$

After time Δt_2 , the conditional reliability of the system falls to the predefined minimum level of reliability R_{th} and then a second PM action is required. In this PM action, either the same segment (i.e. segment one) or a different one (defined as segment two according to the numbering rule) are preventively maintained. If segment one is maintained again, the conditional reliability of the system is:

$$R_{sc}(\tau)_2 = \frac{R_1(\tau)_2 R_s(\tau + \sum_{m=1}^2 \Delta t_m)_0}{R_1(\tau + \sum_{m=1}^2 \Delta t_m)_0} \quad (3.25)$$

The reliability of the system is subsequently given by:

$$R_s(\tau)_2 = \prod_{m=0}^1 R_1(\Delta t_{m+1})_m R_{sc}(\tau)_2 \quad (3.26)$$

If segment two is maintained, the conditional reliability of the system becomes:

$$R_{sc}(\tau)_2 = \frac{R_2(\tau)_2 R_1(\tau + \Delta t_2)_1 R_s(\tau + \sum_{m=1}^2 \Delta t_m)_0}{R_2(\tau + \sum_{m=1}^2 \Delta t_m)_0 R_1(\tau + \sum_{m=1}^2 \Delta t_m)_0} \quad (3.27)$$

The overall reliability of the system is:

$$R_s(\tau)_2 = R_2(\sum_{m=1}^2 \Delta t_m)_0 R_1(\Delta t_1)_0 R_{sc}(\tau)_2 \quad (3.28)$$

The conditional reliability of a system after the m th PM cycle is given by

$$R_{sc}(\tau)_m = \frac{R_s[\tau + \sum_{k_c=1}^m (T_{k_c} - T_{k_c-1})]_0 \prod_{u_A=1}^{M_p} R_{u_A}[\tau + \sum_{k_c=l_u+1}^m (T_{k_c} - T_{k_c-1})]_{l_u}}{\prod_{u_A=1}^{M_p} R_{u_A}[\tau + \sum_{k_c=1}^m (T_{k_c} - T_{k_c-1})]_0} \quad (3.29)$$

$(0 \leq \tau < (T_{m+1} - T_m), \text{ for } m = 0, 1, 2, \dots, M-1 \text{ and } 0 \leq \tau < (T_{M_T} - T_M) \text{ when } m = M)$

where l_u indicates that the last PM of segment u_A ($u_A \leq M_p$) is carried out in the l_u th PM action ($l_u \leq m$ and $m=1,2,\dots,M$), $\sum_{k_c=l_u+1}^m (T_{k_c} - T_{k_c-1}) = 0$ when $l_u+1 > m$ and $\sum_{k_c=1}^m (T_{k_c} - T_{k_c-1}) = 0$. The system reliability can be calculated by using a heuristic

methodology as the one implemented next in the numerical application of the 2nd case study.

3.4.2 Linear Approximations

The evaluation of the reliability function of a single pipe segment is conducted by means of Monte Carlo sampling. Each sample is defined by one realization of each random variable at the initial time of the analysis and then at the next discrete points dt , as the corrosion process evolves, until the end of the lifetime considered. After the computations are performed at dt , linear approximations can be employed to bridge the time intervals among the reliability values of the discrete time points. This can be achieved by considering that among discrete time point values, the reliability decreases in a linear manner. That is, to avoid discretization error when estimating the exact time the reliability falls to a predefined reliability control limit R_{th} , when applying the RBPM strategy, as in the following numerical application of this chapter for the ECDA-based 2nd case study. Fig. 3.7 provides a schematic representation of the linear approximation.

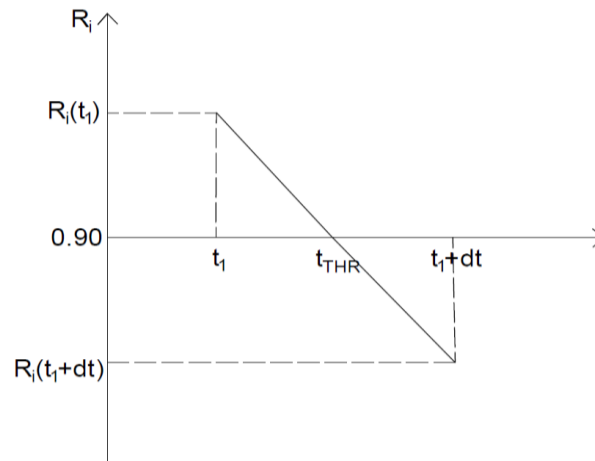


Figure 3.7 Linear approximations to determine the exact time of reliability falling to 0.9

3.5 Numerical Application for the 1st Case Study based on In-line Inspections

An application of the approach presented in Sections 3.2 and 3.3 is illustrated in the following. The analysis is segment-based and is applied on a reference segment. The proposed SRA methodology estimates failure probabilities due to external metal-loss

corrosion. Therefore, reported rupture incidents due to external metal-loss corrosion were gathered for the period 2002-2014 from the PHMSA database and a reference pipeline was built based upon the characteristics of the ruptured pipelines. In specific, the reference segment's random variables D , w_t , UTS , P_{Sop} were defined by mean values equal to the average of the corresponding actual values of the 52 ruptured segments and with suitable corresponding probability distributions and standard deviations from the literature (Zhang and Zhou, 2014; Zhou and Zhang, 2015). It is noted that only external metal-loss corrosion incidents, as opposed to stress corrosion cracking, were taken into account. Moreover, average data from the literature, which are based on extensive field studies on buried onshore energy pipelines, were adopted to characterise the defect density and defect growth rate (Velázquez et al., 2009; Gomes et al., 2013; Valor et al., 2014). All the aforementioned values are summarized in Tables 3.1 and 3.3.

The service life considered for reliability prediction is 100 years. The number of defects on the reference segment is characterised by Eq. (3.1), where λ_o and δ are set to 0.0278 and unity respectively, i.e. $S(t)=0.0139t^2$, so that the expected number of defects over the first 17 years is 0.321 per metre, according to the assumed average defect density herein (Valor, 2014). The initiation time of the first defect is obtained from a uniform distribution with a lower bound of 2.57 and an upper bound equal to 3.06. The growth of each defect is realised by means of the PSWP model defined through Eq. (3.6), by adopting the probabilistic characteristics presented in Table 3.1, as per Section 3.2.2. Average values from literature, are adopted for the characterisation of the defect length; that is assumed to have a mean value of 80mm and a COV of 130% (Nessim and Stephens, 2006; Zhang and Zhou, 2014; Zhou and Zhang, 2015). Finally, the segment diameter (D), wall thickness (w_t) and ultimate tensile strength (UTS) are invariant within the pipe segment.

The ILI measured defect depths and lengths, are assumed to be unbiased and therefore the parameters from Eqs. (3.15a) and (3.15b) are set equal to $c_1=c_{l1} = 0$ and $c_2 = c_{l2} = 1$. The random scattering errors ε_i and ε_{li} are defined as $7.8\% w_t$ and 7.8mm respectively, according to standard tool specifications (Zhou and Zhang, 2015). The PoD associated with the ILI tool is estimated from Eq. (3.14) with $q = 3.262 \text{ (mm}^{-1}\text{)}$, i.e. the PoD is equal to 90% for a defect depth of $10\% w_t$. Out of the 52 external corrosion rupture incidents found in the PHMSA, 43 belong to Class 1 and the rest to Class 2; thus the safety parameters ξ_A and η_A of Eq. (3.13a) and (3.13b) are equal to 0.5 and 1.39 respectively, according to Table 3.2. Since the majority belongs to Class 1 pipelines, the initial

inspection time for the reference pipe segment is assumed to take place at 10 years. Furthermore, an interval of 10 years is also selected for subsequent inspections, based on the repair criteria of Table 3.2. The reliability of the reference pipe segment is evaluated through 10^6 Monte Carlo simulation trials, using MATLAB software.

Table 3.3 Probabilistic characteristics of the random variables

Random variable	Nominal value	Unit	Mean/nominal	COV	Distribution type	Source of probabilistic characteristics
Annual maximum internal pressure, P_{Sop}	5.51	MPa	1.0	3%	Gumbel	Zhou and Zhang (2015)
Diameter, D	493	mm	1.0	0	Deterministic	Zhou and Zhang (2015)
Wall thickness, w_t	7.09	mm	1.0	1.5%	Normal	Zhou and Zhang (2015)
Tensile strength, UTS	434	MPa	1.09	3%	Normal	Zhou and Zhang (2015)
Defect length L	N/A	mm	80	130%	Lognormal	Zhou and Zhang (2015); Zhang and Zhou (2014)

3.5.1 Results and Discussion

The results of the ILI-based SRA methodology are illustrated in Fig. 3.8. In specific, the reliability of the reference pipe segment without the consideration of maintenance activities derived from Eq. (3.12) is presented, along with the conditional reliability and the segment's overall reliability from Eq. (3.16) and (3.17) respectively, both of which account for the maintenance actions. The MC simulation returned one maintenance action at 50 years, in which the segment is fully repaired and restored to pristine condition. As a result, the conditional reliability (availability) is equal to 1 on year 50, whilst the overall reliability (survival function) as expected does not increase, but is nonetheless positively affected by the maintenance action.

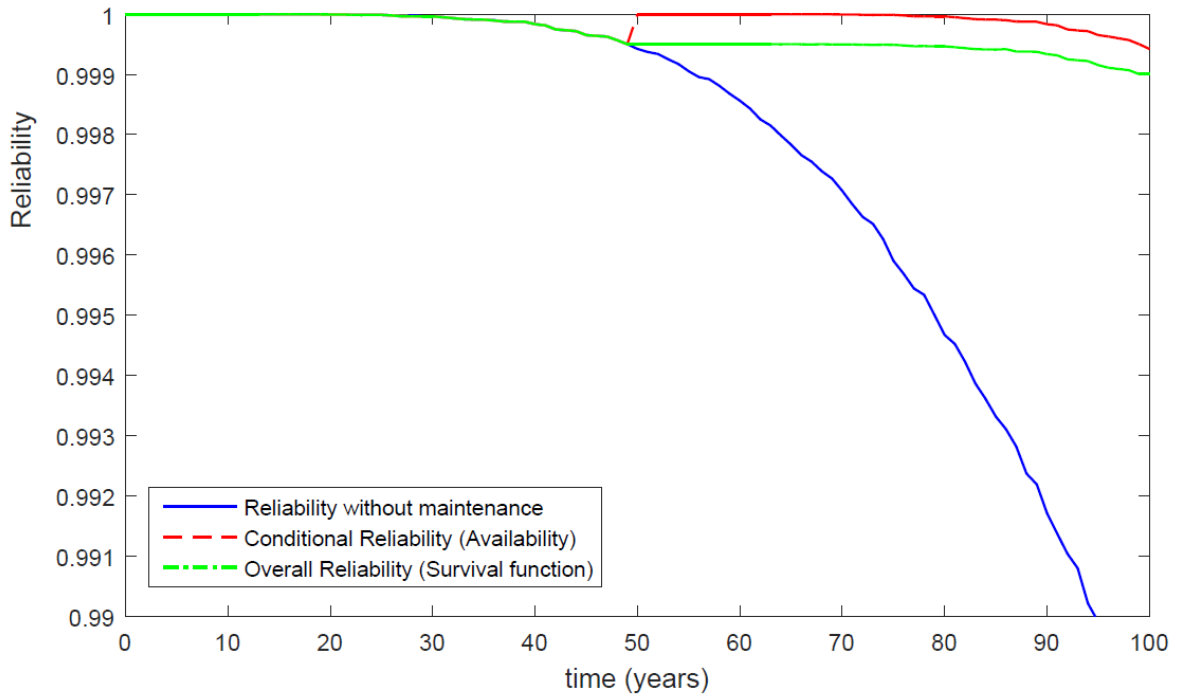


Figure 3.8 Results of the structural reliability approach

The overall reliability result of Fig. 3.8 is compared in the following chapter (Chapter 4) with the result of a statistical methodology applied on the same set of data of PHMSA from 2002 to 2014. The results are discussed in detail in Section 4.5.2.1. It is noted though that the relative values adopted in the above-described SRA methodology to characterise defect density, growth rate and defect length, can generally be subject to further investigation by means of parametric studies. The aim would be to increase proximity with the respective reliability curve from the statistical methodology proposed next in Section 4.3. This can be of great pertinence to operators that wish to determine values of specific defect parameters or other attributes that define risks in existing or new pipelines, based on failure probabilities obtained from significant empirical evidence.

3.6 Numerical Application for the 2nd Case Study based on ECDA

An onshore underground gas transmission pipeline is considered as a case study to illustrate the efficiency of the methodology for the ECDA-based integrity management strategy. The pipeline is assumed to be located in a rural, remote area and to be part of a

line that entails technical challenges that render it unpiggable. Even though it has been in operation since 1995, it is assumed that no maintenance action has been conducted since commissioning. The need to set a long-term integrity management plan based on reliability is identified by operators in order to ensure proper planning of the various resources, whilst ensuring safe performance. If real data from above ground indirect inspections, sampling bell-hole examinations or historical failure data from the region are available, then the defect generation and growth models can be calibrated to these data. However, in this chapter the proposed methodology is illustrated through parametric analyses and actual data are not considered. The data employed are based on reasonable assumptions though, which are supported by empirical findings derived from well-established scientific articles. In specific, average data which are based on extensive field studies regarding buried onshore energy pipelines were adopted (Velázquez et al., 2009; Gomes et al., 2013; Valor et al., 2014), in order to characterise the defect generation rate and defect growth rate. Since average data are used, the proposed methodology is illustrated through parametric analyses, so that the significance and impact of each of the parameters can be further investigated.

The pipeline at the time of installation is assumed to be defect-free. The number of defects and their corresponding initiation times are estimated according to Eqs. (3.1), (3.2) and (3.3). Specifically, δ is assumed to be unity while three values are assumed for λ_o , namely 0.0064, 0.0128, 0.0256. This means that, for $\lambda_o = 0.0064$ for example, Eq. (3.1) results in $S(t) = 0.0064t^2$ and thus, the expected number of defects over the lifetime of 100 years is 64. For all three scenarios of the parametric study, the expected number of defects at 17 years of operation is 0.077, 0.154 and 0.308 per metre. According to a comprehensive field study on buried energy pipelines presented in Valor et al. (2014), the average defect density at 17 years was found to be 0.321 per meter; therefore, the values selected in the parametric study of the present study, do not deviate significantly from real life pipeline conditions. An illustration of NHPP is given in Fig. 3.9, for one realization of the NHPP and one of the expected number of defects, for the assumed λ_o and δ values. The growth of each defect is evaluated based on Eq. (3.4), for their estimated unique initiation times, assuming that the growth rates of the depths are independent and identically distributed with the parameters of Table 3.1. These parameters are based on extensive empirical findings, from well-established studies (Velázquez et al., 2009; Gomes et al., 2013).

The defect length characteristics are presented in Table 3.4. Specifically, the length is assumed to be static and follow a lognormal distribution with a mean of 105 mm and a COV of 130%, while the wall thickness (w_t) and yield strength (σ_y) are assumed to be invariant within the pipe segment. The PCORRC model is adopted to evaluate the capacity of the pipeline against burst (either large leak or rupture). Finally, the internal pressure is assumed to be time-dependent according to a PSWP model, as presented in Section 3.2.3. A parametric analysis is conducted, in order to characterise the generation rate λ of the model. Three values are assumed, namely 0.75, 1.00, and 1.50. The probability distribution of the magnitude of the internal pressure is presented in Table 3.4. The simulated time-dependent internal pressure curves corresponding to $\lambda = 0.75$, $\lambda = 1.00$ and $\lambda = 1.50$ are presented in Fig. 3.10 for a period of 100 years. All the pipeline probabilistic characteristics are summarised in Tables 3.4 and 3.5.

Table 3.4 Probabilistic characteristics of the random variables

Random variable	Nominal value	Unit	Mean/nominal	COV	Distribution type
Annual maximum internal pressure, P_{Sop}	10.34	MPa	1.05	2%	Gumbel
Diameter, D	762	mm	1.0	0	Deterministic
Wall thickness, t	8.96	mm	1.0	1.5%	Normal
Yield strength, σ_y	550	MPa	1.08	3%	Normal
Defect length L	N/A	mm	105	130%	Lognormal

A pipeline system of three identical pipe segments is selected for the implementation of the methodology. The adopted pipe segment characteristics are from the study of Zhang and Zhou (2014). The nominal outside diameter of the pipeline is 762 mm and the operating pressure is 10.34 MPa. The material is made from API 5L Grade X80 steel, with a specified minimum yield and tensile strength of 550 MPa and 625 MPa respectively. Finally, the pipeline has a nominal wall thickness of 8.96 mm. Each segment is 12m long and the reliability of the single segment is estimated based on the limit state function for burst. The Monte Carlo approach provides the calculation of the segment reliability. This corresponds to a single realisation, for one generation of the total number of s defects and 104 iterations of random variable samples. However, in order to achieve more stable results that more accurately depict the reliability prediction, $100 \cdot 10^4$ iterations are chosen.

In other words, 100 generations of s defects are realised, for which 10^4 subsequent MC iterations take place. After applying the MC at each discrete point in time for the lifetime of $T=100$ years, linear approximations are subsequently conducted. The time step is $dt = 0.125$ years, which means the reliability is calculated every 1.5 month and the number of discrete points is 800.

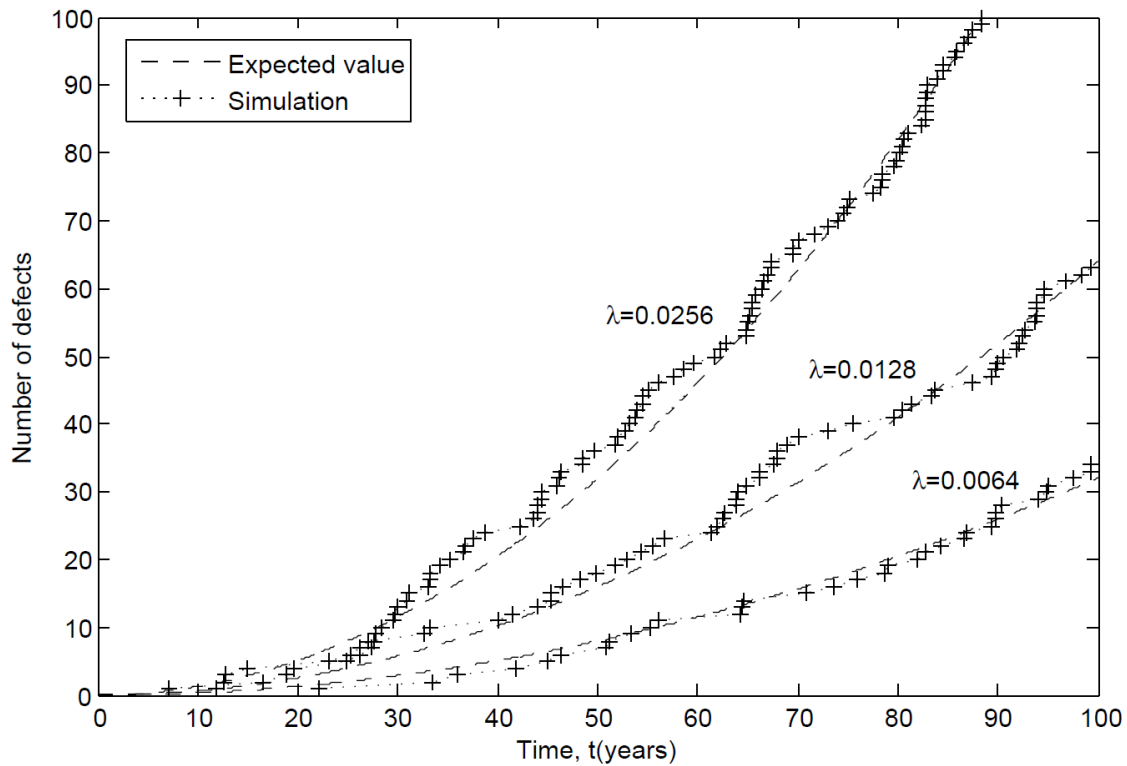


Figure 3.9 Illustration of the NHPP

According to the reliability theory, the original reliability of a series system of three identical and independent segments without PM is $R_s(t) = R_{s_1}(t) \cdot R_{s_2}(t) \cdot R_{s_3}(t)$ (Sun et al, 2007). Subsequently, a PM strategy based on a reliability constraint is employed. This study does not consider the costs associated with the PM or the failure costs and its consequences, but illustrates the maintenance impact only from the safety viewpoint. Therefore, the PM strategy unfolds according to the steps described next. Whenever the system reliability threshold is reached, a direct excavation and examination of one of the three segments takes place, along with the appropriate repair actions, aiming at restoring the specific pipe segment to pristine condition. The proposed maintenance plan, considers no indirect inspections or selected sampling direct examinations at bell-hole locations, but

only 100 percent direct examination and repair of the segment of interest. This is an industry consistent practice, specified at the Standard of NACE International (2010), as part of ECDA methodologies.

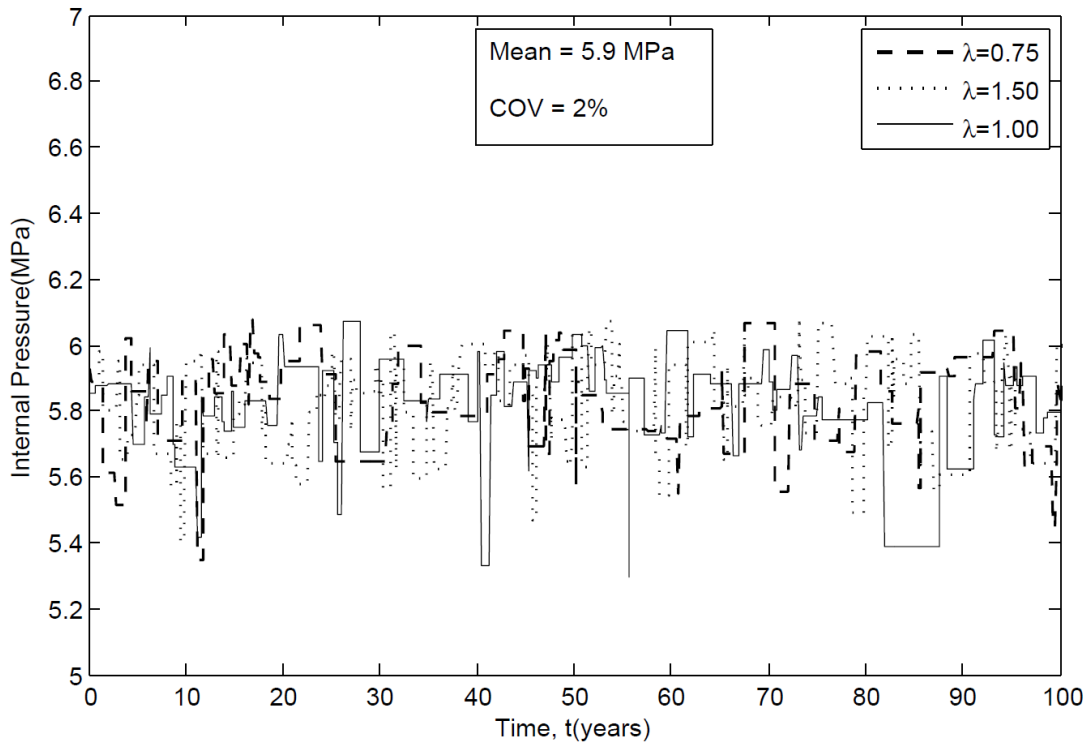


Figure 3.10 Simulated time-dependent internal pressure based on the PSWP model

In this maintenance strategy, the most critical pipe segment is expected to be preventively excavated, assessed and repaired, every time the system reliability reaches the threshold value R_{th} . However, since it is assumed that no prior knowledge regarding the condition of the system exists and the maintenance management plan is the first one to be set by the operators, which can be later updated by inspection and direct assessment information, a sequential PM plan is considered. Three different values are employed, namely 0.90, 0.95 and 0.975, and the impact of the threshold magnitude on the PM strategy is investigated. The reliability threshold is the only decision variable in the RBPM decision making. It is expected that in order to meet a higher reliability requirement, more frequent PM actions are required and in contrast, lowering the reliability threshold will result in the increase of the failure probability.

The parametric analysis conducted in this study, serves to investigate the parameter impact on the conditional and overall system reliability, as well as on the reliability of a single pipe segment. These scenarios are summarized in Table 3.5. It is noted that the parametric study serves as a sensitivity analysis for the parameters summarised in Table 3.5. A more comprehensive sensitivity analysis should also include the parameters of Table 3.4 (i.e. internal pressure P_{sop} , diameter D , wall thickness t , yield strength σ_y , defect length L). This would provide further insight on the impact of all parameters (i.e. random variables of the probabilistic analysis) on the system reliability. The proposed methodology aims to predict the system reliability over a period of 100 years and evaluate the effectiveness of the maintenance strategy. The focus is on the outcome of the proposed segment-based methodology, which can allow accurate reliability predictions in the context of the industry-consistent maintenance strategy. The defect generation and growth models can be calibrated to match real data, if the latter is available (Bazán and Beck, 2013; Valor et al., 2014, Qin et al., 2015). The defect information obtained from the multiple future maintenance actions, can be also used to update the various parameters of the defect generation and growth models. The updated parameters can then be used to re-evaluate the reliability predictions, based on the proposed maintenance strategy.

Table 3.5 Scenarios of the parametric analysis

<i>Scenario</i>	λ_o_NHPP	λ_PSWP	R_{th}
<i>Baseline</i>	0.0128	1.00	0.90
<i>I</i>	0.0256	1.00	0.90
<i>II</i>	0.0064	1.00	0.90
<i>III</i>	0.0128	1.50	0.90
<i>IV</i>	0.0128	0.75	0.90
<i>V</i>	0.0128	1.00	0.95
<i>VI</i>	0.0128	1.00	0.975

3.6.1. Results and Discussions

First, the application of the SRA methodology in conjunction with the SSA is carried out with respect to the baseline scenario of Table 3.5. Fig. 3.11 presents the reliability results based on the aforementioned methodology. This result is afterwards used for the reliability evaluation at the system level, by means of the SSA. In Fig. 3.11, it can be observed that only after the first 30 years, the reliability starts to decrease significantly. This type of result is relevant to integrity management decision making, as it constitutes the initial

indication for preventive inspection and repair strategies. In specific, the first inspection time can be determined for a risk optimization analysis that takes into consideration costs and reliability. In any case, Fig. 3.11 indicates that the first inspection should take place at sometime between 30 and 45 years.

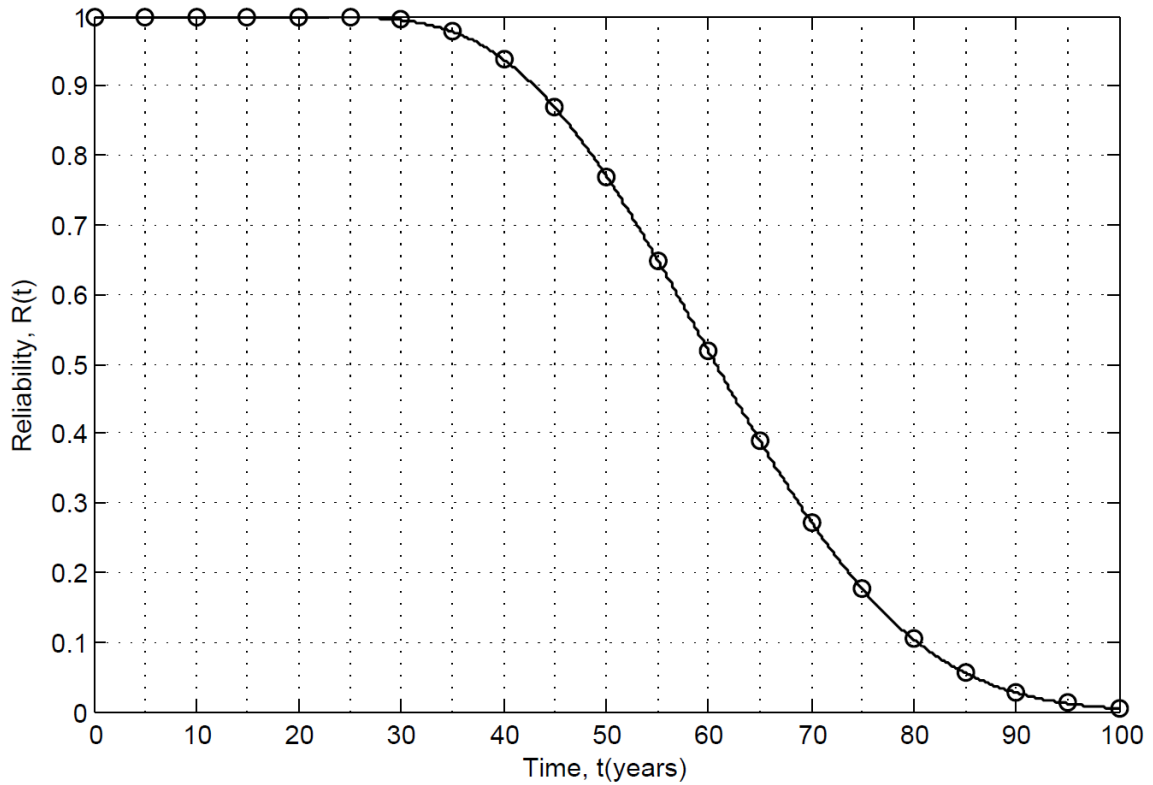


Figure 3.11 Time-dependent reliability prediction for an externally corroded 12m pipe segment

Next, the SSA result for the baseline scenario is illustrated in Fig. 3.12. It presents the conditional reliability changes and the subsequent resulting PM intervals, as well as the fluctuations of the overall reliability throughout the entire period considered. In addition, the difference between the system and single segment reliability, without any PM, is illustrated. The conditional reliability after the first and second PM actions is higher than its reliability before PM, but it does not get restored to the value of 1. In other words, the system is imperfectly repaired in these two first PM actions, although the repair of each segment renders it as good as new, since each of them is restored to pristine condition. After the third PM, the conditional reliability of the system becomes higher, compared to the conditional reliability of the system after the two previous PM actions, because all three old segments are now brought back to pristine condition.

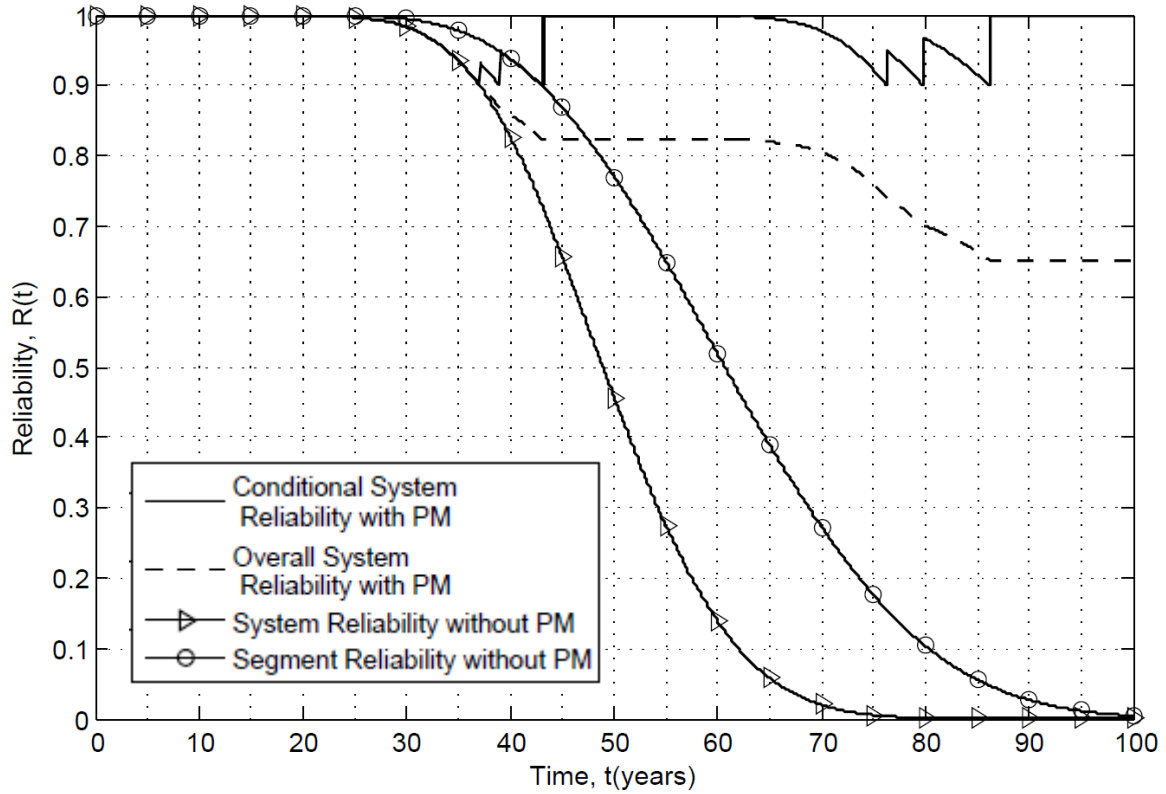


Figure 3.12 Comparison of reliability with and without PM

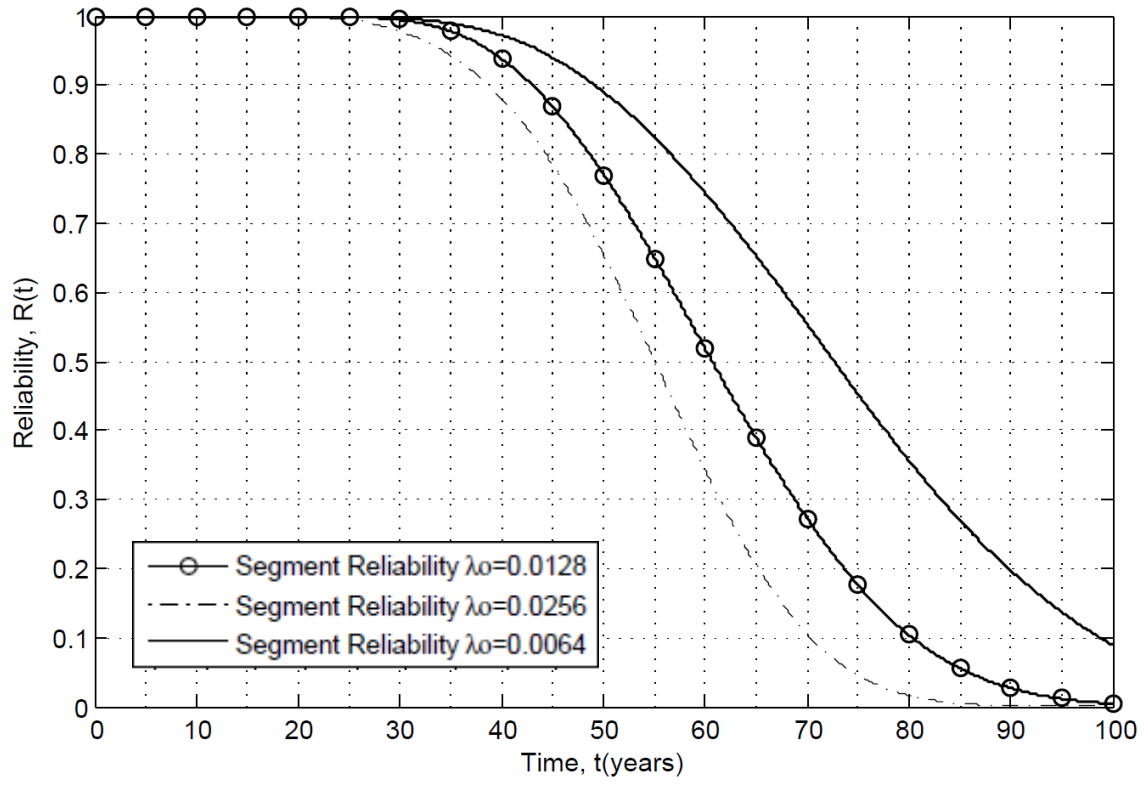
In specific, after the third PM the system is considered fully repaired (conditional reliability equals one), which is something expected considering the degradation rate of each segment, i.e. Fig. 3.11, and the time interval between the first and the third PM action for the whole system, i.e. Fig. 3.12. This is also thought to be industry consistent, given that after every PM each repaired segment is assumed to be restored to pristine condition and that a new pipeline normally has a guaranteed lifetime which is significantly higher than the aforementioned time interval. Furthermore, Fig. 3.11 illustrates that the overall reliability of the pipeline system is much higher compared to the system reliability without PM. This leads to the conclusion that the implemented PM strategy is effective. Besides, it is apparent that the conditional reliability is always higher than the overall system reliability. This is attributed to the failure probabilities of each segment before their preventive repair, as described in Section 3.4.

The impact of the instantaneous generation rate of the NHPP model on the single segment, conditional and system reliability, is depicted in Figs. 3.13a-c respectively. The proportional constant λ_o of the instantaneous rate in Eq. (3.1) is assumed equal to 0.0064,

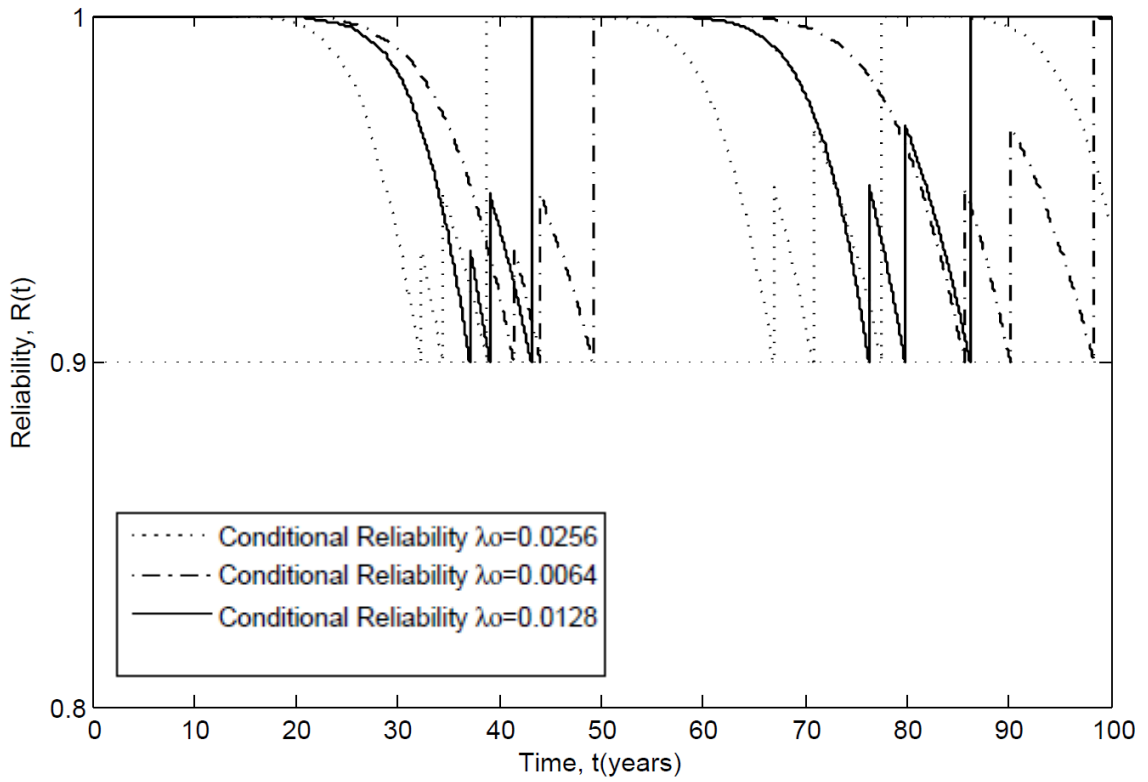
0.0128 and 0.0256. Results shown in Fig. 3.13a indicate that for $\lambda_o=0.0064$ and $\lambda_o=0.0128$, the reliability starts to decrease at approximately the same time, which is 30 years. This is expectable, since although the probability of failure is directly linked to the number of defects, it is also governed by the corrosion growth and material characteristics, which are the same for all three cases. For $\lambda_o=0.0256$ the degradation initiates around 25 years, which is attributed to the significantly higher number of expected defects on the segment. Comparing all three cases, the reliability is minimum for $\lambda_o=0.0064$ and maximum for $\lambda_o=0.0256$ as a higher number of defects leads to higher probabilities of failure. Besides, it is observed that the degradation rate for $\lambda_o=0.0128$ and $\lambda_o=0.0256$ follows a similar pattern for the most part during their lifetimes, while for $\lambda_o=0.0064$ the degradation is much more slow.

In Fig. 3.13b, it is observed that among the three cases, the results are similar with regards to the PM interval and the number of PM actions for the R_{th} of the baseline scenario. For $\lambda_o=0.0256$, the first PM is required at 32 years, for $\lambda_o=0.0128$ at 37 years and for $\lambda_o=0.0064$ at 40 years. It is observed that the time of the first PM for all three cases, is proportional to their values, i.e. the first PM for $\lambda_o=0.0064$ takes place after the second PM for $\lambda_o=0.0128$ and the first PM of $\lambda_o=0.0128$ after the second PM of $\lambda_o=0.0256$. However, this is not exactly the case for the rest of the PM times for these three cases, although some level of proportionality remains. Finally, Fig. 3.12b shows that for all three cases, the same number of PM actions is required, namely six, and that the PM actions are required earlier, for a higher number of defects.

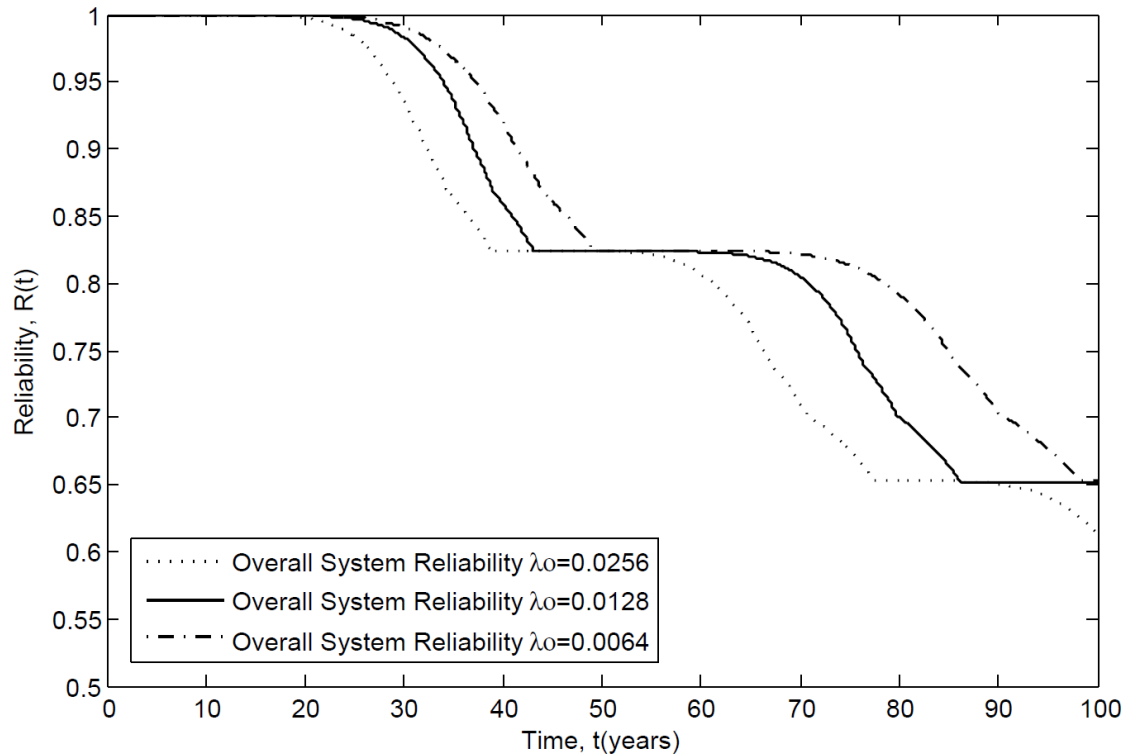
Fig. 3.13c shows that the overall reliability, which is linked with the probability of survival of the system, follows a similar pattern with the conditional reliability. In other words, for $\lambda_o=0.0064$ and $\lambda_o=0.0128$, the overall reliability at the end of the time period considered is the same. This is something plausible, given the same number of identical PM actions, as indicated by the conditional reliability result and the same construction and material conditions of the pipeline system. However, for $\lambda_o=0.0256$ the overall reliability at the end of 100 years decrease even further, compared to the other two cases, since the conditional reliability starts to decrease again after the 6th PM at around 85 years. Again, this is attributed to the marked impact of the higher number of defects on the reliability of the pipeline. It is also noted that the overall system reliability tends to decrease less sharply for a lower number of defects.



(a)



(b)

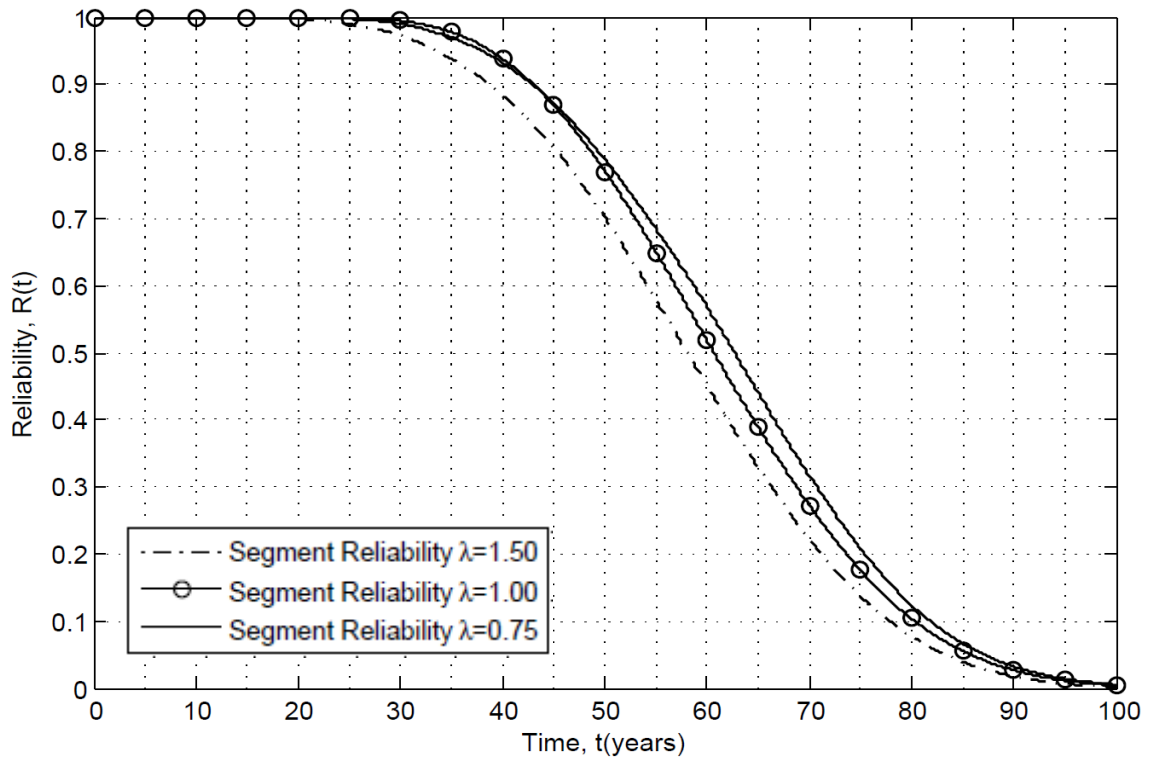


(c)

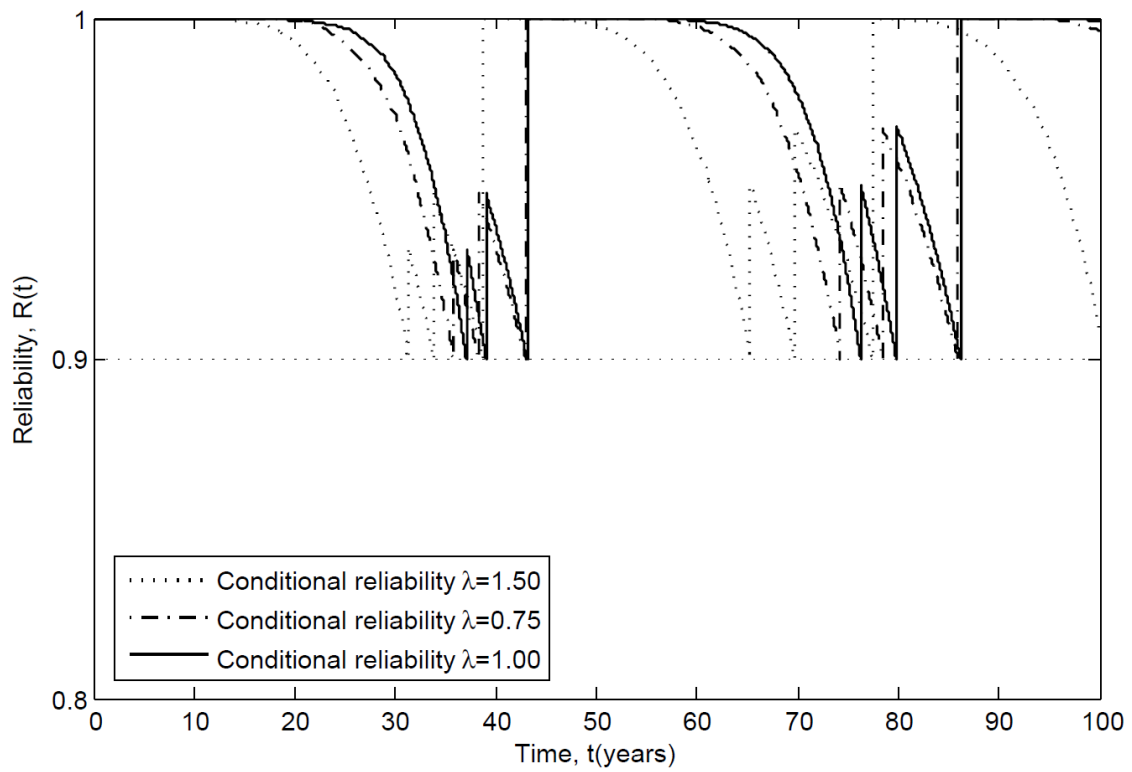
Figure 3.13 (a-c) Comparison of reliability predictions in terms of the proportional constant λ_o of the defect generation model

The predictions for the single segment, conditional and system reliability are next realised for the three parametric scenarios regarding the generation rate λ of the PSWP model and are illustrated in Fig. 3.14a-c. Three values are assumed, namely 0.75, 1.00, and 1.50. It is observed that the different values of λ have a relatively uniform impact on reliability, proportional to the magnitude of λ . Therefore, single segment reliability in Fig. 3.14a increases more significantly for a higher value of λ (1.50), while the difference among the other two cases (0.75 and 1.00) is marginal. In specific, the reliability for $\lambda=0.75$ starts to decrease slightly earlier compared to the one for $\lambda=1.00$, while both reach the reliability control limit of $R_{th}=0.90$ simultaneously. Although for $\lambda=0.75$ the reliability remains higher during the majority of the lifetime considered, at the end both become exactly equal. This slight deviation can be attributed to the stochastic nature of the PSWP model and the marginal difference among the λ values. A similar impact is shown in Fig. 3.14b, with the conditional reliability curves indicating a shorter first PM interval for $\lambda=1.50$, then

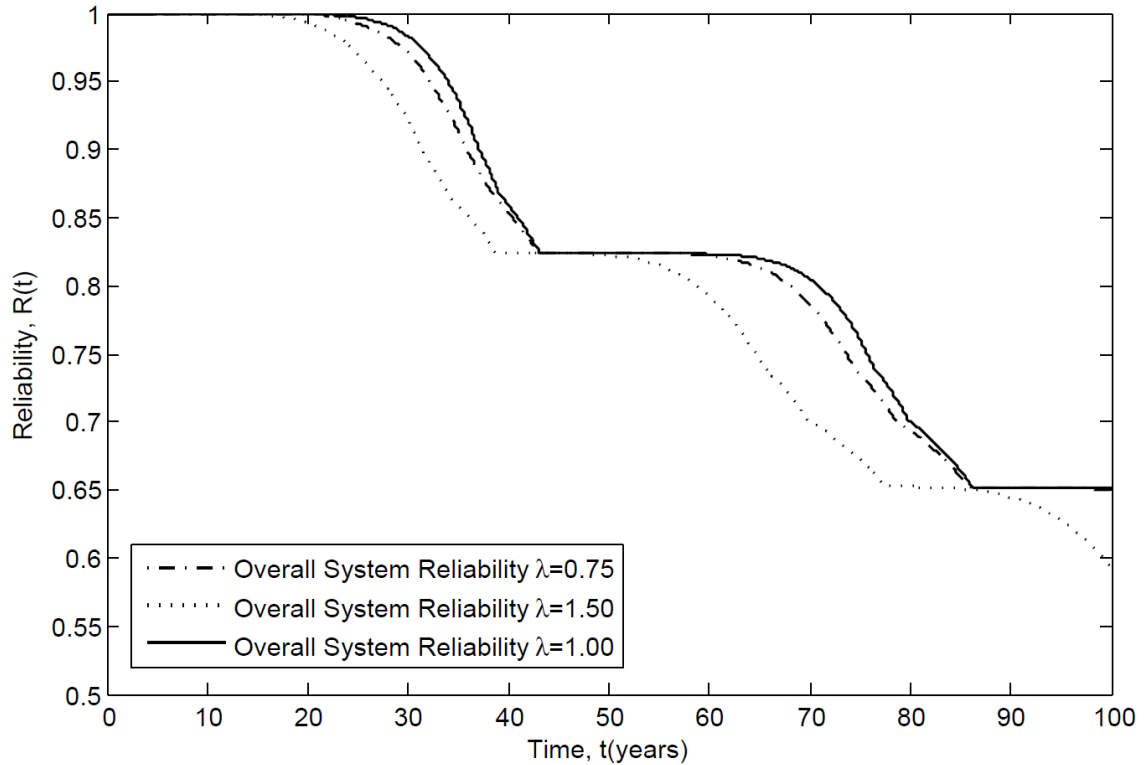
an increased for $\lambda=0.75$ and an even higher for $\lambda=1.00$. Finally, the same level of analogy among the changes in λ and reliability is indicated in Fig. 3.14c.



(a)



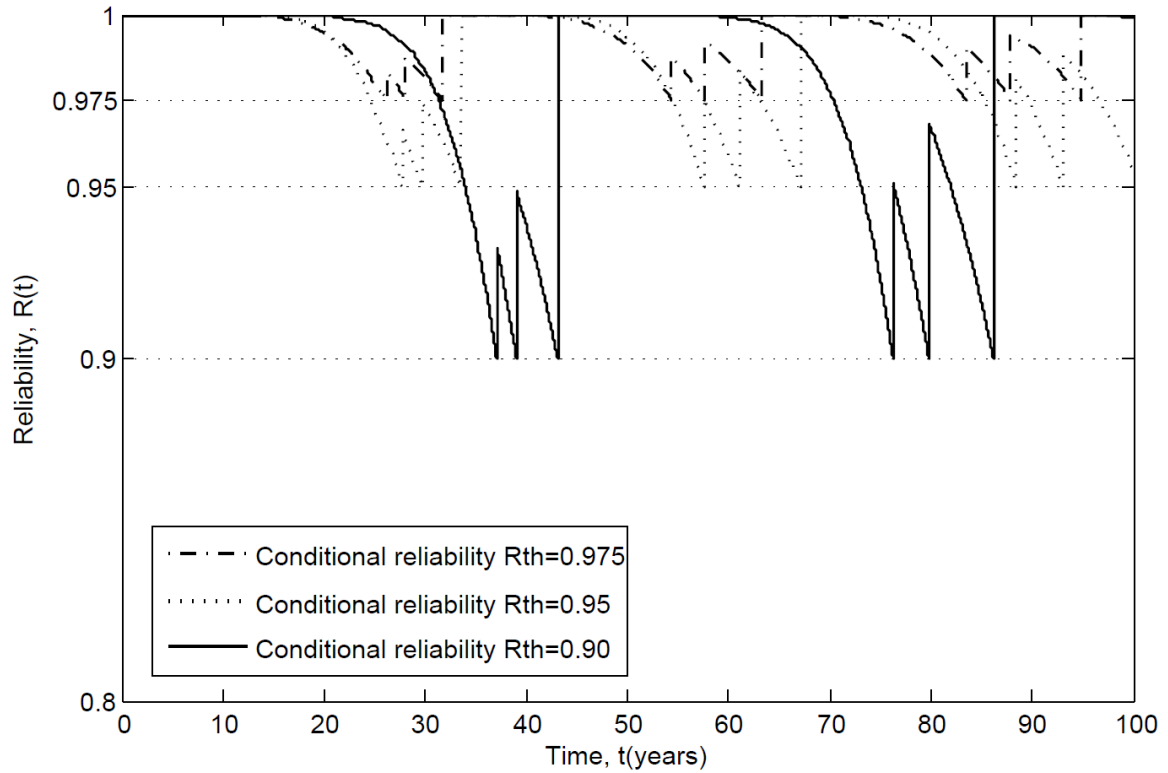
(b)



(c)

Figure 3.14 (a-c) Comparisons of reliability predictions in terms of the generation rate λ of the PSWP internal pressure model

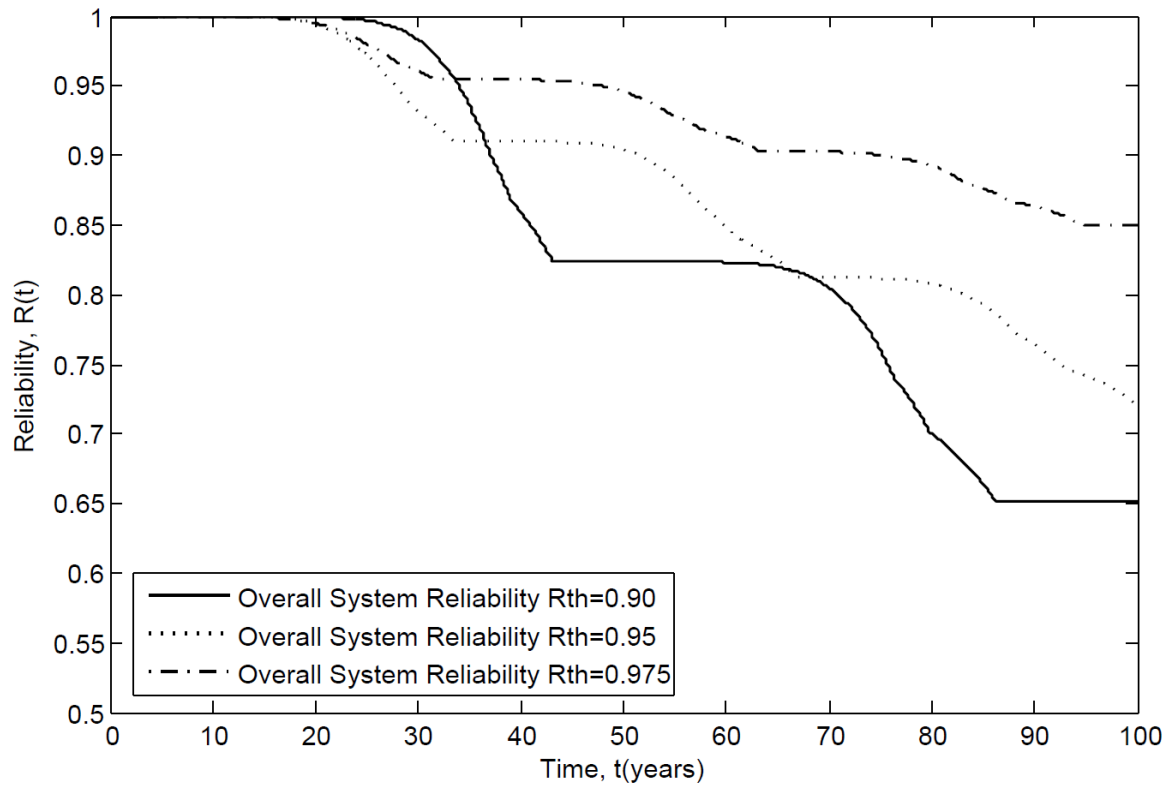
The conditional and overall system reliability predictions corresponding to the different reliability constraint scenarios, are examined in Fig. 3.15a-b. Three values are defined as reliability control limits in the RBPM policy, namely R_{th} equal to 0.90, 0.95 and 0.975, and their effect on the conditional and overall reliability is studied. In Fig. 3.15a, it is shown that the strategies for $R_{th}=0.95$ and $R_{th}=0.975$ have a marginal difference with respect to the times of PM actions, while both produce almost the same number of PM actions (the 9th PM action for $R_{th}=0.95$ would take place at around 101 years according to Fig. 3.15a). On the other hand, for the strategy with $R_{th}=0.90$, a smaller number of PM actions is required, i.e. six, and as expected the PM actions have posterior times.



(a)

Figure 3.15a Comparisons of reliability predictions in terms of the reliability threshold R_{th}

The marked impact of the different R_{th} values on the overall system reliability is illustrated in Fig. 3.15b. In specific, after 100 years of operation the overall reliability of the pipeline system is 0.65 when $R_{th}=0.90$, 0.725 when $R_{th}=0.95$ and 0.85 when $R_{th}=0.975$. In addition, a higher R_{th} value results in a significantly higher overall reliability, throughout the entire lifetime of the system. It is indicative that halfway through the period examined, i.e. 50 years, the overall reliability is 0.83 for $R_{th}=0.90$, 0.92 for $R_{th}=0.95$ and 0.95 for $R_{th}=0.975$. Finally, it is noted that $R_{th}=0.95$ and $R_{th}=0.975$ result in three additional PM actions compared to $R_{th}=0.90$, which denote substantially higher costs that affect the respective decision making markedly.



(b)

Figure 3.15b Comparisons of reliability predictions in terms of the reliability threshold R_{th}

3.7 Conclusions

Two probabilistic methodologies were proposed herein, both based on a robust integration of stochastic processes within a structural reliability analysis (SRA) framework. For their illustration, two realistic case studies were conducted. These were based on two different inspection and maintenance plans, namely DA and ILI inspections and repairs, while both concerned onshore gas transmission pipelines subjected to external metal-loss corrosion. The first methodology focuses on the analysis of external metal-loss corrosion of gas pipelines and provides estimates of rupture probabilities on a reference pipe segment, which was constructed by employing the average characteristics of ruptured pipes from the PHMSA database for the period 2002-2014. The uncertainties were modelled explicitly through stochastic modelling of the segment-based loads and resistances. The non-homogeneous Poisson process was employed for the generation of new defects and the Poisson square wave process to model the growth of the defects. The internal pressure load

was modelled through a discrete Ferry-Borges stochastic process. An implicit ILI inspection and maintenance plan was incorporated thereafter, based on standardised codes of practice along with the corresponding uncertainties of the inspection procedure. Considering the use of realistic characteristics from the PHMSA database, it can be inferred that this model provides additional knowledge on the state of the PHMSA onshore gas transmission network in 2002-2014, a period rather representative of the up-to-date techniques and strategies for pipeline operation and rehabilitation in the industry, amplifying the relevance of the results to reliability analyses of new or existing pipelines.

The second probabilistic methodology can accurately predict the time-dependent reliability for unpiggable pipeline systems subjected to external metal-loss corrosion. The application of the proposed methodology on an example pipeline system was conducted by considering a direct excavation, assessment and repair strategy that is preventive in nature. The non-homogeneous Poisson process was again employed for the generation of corrosion defects over time and an empirical power law model for the defect growth, with respect to a single pipe segment of 12m. A Poisson square wave process model was adopted for the the internal pressure loading. The reliability of the corroding pipe segment was evaluated by means of a Monte Carlo simulation technique against the failure mode of burst. Next, a SSA, which is a heuristic method, was employed in order to update the reliability corresponding to a linear system composed of a series of pipe segments. The estimated single segment reliability, which is directly associated with the failure mode of burst, was used in the SSA analysis, instead of the hazard function associated with the time to failure. The pipeline system was assumed to be imperfectly repaired in every future PM action. This is considered industry consistent due to human and financial constraints. The SSA method can accurately quantify changes in reliability due to the imperfect repairs. The type of maintenance strategy illustrated in the numerical application can be useful to decision-making for reliability prediction of pipeline systems, both as a realistic ECDA strategy and for comparison with other strategies, such as the ILI-based ones. The results indicate the efficiency of the methodology in predicting reliability of pipeline systems over time, while incorporating the effects of failure probabilities of repaired and unrepaired segments.

Furthermore, the impact of certain parameters on the reliability predictions were examined through a parametric study. The instantaneous generation rate λ_o of the defect generation model had a significant impact on the single segment and overall system reliability, as well

as on the conditional reliability. A higher number of λ_o led to a proportionally higher number of defects generated by the NHPP model and a respective proportional decrease of pipeline reliability. The generation rate λ of the PSWP model had a marginal impact on the different types of reliability examined, compared to λ_o . Also, the reliability constraint R_{th} affected significantly the number and times of PM actions. It was found that even relatively little changes in the magnitude of R_{th} can have a marked impact on the overall system reliability after the PM actions. For instance, the parametric study showed that even though $R_{th}=0.95$ and $R_{th}=0.975$ resulted in almost the same number of PM actions and relatively similar PM times, the latter presented a significantly higher reliability during the entire lifetime and especially at the end of it. The probabilistic methodologies proposed in this chapter can assist pipeline operators in selecting efficient preventive ECDA and repair strategies for unpiggable pipelines, as well as ILI and repair strategies for piggable ones. In fact, for piggable pipelines, the two methodologies can be compared and then the optimal one can be derived from an analysis that integrates failure risks and maintenance costs. The methodologies of this chapter can therefore assist operators in making informed maintenance decisions, based on reliability and risk.

4. Statistical Analyses for Reliability Predictions in Energy Pipelines

4.1 Introduction

When it comes to statistical analyses of failures in literature, pipelines are typically examined as repairable systems. In other words, following a failure the system is assumed to return to operation by repairing or even replacing some parts of it, instead of replacing the entire system. The corresponding failure rate refers to a sequence of failure times within a time interval, as opposed to a single time to failure distribution. In this chapter, the times to failure of gas transmission pipelines are grouped and a non-repairable system approach is implemented. There is often confusion among the two analyses, which can lead to unsuitable analysis and wrong conclusions, since the failure rates derived from the two methods are fundamentally different. An excellent discussion about the discrimination between the two can be found in Ascher and Feingold (1984). The Pipeline and Hazardous Material Safety Administration (PHMSA) database provides information on the installation date of each pipeline for which an incident has been reported, as opposed to other established databases that do not report raw data. As a result, inductive inferences can be derived from the pipeline time to failure.

It is assumed that ruptured pipes are non-repairable segments functioning within a repairable system, which is the entire pipeline network. This is thought to be a realistic assumption since a pipe segment is discarded post rupture and replaced by a new one, considering the typically detrimental effect of rupture. Even if a pipe segment has been repaired or even restored to pristine condition before the rupture as part of a maintenance and repair plan, when it eventually ruptures it becomes non-functional. In other words, with regard to rupture, the lifetime of a pipe segment is a random variable defined by a single time to failure. For a group of identical segments, the lifetimes are assumed to be independent and identically distributed. The lifetimes of ruptured segments are arranged by magnitude, whereas their individual rupture year is not of interest (Ascher and Feingold, 1984; Leemis, 1995). Then, their reliability against rupture can be investigated for a range of possible and competing failure causes.

Two distinct statistical methodologies are proposed in this chapter that account for multiple integrity threats. In both of them, a non-repairable system approach is considered

and actual incidents derived from the PHMSA database are used for their numerical application. In the first methodology, a well-established approach from reliability and survival analysis is employed, known as nonparametric predictive inference (NPI). NPI provides interval probabilities, also known as imprecise probabilities, which are quantified via upper and lower bounds. The focus is on the rupture of a future pipe segment due to a specific integrity threat, among a range of competing risks. The second statistical methodology proposes a parametric hybrid empirical hazard model, in conjunction with a robust data processing technique known as the non-linear quantile regression, for reliability analysis and prediction. It provides inferences on the complete lifecycle reliability of the average pipe segment of a region.

The content of this chapter is structured as follows. The specific analysis of the rupture incident data from the PHMSA database, along with the basics of the NPI for different failure causes are described in Section 4.2. The hybrid empirical hazard model and the non-linear quantile regression methodology are presented in section 4.3. In Sections 4.4 and 4.5, the case studies are carried out for the NPI and hybrid parametric methodologies, respectively. Finally, some concluding remarks are presented in Section 4.6, based on the outcomes of the case studies.

4.2 Competing Risks Analysis of Failures based on the NPI Approach

4.2.1 General

The NPI statistical model deals efficiently with competing risks, as suggested in Coolen et al. (2002) and Maturi et al. (2010). It provides insights into reliability of a pipeline population under study, when little information is available and also when several failure causes coexist. NPI enables statistical inference on future observations based on past ones and assumes that failure causes are independent. The method is based on Hill's assumption $A_{(x)}$ (Hill 1988; 1993) which gives a direct conditional probability for a future observable random quantity, conditioned on observed values of related random quantities and the mathematical concept of exchangeability. Furthermore, it provides interval probabilities, which are also referred to in literature as imprecise probabilities. In other words, this means that uncertainty is quantified via lower and upper probabilities. Thus, survival functions are estimated in bounds too. The NPI method enables inferences with regard to

the actual failure time of an exchangeable future unit and also deals with right-censoring data, providing consequently inferences on each separate failure cause or competing risk. The use of the NPI is tailored to the specifications of energy pipeline reliability analysis and real world inferences for a complete pipeline lifecycle are derived, based on historical failure records.

The aim of the first statistical methodology thus, is to apply the competing risks theory by means of the NPI on the dataset of rupture incidents, in order to obtain realistic probabilities of rupture, broken down by specific causes. This kind of information is pivotal for fully understanding risks and their time-dependent implications. It is illustrated how the NPI method can be applied on the PHMSA data to derive an evaluation of the survival function of onshore gas transmission pipelines against rupture failures. The application corresponds to only a population of ruptured components and not the entire pipeline network. As a result, inferences concern a future segment that will rupture due to a specific failure cause and lower and upper probabilities for this event are obtained. The survival functions obtained represent the complementary probability of rupture for this future segment, at a given time instant. Detailed mathematical justifications of the aforementioned definitions should be sought in the references of this study and most specifically in Maturi et al. (2010).

4.2.2 PHMSA Rupture Incidents from 2002-2014

The PHMSA database is updated on an annual basis. At the time of this study, the PHMSA database for onshore gas transmission pipelines included the incident data from 1970 to 2015 and the mileage data from 1970 to 2014. In brief, pipeline operators report incidents to PHMSA on a standardised form, which was subject to major changes on 1984 and 2002. This study utilised the incident data from 2002 up to the end of 2014. The pre-2002 data is excluded from the study because it is significantly less detailed and the description of most data fields is very different compared to the post-2002 ones. Therefore, it is very difficult to combine the data of those periods. Furthermore, the incident data between 2002 and until 2014 is considered reasonably representative of the current state of onshore gas transmission pipelines in the US, as well as the up-to-date inspection and maintenance techniques. The history of in-line inspection tools shows that these were not fully developed and applied in industry practice prior to 1980. Also, high-resolution tools were

used after 1990. This is important information when calculating failure rates, in that the aim is to obtain comprehensive results, which allow for improvement of current practices and reduction of incidents.

Lam and Zhou (2016) analysed the PHMSA database and evaluated respective failure rates, in an effort to derive baseline failure probabilities for carrying out system-wide risk assessments of pipelines. The causes and the failure modes of the pipeline incidents were considered. It is noted that the format of the incident data before 2010 is different from that afterwards. Therefore, the data from the two periods had to be aggregated. A similar aggregation strategy is employed herein. The main and secondary failure causes, as well as the rupture failure mode, for the periods 2002-2009 and 2010-2014 are presented in Tables 4.1 and 4.2.

Table 4.1 Mapping of the failure causes for the period 2002-2014

2002-2009		2010-2014		Failure causes adopted in this study
Corrosion	Internal corrosion	Corrosion	Internal corrosion	Internal corrosion (IC)
	External corrosion		External corrosion	External corrosion (EC)
Material and welds	Body of pipe			Material failure (MF)
	Component			
	Joint			
	Butt			
	Fillet			
	Pipe seam			
			Construction-, installation-, or fabrication-related	
			Original manufacturing-related(not girth weld or other welds formed in the field)	
	Environmental cracking-related			
Excavation	Third party excavation damage	Excavation	Excavation damage by third party	Excavation Damage (ED)
	Operator excavation damage (includes contractors)		Excavation damage by operator (first party)	
			Excavation damage by operator's contractor (second party)	

Table 4.1 Mapping of the failure causes for the period 2002-2014

Other outside forces	Rupture of previously damaged pipe	Other outside forces	Previous damage due to excavation activity	Previously damaged pipe (PDP)
			Previous mechanical damage not related to excavation	
	Car, truck or other vehicle not related to excavation activity		Damage by car, truck, or other motorized vehicle/equipment not engaged in excavation	Other (O)
	Fire/explosion as primary cause of failure		Nearby industrial, man-made, or other fire/explosion as primary cause of incident	
	Vandalism		Intentional damage	
			Damage by boats, barges, drilling rigs, or other maritime equipment or vessels set adrift or which have otherwise lost their mooring	
			Routine or normal fishing or other maritime activity not engaged in excavation	
			Electrical arcing from other equipment or facility	
	Other outside force damage			
Equipment and operations	Malfunction of control/relief equipment	Equipment failure	Malfunction of control/relief equipment	
	Threads stripped, broken pipe coupling		Threaded connection/coupling failure	
	Ruptured or leaking seal/pump packing			
Equipment and operations		Equipment failure	Compressor or compressor-related equipment	
			Non-threaded connection failure	
			Defective or loose tubing or fitting	
			Failure of equipment body (except compressor), vessel plate, or other material	
			Other equipment failure	
	Incorrect operation	Incorrect operation	Damage by operator or operator's contractor not related to excavation and not due to motorized vehicle/equipment damage	
			Underground gas storage, pressure vessel, or cavern allowed or caused to overpressure	
			Valve left or placed in wrong position, but not resulting in an overpressure	
Pipeline or equipment over pressured				

Table 4.1 Mapping of the failure causes for the period 2002-2014

			Equipment not installed properly Wrong equipment specified or installed	
			Other incorrect operation	
Other	Miscellaneous		Miscellaneous	
	Unknown		Unknown	
Natural forces	Heavy rains/floods		Heavy rains/floods	
	Temperature		Temperature	
	High winds		High winds	
	Lightning		Lightning	
			Other natural force damage	
	Earth movement		Earth movement	Earth movement (EM)

It is also noted that incidents in the PHMSA database are classified as either pipe-related or non-pipe related. Pipe-related incidents include those occurring on the body of pipe and pipe seam, whereas non-pipe related incidents include those occurring on compressors, valves, meters, hot tap equipment, filters and so on. Only pipe-related incidents are analysed in this study. The failure data utilised are associated with the onshore (as opposed to offshore) gas transmission (as opposed to gathering) pipelines, which account for the vast majority of gas pipelines in the US. The main assumption of the methodology is the exchangeability that is inherent in the NPI approach and concerns failed units and a future one. Of course, in reality the PHMSA database covers thousands of miles of onshore gas transmission pipelines and thus, differences exist in materials, diameters, installation years and other attributes. To take into consideration all these differences and derive separate inferences for pipelines with the exact same characteristics is not feasible, since the available data is not that detailed in the first place.

Table 4.2 Mapping of failure modes for the period 2002-2014

2002-2009		2010-2014		Failure modes adopted in this study
Leak	Pinhole	Leak	Pinhole	Leak
			Crack	
	Connection failure		Connection failure	
			Seal or packing	

Table 4.2 Mapping of failure modes for the period 2002-2014

			Other leak type	
	Puncture	Mechanical Puncture		Puncture
Rupture	Circumferential	Rupture	Circumferential	Rupture
	Longitudinal		Longitudinal	
			Other of rupture type	
	Other	Other		Other

Kiefner et al. (2001) and Lam and Zhou (2016) further highlighted the lack of exhaustive information in the PHMSA database, as they could not evaluate incident rates considering more than one pipeline attribute and they suggested the revision of the PHMSA reporting format of the pipeline mileage data. Furthermore, Lam and Zhou (2016) summarised some of the major attributes of the operating onshore gas transmission pipeline network for the years 2002-2013, available in the PHMSA mileage data. In brief, steel is the predominant pipe material, since it accounts for over 99% of the total pipeline length between 2002 and 2013. About 97-98% of the steel pipelines are cathodically protected and coated and 80% of them belong to the so-called class 1 areas (low-population-density areas). Regarding diameters, 40-50% of the network is between 254-711mm (10-28 inches), while around 25% is over 711mm (28 inches). Finally, it is noted that during the design phase the wall thickness of a steel gas transmission pipeline in USA is estimated as a function of the diameter, design pressure, specified minimum yield strength (SMYS) and a safety factor that depends on the location class. The wall thickness of a higher location class pipeline is therefore greater than that of a lower location class pipeline, to allow higher protection for the pipeline, as well as its surrounding population (Lam and Zhou, 2016). However, due to the exchangeability property of the NPI method considered herein, all failed pipeline segments are assumed to fall into a unique category and only be examined as onshore gas transmission pipeline segments.

Only ruptures (as opposed to leaks, punctures or others) are considered herein. Pipeline incidents that meet at least one of the following criteria must, by law, be reported to the U.S. Department of Transportation (DOT), Office of Pipeline Safety. The criteria for reporting are stated in the Code of Federal Regulations. A report is required if the incident results in an event that involves a release of gas from a pipeline and either a death or personal injury necessitating in-patient hospitalization, or an estimated property damage, including cost of gas lost, of operator or others, or both, of \$50,000 or more. Also, an event

that is significant in the judgment of the operator, even though it did not meet the two abovementioned can also be reported (Bolt et al., 2006). Given the aforementioned reporting criteria and the implications of a typical rupture incident, it can be assumed that most, if not all, of the actual ruptures were reported to PHMSA. On the other hand, the real number of leaks or punctures that did not meet the reporting criteria may be significant, compared to the number of reported leaks and punctures. Therefore, the rupture rate evaluated using the PHMSA database is thought to be representative of the actual rupture rate. Moreover, the consequences associated with ruptures are far more severe than those associated with leaks and punctures. This is evident if one considers that most leaks (about 97%) and punctures (about 90%) did not result in ignition, while the majority of fatalities and injuries (75% and 83% respectively) were due to ruptures. Therefore, the rupture incidents are thought to be much more critical for analysis from the risk perspective, compared to the leak and puncture rates (Lam and Zhou, 2016).

4.2.3 NPI for Competing Failure Causes

Competing risks theory constitutes a credible way of obtaining real world probabilities, where a pipe segment is not only at risk of rupturing from a specific cause, but also from any other rupture cause (Hinchliffe and Lambert, 2013). Competing risks theory allows for breaking down probabilities of failure, to give operators a clearer indication of the risks they face with each decision they make. This decision-making can regard selection of maintenance plan, how to optimally allocate resources and finally understanding the longer-term implications of failure mechanisms.

In this section, an overview of NPI for competing risks is realised, following Coolen and Yan (2004) and Maturi et al. (2010). According to Hill (1988), $A_{(x)}$ is a Bayesian, fiducial and a confidence/tolerance procedure. It is simple, coherent and plausible, whilst at the same time it is supported by all the serious approaches for statistical inference. According to Hill (1988), $A_{(x)}$ constitutes the fundamental solution to the problem of induction. Let $Y_{B_1}, \dots, Y_{B_x}, Y_{B_{x+1}}$ be continuous and exchangeable random quantities. The values Y_{B_1}, \dots, Y_{B_x} are assumed to be observed and the corresponding ordered values are denoted by $-\infty < y_{B_1} < \dots < y_{B_x} < \infty$ ($y_{B_0} = -\infty$). It is assumed that no ties occur among the observed values and if they do, the tied observations differ by trivial amounts (Maturi et al., 2010).

For $Y_{B_{x+1}}$, which represents a future observable random quantity conditional on x observations, $A_{(x)}$ is (Hill, 1988):

$$P(Y_{B_{x+1}} \in (y_{B_{\omega-1}}, y_{\omega})) = \frac{1}{x+1}, \omega = 1, \dots, x, \text{ and}$$

$$P(Y_{B_{x+1}} \in (y_{B_x}, \infty)) = \frac{1}{x+1} \quad (4.1)$$

NPI is a statistical method based on Hill's assumption $A_{(x)}$, which can be interpreted as a post-data assumption, related to exchangeability (Coolen et al., 2002; Maturi et al., 2010). Inferences based on $A_{(x)}$ are predictive and nonparametric and are particularly suitable when there is no additional information, or one does not wish to use such information, for instance to study effects of additional assumptions underlying other statistical methods. Such inferences are exactly calibrated (Lawless and Fredette, 2005), which strongly justifies their use from the frequentist statistics perspective. Instead, $A_{(x)}$ does not provide precise probabilities for the events of interest but bounds for probabilities with strong consistency properties in the theory of interval probability (Walley, 1991; Weichselberger, 2000).

Coolen and Yan (2004) generalised $A_{(x)}$ into right-censoring $A_{(x)}$ or rc- $A_{(x)}$, to take into account the effect of right-censoring for data, on event times that it is only known that the event has not yet taken place, in specific terms. The rc- $A_{(x)}$ uses the additional assumption that the residual lifetime of a right-censored unit is exchangeable with the residual lifetimes of all other units that have not yet failed or been censored, at the time of censoring. To derive the required form of rc- $A_{(x)}$ for NPI for competing risks, notation is required for probability mass assigned to intervals, without further restrictions on the spread within the intervals. The partial specification of probability distributions is called an M -function and the notation is introduced next.

A probability mass assigned within an interval (a_B, b_B) in the above described way is denoted by $M_{Y_B}(a_B, b_B)$ and referred to as M -function value for Y_B on (a_B, b_B) . Since all M -function values for Y_B on all intervals should sum up to one, each M -function value should be in $[0,1]$ and $A_{(x)}$ can be expressed as $M_{Y_{B_{x+1}}}(x_{\omega}, x_{\omega+1}) = 1/(x+1)$, for $\omega=0, \dots, x-1$ and $M_{Y_{B_{x+1}}}(y_{B_x}, \infty) = 1/(x+1)$. The assumption 'right-censoring $A_{(x)}$ ' or rc- $A_{(x)}$, partially specifies the NPI-based probability distribution for a nonnegative random quantity X_{x+1} ,

based on u_B event times and v_B right censoring times. In specific, it is partially specified by ($\omega=0, \dots, u_B$; and $k_B = 1, \dots, l_{B\omega}$, with $t_0 = 0$ and $t_{u_B+1} = \infty$):

$$M_{X_{x+1}}(t_\omega, t_{\omega+1}) = \frac{1}{x+1} \prod_{\{r_B:c_{r_B} < t_\omega\}} \frac{\tilde{x}_{c_{r_B}+1}}{\tilde{x}_{c_{r_B}}} \quad (4.2)$$

$$M_{X_{x+1}}(c_{k_B}^\omega, t_{\omega+1}) = \frac{1}{(x+1)\tilde{x}_{c_{k_B}^\omega}} \prod_{\{r_B:c_{r_B} < c_{k_B}^\omega\}} \frac{\tilde{x}_{c_{r_B}+1}}{\tilde{x}_{c_{r_B}}} \quad (4.3)$$

The product terms are defined as one, if the product is taken over an empty set. This implicitly assumes non-informative censoring, as a post-data assumption related to exchangeability, for all items known to be at risk at any time t . If there are no censorings, then $rc-A_{(x)}$ is identical to $A_{(x)}$ (Coolen et al., 2002; Coolen and Yan 2004; Maturi et al., 2010). The terms $\tilde{x}_{c_{r_B}}$ and $\tilde{x}_{c_{k_B}^\omega}$ describe the number of units in the risk set prior to time c_{r_B} and $c_{k_B}^\omega$, respectively. The definition $\tilde{x}_0 = x+1$ is used throughout this chapter. Summing up all M -function values assigned to intervals of this form (which have positive M -function values and sum up to one over all these intervals) and having the same $x_{\omega+1}$ as right endpoint, gives the probability as follows:

$$P(X_{x+1} \in (x_\omega, x_{\omega+1})) = \frac{1}{x+1} \prod_{\{r_B:c_{r_B} < x_{\omega+1}\}} \frac{\tilde{x}_{c_{r_B}+1}}{\tilde{x}_{c_{r_B}}} \quad (4.4)$$

where $x_\omega, x_{\omega+1}$ are two sequential failure times.

4.2.3.1 NPI Probabilities for Competing Risks

This study examines the case where a number of k_B distinct failure causes (competing risks) can cause a unit or segment to fail. The unit is assumed to be failing due to the first occurrence of a cause and then withdrawn from further use and observation. It is assumed that such failure observations are obtained for x units and that the cause leading to a failure is known with certainty. For each unit, k_B random quantities are considered and T_ζ is then defined for $\zeta=1, \dots, k_B$, where T_ζ represents the unit's time to failure, under the condition that failure occurs due to cause ζ . These T_ζ are considered to be independent continuous random quantities, which in other words means that the failure causes are assumed to occur independently and the failure time of the unit is the minimum among k_B . Furthermore, T_ζ is assumed to be unique and known with certainty for each unit, while for

the T_ζ corresponding to the other failure causes, which did not cause the failure of the unit, the unit's observed failure time is a right-censoring time. The competing risk data per failure cause consists of several observed failure times for the specific failure cause considered and right-censoring times for failures caused by other failure causes. Consequently, rc- $A_{(x)}$ can be applied per failure cause ζ , for inference on a future unit $N_{B\zeta, x+1}$ (where $N_{B\zeta, x+1}$ corresponds to an observation T for unit $x+1$ and $N_{B\zeta, x+1}$ to T_ζ , as defined above).

It is assumed that the number of failures due to cause ζ is $u_{B\zeta}$, $n_{B\zeta,1} < n_{B\zeta,2} < \dots < n_{B\zeta, u_{B\zeta}}$, and $v_{B\zeta} = (x - u_{B\zeta})$ is the number of the right-censored observations with $c_{\zeta,1} < c_{\zeta,2} < \dots < c_{\zeta, v_{B\zeta}}$, corresponding to failure cause ζ . It is further assumed that there are $s_{B\zeta, \omega_\zeta}$ right-censored observations in the interval $(n_{B\zeta, \omega_\zeta}, n_{B\zeta, \omega_\zeta} + 1)$ denoted by $c_{\zeta,1}^{\omega_\zeta} < c_{\zeta,2}^{\omega_\zeta} < \dots < c_{\zeta, s_{B\zeta, \omega_\zeta}}^{\omega_\zeta}$, such that $\sum_{\omega_\zeta=0}^{u_{B\zeta}} s_{B\zeta, \omega_\zeta} = v_{B\zeta}$. The random quantity representing the failure time of the next unit, with all k_B failure causes considered is $N_{B, x+1} = \min_{1 \leq \zeta \leq k_B} N_{B\zeta, x+1}$. It is noted that it is assumed that $n_{B\zeta,0} = 0$ and $n_{B\zeta, u_{B\zeta}} = \infty$ for notational convenience (Maturi et al., 2010).

The NPI M -functions for $N_{B\zeta, x+1}$ ($\zeta = 1, \dots, k_B$), similar to Eqs (4.2) and (4.3) are:

$$M^\zeta(t_{\zeta, \omega_\zeta^*}^{\omega_\zeta}, n_{B\zeta, \omega_\zeta+1}) = M_{N_{B\zeta, x+1}}(t_{\zeta, \omega_\zeta^*}^{\omega_\zeta}, n_{B\zeta, \omega_\zeta+1}) = \frac{1}{(x+1)} (\tilde{x}_{t_{\zeta, \omega_\zeta^*}^{\omega_\zeta}})^{\delta_{\omega_\zeta^*}^{\omega_\zeta} - 1} \prod_{\left\{ r_B: c_{\zeta, r_B} < t_{\zeta, \omega_\zeta^*}^{\omega_\zeta} \right\}} \frac{\tilde{x}_{c_{\zeta, r_B}}^{+1}}{\tilde{x}_{c_{\zeta, r_B}}} \quad (4.5)$$

where $\omega_\zeta = 0, 1, \dots, u_{B\zeta}$, $\omega_\zeta^* = 0, 1, \dots, s_{B\zeta, \omega_\zeta}$ and

$$\delta_{\omega_\zeta^*}^{\omega_\zeta} = \begin{cases} 1 & \text{if } \omega_\zeta^* = 0 \\ 0 & \text{if } \omega_\zeta^* = 1, \dots, s_{B\zeta, \omega_\zeta} \end{cases}$$

i.e. $t_{\zeta, 0}^{\omega_\zeta} = n_{B\zeta, \omega_\zeta}$ and $t_{\zeta, \omega_\zeta^*}^{\omega_\zeta} = c_{\zeta, \omega_\zeta^*}^{\omega_\zeta}$ for failure time, or time 0 and for censoring time, respectively. The numbers of units in the risk set just prior to times c_{r_B} and $t_{\zeta, \omega_\zeta^*}^{\omega_\zeta}$ are $\tilde{x}_{c_{r_B}}$ and $\tilde{x}_{t_{\zeta, \omega_\zeta^*}^{\omega_\zeta}}$, respectively. The corresponding NPI probabilities, similarly to Eq. (4.4) are:

$$P^\zeta(n_{B\zeta, \omega_\zeta}, n_{B\zeta, \omega_\zeta+1}) =$$

$$P(N_{B\zeta, x_{\zeta+1}} \in (n_{B\zeta, \omega_\zeta}, n_{B\zeta, \omega_{\zeta+1}})) = \frac{1}{(x+1)} \prod_{\{r_B: c_{\zeta, r_B} < n_{B\zeta, \omega_{\zeta+1}}\}} \frac{\tilde{x}_{c_{\zeta, r_B}+1}}{\tilde{x}_{c_{\zeta, r_B}}} \quad (4.6)$$

where $n_{B\zeta, \omega_\zeta}$ and $n_{B\zeta, \omega_{\zeta+1}}$ are two consecutive observed failure times, triggered by failure cause ζ .

The notation for the NPI lower and upper probabilities, for the event that a single future unit $x+1$ fails due to a specific failure cause l_B , for each $l_B = 1, \dots, k_B$ and assuming that the future unit undergoes the same process as the x units, is as follows:

$$\underline{P}^{(l_B)} = \underline{P}(N_{B l_B, x+1} = \min_{1 \leq \zeta \leq k_B} N_{B \zeta, x+1}) = \underline{P}\left(N_{B l_B, x+1} < \min_{\substack{1 \leq \zeta \leq k_B \\ \zeta \neq l_B}} N_{B \zeta, x+1}\right) \quad (4.7)$$

$$\overline{P}^{(l_B)} = \overline{P}(N_{B l_B, x+1} = \min_{1 \leq \zeta \leq k_B} N_{B \zeta, x+1}) = \overline{P}\left(N_{B l_B, x+1} < \min_{\substack{1 \leq \zeta \leq k_B \\ \zeta \neq l_B}} N_{B \zeta, x+1}\right) \quad (4.8)$$

These NPI lower and upper probabilities for the event that the next unit fails due to failure cause l_B are:

$$\underline{P}^{(l_B)} = \sum_{C_{l_B}(\zeta, \omega_\zeta, \omega_\zeta^*)} \left[\sum_{\omega_{l_B}=0}^{u_{B l_B}} \mathbf{1}(n_{B l_B, \omega_{l_B}+1} < \min_{\substack{1 \leq \zeta \leq k_B \\ \zeta \neq l_B}} \{t_{\zeta, \omega_\zeta^*}^{\omega_\zeta}\}) P^{l_B}(n_{B l_B, \omega_{l_B}}, n_{B l_B, \omega_{l_B}+1}) \right] \times \prod_{\substack{\zeta=1 \\ \zeta \neq l_B}}^{k_B} M^\zeta(t_{\zeta, \omega_\zeta^*}^{\omega_\zeta}, n_{B l_B, \omega_{l_B}+1}) \quad (4.9)$$

$$\underline{P}^{(l_B)} = \sum_{C_{l_B}(\zeta, \omega_\zeta)} \left[\sum_{\omega_{l_B}=0}^{u_{B l_B}} \sum_{\omega_{l_B}^*=0}^{s_{B l_B, \omega_{l_B}}} \mathbf{1}(t_{l_B, \omega_{l_B}^*}^{\omega_{l_B}} < \min_{\substack{1 \leq \zeta \leq k_B \\ \zeta \neq l_B}} \{n_{B \zeta, \omega_{\zeta+1}}\}) M^{l_B}(t_{\zeta, \omega_\zeta^*}^{\omega_\zeta}, n_{B l_B, \omega_{l_B}+1}) \right] \times \prod_{\substack{\zeta=1 \\ \zeta \neq l_B}}^{k_B} P^\zeta(n_{B \zeta, \omega_\zeta}, n_{B \zeta, \omega_{\zeta+1}}) \quad (4.10)$$

where $\sum_{C_{l_B}(\zeta, \omega_\zeta, \omega_\zeta^*)}$ denotes the sums over all ω_ζ^* , from 0 to $s_{B \zeta, \omega_\zeta}$ and over all ω_ζ , from 0 to $u_{B \zeta}$, for $\zeta=1, \dots, k_B$, but not including $\zeta=l_B$. Similarly, $\sum_{C_{l_B}(\zeta, \omega_\zeta)}$ denotes the sums over all ω_ζ , from 0 to $u_{B \zeta}$, for $\zeta=1, \dots, k_B$, but not including $\zeta=l_B$.

4.2.3.2 Survival Functions for Competing Risks

The survival function, which is also known as reliability function, represents the probability of survival for a unit past a certain moment of time. The present methodology

does not produce precise probabilities and thus precise values for the survival function, but aims to derive maximum and minimum upper bounds, which are consistent with the probability assessment according to $A_{(x)}$. The formulae for these NPI lower and upper survival functions $\underline{S}_{N_{B_{x+1}}}(t)$ and $\overline{S}_{N_{B_{x+1}}}(t)$ are considered relevant and applicable in multiple ways in reliability and survival analysis (Coolen et al., 2002). These NPI lower and upper survival functions were first introduced by Coolen et al. (2002), but Maturi et al. (2010) introduced the simple closed-form formulae for these survival functions as presented in Eqs. 4.11 and 4.12. First, it is assumed that $t_{s_{B_{\omega+1}}}^{\omega} = t_0^{\omega+1} = n_{B_{\omega+1}}$, for $\omega = 0, 1, \dots, u_B - 1$. The NPI lower survival function can then be expressed as follows, for $t \in [t_{a_B}^{\omega}, t_{a_{B+1}}^{\omega})$ with $\omega = 0, 1, \dots, u_B$ and $a_B = 0, 1, \dots, s_{B_{\omega}}$:

$$\underline{S}_{N_{B_{x+1}}}(t) = \frac{1}{(x+1)} \tilde{x}_{t_{a_B}^{\omega}} \prod_{\{r_B:c_{r_B} < t_{a_B}^{\omega}\}} \frac{\tilde{x}_{c_{r_B}+1}}{\tilde{x}_{c_{r_B}}} \quad (4.11)$$

and the corresponding NPI upper survival function for $t \in [n_{B_{\omega}}, n_{B_{\omega+1}})$, with $\omega = 0, 1, \dots, u_B$:

$$\overline{S}_{N_{B_{x+1}}}(t) = \frac{1}{(x+1)} \tilde{x}_{n_{B_{\omega}}} \prod_{\{r_B:c_{r_B} < n_{B_{\omega}}\}} \frac{\tilde{x}_{c_{r_B}+1}}{\tilde{x}_{c_{r_B}}} \quad (4.12)$$

For proofs and further discussion of the above formulae, the interested reader is referred to Maturi et al. (2010).

4.3 Statistical Analysis based on a Parametric Hybrid Methodology

4.3.1 General

In this section, a second statistical analysis methodology is proposed, which can estimate the overall reliability of a pipe segment that belongs to a pipeline network. Pipes are likewise examined as non-repairable segments functioning within a repairable system, i.e. the entire pipeline network. The proposed model provides reliability inferences on the pipe segment's entire service life, even when available data are scarce, incomplete and both left and right censored. The pipe segment examined is thought to exhibit the average conditions of any given region under study.

To illustrate the proposed model, the data of Section 4.2.2, i.e. from the PHMSA database for the period 2002-2014, are employed, with regard to rupture incidents of onshore gas transmission pipelines. The incident data for the period 2002-2014 are considered fairly representative of the current state and rehabilitation applications in regards to onshore gas transmission pipelines. Undoubtedly, PHMSA database covers thousands of miles of onshore gas transmission pipelines and thus differences exist in materials, diameters, soil conditions and many other attributes. Furthermore, there is discrepancy among the annual report database (that contains the pipeline details and mileage information) and the incident database, which further hinders credible statistical analyses. These uncertainties, associated with the statistical analysis of the PHMSA database, are taken into consideration by adopting a hybrid empirical hazard model in liaison with a robust data processing technique, known as the non-linear quantile regression. This proposed combined model is thought to produce a credible expectation range of reliability performance of the infrastructure under consideration, for a complete service life of 100 years, as opposed to the ROCOF approach that can produce average annual failure rates only for the time period under study, i.e. 13 years for the period 2002-2014.

4.3.2 Hazard Functions and Corresponding Reliability

Gas pipelines, like a lot of the typical large-scale engineering structures, are considered to follow some similar patterns when it comes to their failure or hazard rate. One of the most commonly adopted hazard patterns in literature for large-scale engineering structures is the bath-tub pattern (Sun et al., 2011; Shafiee et al., 2011). This one is adopted in this study and is assumed to cover the whole lifecycle of gas transmission pipelines, consisting of three phases as shown in Fig. 4.1. Phase 1 represents the incipient failure phase or ‘infant mortality’ and the failure rate decreases with time. Phase 2 represents random failures and the probability of failure is constant. Phase 3 is called the wear-out or degradation phase, where the number of failures, and thus the failure rate, increase with time. Many models can be successfully employed to describe these mixed distributions. In this study, the exponential failure distribution with a constant failure rate λ_B is employed for phase 2 and mixed exponential and Weibull distributions for phase 3. These are presented in Eq. (4.13) and (4.14).

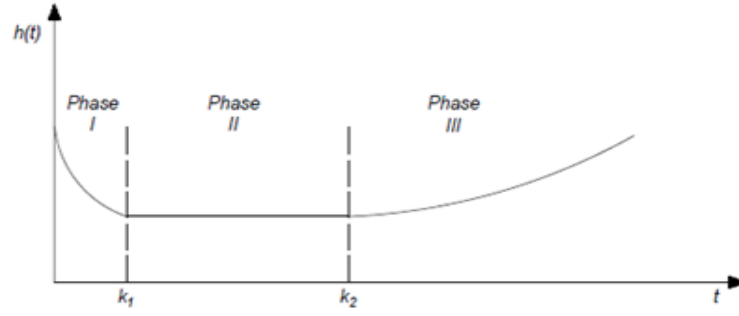


Figure 4.1 Bath-tub failure pattern

Phase 1 can be neglected for gas transmission pipelines and is not taken into consideration herein. It is thought to regard failures at the initial operation years that are mainly caused by construction and/or manufacturing defects, human errors, as well as random reasons. However, since gas pipelines are generally large cross-country infrastructure with long lifetimes, this first phase can be regarded trivial in terms of both duration and magnitude. As a result, the hazard pattern considered includes only phase 2 and 3, as presented in Fig. 4.2.

$$h(t) = \lambda_B \quad \text{for } k_1 \leq t \leq k_2 \quad (4.13)$$

$$h(t) = \lambda_B + \left(\frac{\beta_2}{\alpha_2}\right)\left(\frac{t - k_2}{\alpha_2}\right)^{\beta_2 - 1} \quad \text{for } t \geq k_2, \alpha_2 > 0, \beta_2 > 1 \quad (4.14)$$

where $h(t)$ is the hazard function and t is the age of the pipeline under consideration. Parameter λ_B is a constant failure rate and α_2, β_2 are the scale and shape parameters of the Weibull distribution. Parameters k_1 and k_2 refer to the start and the end of phase 2, respectively.

Once the hazard functions are obtained, the reliability functions can be derived from them. Eq. (4.15) and (4.16) give continuous reliability curves that correspond to continuous hazard curves. The reliability functions corresponding to Eq. (4.13) and (4.14) are:

$$R_{s_1}(t) = e^{-\lambda_B t} \quad \text{for } k_1 \leq t \leq k_2 \quad (4.15)$$

$$R_{s_2}(t) = e^{-\lambda_B t} + e^{-\left(\frac{t - k_2}{\alpha_2}\right)^{\beta_2}} \quad \text{for } t \geq k_2, \alpha_2 > 0, \beta_2 > 1 \quad (4.16)$$

Eq. (4.13)-(4.16) entail the assumption that random failures occur throughout both phase 2 and phase 3, but in phase 3 an accelerating degradation of the structure over time takes place and this is described by a Weibull distribution.

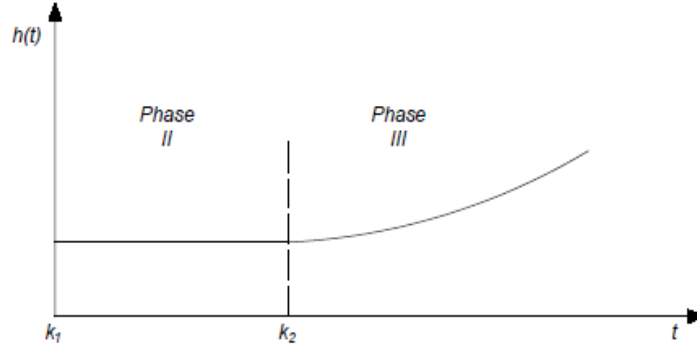


Figure 4.2 Bath-tub failure pattern for gas transmission pipelines

Setting $\alpha_{FT} = \frac{\beta_2}{\alpha_2 \beta_2}$ and $\beta_{FT} = \beta_2 - 1$, Eq. (4.14) becomes:

$$h(t) = \lambda_B + \alpha_{FT}(t - k_2)^{\beta_{FT}} \quad (4.17)$$

According to Cox and Oaks (1984) and Leemis (1995), a discrete hazard function can be defined as:

$$h_t = \frac{f_t}{R_s(t_{t-1})}, \quad t = 1, 2, \dots, \quad (4.18)$$

where h_t is the hazard function, $R_s(t_{t-1})$ is the reliability function, which is also referred to as the survival function and f_t is a discrete failure probability function that is equal to:

$$f_t = R_s(t_{t-1}) - R_s(t_t), \quad t = 1, 2, \dots, \quad (4.19)$$

In the limit of small time intervals Δt , the discrete hazard rate measures the rate of failure in the next instant on time, for those segments of the population (conditioned on) surviving to time t :

$$h_t = \frac{N_s(t_{t-1}) - N_s(t_t)}{\Delta t \cdot N_s(t_{t-1})}, \quad t = 1, 2, \dots, \quad (4.20)$$

where $N_s(t_{t-1})$ and $N_s(t_t)$ are the numbers of functional segments of a population at time t_{t-1} and t_t respectively.

Eq. (4.20) is also called the force of mortality and is a property of a time to failure distribution (Ebeling, 1997). This approach is considered adequate for the purpose of deriving the hazard function of gas transmission pipelines, since these can be divided in

segments of same or similar characteristics, as described in the following example of section 4.5. Also, this approach can efficiently deal with scarce, left or right-censored data, by estimating discrete hazards solely at times that failure data are available (Sun et al., 2011).

Once the hazard function has been derived, parameters of Eq. (4.17) should be then estimated. The adopted approach for parameter estimation is comprised of two parts. The first part is a heuristic method proposed elsewhere (Sun et al., 2011) and regards parameters λ_B and k_2 . In specific, parameter k_2 can be determined by the discrete hazard bar chart that is produced from Eq. (4.20). Parameter k_2 is thought to be easily attainable in the presence of complete and consistent data, but due to statistical uncertainties and fluctuations, this is not always the case and expert opinion is usually necessary. Furthermore, λ_B is a constant rate of the exponential failure distribution and represents the random failure phase. The value of λ_B can be obtained as the average of discrete hazard values that belong to this phase, i.e. phase 2. It can be defined as:

$$\lambda_B = \frac{1}{N_k} \sum_{1 < t \leq N_k} h_t \quad (4.21)$$

where $k=k_2-k_1$

Finally, parameters α_{FT} and β_{FT} need to be estimated from the wear-out phase, i.e. phase 3, by means of the robust graphical method described in the next section.

4.3.3 Non-linear Quantile Regression

The most commonly adopted methods in literature for parameter estimation of probabilistic models are the maximum likelihood method and the linear (or non-linear) least-squares regression method (Rigdon and Basu, 2000; Basile et al. 2004; Caleyó et al. 2008; Tee et al., 2013; Morrison and Spencer, 2014). Maximum likelihood method has the limitation that requires sufficient failure data to produce credible results. Least-squares regression has often been applied to derive the mean response of the dependent variable (hazard function herein), as a function of the independent variable (time herein). However, both of these are thought to have difficulty in describing scarce and censored data and also fail to yield a complete picture of the variables' relationships. This is especially the case

for heteroscedastic data, data with non-Gaussian error distributions and data derived from sample selections. Also, they are sensitive to extreme outliers that can distort the results significantly. Furthermore, many times the researcher aims to obtain an upper bound of the relationship such that the final result is conservative. This is especially the case in applications such as gas pipelines, where extremes are important and upper quantiles of rupture incident levels are critical from a public health perspective. This can be achieved by the quantile regression, since it can estimate multiple rates of change, i.e. slopes, from the minimum to maximum response (Cade and Noon, 2003; Chen, 2005).

Non-linear quantile regression is considered to be able to deal with the aforementioned challenges and is employed for the data analysis and estimation of the parameters α_{FT} and β_{FT} , contained in Eq. (4.17). It is a quantifiable, repeatable and non-biased statistical methodology that provides estimates for a given quantile or, equivalently, a given probability of exceedance. The greatest quantile that can be calculated by the method, depends on the number of data points available in the dataset. For datasets with small numbers of data, for instance less than 20 data points, it is likely that the quantile regression lines for quantiles $\tau_q = \{0.95, 0.98, \text{ and } 0.99\}$, might be represented by the same line. The existence of various slope estimates for different quantiles, constitutes an indirect confirmation of the heteroscedasticity of the dataset (Morrison and Spencer, 2014). Errors are assumed to be independent and identically distributed (iid) in this study.

Typically a response variable y_B is some function of predictor variables x_B , so that $y_B = f(x_B)$. To this end, Eq. (4.17) is rearranged and set as follows:

$Q_{y_B} = h(t) - \lambda_B$ and $x_B = t - k_2$, so that the following non-linear relationship can be defined:

$$Q_{y_B} = \alpha_{FT} \cdot x_B^{\beta_{FT}} \quad (4.22)$$

The conditional quantiles denoted by $Q_{y_B}(\tau_q|x_B)$ are the inverse of the conditional cumulative distribution function of the response variable $F_{y_B}^{-1}(\tau_q|x_B)$, where $\tau_q \in [0,1]$ denotes the quantiles (Koenker and Machado, 1999). For example, for $\tau_q = 0.90$, $Q_{y_B}(0.90|x_B)$ is the 90th percentile of the distribution of y_B conditional on the values of x_B , i.e. 90% of the values of y_B are less than or equal to the specified function of x_B . In contrast to the mean regression technique, which employs the least-squares procedure, parameters from the quantile regression are obtained by minimizing (Cao and Dean, 2015):

$$S_Q = \sum_{Q_{y_{B_t}} \geq \hat{Q}_{y_{B_t}}} \tau_q [Q_{y_{B_t}} - \hat{Q}_{y_{B_t}}] + \sum_{Q_{y_{B_t}} < \hat{Q}_{y_{B_t}}} (1 - \tau_q) [Q_{y_{B_t}} - \hat{Q}_{y_{B_t}}] \quad (4.23)$$

The non-linear iid quantile regression problem is solved using an interior point algorithm. It is analytically described in Koenker and Park (1996). More references to the methodology and code of non-linear regression are provided herein. The non-linear quantile regression method is part of the quantile regression package `quantreg` in R software, which was used for the respective estimations herein (Koenker, 2012). The method directly generates quantiles at a specified exceedance level, removing the requirement for subjectively processing the data and therefore results in a method that produces a unique answer (Morrison and Spencer, 2014; Cao and Wang, 2015).

4.4 Case Study based on the NPI methodology

4.4.1 General

The purpose of this case study is to numerically apply the NPI for competing risks in the aforementioned PHMSA dataset and then derive lower and upper probabilities, as well as survival functions for different competing failure causes, for the future onshore gas transmission pipe segment that will fail due to rupture. Only ruptured pipes are of interest in this study. Given that only a tiny fraction of the overall number of pipes fails in the entire US gas transmission pipeline network, applying the competing risks theory on the entire network would be unfruitful, since the impact of incidents is trivial and the same results are produced, either for realistic competing risks' probabilities or for net probabilities. A net survival probability is for instance one that describes the probability of surviving external corrosion in the hypothetical world where a pipeline cannot rupture from any other cause. Relative survival and cause-specific survival attempt to estimate this, under specific assumptions. The second methodology proposed in this chapter covers such an analysis, one that takes into account the entire US gas transmission pipeline network. The focus thus herein, is to analyse the rupture incidents, so that realistic marginal expectations of the interdependency among failure causes can be derived and a cumulative rupture function of pipe segment ruptures can be defined in a comprehensive way.

The main assumption of the methodology is that the future pipe segment undergoes the same process and conditions, as the ones that have reportedly failed thus far. Taking into consideration that only a very specific category of pipelines, i.e. onshore gas transmission, is examined, it is reasonable to assume that similar behaviour is expected from this type of pipelines. Besides, as described in Section 4.2, there are certain attributes that are common for the majority of onshore gas transmission pipelines that operated between 2002-2014 (class location 1, carbon steel material of construction and cathodic and coating protection). The future pipe segment that is examined against rupture is assumed to be a typical 12m long pipe segment. For the sake of exchangeability which is inherent in the NPI approach, each one of the 179 reported ruptures is assumed to originate from one or a number of defects confined to the 12m pipe segment, irrespective of the propagation length, post rupture initiation. The rupture lengths reported by pipeline operators in the database besides, were found to be on average around 10m, which corroborates this assumption.

Next, from the different types of failure that stem from different (thus competing) failure causes, only rupture is examined. In the period 2002-2014, 189 pipe-related rupture incidents were found in the database. The time to failure is of interest in the methodology and as a result the installation dates of the pipelines that failed due to rupture were listed. However, 10 rupture incidents concerned pipelines whose installation dates were unknown (had not been reported to PHMSA). These 10 rupture incidents were not taken into consideration, without significantly distorting the analysis. In Tables 4.3 and 4.4 a breakdown of the numbers and percentages of the different failure causes for the 189 and the 179 rupture cases is presented. It can be observed that ignoring the incidents with unknown installation dates (and thus times to failure), does not impact rupture frequencies due to different failure causes significantly. The time to failure is estimated by subtracting the year of installation from the year of failure, for each rupture incident.

Table 4.3 179 Rupture failure data with known installation dates

Failure cause	Number	Percentage %
IC	19	10.61
EC	64	35.75
ED	27	15.08
PDP	9	5.03
MF	33	18.43
EM	10	5.59
O	17	9.50

Table 4.4 189 Rupture failure data with both known and unknown installation dates

Failure cause	Number	Percentage %
IC	19	10.05
EC	64	33.86
ED	31	16.40
PDP	10	5.29
MF	35	18.52
EM	10	5.29
O	20	10.58

4.4.2 Results and Discussion

The NPI for competing risks assumes that there are no ties among the data to avoid notational difficulties (Maturi et al., 2010). However, among the 179 rupture incidents there are many tied observations. The time to failure for each one of them was initially expressed in years. To deal with ties though, the years are converted in weeks (1 year was assumed to be equal to 52 weeks) and then a trivial difference of one week is assumed among tied observations. This difference is considered to be sufficiently low, in that it does not affect the order of observations in other (failure cause) groups. Ties among different failure cause groups were also notable and were treated distinctively for upper and lower bounds. They were handled in such a way that upper and lower probabilities became maximal and minimal respectively, over the possible ways of splitting such ties, without affecting the ordering of the rest of the observations (Maturi, 2010).

A rupture observation due to a specific failure cause is simultaneously a right-censored observation for all other failure causes. When one observation is right-censored for two or

more failure causes, then this is also dealt with by assuming that right censoring observations occurred marginally postliminary for one of the failure causes. Likewise, different possible orderings of the untied right-censoring times are considered, in an effort to maximise and minimise the upper and lower bounds respectively (Maturi, 2010). Next, Eqs. (4.9) and (4.10) are used to obtain the NPI upper and lower probabilities and compare different failure causes with respect to rupture of the future pipe segment.

The NPI upper and lower probabilities for the rupture event of unit 180 (the future pipe segment) due to external corrosion (EC) are:

$$\bar{P}(X_{180}^{EC} < X_{180}^{OFC}) = 0.3755$$

$$\underline{P}(X_{180}^{EC} < X_{180}^{OFC}) = 0.3427$$

while the corresponding NPI lower and upper probabilities for unit 180 to rupture due to other failure modes (OFC) are:

$$\bar{P}(X_{180}^{OFC} < X_{180}^{EC}) = 0.6573$$

$$\underline{P}(X_{180}^{OFC} < X_{180}^{EC}) = 0.6245$$

In the above, OFC refers to all failure causes except EC. These are all grouped together in one group named OFC and are jointly considered as a single failure cause and then compared with EC. OFC grouping is done in a similar way in the following, for different cases examined.

The NPI upper and lower probabilities for the rupture event of unit 180 due to material failure (MF) are:

$$\bar{P}(X_{180}^{MF} < X_{180}^{OFC}) = 0.2087$$

$$\underline{P}(X_{180}^{MF} < X_{180}^{OFC}) = 0.1765$$

while the corresponding NPI lower and upper probabilities for unit 180 to rupture due to other failure causes (OFC) are:

$$\bar{P}(X_{180}^{OFC} < X_{180}^{MF}) = 0.8235$$

$$\underline{P}(X_{180}^{OFC} < X_{180}^{MF}) = 0.7913$$

The NPI upper and lower probabilities for the rupture event of unit 180 due to external damage (ED) are:

$$\bar{P}(X_{180}^{ED} < X_{180}^{OFC}) = 0.1798$$

$$\underline{P}(X_{180}^{ED} < X_{180}^{OFC}) = 0.1474$$

while the corresponding NPI lower and upper probabilities for unit 180 to rupture due to other failure causes (OFC) are:

$$\bar{P}(X_{180}^{OFC} < X_{180}^{ED}) = 0.8526$$

$$\underline{P}(X_{180}^{OFC} < X_{180}^{ED}) = 0.8202$$

It is observed that for each one of the above three pairs of failure causes (EC and OFC, MF and OFC, ED and OFC) examined, the lower and upper probabilities satisfy the conjugacy property (Coolen, 1996). This is due to the fact that implicit in this method is the assumption that the future segment eventually ruptures and this is assumed to happen with certainty. When comparing one failure cause group with another group (or more than one group as shown next), the resulting NPI upper and lower probabilities can provide either a weak or a strong indication about the future unit's failure (Maturi et al., 2010). For example, the NPI lower and upper probabilities presented above, contain a strong indication that the future segment will rupture due to another failure cause (OFC) when all the other failure causes are grouped together, instead of when EC, MF and ED failure causes are separate. This holds because:

$$\underline{P}(X_{180}^{OFC} < X_{180}^{EC}) > \bar{P}(X_{180}^{EC} < X_{180}^{OFC}) \text{ and likewise for MF and ED.}$$

In the next example, the weak indication term is also discussed. A different grouping of the same time to failure data is illustrated. In specific, groups with three failure causes are considered each time and inferences in the form of weak and strong indications are derived in a similar manner to the case of two groups.

The NPI upper and lower probabilities for the event that unit 180 will rupture due to either EC, MF or OFC are as follows:

$$\bar{P}(X_{180}^{EC} < \min\{X_{180}^{MF}, X_{180}^{OFC}\}) = 0.3755$$

$$\underline{P}(X_{180}^{EC} < \min\{X_{180}^{MF}, X_{180}^{OFC}\}) = 0.3321$$

$$\bar{P}(X_{180}^{OFC} < \min\{X_{180}^{MF}, X_{180}^{EC}\}) = 0.4806$$

$$\underline{P}(X_{180}^{OFC} < \min\{X_{180}^{MF}, X_{180}^{EC}\}) = 0.4407$$

$$\bar{P}(X_{180}^{MF} < \min\{X_{180}^{EC}, X_{180}^{OFC}\}) = 0.2087$$

$$\underline{P}(X_{180}^{MF} < \min\{X_{180}^{EC}, X_{180}^{OFC}\}) = 0.1707$$

The fact that $\underline{P}(X_{180}^{EC} < \min\{X_{180}^{MF}, X_{180}^{OFC}\}) > \bar{P}(X_{180}^{MF} < \min\{X_{180}^{EC}, X_{180}^{OFC}\})$ provides a strong indication that EC is more likely than MF to cause a rupture, with all other failure causes grouped together as OFC.

The NPI upper and lower probabilities for the event that unit 180 will rupture due to either EC, excavation damage (ED) or OFC are as follows:

$$\bar{P}(X_{180}^{EC} < \min\{X_{180}^{ED}, X_{180}^{OFC}\}) = 0.3755$$

$$\underline{P}(X_{180}^{EC} < \min\{X_{180}^{ED}, X_{180}^{OFC}\}) = 0.3321$$

$$\bar{P}(X_{180}^{OFC} < \min\{X_{180}^{ED}, X_{180}^{EC}\}) = 0.5097$$

$$\underline{P}(X_{180}^{OFC} < \min\{X_{180}^{ED}, X_{180}^{EC}\}) = 0.4667$$

$$\bar{P}(X_{180}^{ED} < \min\{X_{180}^{EC}, X_{180}^{OFC}\}) = 0.1798$$

$$\underline{P}(X_{180}^{ED} < \min\{X_{180}^{EC}, X_{180}^{OFC}\}) = 0.1449$$

The NPI upper and lower probabilities for the event that unit 180 will rupture due to either MF, ED or OFC are as follows:

$$\bar{P}(X_{180}^{ED} < \min\{X_{180}^{MF}, X_{180}^{OFC}\}) = 0.1798$$

$$\underline{P}(X_{180}^{ED} < \min\{X_{180}^{MF}, X_{180}^{OFC}\}) = 0.1449$$

$$\bar{P}(X_{180}^{MF} < \min\{X_{180}^{ED}, X_{180}^{OFC}\}) = 0.2087$$

$$\underline{P}(X_{180}^{MF} < \min\{X_{180}^{ED}, X_{180}^{OFC}\}) = 0.1707$$

$$\bar{P}(X_{180}^{OFC} < \min\{X_{180}^{ED}, X_{180}^{MF}\}) = 0.6761$$

$$\underline{P}(X_{180}^{OFC} < \min\{X_{180}^{ED}, X_{180}^{MF}\}) = 0.6284$$

In a similar manner, these NPI lower and upper probabilities can also provide weak indications, for the event that the future segment ruptures due to a specific failure cause. For example, the future rupture event due to ED is slightly less likely compared to rupture due to MF, with all other failure causes grouped together (OFC). This is because:

$\bar{P}(X_{180}^{ED} < \min\{X_{180}^{MF}, X_{180}^{OFC}\}) < \bar{P}(X_{180}^{MF} < \min\{X_{180}^{ED}, X_{180}^{OFC}\})$ and

$\underline{P}(X_{180}^{ED} < \min\{X_{180}^{MF}, X_{180}^{OFC}\}) < \underline{P}(X_{180}^{MF} < \min\{X_{180}^{ED}, X_{180}^{OFC}\})$, respectively.

However, $\bar{P}(X_{180}^{ED} < \min\{X_{180}^{MF}, X_{180}^{OFC}\}) > \underline{P}(X_{180}^{MF} < \min\{X_{180}^{ED}, X_{180}^{OFC}\})$ means that there is not a strong indication for this event.

It is noted that, for all the cases illustrated above, there is a strong indication that the future segment will rupture due to OFC, instead of the EC, MF and ED failure causes, similarly to the result obtained when only two groups of failure causes were considered. All the above results are in line with the basic underlying theory of statistics corresponding to imprecise probabilities. Thus, when three separate groups of failure causes are considered instead of two, which means that the data is represented in more detail, the upper and lower probabilities entail more imprecision. For instance, the upper and lower probabilities of rupture due to EC is [0.3427, 0.3755] for two groups and [0.3321, 0.3755] for three groups. According to Maturi et al. (2010), this is in line with the fundamental principle of NPI, in the context of multinomial data.

Another inference from the above-described upper and lower probabilities, is that relatively early failures, when compared with later ones, do not impact the final result. While, for example, ED and MF have many more early failures than EC, this does not affect the final result. This is something expected though, since data correspond to competing risks on the same segments and not completely independent failure times per group. Nevertheless, this method is considered advantageous, since it enables inferences with regard to actual failure times, as opposed to other standard statistical methods that measure only frequency of failures. Finally, it can be observed that the upper probability for the future rupture event due to either EC, MF or ED, is the same irrespective of whether two or three groups were considered. When it comes to EC for instance, the upper probability is realised with the extreme assignments of probability masses in the intervals created by the data, in accordance to the lower survival function for EC and the upper survival function for the other failure causes. Since all failure causes are assumed independent, the upper survival function for the other failure causes is the same, irrespective of the number of separate groups considered.

It is noted that, there is no limited time period considered for the estimated upper and lower probabilities. For insights into time of rupture occurrence, the upper and lower

survival functions presented next can be examined, either for one specific failure cause or for multiple combined. The survival function is directly linked to the probability of rupture of the future pipe segment, without any knowledge of underlying distributions, by only adopting the observed data (Coolen-Schrijner and Coolen, 2004; Barone and Frangopol, 2014). The survival functions illustrated in Fig. 4.3, result from completely neglecting the information on different failure causes and correspond to the situations of two and three groups of failure causes, respectively. The lower survival function $\underline{S}_{180}^{2CR}$ concerns two groups of failure causes and is assessed by multiplying the conditional (on different failure causes) lower survival functions. The lower survival function $\underline{S}_{180}^{3CR}$ is derived in a similar manner, for three groups of failure causes. These lower and upper survival functions demonstrate the expected nested structure according to the level of detail of data representation, similarly to the lower and upper probabilities.

Then, in Fig. 4.4 the NPI lower and upper survival functions, corresponding to two separate failure causes (EC and MF), are presented. For example, \underline{S}_{180}^{EC} is obtained by considering the 64 ruptures caused by EC as actual failure time observations and the rest 115 observations as right-censored data. The same procedure was implemented and is illustrated for MF in Fig. 4.4 and for the rest of the failure causes in Fig. 4.5 and Fig. 4.6. The inferences derived from Figs. 4.4-4.6, are relevant to the nature and magnitude of ruptures caused by each cause. For instance, the fact that EC causes less early failures than MF, IC, ED, OTHER, EM is evident in Figs. 4.4-4.6. Also, it is noted that the fewer the total failures due to any failure cause, the higher the imprecision (difference between corresponding upper and lower survival functions), at larger service life times. The fact that in all results, the lower survival function is always equal to zero beyond the largest observation, while the upper survival function remains positive, is something inherent in the NPI approach. Finally, it can be inferred that these survival functions can be used to define relevant maintenance strategies, in the form of upper and lower bounds or even more robustly, by adopting only the lower survival function.

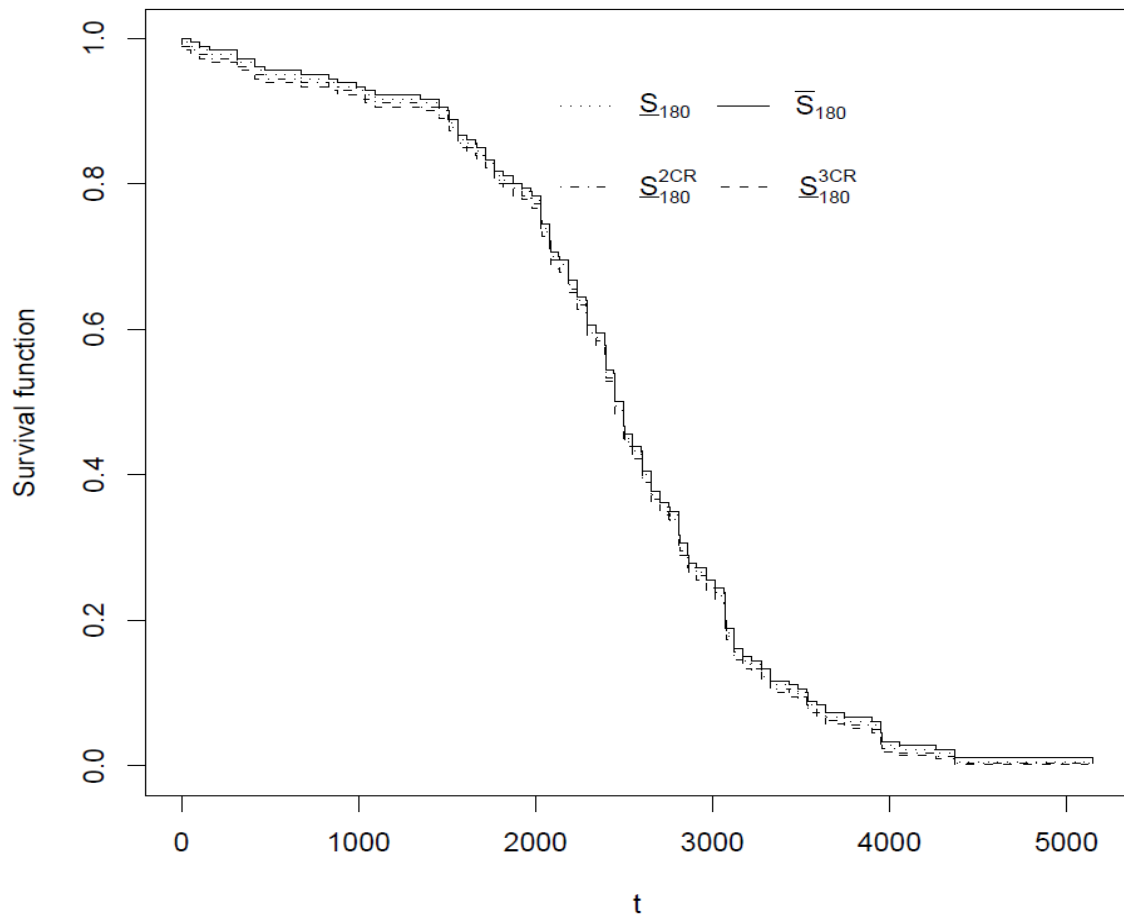


Figure 4.3 NPI lower and upper survival functions for a future pipe segment with t in weeks

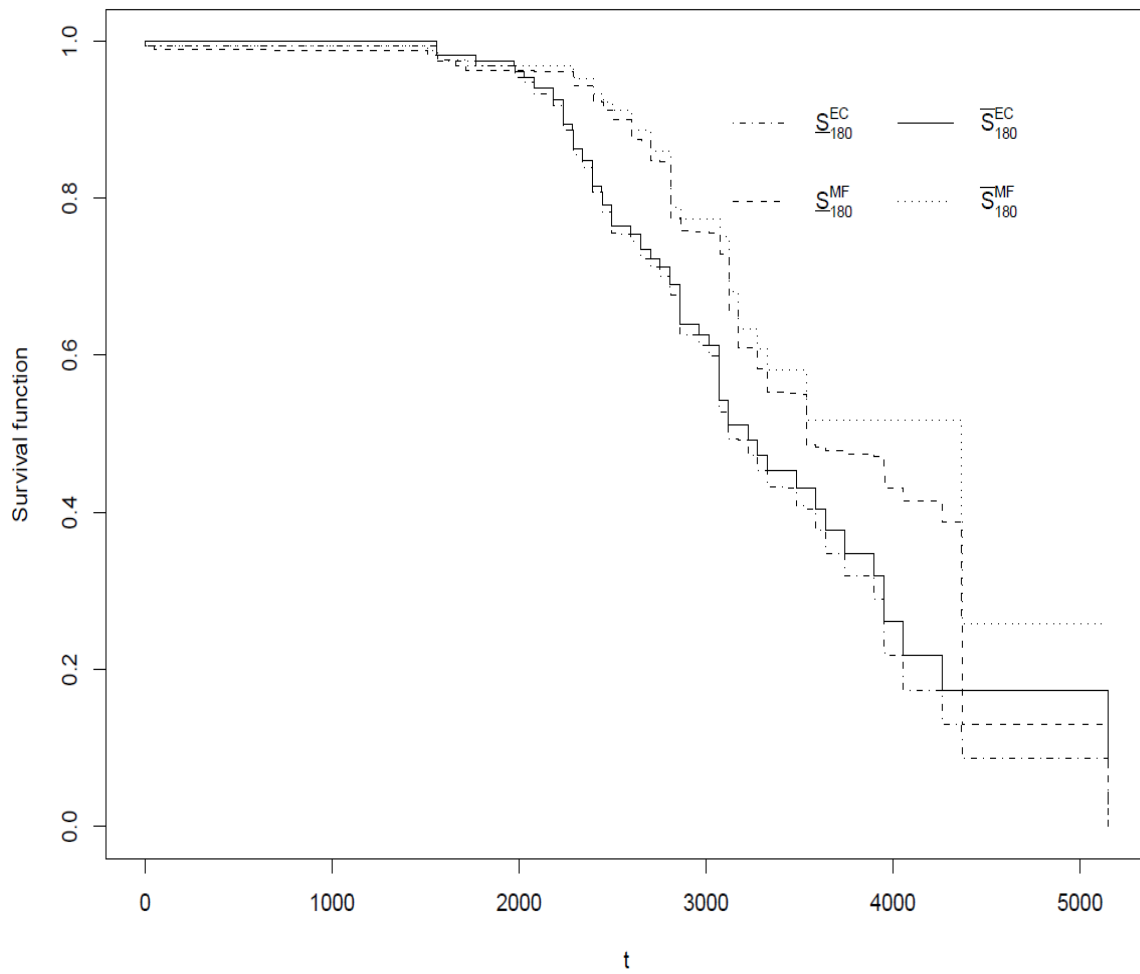


Figure 4.4 NPI conditional (EC, MF) lower and upper survival functions for a future pipe segment with t in weeks

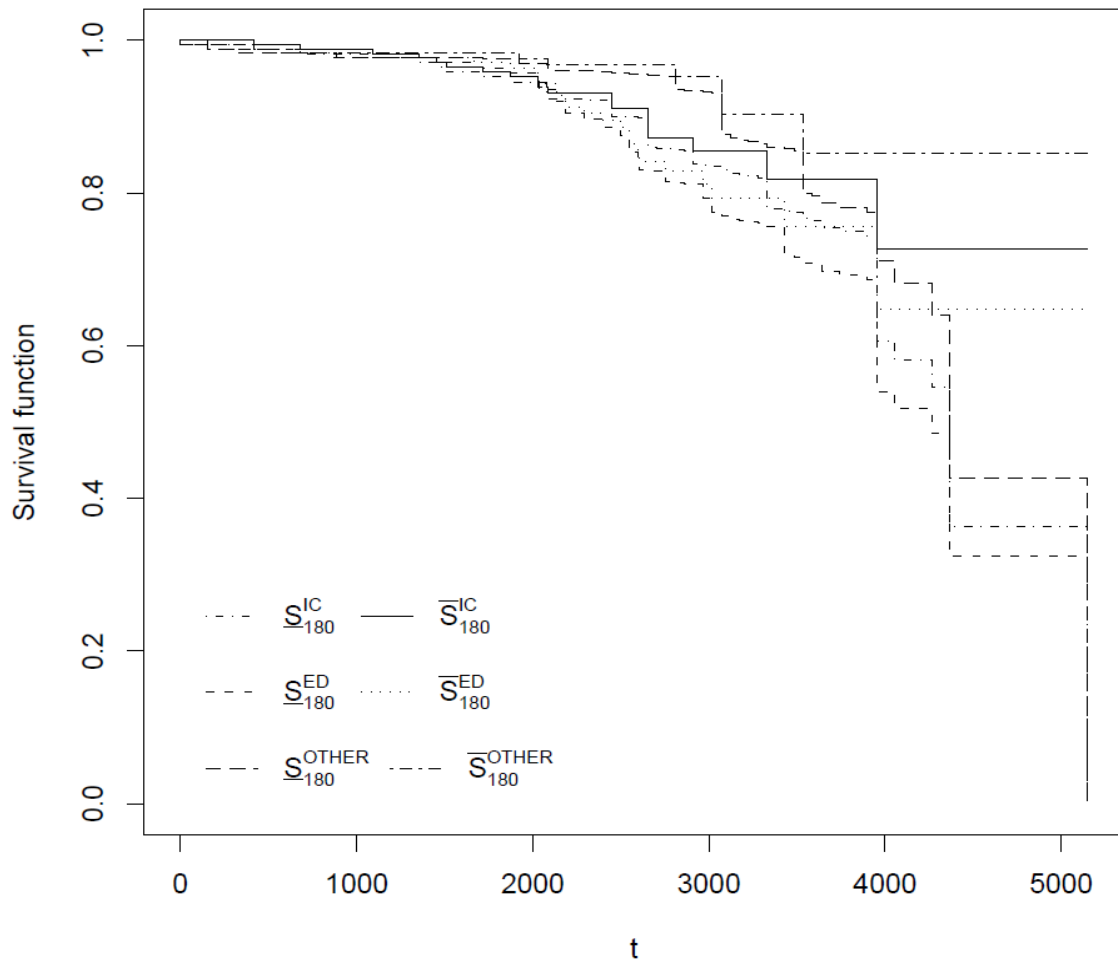


Figure 4.5 NPI conditional (IC, ED, OTHER) lower and upper survival functions for a future pipe segment with t in weeks

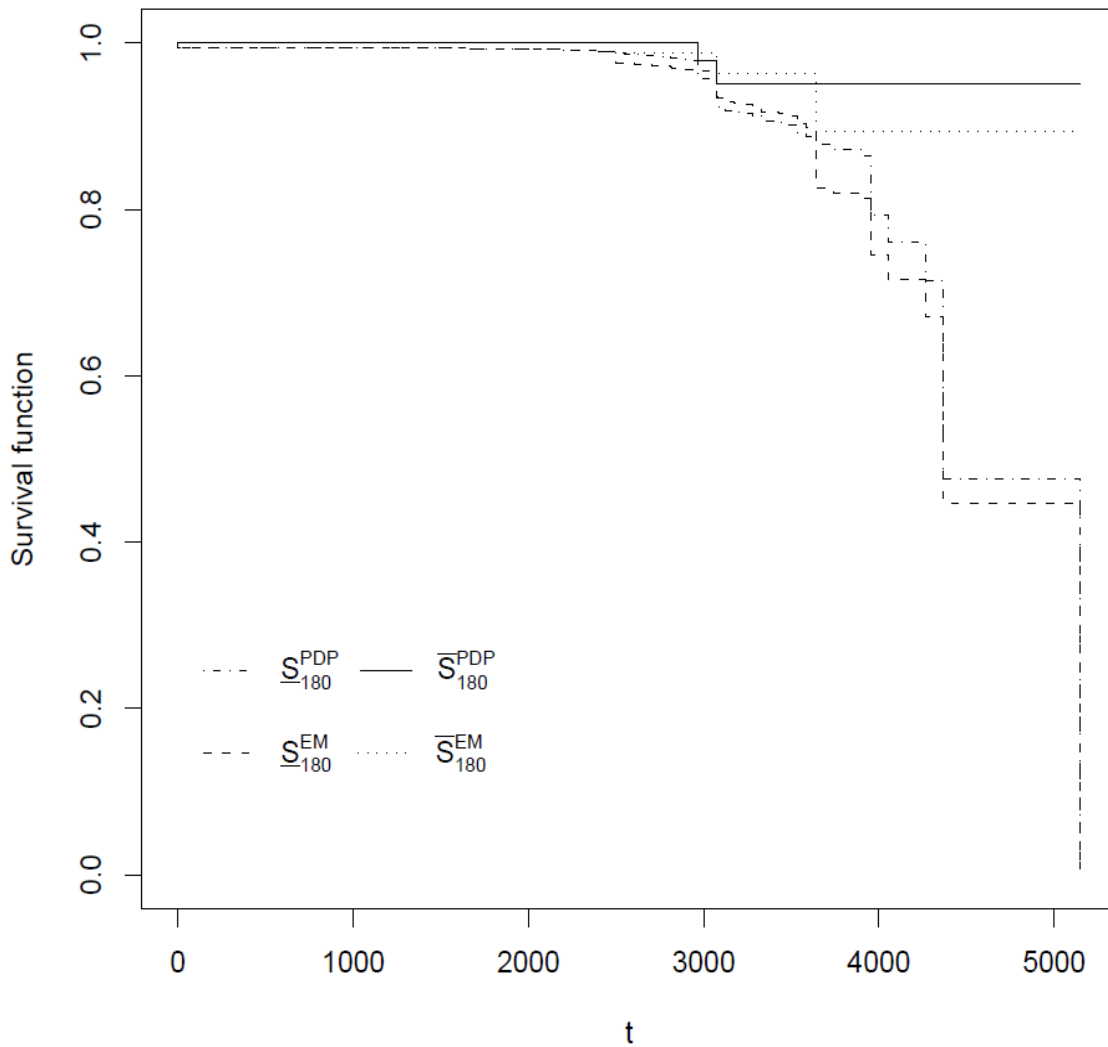


Figure 4.6 NPI conditional (PDP, EM) lower and upper survival functions for a future pipe segment with t in weeks

4.5. Case Study based on the Parametric Hybrid Methodology

4.5.1. General

The statistical analysis methodology presented in Section 4.3 is applicable to any energy pipeline network with a large population of segments and available historical rupture data. In fact, it is efficient with scarce and/or censored historical data. Similarly to the first case study, the rupture data from PHMSA database for the period 2002-2014 are employed,

with respect to onshore gas transmission pipelines. Moreover, the installation dates of pipes are used, in order to derive the respective hazard and reliability functions. Upon rupture, the pipe segment is assumed to be discarded and replaced by a new one, considering the segments as non-repairable. The proposed statistical analysis methodology, assumes that the network under consideration, can be divided into a number of similar pipe segments, based on an adequate segmentation length. The resulting population of segments is considered to operate under similar conditions. This is also assumed for those pipe segments that have reportedly failed. This assumption certainly entails some level of approximation but, as already analysed in Section 4.3, only one category of pipelines (onshore gas transmission) is examined and thus, it is considered reasonable to expect, at a significant extent, similar behaviour from this specific type of pipelines.

The segmentation length is assumed to be 12.5m, which is approximately the typical length of a newly-constructed pipe segment in industry. Also, rupture incidents are assumed to be confined to the 12.5m pipe segment. The rupture lengths of the 189 incidents, which are reported by pipeline operators in the database for the period 2002-2014, was found to be around this magnitude (on average around 10m). As a result, the assumption that a pipe segment of 12.5m is discarded after rupture and replaced by a new one is considered fairly representative of real industry practice. Thus, the gas transmission pipelines are assumed to form a statistically-related population of 12.5m long segments, performing a similar function in a similar location. As mentioned already, 189 pipe-related rupture incidents were reported in PHMSA, in the period 2002-2014. The time to rupture is of interest and as a result the installation dates of the ruptured pipes are considered. However, 10 rupture incidents concerned pipes whose installation dates are unknown (not reported in the PHMSA). These 10 rupture incidents are not taken into consideration, adding extra uncertainty when all failure cause rupture incidents are examined. However, this uncertainty is thought to be counterbalanced at a significant extent, by the fact that a percentage of approximately 2% of the total mileage on an annual basis is of unknown age (installation date) as well and thus neglected in the analysis.

Furthermore, the lack of detailed information in the PHMSA mileage database, with respect to the age of the operating network, necessitates the estimation of average values. For every year between 2002 and 2014, the installation dates are available per decade. As a result, different age groups of operating pipelines can be inferred for every year between 2002 and 2014. A careful examination of the yearly changes of pipeline lengths for each

installation date group, for the period 2002-2014, indicates that each year 4000km to 5000km of new pipelines are added to the network on average. Some pipelines are replaced throughout the period 2002-2014 and thus the total network mileage remains almost unchanged. In this study, the installation dates for years 2004 and 2014 were selected and the mean time of their values were used to derive the respective pipeline age groups as presented in Table 4.5. It is noted that, only pipeline ages up to 64 years were considered, since beyond that value was impossible to derive plausible inferences about the respective mileage per year.

Table 4.5 Approximation of the onshore gas transmission pipeline network age groups in 2002-2014

Pipeline age (years)	Length (km)	Total number of Segments	Number of Segments per year
0-4	18.477,255	1.478.180	369.545
5-14	49.254, 3525	3.940.348	394.034
15-24	46.207,805	3.696.624	369.662
25-34	45.487,671	3.639.013	363.901
35-44	83.936,3135	6.714.905	671.490
45-54	116.157,758	9.292.620	929.262
55-64	73.381,536	5.870.522	587.052

The use of average values for 2004 and 2014, returns a value of 18.477,255 km for 0-4 year old pipelines. Compared to the initial observation that 4.000-5.000 km of new pipelines are installed every year for the period 2002-2014, it is evident that the mean values for 2004 and 2014, represent satisfactorily the entire period 2002-2014. The same level of accuracy is expected for the rest of age groups, amplified by the fact that 2004 is a very early year (3rd year) and 2014 is the final year of the studied period. Therefore, it can be inferred that the totality of pipe segments added and discarded from this network, are well taken into account in this approximate approach. Furthermore, for every age group listed in Table 4.5, the lengths are first converted to segments (with segmentation length 12.5m) and then divided by the number of years of each group, in order to derive the average number of pipe segments based on their age per year. Finally, for every year the number of incidents is estimated, based on the time to rupture of each reported incident. The respective discrete hazards are then derived from Eq. (4.20). The resulting discrete hazard rate chart is illustrated in Fig. 4.7. Within PHMSA, there are 20 rupture incidents

corresponding to pipe segments aged 65 years or more, with the older one being a 99 years old segment that ruptured due to external corrosion in 2009. These are not part of the hazard bar chart of Fig. 4.7, since the hazard dataset is right-censored at 64 years and only the remaining 159 reported incidents are accounted for. Finally, a service life of 100 years is considered for reliability prediction.

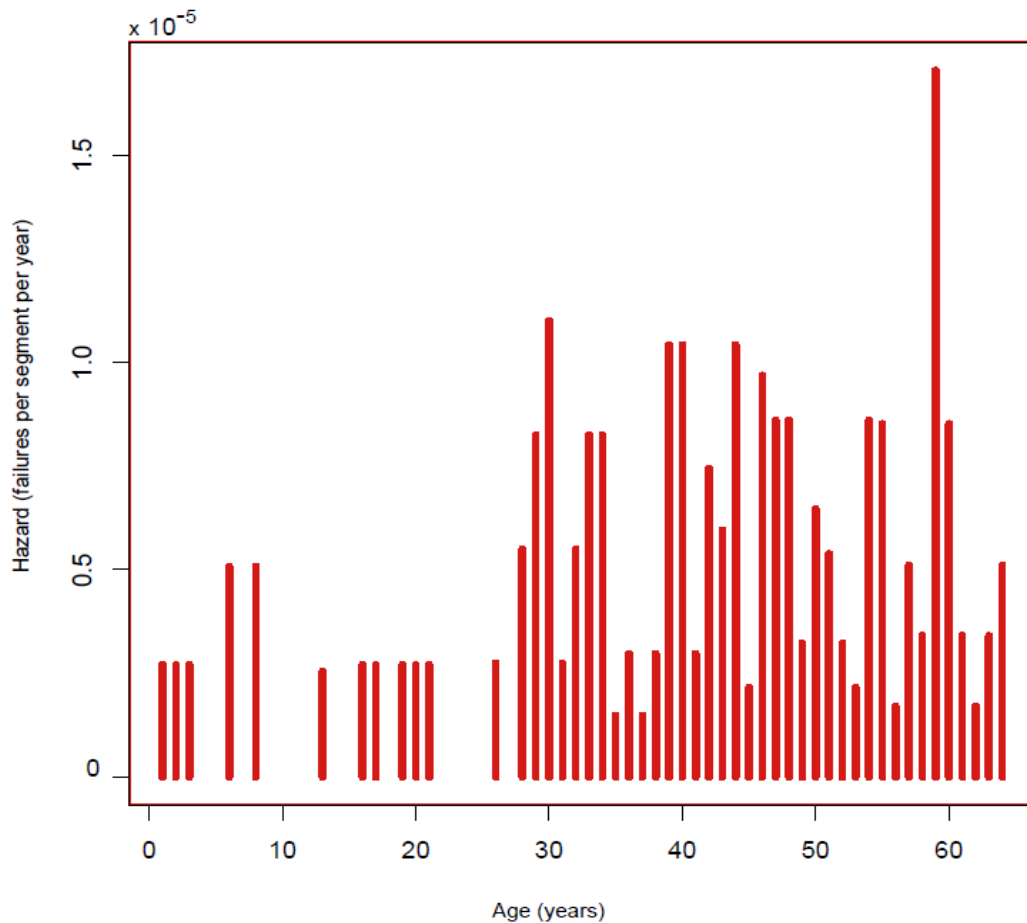


Figure 4.7 Rupture hazard bar chart of the onshore gas transmission pipeline network in 2002-2014

4.5.2 Results and Discussions

Following the formation of the discrete hazard bar chart presented in Fig. 4.7, the methodology presented in Sections 4.3.2 and 4.3.3 for hazard and reliability estimation is applied next. First, the hazard bar chart needs to be distinguished in random failure and wear-out phases, by deterministically defining parameter k_2 , which is the point that

separates them. In the example herein, it is easily obtained directly from observation of the chart and is evaluated as $k_2 = 27$ years. This is thought to be the year after which wear out initiates and thereupon increases in a rather consistent manner. This is verified not only by the fact that the majority of discrete hazards after k_2 have higher values, but also because there are no years with zero hazards. Furthermore, for the random failure period from year $k_1 = 0$ to $k_2 = 27$ years, the hazard rate is defined as the average of the discrete hazards within that period. The obtained average value is considered representative of the hazard trend for this period, since the respective values hardly fluctuate, whilst there are many zero values.

Next, the non-linear quantile regression method is adopted, as per Section 4.3.3, to evaluate the parameters α_{FT} and β_{FT} of Eq. (4.17). As mentioned already, the non-linear (iid) quantile regression problem is solved using an interior point algorithm, which is an iterative procedure that begins with initial estimates of the parameters. Different starting values of α_{FT} and β_{FT} of Eq. (4.17), could return slightly different final estimates of α_{FT} and β_{FT} . The results verify what is implied by the hazard bar chart format; the heteroscedasticity of the data. This is verified in an indirect way, since for different quantiles, different slope estimates are obtained. However, after 0.99 quantile, all slope estimates are the same and therefore are represented by the same line. Thus, the 0.99 is chosen as the adequate quantile for parameter evaluation, in this example. The reason is that an upper bound estimation is desirable from the safety viewpoint. Rupture incidents of gas pipelines are very critical from the public health perspective and thus a conservative estimation of the hazard function is of interest, so that all future hazard rates will be below the upper bound with a 1% probability of exceedance. Non-linear quantile regression has proven to be robust with outliers in this application, as they are efficiently taken into consideration with the 0.99 quantile estimation. Therefore, this method is thought to produce a credible characterisation of parameters α_{FT} and β_{FT} . Finally, in liaison with the discrete hazard estimation model, a reliability prediction for 100 years can be obtained, even though the dataset is incomplete and right-censored at 64 years. In other words, the hazard curve can be extended after 64 years, until 100 years are reached. The resulting parameters of Eq. (4.17) are presented in Table 4.6. The derived hazard function curve for all failure causes is presented in Fig. 4.8. The respective reliability function curve, for a prediction period of 100 years, is presented in Fig. 4.9.

Table 4.6 Parameter estimation results of Eq. (4.17) for all failure causes

Non-linear (iid) Quantile Regression (Starting Estimates: $\alpha_{FT}=4\cdot 10^{-6}$ $\beta_{FT}=10^{-2}$)		
Including Standard Errors		
Quantile	Power Law Fit	Including Standard Errors
0.99	$1.373\cdot 10^{-6}+7.655\cdot 10^{-6}\cdot (t-27)^{0.206}$	$1.373\cdot 10^{-6}+ 7.655\cdot 10^{-6}$ $(\pm 6.685\cdot 10^{-7})\cdot (t-27)^{0.206}$

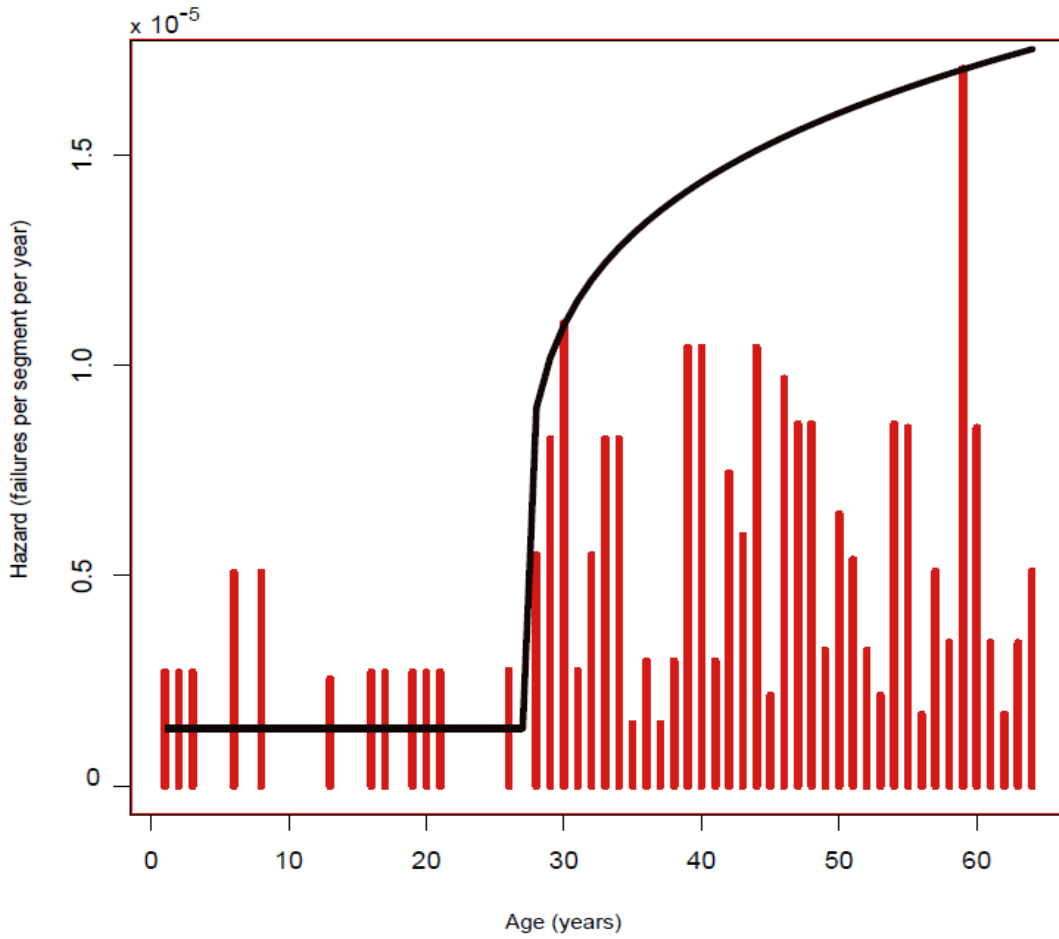


Figure 4.8 Hazard function curve for $\tau_q = 0.99$ quantile (all failure causes)

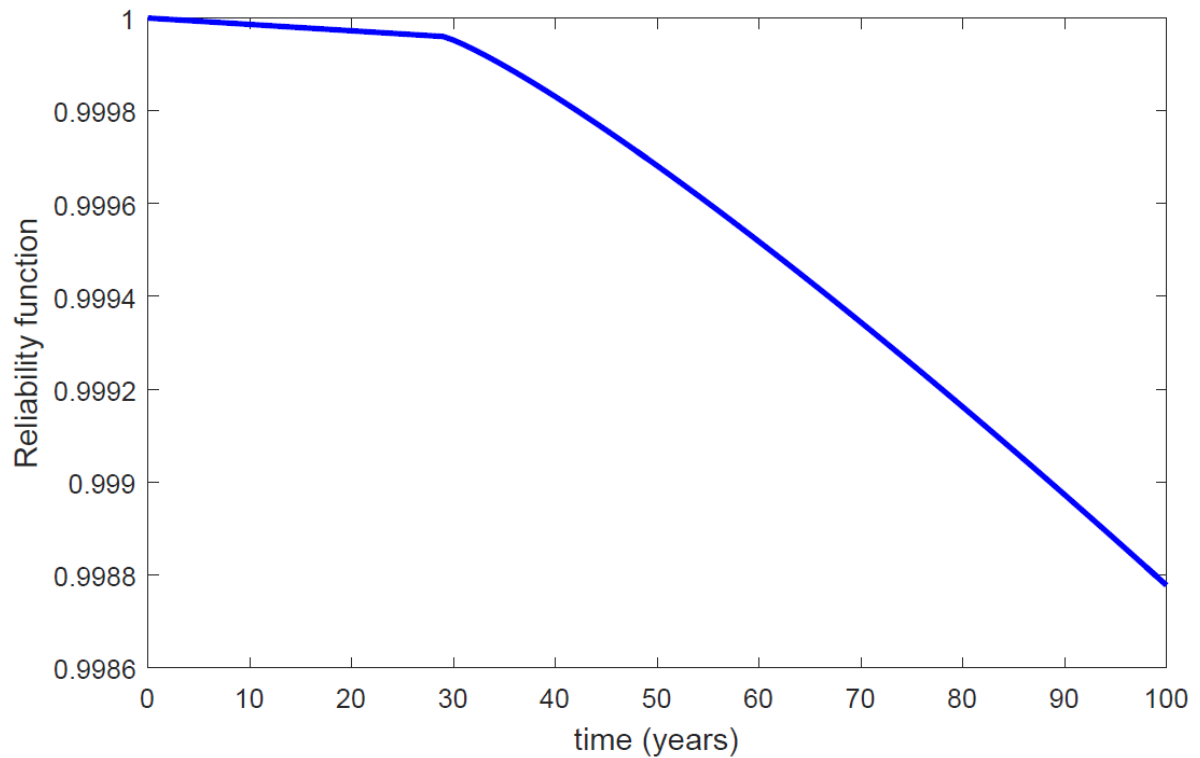


Figure 4.9 Reliability function against rupture of the average segment of the onshore gas transmission pipeline network in 2002-2014

4.5.2.1 Comparison and Cross-Verification of the Methodology

For the purpose of validation, the above statistical methodology was applied for rupture incidents caused by external corrosion, as reported to PHMSA between 2002-2014. Again, those incidents concerned pipelines of maximum 64 years of age, whilst stress corrosion cracking incidents were not counted. Even though external corrosion is considered a gradual deterioration failure mechanism, a random failure phase was nonetheless considered and the same methodology described in Section 4.3 was carried out. The rationale behind this lies in the particular nature of the external corrosion mechanism. According to practical experience, substantial time is normally required for metal-loss to reach the failure depth. As a result early external corrosion failures, in less than 10 years for example, are thought to be random in nature, caused typically from extremal conditions.

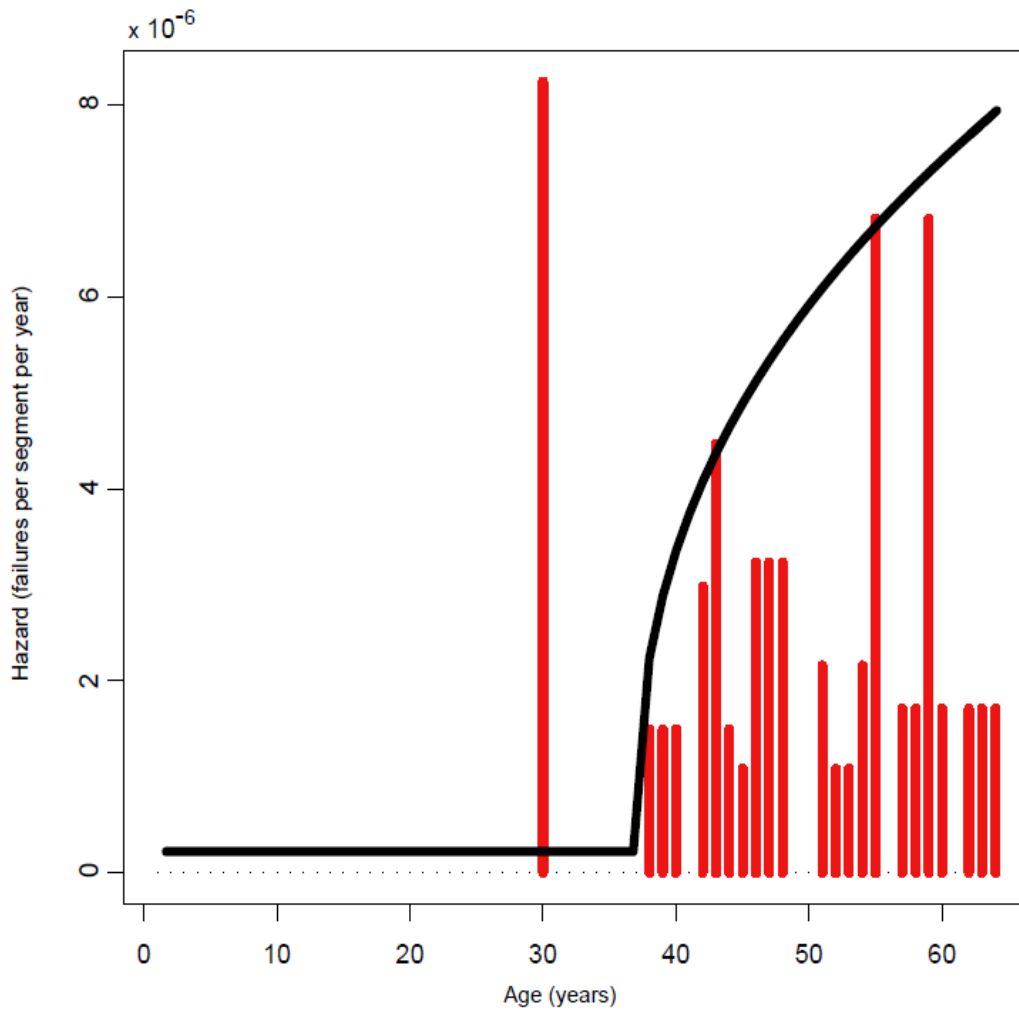


Figure 4.10 Hazard bar chart for rupture due to external metal-loss corrosion

Table 4.7 Parameter estimation results of Eq. (4.17) for external corrosion incidents

Non-linear (iid) Quantile Regression (Starting Estimates: $\alpha_{FT}=10^{-6}$ $\beta_{FT}=10^{-1}$) Including Standard Errors		
Quantile	Power Law Fit	Including Standard Errors
0.99	$2.228 \cdot 10^{-7} + 1.958 \cdot 10^{-6} \cdot (t-37)^{0.418}$	$2.228 \cdot 10^{-7} + 1.958 \cdot 10^{-6} (\pm 1.302 \cdot 10^{-7}) \cdot (t-37)^{0.418}$

Following this, the end point of the random failure phase for external corrosion ruptures was evaluated to be $k_2 = 37$ years by the respective hazard bar chart and then the upper bound for the wear out phase was estimated, based on the 0.99 quantile. It is noted that the end point of the random failure phase was not set as 30 years, even if the hazard rate

presents a peak value there. However, except for the highest rate values, the wear out phase is expected to also entail a consistent number of non-zero rate values. As it can be observed from Fig. 4.10, after 30 years there are 7 years of zero incidents, while beyond year 38 incidents take place far more consistently. Therefore, it can be deduced that the ruptures of year 30 belong to the random failure phase, which ends at 37 years. The resulting parameters of Eq. (4.17) for the external corrosion incidents are presented in Table 4.7 and the respective hazard curve in Fig. 4.10.

The resulting reliability function for 100 years that corresponds to the hazard curve of Fig. 4.10, is presented next in a comparative Fig. 4.11. The aim is to compare and validate this result, against the overall reliability result illustrated in Fig. 3.8 of Section 3.5.1. The latter is derived from the respective structural reliability analysis methodology that corresponds to a conceptual reference pipe segment, built upon the average characteristics of the ruptured pipe segments reported in PHMSA from 2002 to 2014. The comparative Fig. 4.11 presents the two reliability curves, obtained from the two different methods. These are considered to be in sufficiently good agreement, taking into consideration the generic and approximate nature of the mileage analysis, as well as the fact that some relative values had to be adopted in the structural reliability analysis. Therefore, the validity of both, as comprehensive methodologies, each one in their particular area, is considered to be cross-verified. Moreover, a better knowledge of the state of onshore gas transmission pipelines, as reported in PHMSA from 2002 to 2014, is also thought to have been obtained. This was achieved through reliability curves that depict reliability changes explicitly, throughout a complete service life of 100 years, as opposed to average annual failure rates for the 13 years among 2002 and 2014 that can be derived from the typically adopted ROCOF methods. As mentioned in Section 3.5.1, the defect density, growth rate and defect length values can be accurately defined based on a parametric study, if the aim is to increase the proximity among the results obtained from the structural reliability analysis and statistical analysis methodologies. This can be particularly relevant for pipeline operators that wish to evaluate specific defect parameters or other integrity threats, based on probabilistically assessed empirical evidence.

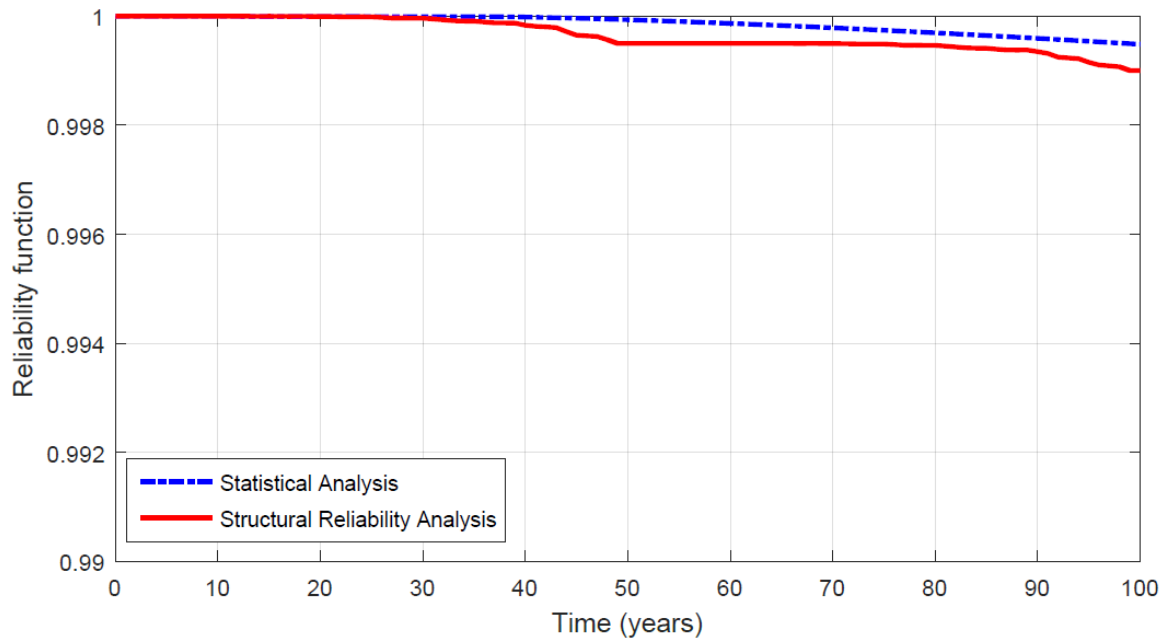


Figure 4.11 Comparison of the reliability function curves of the two different methodologies

4.6 Conclusions

The first methodology of this chapter employed the NPI approach in an attempt to derive inductive inferences from the lifetimes of a set of ruptured pipelines. This approach was applied in a PHMSA dataset of rupture incidents of onshore gas transmission pipelines for the period 2002-2014. The NPI method analysed the rupture incidents from a non-repairable systems perspective, based on the time to rupture of the pipe segments. It was shown that NPI is advantageous in deriving inferences for the future pipe segment that ruptures due to a specific failure cause, by providing imprecise probabilities and survival functions for this event, based on historical failure data. The results indicated external corrosion as the predominant rupture cause for the aforementioned database under consideration, with ruptures taking place mainly after 30 years. The predicted imprecise probabilities and survival functions, can be used to examine and implement maintenance strategies based on relative risk prioritization.

The second methodology was based on the PHMSA data for the period 2002-2014 as well. An empirical discrete hazard model was adopted in conjunction with a non-subjective parameter estimation technique, namely non-linear quantile regression, to evaluate the hazard and reliability functions. The model provided inferences on the reliability of a

region's reference pipe segment for its complete lifecycle, even in the case of scarce, incomplete and censored data, as opposed to the commonly adopted ROCOF methods in literature that only account for the limited time period under study. Furthermore, non-linear quantile regression is thought to have yielded a complete picture regarding the hazard dataset. Thus, it is considered that the generic nature of the historical data was reasonably accounted for and the resulting reliability lies within a credible expectation range. The results of the second statistical methodology were also compared with these of the structural reliability model of Section 3.5.1, which was based on the same set of PHMSA data. The results demonstrated reasonable proximity, which constitutes an inherent validation of the soundness of both methodologies and their estimations. The second statistical methodology can thus help pipeline operators to derive plausible expectations for the performance of either new or existing pipelines. These expectations can also be linked to specific parameters by means of parametric studies. The results of both methodologies are thought to provide additional knowledge on the state of the PHMSA onshore gas transmission network among 2002-2014 with respect to rupture, as opposed to results from the ROCOF-based approaches typically employed in literature. In addition, this period is considered representative of the most current operation and rehabilitation techniques and practices in industry, corroborating the significance of the results for new or existing pipelines. The methodologies of this chapter can therefore assist pipeline operators in making informed maintenance decisions, based on reliability and risk.

5. Bayesian Analysis of Pipeline Reliability Based on Imperfect Inspection Data

5.1 Introduction

Apart from metal-loss corrosion, environmental defects stemming from stress corrosion cracking (SCC) are also major threats to the safe operation and structural integrity of energy pipelines. A typical industry mitigation response to both of these, includes high-resolution in-line inspections (ILI) to measure defects on the pipeline body and estimate failure probabilities based on the inspection results. This chapter focuses on cases where ILI data is available on the model response, where Bayesian analysis serves the requirement to inversely determine the probabilistic input parameters given output data. The analytical estimation of the high-dimensional integrals involved in the Bayesian updating is impractical in pipeline problems and typically Markov Chain Monte Carlo (MCMC) sampling techniques are adopted to numerically perform the task (Al-Amin and Zhou, 2014).

The limitations of MCMC include the uncertainty around ensuring that the final samples have reached the posterior distribution and also the difficulty in ultimately quantifying small probabilities of rare failure incidents (Straub et al., 2016); particularly rupture due to metal-loss corrosion in the setting of energy pipelines (Zhang and Zhou, 2013). An alternative method to MCMC is Bayesian Updating with structural reliability methods (BUS), which sets an analogy between Bayesian updating and a reliability problem (Straub and Papaioannou, 2014a). This formulation enables the use of established Structural Reliability methods for the Bayesian updating. The Structural Reliability method adopted herein is Subset Simulation (SuS). The whole methodology is referred to as BUS-SuS and is considered to be an improved reinterpretation of the classical rejection sampling approach, to Bayesian analysis with subset simulation. BUS-SuS facilitates the estimation of small posterior failure probabilities directly within the same analysis framework, without the requirement of either explicit knowledge or approximation of the posterior joint probability distribution of the random variables (Straub et al., 2016).

In the present chapter, two case studies involving existing gas pipelines are used to illustrate and validate the proposed methodology. In the first case study, BUS-SuS is applied in an existing gas pipeline containing metal-loss corrosion defects. The pipeline is

subjected to high-pressure internal loading and BUS-SuS is validated against field data. The growth of multiple active metal-loss corrosion defects is characterised through adopting the gamma stochastic process and incorporating it into an hierarchical Bayesian framework based on multiple ILI data, along with a comprehensive consideration of associated measurement errors. A Ferry-Borges stochastic process is employed to model the internal process in the subsequent reliability analysis. The system reliability of the pipeline is evaluated in terms of three distinctive failure modes, namely small leak, large leak and rupture.

In the second case study, Bayesian updating is conducted by using BUS-SuS in conjunction with a data augmentation (DA) technique. Simulated data corresponding to an existing gas pipeline with high-pH SCC features and subjected to static internal pressure loading were used to illustrate and validate the proposed methodology. The growth of multiple active SCC features is characterised through adopting a non-homogeneous gamma process (NHGP) model and incorporating it into the Bayesian framework based on multiple ILI data, with the associated measurement errors comprehensively accounted for. Furthermore, the dependence among the growths of different crack features is considered in the analysis, using the Gaussian copula. The growth modeling focuses on the crack depth, as this is the most critical crack dimension for high-pH SCC under constant loading (Song et al., 2011). At the end, the system reliability is evaluated by means of the Battelle model (Yan et al., 2014) and the sensitivity of both the growth model and system reliability to different dependence scenarios is investigated.

The content of this chapter is organised as follows. Section 5.2 defines the uncertainties involved in the ILI data. The formulations of the stochastic models for the crack generation and growth are presented in Section 5.3. The Bayesian method for updating the model parameters by means of BUS-SuS and DA are described in section 5.4. The system reliability derivation is described in Section 5.5, for both metal-loss corrosion defects and SCC cracks. In Section 5.6, a numerical application is presented based on an real gas pipeline containing multiple active metal-loss corrosion defects. In Section 5.7, a case study involving simulated ILI data that correspond to another existing in-service gas pipeline that has presented high-pH SCC in the past is implemented, in order to illustrate and validate the proposed methodology. Finally, some concluding remarks are presented in section 5.8, on the basis of the outcomes of the study.

5.2 Uncertainties Associated with ILI Data

The probability distributions of the parameters of the gamma process model are updated based on the observation data. However, the ILI data are subject to measurements errors and sizing uncertainties associated with the ILI tools (Al-Amin et al., 2012). Herein, k corrosion defects of a pipeline segment are considered, which have been inspected l times over a given period and the measurement errors of the observations are taken into consideration extensively. As a result, the measured depth y_{ij} of the i^{th} defect ($i=1, 2, \dots, s$) at inspection j ($j=1, 2, \dots, l$) has the following relationship with the actual depth y_{ij} :

$$y_{ij} = c_{1j} + c_{2j}d_{ij} + \varepsilon_{ij} \quad (5.1)$$

The parameters c_{1j} , c_{2j} are the constant and non-constant biases associated with the ILI tool of the j^{th} inspection, which are assumed to be deterministic quantities. For instance, for $c_{1j} = 0$ and $c_{2j} = 1$ the tool is considered unbiased. Furthermore, ε_{ij} denotes the random scattering errors with respect to the measured depth, which are assumed to have zero means and known standard deviations (i.e. from the inspection tool specifications). Herein, it is assumed that ε_{ij} are spatially independent and identically distributed for a given inspection j . For a specific defect i , ε_{ij} are considered correlated and follow a multivariate normal distribution with a zero mean and known covariance matrix Σ_{ε} of the random scattering errors associated with different inspections (Al-Amin et al., 2012).

The PDF of $\boldsymbol{\varepsilon}_i = (\varepsilon_{i1}, \varepsilon_{i2}, \dots, \varepsilon_{il})^{\text{T}}$, with ‘‘T’’ denoting transposition, is given by:

$$f_{\boldsymbol{\varepsilon}_i}(\boldsymbol{\varepsilon}_i | \Sigma_{\varepsilon_i}) = (2\pi)^{-\frac{l}{2}} |\Sigma_{\varepsilon_i}|^{-\frac{1}{2}} \exp\left(-\frac{1}{2} \boldsymbol{\varepsilon}_i^{\text{T}} \Sigma_{\varepsilon_i}^{-1} \boldsymbol{\varepsilon}_i\right) \quad (5.2)$$

where Σ_{ε} is an l -by- l matrix with elements equal to $\rho_{fq}\sigma_f\sigma_q$ ($f = 1, 2, \dots, l$; $q = 1, 2, \dots, l$), with ρ_{fq} being the correlation coefficient between the random scattering errors associated with the f^{th} and the q^{th} inspections and σ_f , σ_q denoting the standard deviations of the random scattering errors associated with the tools used in inspections f and q , respectively.

The probability distribution of the random scattering error ε_{ij} associated with the reported defect i in the j^{th} inspection, can be determined from tool specifications that characterise the sizing accuracy, in terms of the probability of the error falling within prescribed bounds e_{min} and e_{max} . For instance, a tool that reportedly estimates defect depths within an error band of $\pm 10\%$ of the pipe wall thickness, with a probability of 90%. This information can be used to estimate the mean value (μ) and standard deviation (σ) of the random scattering error for any distribution type. Assuming that the mean and standard deviation

of the error are derived from a multivariate normal distribution, these can be calculated from the following, as illustrated in Fig. 5.1:

$$\mu = (e_{\min} + e_{\max}) / 2 \quad (5.3)$$

$$\sigma = (e_{\max} - \mu) / \left[\Phi^{-1} \left(\frac{1 + p_e}{2} \right) \right] \quad (5.4)$$

where Φ^{-1} is the inverse standard normal distribution function (Stephens and Nessim, 2006).

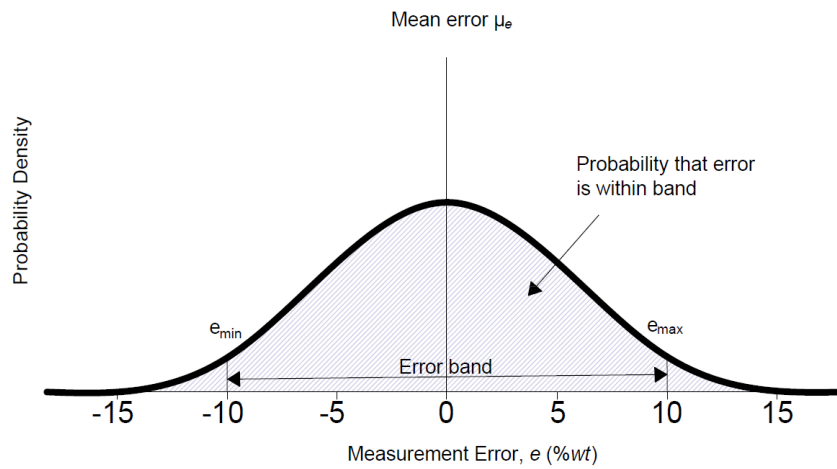


Figure 5.1 Measurement error band and corresponding probability

The probability of detection (PoD) for each corrosion defect can be estimated as per Eq. (3.14) of Section 3.3.1. This can be modified to include a detection threshold d_t , i.e. the smallest defect that can be detected, as follows:

$$\text{PoD} = 1 - e^{-q(d-d_t)} \text{ for } d \geq d_t \quad (5.5)$$

In brief, q defines the inherent tool detection capability and can be quantified from vendor-supplied tool specifications, e.g. 90% probability of detecting a defect with a depth of 10% of the pipe wall thickness (i.e. 10% w_t). The value of q is a constant that can be estimated if d_t and PoD values are known from tool specifications.

5.3 Stochastic Models for Corrosion Defect Generation and Growth

5.3.1 Generation of both Detected and Undetected Corrosion Defects

The non-homogeneous Poisson process (NHPP) was employed to model the generation of new corrosion defects on a given segment of the pipeline as per Eq. (3.1) of Section 3.2.1. In case of l ILIs that have taken place on a pipe segment of interest over a certain time period, it is thought that each inspection has the capacity to track new and existing defects, in terms of their spatial positions (Qin et al., 2015). Given the time of the j th inspection ($j = 1, 2, \dots, l$) t_j , the total number of defects S_j , can be distinguished into those defects that have initiated prior to the $(j-1)$ th inspection S_j^0 and those ones that have initiated between the $(j-1)$ th and j th inspections S_j^k . The value of S_j^k can then be estimated by assuming it follows a Poisson distribution with PMF given by:

$$f_p(S_j^k | \lambda_o, \delta) = \frac{(\Lambda_j)^{S_j^k} e^{-\Lambda_j}}{S_j^k!} \quad (5.6)$$

where $\Lambda_j = \int_{t_{j-1}}^{t_j} \lambda_o \tau^\delta d\tau$ and $t_0 = 0$.

The number of detected defects is typically smaller compared to the actual number of defects and that is due to the imperfect detectability of the ILI tool (Qin et al., 2015). Suppose that S_j^{kde} and S_j^{kun} are the detected and undetected values, respectively, that form the total number S_j^k . Following the Poisson splitting property (Qin et al., 2015, Kulkarni, 1995), S_j^{kde} and S_j^{kun} are assumed to be following the Poisson distributions with the respective PMFs:

$$f_p(S_j^{kde} | \lambda_o, \delta) = \frac{(\overline{\text{PoD}}_j \Lambda_j)^{S_j^{kde}} e^{-\overline{\text{PoD}}_j \Lambda_j}}{S_j^{kde}!} \quad (5.7)$$

$$f_p(S_j^{kun} | \lambda_o, \delta) = \frac{[(1 - \overline{\text{PoD}}_j) \Lambda_j]^{S_j^{kun}} e^{-(1 - \overline{\text{PoD}}_j) \Lambda_j}}{S_j^{kun}!} \quad (5.8)$$

where $\overline{\text{PoD}}_j$ denotes the average PoD that corresponds to the S_j^k defects and can be estimated as follows:

$$\overline{\text{PoD}}_j = \int \text{PoD}(x) f_{x_j^k}(x) dx \quad (5.9)$$

with $f_{x_j^k}(x)$ denoting the probability density function (PDF) of the depths of the S_j^k defects at time t_j .

5.3.2 Stochastic Growth of Corrosion Defects

In this chapter, the growth of each active corrosion defect depth is modelled through both a homogeneous (HGP) and a non-homogeneous gamma process (NHGP). Gamma process is a non-decreasing stochastic process that consists of a series of independent and gamma distributed increments. The distribution of the depth of the corrosion defect at time t , $d_r(t)$ is given by (Maes et al., 2009; Zhang and Zhou, 2013):

$$f_{d_r(t)}(d_i(t) | \alpha(t-t_{i0})^\kappa, \beta_i) = \beta_i^{\alpha(t-t_{i0})^\kappa} d_i(t)^{\alpha(t-t_{i0})^\kappa - 1} e^{-d_i(t)\beta_i} / \Gamma(\alpha(t-t_{i0})^\kappa) I_{G(0,\infty)}(d_i(t)) \quad (5.10)$$

where $\alpha(t-t_{i0})^\kappa$ and β_r represent the time-dependent shape parameter and rate parameter (or equivalently the inverse of the scale parameter) of defect r , respectively, and t_{r0} the initiation time of the r^{th} defect ($r=1, 2, \dots$). It is noted that the index r is used to characterise both detected and undetected corrosion defects, as opposed to the index i that is used to enumerate detected defects. Also, $I_{G(0,\infty)}(d_r(t))$ denotes an indication function which equals one if $d_r(t) > 0$ and zero otherwise, while $\Gamma(x) = \int_0^\infty s^{x-1} e^{-z} dz$ for $x > 0$ (Van Noortwijk, 2009).

Eq. (5.10) denotes the probability density function (PDF) of a gamma distributed random variable $d(t)$ with mean equal to $\alpha(t-t_0)^\kappa/\beta_r$ and variance equal to $\alpha(t-t_0)^\kappa/\beta_r^2$. For the growth of the r^{th} defect within one year, the incremental depth is a gamma distributed random variable with a mean value of α/β_r and a variance of α/β_r^2 , when it comes to homogeneous gamma process (HGP). For the non-homogeneous gamma process (NHGP), the aforementioned values refer only to the first unit increment of time since t_{r0} (Zhang and Zhou, 2013). For the rest of the increments, the mean and variance are $\alpha(t_{(incr+1)}^\kappa - t_{incr}^\kappa)/\beta_i$ and $\alpha(t_{(incr+1)}^\kappa - t_{incr}^\kappa)/\beta_i^2$, respectively. It is noted that Eq. (5.10) is a HGP when the shape parameter (i.e. $\alpha(t-t_0)^\kappa$ for $t \geq 0$) is a linear function of time ($\kappa = 1$) and a NHGP when non-linear ($\kappa > 1, \kappa < 1$). In this study, α and κ are assumed to be common for all the defects of a pipeline segment, while β_r and t_0 are assumed to be defect specific. It is further assumed

that the prior distributions of β_r and t_{r0} associated with different defects are identical and mutually independent (iid).

It follows that the growth of the r^{th} defect among two consecutive inspections is gamma distributed with a PDF as follows:

$$f_{\Delta d_{ij}}(\Delta d_{ij} | \Delta \alpha_{ij}, \beta_i) = \beta_i^{\Delta \alpha_{ij}} \Delta d_{ij}^{\Delta \alpha_{ij}-1} e^{-\Delta d_{ij} \beta_i} / \Gamma(\Delta \alpha_{ij}) \quad (5.11)$$

where β_r is the defect-specific rate parameter and $\Delta \alpha_{rj}$ is the time-dependent shape parameter associated with Δd_{rj} . It follows:

$$\Delta \alpha_{ij} = \alpha(t_j - t_{i0})^\kappa \quad (j = 1) \quad (5.12a)$$

$$\Delta \alpha_{ij} = \alpha(t_j - t_{i0})^\kappa - \alpha(t_{j-1} - t_{i0})^\kappa \quad (j = 2, 3, \dots, l) \quad (5.12b)$$

with t_{rj} denoting the time of the j^{th} inspection for the r^{th} defect, while $t = t_0$ corresponds to the initiation time of the r^{th} defect. For the HGP model ($\kappa = 1$), Eq. (5.12) is simplified as:

$$\Delta \alpha_{ij} = \alpha(t_j - t_{j-1}) \quad (j = 1, 2, \dots, l) \quad (5.12c)$$

Based on the above, the depth of each defect r at the time of each inspection j , d_{ij} , can be defined as the sum of consecutive incremental depths between t_{j-1} and t_j , as follows:

$$d_{rj} = d_{r,j-1} + \Delta d_{rj} \quad (5.13)$$

where d_{r0} is assumed to equal zero.

5.3.3 Correlations among stochastic degradations through Gaussian copula

The growths of different corrosion defects are usually partially correlated (dependent) within a pipe segment, given that they experience similar manufacturing practice and service environment (Hong et al., 2014). The assignment of the joint probability distribution with dependency structure, can be accomplished by using the Gaussian copula function (Zhou et al., 2017). Copula can be used to characterise the correlations of the stochastic growths d_{jk0} ($j = 1, 2, \dots, l$), ($k_0=1, 2, \dots, k_F$) separately, from the marginal distribution functions (Zhou et al., 2017, Schneider et al., 2017). Copula functions are joint distribution functions of k standard uniformly distributed variables U_{Ck_0} ($k_0=1, 2, \dots, k_F$) (Zhou et al., 2012; Hong et al., 2014):

$$C(u_{C1}, u_{C2}, \dots, u_{Ck_F}) = P(U_{C1} \leq u_{C1}, U_{C2} \leq u_{C2}, \dots, U_{Ck_F} \leq u_{Ck_F}) \quad (5.14)$$

A copula with components $F(v_1, v_2, \dots, v_{k_F})$ is a multivariate distribution function, with marginal distribution functions $F_r(v_{k_F})$ and in addition to that, any multivariate distribution

function F can be written as a copula representation as follows (Chang et al., 1994; Qian et al., 2013):

$$C(F_1(V_1), F_2(V_2), \dots, F_{k_F}(V_{k_F})) = F(v_1, v_2, \dots, v_{k_F}) \quad (5.15)$$

where $F_y(v_{k_0})$ ($y=1, 2, \dots, k_F$) are the marginal probability distribution functions of the random variables V_{k_0} evaluated at v_{k_0} .

Herein, the Gaussian copula presented next is chosen to define the dependence structure among the growths of different defects, which are characterised stochastically by gamma processes:

$$C(u_{C_1}, u_{C_2}, \dots, u_{C_{k_F}}) = \Phi_{k_F}(\Phi^{-1}(u_{C_1}), \Phi^{-1}(u_{C_2}), \dots, \Phi^{-1}(u_{C_{k_F}}); \mathbf{R}) \quad (5.16)$$

where $\Phi_{k_F}(\cdot; \mathbf{R})$ is the k_F -variate standard normal distribution function with the $(k_F \times k_F)$ matrix of correlation coefficients \mathbf{R} and $\Phi^{-1}(\cdot)$ is the inverse of the standard normal distribution function. The off-diagonal element of \mathbf{R} is Pearson's linear correlation coefficient and the diagonal elements are equal to unity. Given the correlation matrix \mathbf{R} , the Gaussian copula-based stochastic dependence between d_{jk_0} is realised by generating dependent samples Δd_{jk_0} on the pre-defined inspection times. The value of Δd_{jk_0} is evaluated as:

$$\Delta d_{jk_0} = F_G^{-1}[\Phi(u_{C_{k_0}})] \quad (5.17)$$

where $F_G^{-1}(\cdot)$ is the inverse function of the gamma distribution function for Δd_{jk_0} .

5.4 Bayesian Updating of the Stochastic Generation and Growth Models

5.4.1 Prior Distributions and Hierarchical Representation of the Deterioration Model

Physical models offer a comprehensive way of assessing loads and resistances associated with failure modes, accounting for the separate effect of each random variable on the pipeline (Frangopol and Soliman, 2016). Most of the parameters are assumed to be uncertain and are modelled probabilistically as random variables $\boldsymbol{\theta}$, through their joint probability density function (PDF) $f(\boldsymbol{\theta})$. In the context of energy pipelines, the physical model can be learned from new observation data, which usually come in the form of ILIs. Since the uncertainty in the parameters of the physical model is expressed through $\boldsymbol{\theta}$, the

information obtained from the inspection data can be used to update the distribution of θ . Given the critical role of the defect growth model in corroding energy pipelines physical models, updating its parameters is considered to satisfactorily describe the updated θ .

The gamma distribution is selected as the prior distributions of α , κ and β_i parameters of the corrosion growth model and also for the λ_o and δ parameters of the generation model. This distribution ensures positive quantities and can be conveniently constructed to be non informative. The truncated normal distribution, with an upper bound equal to the time of the inspection that each corrosion defect is detected for the first time and a lower bound of equal to the time of the previous inspection (as per Section 5.3.1), is chosen as the prior distribution of t_{i0} . The prior distributions for t_{i0} , α , κ and β_i for different defects are assumed to be mutually independent. The shape (rate) parameters of the gamma prior distributions for α , β_i , κ and λ_o , δ are defined as γ_1 , ξ_1 , γ_3 , ξ_3 , γ_4 , ξ_4 , γ_5 , ξ_5 , γ_6 , ξ_6 , respectively.

The uncertainties contained in the aforementioned corrosion growth model can be expressed by three levels of parameters for every specific defect, which combined form the entirety of the system uncertainties, described by the gamma process (Briš, 2008; Maes et al., 2009; Zhang and Zhou, 2013). The representation of an indicative deterioration HGP model is depicted in Fig. 5.2. The first level concerns location and/or element-specific uncertainties, expressed by the basic parameters of the HGP model (α , β_i , t_{i0}). The second level includes the temporal uncertainties of the deterioration increments for each defect i . It consists of the expected depths at inspection times and their increments between two consecutive inspections, along with the respective scale parameters Δa_{ij} ($i=1, 2, \dots, s$; $j=1, 2, \dots, l$). Finally, the third level associates the inspection data with measurement errors c_{1j} , c_{2j} and Σ_ϵ , accounting for observational uncertainties and the imprecise nature of inspections. Ellipses and rectangles in Fig. 5.2 characterise stochastic and deterministic (known) variables, whereas single- and double-edged arrows symbolise the stochastic and deterministic links, respectively. The known quantities, as shown in Fig. 5.2, include the parameters of the distributions of the basic parameters (i.e. γ_1 , ξ_1 , γ_2 , ξ_2 , γ_3 , ξ_3), the inspection times t_j ($j=1, 2, \dots, l$) and the measurement errors.

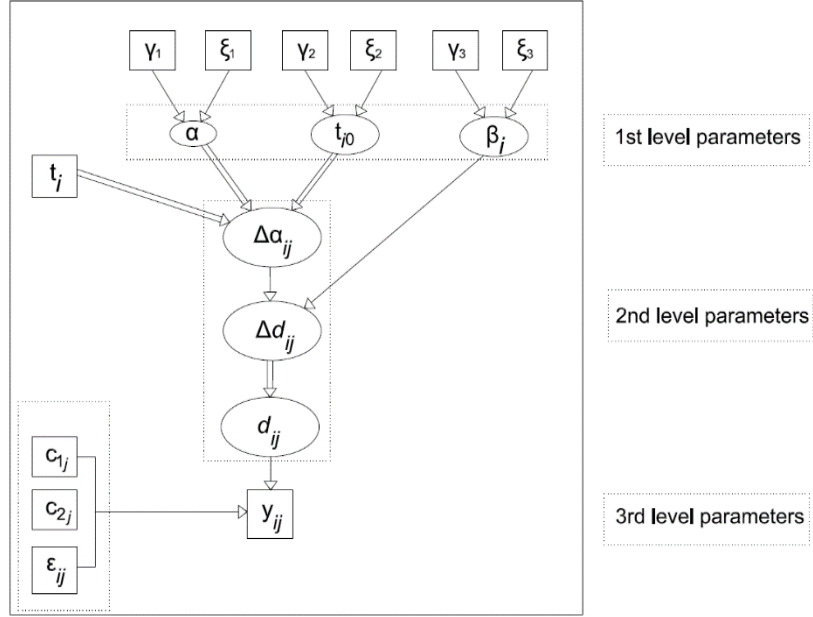


Figure 5.2 Hierarchical Bayesian HGP-based model for the j^{th} inspection of the i^{th} defect

5.4.2 General Formulation

The s metal-loss corrosion defects characterised by gamma process include $2s+2$ parameters, two common for all the defects parameters (α and κ), along with s defect specific rate parameters β_i and defect growth initiation times t_{i0} ($i = 1, 2, \dots, s$). Given the inspection data \mathbf{D} , Bayes' rule enables updating of the joint 'prior' distribution of the parameters $\boldsymbol{\theta}$, which is denoted by $f(\boldsymbol{\theta})$, to a 'posterior' probability distribution $f(\boldsymbol{\theta}|\mathbf{D})$, as follows (Zhang and Zhou, 2013; Straub and Papaioannou, 2014a; Caleyó et al., 2015):

$$f(\boldsymbol{\theta}|\mathbf{D}) = \frac{L(\mathbf{D}|\boldsymbol{\theta})f(\boldsymbol{\theta})}{\int_{\Theta} L(\mathbf{D}|\boldsymbol{\theta})f(\boldsymbol{\theta})} \quad (5.18)$$

Θ represents the space for $\boldsymbol{\theta}$ and $L(\mathbf{D}|\boldsymbol{\theta})$ is the likelihood function, which describes the inspection data conditional on the parameters of the model. Based on Eq. 5.1, ε_{ij} denotes the deviation of the inspection data from the model prediction, given that the ILI tools measurement errors have already been taken into consideration. Thus, the likelihood function characterising these inspections can be described comprehensively through Eq. 5.2. It follows that the likelihood of the inspection data y_i conditional on Δd_{ij} can be defined as:

$$L(\mathbf{y}_i|\Delta \mathbf{d}_i) = (2\pi)^{-\frac{l}{2}} |\boldsymbol{\Sigma}_\varepsilon|^{-\frac{1}{2}} \exp \left[-\frac{1}{2} \left(\mathbf{y}_i - (\mathbf{c}_1 + \mathbf{c}_2 \mathbf{A}_{\Delta d_i}) \right)' \boldsymbol{\Sigma}_\varepsilon^{-1} \left(\mathbf{y}_i - (\mathbf{c}_1 + \mathbf{c}_2 \mathbf{A}_{\Delta d_i}) \right) \right] \quad (5.19)$$

where $\mathbf{A}_{\Delta d_i}$ is an $l \times 1$ vector with the j th element equal to $\sum_{w=1}^j \Delta d_{iw}$.

For the evaluation of Eq. 5.18, simulation techniques such as MCMC can be employed to generate samples of the posterior distribution. Furthermore, when the computation of the probability of failure conditional on the posterior distribution is of interest, a reliability analysis can be performed as a post-processing step after the Bayesian analysis. Typically, a crude Monte Carlo simulation is adopted to carry out this reliability analysis (Zhou, 2010; Zhang and Zhou, 2013; Valor et al., 2014). However, crude Monte Carlo cannot efficiently estimate rare event probabilities (e.g. $<10^{-6}$), such as rupture of energy pipelines (Zhang and Zhou, 2013; Al-Amin and Zhou, 2014; Lam and Zhou, 2016). Thus, a structural reliability method that can efficiently estimate small posterior probabilities is necessary. Such a method would require an explicit knowledge of the joint posterior distribution, which must thus be approximated from the posterior samples. This can lead to considerable errors, especially in the tails of the distributions. In this study a new methodology, which was proposed in Straub and Papaioannou (2014a) and Straub et al. (2016) as an extension of the classical rejection sampling approach to Bayesian analysis, is applied for sampling from the posterior distribution. In addition to that, it enables the computation of the small posterior failure probabilities, directly within the same single framework.

BUS-SuS can be interpreted as an extension of the classical rejection sampling approach to Bayesian analysis. Details of the connection between the classical rejection sampling approach and BUS-SuS can be found in Straub and Papaioannou (2014a). The simple rejection sampling algorithm however, is thought to be inefficient, especially in the presence of increasing amount of inspection data, such as often is the case with corroding energy pipelines. This is also particularly aggravated when non-informative priors are present. However, an advantage of the rejection sampling algorithm over MCMC is its simplicity and the fact that ensures accurate and uncorrelated samples of the posterior. BUS-SuS developed for corroding pipelines herein, maintains partly the advantages of the simple rejection sampling algorithm, while it is highly efficient by employing Subset simulation which is capable of computing very small probabilities (Au and Beck, 2001; Tee et al, 2014).

Considering the augmented outcome space $[\boldsymbol{\theta}; p]$ is the first step of the analysis. Then, by defining the domain $Z = \{p \leq cL(\boldsymbol{\theta})\}$, the posterior distribution $f(\boldsymbol{\theta}|\mathbf{D})$ can be obtained by censoring the joint distribution of p and $\boldsymbol{\theta}$ to Z and marginalizing $\boldsymbol{\theta}$:

$$f(\boldsymbol{\theta}|\mathbf{D}) \propto \int_0^1 I_Z([\boldsymbol{\theta}, p] \in Z) f(\boldsymbol{\theta}) dp \quad (5.20)$$

where I_Z is an indicator function which takes value one if $\{p \leq cL(\boldsymbol{\theta})\}$ and zero otherwise, and p is a standard uniform random variable. Furthermore, c is defined as a positive constant that ensures $cL(\boldsymbol{\theta}) \leq 1$ for all $\boldsymbol{\theta}$. The selection of c is discussed in section 5.4.3. In the structural reliability convention, the domain Z describes an observation event (in terms of the Bayesian updating) through a limit state function r_A , such that it corresponds to a respective domain $\{r_A(p, \boldsymbol{\theta}) \leq 0\}$:

$$r_A(p, \boldsymbol{\theta}) = p - cL(\boldsymbol{\theta}) \quad (5.21)$$

The probability of the observation event $\Pr(Z)$ is equal to the acceptance rate of the simple rejection sampling algorithm which typically is too small for Monte Carlo simulation to be efficient. Therefore, SuS is employed to explore the domain Z and compute $\Pr(Z)$. It is advantageous to apply SuS in the standard Normal space (Papaioannou et al., 2015; Straub et al., 2016), thus the outcome space of the original random variables p and $\boldsymbol{\theta}$ is transformed to a space with independent standard Normal random variables \mathbf{V} . Moreover, p and $\boldsymbol{\theta}$ are a-priori independent, as a result they can be transformed separately. The corresponding limit-state function expressed through the underlying standard Normal random variables can be described in terms of a function R_A :

$$R_A(\mathbf{v}) = v_0 - \Phi^{-1}(cL(\mathbf{T}(\mathbf{v}))) \quad (5.22)$$

where Φ is the standard Normal cumulative distribution function (CDF). The transformation \mathbf{T} can be either performed by means of the Rosenblatt transformation or the marginal transformation based on the Nataf model. Next, BUS-SuS can generate samples from the transformed observation domain (Straub and Papaioannou, 2014a). SuS evaluates the probability $\Pr(Z)$ associated with a limit state function $R_A(\mathbf{v})$, defined in the respective domain $\{R_A(\mathbf{v}) \leq 0\}$. This is realised by expressing the event Z as an intersection of M nested intermediate events, such that $Z_0 \supset Z_1 \supset \dots \supset Z_{M_c} = Z$. The probability $\Pr(Z)$ can be defined as:

$$\Pr(Z) = \Pr\left(\bigcap_{\chi=1}^{M_c} Z_\chi\right) = \prod_{\chi=1}^{M_c} \Pr(Z_\chi | Z_{\chi-1}) \quad (5.23)$$

where Z_0 corresponds to the certain event (Au and Beck, 2001). The final probability is expressed through larger conditional probabilities of the intermediate events $Z_\chi = \{R_A(\mathbf{v}) \leq b_\chi\}$, with $b_1 > b_2 > \dots > b_{M_c} = 0$ and $\chi > 0$. The values of b_χ are chosen adaptively, so that the estimates of the conditional probabilities correspond to a specific value p_0 , which is

usually selected to be in the range of [0.1~0.3] (Au and Beck, 2001; Straub and Papaioannou, 2014a). Towards this, H samples are simulated from \mathbf{V} , conditional on each intermediate event $Z_{\chi-1}$ and then the respective limit state function $R_S(\mathbf{v})$ value is estimated. Based on this evaluation, the samples are placed in increasing order of magnitude, whereas the threshold b_χ is set to the p_0 -percentile of the ordered samples. The process is repeated until $b_{M_c} = 0$, whilst b_1 is estimated through unconditional samples of \mathbf{V} based on a crude Monte Carlo. Consecutively, the samples of \mathbf{V} conditional on Z_χ for $\chi = 1, \dots, M_c - 1$ are generated from Markov chains through MCMC sampling, with seeds the samples conditional on $Z_{\chi-1}$ for which $R_A(\mathbf{v}) \leq b_\chi$. Then, $\Pr(Z)$ is estimated as follows:

$$\Pr(Z) = p_0^{M_c-1} p_{M_c} \quad (5.24)$$

where p_{M_c} corresponds to the conditional probability $\Pr(Z_{M_c} | Z_{M_c-1})$ as follows:

$$p_{M_c} = \frac{1}{G} \sum_{\lambda_c=1}^G I_R(\mathbf{v}_{\lambda_c}^{M_c-1}) \quad (5.25)$$

where I_{RA} is an indication function of the observation event and $\{\mathbf{v}_{\lambda_c}^{M_c-1}, \lambda_c = 1, \dots, H\}$ are samples of \mathbf{V} conditional on Z_{M_c-1} .

In Bayesian updating, apart from $\Pr(Z)$ one is interested in obtaining samples that fall into the domain Z , thus a final step should be defined. That is an extra step, where W additional samples conditional on Z are produced, so that a total number of (at least) H samples from the posterior distribution can be obtained.

5.4.3 Constant c

The required choice of constant c in BUS-SuS should ensure $cL(\boldsymbol{\theta}) \leq 1$ for all $\boldsymbol{\theta}$. Choosing the constant c too low might undermine the efficiency of the method significantly, since the acceptance probability is linearly related to c . Contrarily, if it is chosen too large, this might lead to samples that do not follow the posterior distribution (Betz et al., 2014). An optimal choice of c can be approximated based on (Straub and Papaioannou, 2014a):

$$c = \frac{1}{\sup L(\boldsymbol{\theta})} \quad (5.26)$$

For a given defect i that has been inspected and sized by multiple inspections, $\sup L(\boldsymbol{\theta})$ is equal to the maximum of the PDF of the random scattering error ε_{ij} with respect to the measured defect depth (Straub and Papaioannou, 2014b). This is correlated, following a

multivariate normal distribution with a zero mean and known covariance matrix Σ_ϵ associated with the total number of different inspections l . $\sup L(\boldsymbol{\theta})$ occurs at the location of the maximum likelihood and thus it is possible to evaluate it by employing an optimization algorithm such that $\sup L(\boldsymbol{\theta}) = L(\boldsymbol{\theta}_{MLE})$, where $\boldsymbol{\theta}_{MLE}$ denotes the maximum likelihood estimator (Straub and Papaioannou, 2014a). In case of a relatively small number of individual inspections (e.g. <5), an alternative choice is thought to produce equally accurate results, that is:

$$c = \frac{1}{\prod_{j=1}^l [\sup L_j(\boldsymbol{\theta})]} \quad (5.27)$$

It should be mentioned that alternative methods of selecting the constant c when using SuS have been described in Betz et al. (2014), DiazDelaO et al. (2017) and Betz et al. (2018).

5.4.4 Likelihood Function for the Growth Model of Detected Corrosion Defects

Suppose that a number of defects have been detected in a total of l inspections and a defect i is first detected in the j th ($j = 1, 2, \dots$ or l) inspection. Furthermore, $\mathbf{y}_i = (y_{ji}, y_{j+1,i}, \dots, y_{j+g,i}, \dots, y_{li})'$ and $\mathbf{d}_i = (d_{ji}, d_{j+1,i}, \dots, d_{j+g,i}, \dots, d_{li})'$ denote the vector of the ILI-reported depths for defect i and the vector of the corresponding actual depths of defect i , respectively. Given the measurement error described in Section 5.2, the likelihood of \mathbf{y}_i conditional on \mathbf{d}_i can be defined as follows:

$$L(\mathbf{y}_i | \mathbf{d}_i) = (2\pi)^{-\frac{(l-j+1)}{2}} |\Sigma_{\mathbf{E}_i}|^{-\frac{1}{2}} \exp\left[-\frac{1}{2} (\mathbf{y}_i - \mathbf{b}_1 - \mathbf{b}_2 \mathbf{d}_i)' \Sigma_{\mathbf{E}_i}^{-1} (\mathbf{y}_i - \mathbf{b}_1 - \mathbf{b}_2 \mathbf{d}_i)\right] \quad (5.28)$$

where $\mathbf{b}_1 = (b_j, b_{j+1}, \dots, b_l)'$ and \mathbf{b}_2 is an $l-j+1 \times l-j+1$ diagonal matrix with the g th element equal to b_{2j+g} . Inherent in this formulation is the assumption that once a defect is detected, it will be detected in the following inspections as well. This assumption can be relaxed via the use of the multiple imputation technique (Qin et al., 2015; Rubin, 2004). In other words, a feature that has been detected once by the ILI tool, might not be detected in a later inspection and will be dealt as missing data, by means of the multiple imputation technique.

5.4.5 Likelihood Function for the Generation Model of Corrosion Defects

Likewise the likelihood function of the growth model, the updating of the number of detected defects inherently contains the possibility that some of the newly detected defects in the j th inspection, might have actually been generated prior to the exactly previous inspection, i.e. $(j-1)$ th, but remain undetected until then. However, in order to simplify the likelihood functions for NHHP, it is assumed that the newly detected defects in the j th inspection have initiated between the $(j-1)$ th and j th inspections. That is a conservative approach, since it finally leads to overestimation of the instantaneous rate of defect generation (Qin et al., 2015). Thus, the likelihood function for the number of newly detected defects in l inspections, S_j^{kde} ($j = 1, 2, \dots, l$), is defined as follows:

$$L(S_j^{kde} | \lambda_0, \delta) = \prod_{j=1}^l \frac{[\overline{\text{PoD}}_j \lambda_0 (t_j^\delta - t_{j-1}^\delta)]^{S_j^{kde}}}{S_j^{kde}} \exp\left\{-[\overline{\text{PoD}}_j \lambda_0 (t_j^\delta - t_{j-1}^\delta)]\right\} \quad (5.29)$$

where $\overline{\text{PoD}}_j$ includes both detected and undetected defects in the j th inspection. The undetected defects are treated as the missing data and the data augmentation (DA) technique is employed to incorporate these in the Bayesian analysis (Tanner and Wong, 1987). This technique is described in more detail in Section 5.5.3. In this methodology thus, the $\overline{\text{PoD}}_j$ serves as a link in the Bayesian updating, between the NHHP and NHGP models.

5.5 Time-dependent Reliability Analysis

5.5.1 Limit State Functions for Metal-Corrosion Defects

The reliability assessments herein are implemented using the PCORRC model to calculate the failure pressure of defects in Pa or kPa or MPa, as per Eq. (3.8) of section 3.2.4. In addition, the rupture pressure is calculated according to Eqs. (3.9a-b) from the same section.

At a given corrosion defect, the limit state function for small leak is defined as:

$$g_1 = P_{sfi} - P_{sop} \quad (5.30)$$

where $P_{S_{fi}}$ is the failure pressure calculated from Eq. (3.8) of section 3.2.4, by substituting $d = 0.0009w_t$. It corresponds to the case where the depth of the defect is equal to the pipe wall thickness, i.e. where the defect penetrates the pipe (Valor et al., 2014). It is noted that $P_{S_{op}}$ is the time dependent internal pressure of the pipe segment under examination.

The limit state function for plastic collapse due to internal pressure at the defect (large leak) is given by:

$$g_2 = P_{S_{fi}} - P_{S_{op}} \quad (5.31)$$

where $P_{S_{fi}}$ is the failure pressure calculated from Eq. (3.8) of section 3.2.4, without changing the defect depth generated from the stochastic growth model (when $d < w_t$). It denotes the burst pressure on a part through wall corrosion defect (Zhang and Zhou, 2013).

The limit state function for unstable defect extension in the axial direction due to internal pressure (rupture) is given by:

$$g_3 = P_{S_R} - P_{S_{op}} \quad (5.32)$$

where P_{S_R} is the pressure resistance of the pipe that contains a through wall defect, which results from the burst at the corrosion defect and is defined by Eq. (3.9a) of section 3.2.4.

The discrimination between small leak, large leak and rupture based on g_1 , g_2 and g_3 follows the scheme described next (Valor et al., 2014). When a defect depth is equal to the pipe wall thickness ($d_i \geq w_t$), then a failure pressure $P_{S_{fi}}$ is calculated from Eq. (3.8) of section 3.2.4, by substituting the defect depth with the delimited value $d_i = 0.0009w_t$ (Valor et al., 2014). Then, if $P_{S_{fi}} \geq P_{S_{op}}$, a small leak is counted. Otherwise if it holds $P_{S_{fi}} < P_{S_{op}}$, it is examined if $P_{S_{fi}} > P_{S_R}$ and if it is the case, a large leak is considered, whereas if not a rupture instead. When $d_i < w_t$ the same procedure is repeated, by considering that if $P_{S_{fi}} \geq 0$ the pipeline is safe (instead of counting a small leak failure).

5.5.2 Limit State Functions for High-pH SCC Defects

The Battelle model, also known as the log secant approach or NG-18 Equation, is a semi empirical model developed at the Battelle Memorial Institute to predict the burst pressure of pipes that are subjected solely to internal pressure and contain longitudinally oriented surface cracks (Yan et al., 2014). The model assumes a rectangular crack profile in the through wall thickness direction, defined by the maximum crack depth and length and

estimates the burst pressure by adopting two criteria; the flow stress- and fracture toughness- based criteria. The former addresses the plastic collapse failure mode, whilst the latter addresses the fracture failure mode. According to the Battelle model, the burst pressure R_{b1} can be defined as follows:

$$R_{b1} = \min \left\{ \frac{2t\sigma_f}{D} \frac{1 - \frac{d_{ij}}{w_t}}{1 - \frac{d_{ij}}{Mw_t}}, \frac{4w_t\sigma_f}{\pi D} \frac{1 - \frac{d_{ij}}{w_t}}{1 - \frac{d_{ij}}{Mw_t}} \arccos \left(\exp \left(-\frac{\pi K_{mat}^2}{8L\sigma_f^2} \right) \right) \right\} \quad (5.33)$$

where D is the outside diameter of the pipe, w_t is the wall thickness, σ_f is the pipe's material flow stress and equals $UTS + 68.95$ MPa, with UTS representing the yield strength of the pipe material. Furthermore, d_{ij} denotes the crack depth in the through pipe wall thickness direction, for the i th crack in the j th inspection, and L is the length of the defect in the longitudinal direction of the pipeline. Finally, K_{mat} refers to the fracture toughness of pipe steel in terms of the stress intensity factor and M is the Folias factor, evaluated as follows:

$$M = \begin{cases} \left[1 + \frac{0.6275(2L)^2}{Dw_t} - 0.003375 \left(\frac{(L)^2}{Dw_t} \right)^2 \right]^{1/2} & L \leq \sqrt{20Dw_t} \\ 3.3 + 0.032 \frac{L^2}{Dw_t} & L > \sqrt{20Dw_t} \end{cases} \quad (5.34)$$

The fracture toughness K_{mat} is evaluated by an empirical equation, i.e. $K_{mat} = (C_v E / A_c)^{0.5}$, with C_v , A_c and E referring to the upper shelf Charpy V-notch (CVN) impact energy, net cross-sectional area of the Charpy impact specimen and Young modulus of steel, respectively.

5.5.3 System Reliability Analysis

The methodology for system reliability analysis of a pipe segment that contains multiple corrosion defects and has been subjected to multiple ILIs, has the core consideration that the pipe segment is a series system. This means that failure at any of the defects can yield the failure of the whole system (Zhang and Zhou, 2013). Nonetheless, only the probability distribution of the maximum depth is not sufficient. The reason is that failure probabilities corresponding to large leak and rupture are affected by the defect length as well. In addition, the maximum depth and length do not necessarily coincide at the same defect. In

Structural Reliability methods, the failure event of interest is expressed in terms of its corresponding limit state function:

$$\Pr(F_{f_m}) = \{ g_{f_m}(\boldsymbol{\theta}) \leq 0 \} \quad (5.35)$$

where $f_m=1,2,3$ denote the small leak, large leak and rupture failure modes, respectively.

The probability of the failure event is equal to the probability of the vector $\boldsymbol{\theta} = [\theta_1; \theta_2; \dots; \theta_n]$ of the n input random variables of the problem, taking a value within the domain in the outcome space of $\boldsymbol{\theta}$ for which $g_{f_m}(\boldsymbol{\theta}) \leq 0$. It can be estimated by integrating the joint probability function of $\boldsymbol{\theta}$, $f(\boldsymbol{\theta})$, over the aforementioned domain:

$$\Pr(F_{f_m}) = \int_{g_{f_m}(\boldsymbol{\theta}) \leq 0} f(\boldsymbol{\theta}) d\theta_1 d\theta_2 \dots d\theta_n \quad (5.36)$$

Furthermore, the probability of the rare event conditional on the inspection data, can be computed by inserting the posterior $f(\boldsymbol{\theta}|\mathbf{D})$ into Eq. (5.36):

$$\Pr(F_{f_m}|\mathbf{D}) = \int_{g_{f_m}(\boldsymbol{\theta}) \leq 0} f(\boldsymbol{\theta}|\mathbf{D}) d\theta_1 d\theta_2 \dots d\theta_n \quad (5.37)$$

Eq. (5.20) suggests that the conditional PDF of $\boldsymbol{\theta}$ given the data \mathbf{D} , is obtained by conditioning the prior distribution on the observation event Z . This definition of the observation domain describes the data exactly in a Bayesian framework, therefore conditioning the probability of F_{f_m} on the data, is equivalent to conditioning it on the observation event Z (Straub et al., 2016):

$$\Pr(F_{f_m}|\mathbf{D}) = \Pr(F_{f_m}|Z) \quad (5.38)$$

The conditional small failure probability given the data, $\Pr(F_i|\mathbf{D})$, is obtained by combining Eqs. (5.20) and (5.37) such that:

$$\Pr(F_{f_m}|Z) = \int_{g_{f_m}(\boldsymbol{\theta}) \leq 0} f(\boldsymbol{\theta}|\mathbf{D}) d\theta_1 d\theta_2 \dots d\theta_n = \frac{\int_{g_{f_m}(\boldsymbol{\theta}) \leq 0} \int_0^1 I_Z(p, \boldsymbol{\theta}) f(\boldsymbol{\theta}) dp d\theta_1 d\theta_2 \dots d\theta_n}{\int_{\boldsymbol{\theta}} \int_0^1 I_Z(p, \boldsymbol{\theta}) f(\boldsymbol{\theta}) dp d\theta_1 d\theta_2 \dots d\theta_n} \quad (5.39)$$

Based on Eq. (5.21), $\Pr(F_{f_m}|Z)$ is redefined as:

$$\Pr(F_{f_m}|Z) = \frac{\int_{g_{f_m}(\boldsymbol{\theta}) \leq 0 \cap r_A(p, \boldsymbol{\theta}) \leq 0} f(\boldsymbol{\theta}) dp d\theta_1 d\theta_2 \dots d\theta_n}{\int_{r_A(p, \boldsymbol{\theta}) \leq 0} f(\boldsymbol{\theta}) dp d\theta_1 d\theta_2 \dots d\theta_n} = \frac{\Pr[g_{f_m}(\boldsymbol{\theta}) \leq 0 \cap r_A(P, \boldsymbol{\theta}) \leq 0]}{\Pr[r_A(P, \boldsymbol{\theta}) \leq 0]} \quad (5.40)$$

Transforming the problem to standard Normal space based on Eq. (5.22), the small failure probability $\Pr(F_{f_m}|\mathbf{D})$ can be expressed by the standard Normal \mathbf{V} , as follows:

$$\Pr(F_{f_m}|Z) = \frac{\Pr[G_{f_m}(\mathbf{V}) \leq 0 \cap R_A(\mathbf{V}) \leq 0]}{\Pr[R_A(\mathbf{V}) \leq 0]} \quad (5.41)$$

where G refers to the transformed limit state function in standard Normal space:

$$G_{f_m}(\mathbf{V}) = g_{f_m}(\mathbf{T}^{-1}(\mathbf{V})) \quad (5.42)$$

To estimate the probability of the intersection of the observation and failure events $\Pr(F_{f_m} \cap Z)$, an equivalent limit state function $\hat{G}_{f_m}(\mathbf{v}) = \max(G_{f_m}(\mathbf{v}), R_A(\mathbf{v}))$ can be defined, such that $F_{f_m} \cap Z = \{\hat{G}_{f_m}(\mathbf{V}) \leq 0\}$. Limit state function $\hat{G}_{f_m}(\mathbf{v})$ can be applied in the same way, as for the estimation of the observation event Z in Eq. (5.22). The updated probability $\Pr(F_{f_m}|Z)$ though, can also be estimated directly, following estimation of $\Pr(Z)$, with a consecutive SuS run, i.e. that starts where the other one ended, by defining a set of intermediate events $F'_0 \supset F'_1 \supset \dots \supset F'_{M_D}$ with $F'_\chi = F_\chi \cap Z$ and $F'_0 = F_0 \cap Z = Z$. The conditional probability is equal to:

$$\Pr(F_{f_m}|Z) = \frac{\Pr(F|Z)}{\Pr(Z)} = \frac{\Pr(\bigcap_{\chi=0}^{M_D} F'_\chi)}{\Pr(Z)} = \Pr\left(\bigcap_{\chi=1}^{M_D} F'_\chi \mid F'_0\right) = \prod_{\chi=1}^{M_D} \Pr(F'_\chi \mid F'_{\chi-1}) \quad (5.43)$$

After estimating $\Pr(F_{f_{m_i}}|\mathbf{D})$ for each defect i , the probability of failure for the f_m th failure mode, with respect to the entire pipe segment with s defects, can be computed:

$$\Pr(F_{f_m}|\mathbf{D})_{segment} = 1 - \prod_{i=1}^s [1 - \Pr(F_{f_{m_i}}|\mathbf{D})] \quad (5.44)$$

A step-by-step procedure for estimating the posterior failure probabilities conditional on the data, $\Pr(F_{f_{m_i}}|\mathbf{D})$, by the use of BUS-SuS, is described in Appendix A. This procedure is the one mentioned above, in which the updated probability is derived through a consecutive SuS run, after the estimation of $\Pr(Z)$.

When both the detected and undetected defects are considered, the real depths of the detected defects are related to the inspection-reported depths, through the likelihood function given by Eq. (5.28), while the real depths of the undetected defects are treated as the missing data and imputed using the DA technique (Qin et al., 2015; Tanner and Wong, 1987). As a result, the joint posterior distribution of the model parameters are evaluated from the depths of the total defect population (both detected and undetected). It is noted that it is straightforward to incorporate DA in the Bayesian updating with BUS-SuS. In specific, DA is an iterative process that contains two steps in each iteration; the imputation and the posterior step (Qin et al., 2015). The imputation step generates the samples of the missing data from its corresponding probabilistic distribution, conditional on the current state of model parameters. The posterior step is used to generate new samples of model parameters from their corresponding posterior distributions, conditional on both the

observed and missing data. More information and details of the DA process can be found in Qin et al. (2015), Tanner and Wong (1987), Rubin (2004), Little and Rubin (2014).

5.6 Metal-loss Corrosion Case Study

5.6.1 General

An application on an underground natural gas pipeline constructed in 1972 is realised in this section, in order to illustrate and validate the proposed methodology. Several segments of this pipeline were excavated in 2010 and the depths of the corrosion defects were measured using an ultrasonic (UT) thickness device at the excavation sites (Zhang, 2014). A set of 17 defects is used herein, among those identified and matched with the defects inspected by high-resolution magnetic flux leakage (MFL) tools in 2000, 2004, 2007, 2009 and 2011. The measurements errors corresponding to these ILI tools, are obtained from Al-Amin et al. (2012), a study on the same pipeline. In their study, the ILI-reported and field-measured depth values were compared for a number of inactive defects that had been recoated and stopped growing. Furthermore, according to Al-Amin et al. (2012), the field-sized depths are considered free of measurement error. Thus, the corrosion depths in 2010 correspond to the actual depths.

The ILI data of 2000, 2004 and 2007 are considered for the application of the proposed methodology. The results are then validated, by comparing the predicted depths with the corresponding field-measured depths in 2010. The ILI data of year 2009 are excluded, so that the prediction corresponds to a reasonably long forecasting period (i.e. 3 years, from 2007 to 2010). The constant and non-constant biases and standard deviations of the random scattering errors of the ILIs are presented next, along with the correlations between the random scattering errors associated with different ILI tools used, for the respective inspections. The values of these parameters are: $c_{11} = c_{12} = 2.04$ ($\% w_t$), $c_{13} = -15.28$ ($\% w_t$), $c_{14} = -10.38$ ($\% w_t$) and $c_{15} = 4.84$ ($\% w_t$); $c_{21} = c_{22} = 0.97$, $c_{23} = 1.4$, $c_{24} = 1.13$ and $c_{25} = 0.84$; $\sigma_1 = \sigma_2 = 5.97$ ($\% w_t$), $\sigma_3 = 9.05$ ($\% w_t$), $\sigma_4 = 7.62$ ($\% w_t$) and $\sigma_5 = 5.94$ ($\% w_t$); $\rho_{12} = 0.82$, $\rho_{13} = \rho_{23} = 0.7$, $\rho_{14} = \rho_{24} = 0.72$, $\rho_{15} = \rho_{25} = 0.82$, $\rho_{34} = 0.78$, $\rho_{35} = 0.71$ and $\rho_{45} = 0.74$, where the subscripts '1', '2', '3', '4' and '5', refer to the ILI tools used in 2000, 2004, 2007, 2009 and 2011, and w_t denotes the pipeline wall thickness.

5.6.2 Application and Validation of the Methodology

BUS-SuS is applied next, to evaluate the probabilistic characteristics of the parameters of the HGP and NHGP corrosion growth models, for each of the 17 defects. The depths of the 17 defects are illustrated in Fig. 5.3. They correspond to ILIs for years 2000, 2004, 2007 and to the excavation measurements of 2010. Some of the defect depths, appear to decrease over time. This is attributed merely to the large impact of the ILI tools measurement errors, since a decrease of a defect depth, would have no physical meaning.

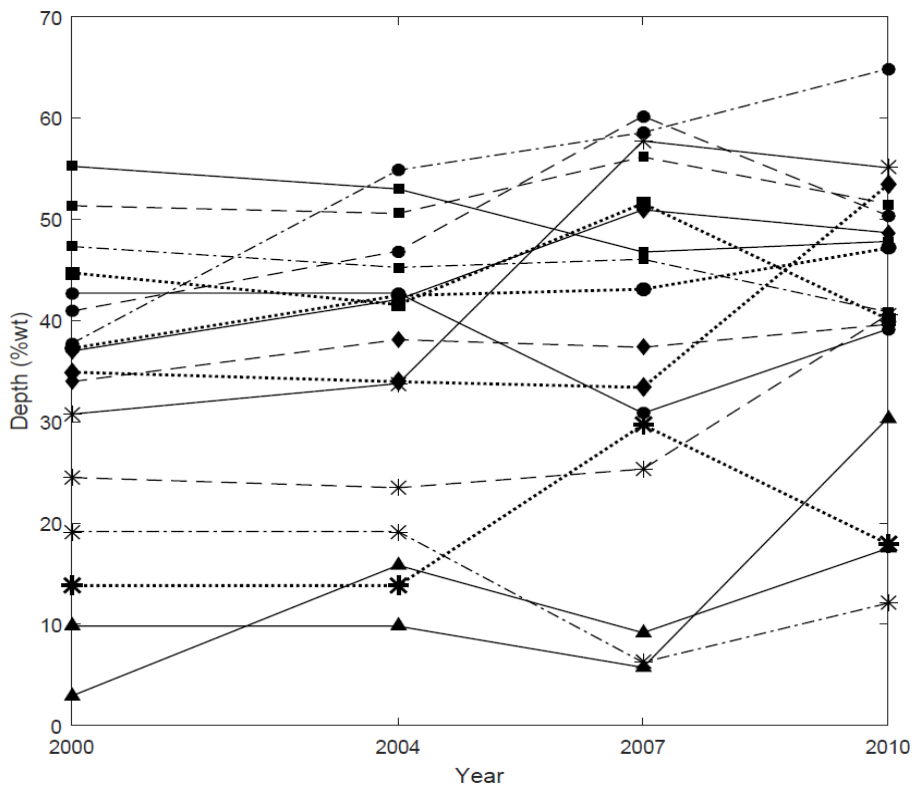


Figure 5.3 ILI-reported depths in 2000, 2004, 2007 and field-measured depths in 2010 for each of the seventeen defects

The gamma distribution is selected as the prior distributions of α , β_i and κ , on the basis that this distribution ensures positive quantities and can be conveniently utilised as a non-informative distribution. The truncated normal distribution with a lower bound of zero and an upper bound of 28 years, i.e. the time elapsed from installation of the pipeline in 1972 until the first inspection in 2000, is chosen as the prior distribution of t_{i0} . Furthermore, it is also assumed that the prior distributions of β_i and t_{i0} are identical and mutually independent for different defects. The parameters at the top of Fig. 5.2, i.e. of the prior distributions,

corresponding to the HGP growth model, are defined as follows: $\gamma_1 = 1$, $\xi_1 = 1$, $\gamma_2 = 1$, $\xi_2 = 1$, $\gamma_3 = 1$, $\xi_3 = 1$. Correspondingly, $\gamma_4 = 1$, $\xi_4 = 1$, denote the parameters of the prior distribution of κ , for the NHGP model.

A total of 20,000 samples were generated for the BUS-SuS, while it was selected that $p_0 = 0.1$. The constant c was evaluated from Eq. 5.27 and was found to be $c = 1975$. A comparison is illustrated in Figs. 5.4 and 5.7, for the HGP and NHGP models, respectively. These concern the defect depth predictions of the BUS-SuS methodology in 2010 and the corresponding field-measured depths in 2010, for the 17 defects. The predicted depth for each defect, presented in both Figs. 5.4 and 5.7, is the mean depth derived from the HGP and NHGP models respectively, with α , β_i , κ and t_{i0} assumed to be deterministic and set equal to the mean values of the corresponding marginal posterior distributions obtained from BUS-SuS. Fig. 5.4 indicates that the predictions given by the HGP-based BUS-SuS model are reasonably accurate, since 14 out of 17 values fall within the range of $\pm 10\% w_i$, when compared with the corresponding actual depth. This range is typically adopted as a confidence interval for inspection tool accuracy in the pipeline industry and, therefore, it can set an adequate metric of accuracy, for the proposed methodology herein.

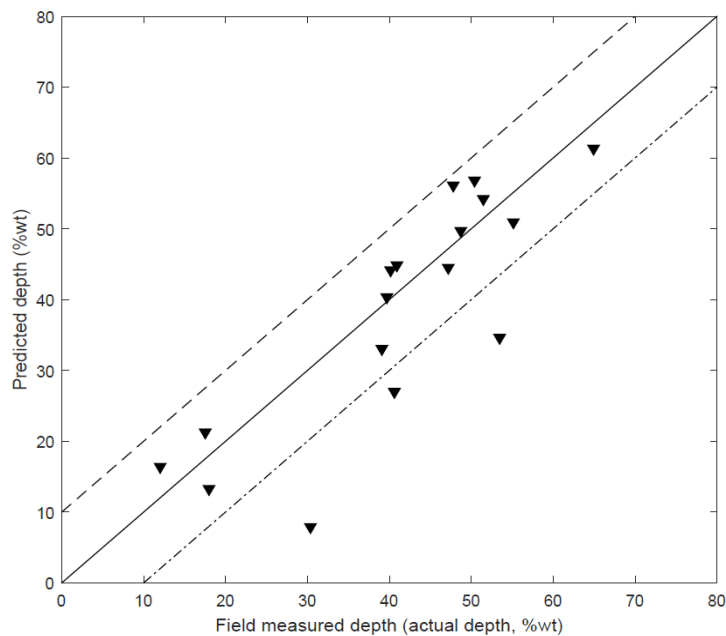


Figure 5.4 Comparison of the HGP model predictions with the field-measured depths in 2010

Two of the three defects, namely defect 4 and 9, for which BUS-SuS could not achieve a prediction in the interval $\pm 10\% w_i$, were further examined in an effort to study the discrepancy in greater depth. The mean, 10- and 90- percentile are estimated for those defects, based on the results of the Bayesian analysis. The mean and standard deviation of defect depths are estimated as $\alpha(t-t_{i0})^\kappa/\beta_i$ and $(\alpha(t-t_{i0})^\kappa/\beta_i^2)^{0.5}$ respectively, for each defect. The parameters α , κ , t_{i0} and β_i are set equal to the deterministic mean values from their corresponding marginal posterior distributions, derived from BUS-SuS. The 10- and 90-percentile predictions have shape parameters $\alpha(t-t_{i0})^\kappa$, rate parameters β_i and CDF $F(d(t) \leq y(t)) = \gamma(\alpha(t-t_{i0})^\kappa, \beta_i y(t)) / \Gamma(\alpha(t-t_{i0})^\kappa)$, where $\gamma(c_\gamma, u)$ is the incomplete gamma function, defined as $\gamma(c_\gamma, u) = \int_0^u z^{c_\gamma-1} e^{-z} dz$ (Zhang, 2014). The above correspond to the NHGP-based model, as well as the HGP-based model when κ is omitted (it is set equal to one). The ILI derived depths are also depicted for comparison with the model predictions. It is indicated in Figs. 5.5 and 5.6 that the ILI results, though similar to each other every inspection year, are very different compared to the actual depth reported in 2010. In that sense, it is reasonable to deduce that ILI tools measurements errors are the main reason behind the discrepancies among ILI reported depths and actual depths, which subsequently lead to underestimations from the proposed BUS-SuS method. Therefore, it can be postulated that BUS-SuS provides credible forecasts and it bears no direct responsibility for the underestimations.

Next, the predicted depths of the 17 defects, based on the NHGP model are derived in a similar fashion, with the parameter κ now additionally present. The joint posterior distribution of the NHGP-based growth model parameters was evaluated based on the same number of samples (i.e. 20,000), as in the HGP-based model. The comparison between the model predictions and the field measurements in year 2010, is illustrated in Fig. 5.7. The predictive accuracy of the NHGP model is satisfactory, in that 14 of the 17 defects fall within the confidence interval region (i.e actual depth $\pm 10\% w_i$). It can be observed that the NHGP model tends to provide less conservative predictions, for the depths of all defects. However, for this set of data, the two models can be considered equally precise. Their differences can be attributed to the growth trend of each defect as suggested by the ILI data, which may resemble either a linear path or a non-linear path. A more detailed comparison of the NHGP and HGP model predictions, is carried out in the following section.

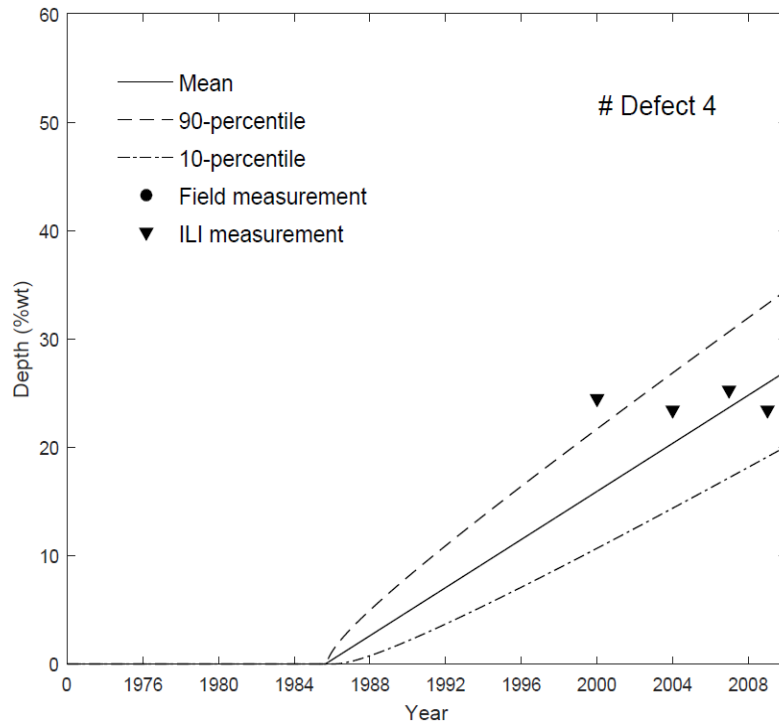


Figure 5.5 Predicted growth path of defect 4 based on the HGP model

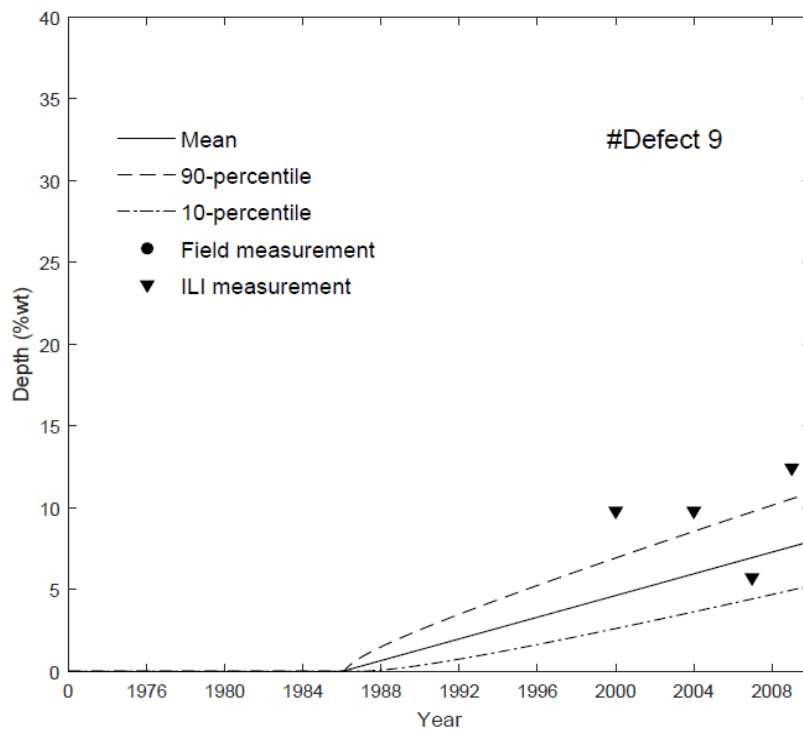


Figure 5.6 Predicted growth path of defect 9 based on the HGP model

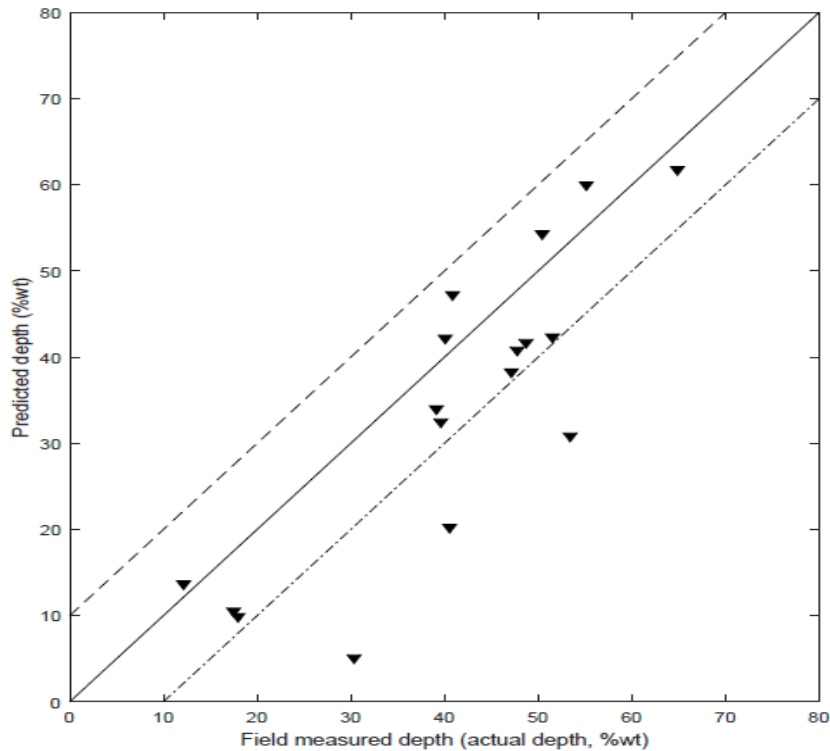


Figure 5.7 Comparison of the NHGP model predictions with the field measured depths in 2010

5.6.3 Comparisons of Growth Models and Time-dependent Reliability Analysis

One of the segments of the pipeline described in Section 5.6.1 is used to evaluate the time-dependent system reliability, by applying the proposed methodology. The pipeline has a nominal outside diameter of 508 mm and is made of API 5L Grade X52 steel, with a specified minimum yield stress (SMYS) of 359 MPa and a specified minimum tensile strength (SMTS) of 456 Mpa. The segment has a nominal wall thickness of 5.56 mm and an operating pressure of 5.654 Mpa. It has a length of 18.13m and contains 10 corrosion defects. It is noted that the 17 defects used previously for the validation of the model, do not belong to this pipe segment. The latter was inspected by MFL tools in 2004, 2007, 2009 and 2011. The ILI-reported depths and the apparent growth paths are illustrated in Fig. 5.8.

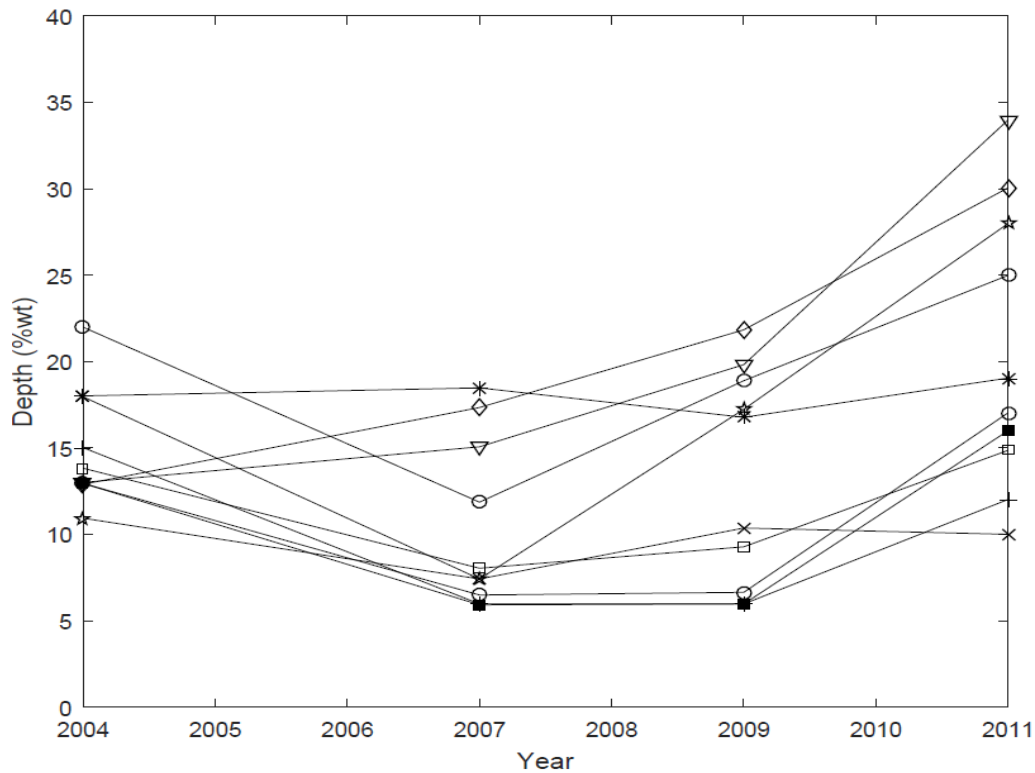


Figure 5.8 ILI-reported depths in 2004, 2007, 2009 and 2011 for each of the ten defects

Furthermore, the aforementioned parameters are characterised probabilistically and described as random variables, with statistical properties as presented in Table 5.1. The ILI-reported lengths in 2011, as presented in Fig. 5.9, are adopted as the initial nominal defect lengths. After this year, the defect lengths were assumed to grow linearly, with random growth rates derived from the lognormal distribution, as indicated in Table 5.1. A time-dependent internal pressure was considered, as per the stochastic Ferry-Borges model of Section 3.2.3.

First, the goal is to further investigate and compare the NHGP and HGP-based predictions and therefore, 20,000 samples are generated for the BUS-SuS, with $p_0 = 0.1$. The constant c was found to be $c = 20,792$ for this pipe segment, based on Eq. 5.27, for the 4 inspections in 2004, 2007, 2009 and 2011. The same values as in Section 5.6.2 are given to the parameters that define the prior distributions of the stochastic growth models. Initially, the result of interest is to obtain samples from the posterior distribution, so that afterwards the predictions of the NHGP and HGP models can be compared. To this end, after deriving $\Pr(Z)$ from the BUS-SuS run, additional samples are generated according to the procedure described in Section 5.4.2, so that a total of 20,000 samples of the posterior distribution

can be obtained. Thereafter, the NHGP and HGP-based predictions for four defects are investigated, through Fig. 5.10, in terms of the predicted growth path, for the period from pipe installation to ten years after the last inspection (i.e. 1972-2021).

Table 5.1 Probabilistic characteristics of the random variables included in the reliability analysis

Random Variable	Nominal value	Unit	Mean/Nominal	COV	Distribution type	Source
Initial $L_1 - L_{10}$	Given by Fig. 5.7	mm	1.0	7.8/ mean	Normal	Leis and Stephens, 1997
Diameter	508	mm	1.0	0.06%	Normal	Zhang and Zhou, 2013
Wall thickness	5.56	mm	1.0	0.25/mean	Normal	Zhang and Zhou, 2013
Tensile strength	456	MPa	1.08	3%	Normal	Zhang and Zhou, 2013
Maximum annual internal pressure	5.654	MPa	1.02	2%	Gumbel	Zhang and Zhou, 2013
Length growth rate	3.0	mm/year	1.0	50%	Lognormal	Zhou, 2010

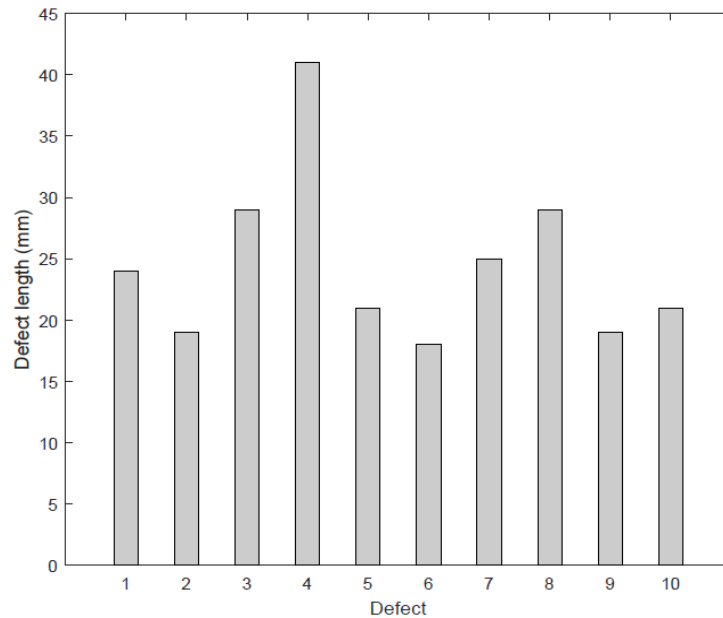


Figure 5.9 Initial defect lengths of the 10 defects derived from the ILI in 2011

It is observed that the predicted growth paths from the two stochastic models differ significantly, resulting in considerably different predictions for each defect depth in 2021. This is expectable to a certain extent, since the HGP model assumes a linear shape parameter with time, whereas the NHGP a power law function of time, for the shape parameter. So, the inference made previously, as to which of the two stochastic models most appropriately describes the defect growth, is amplified in this example.

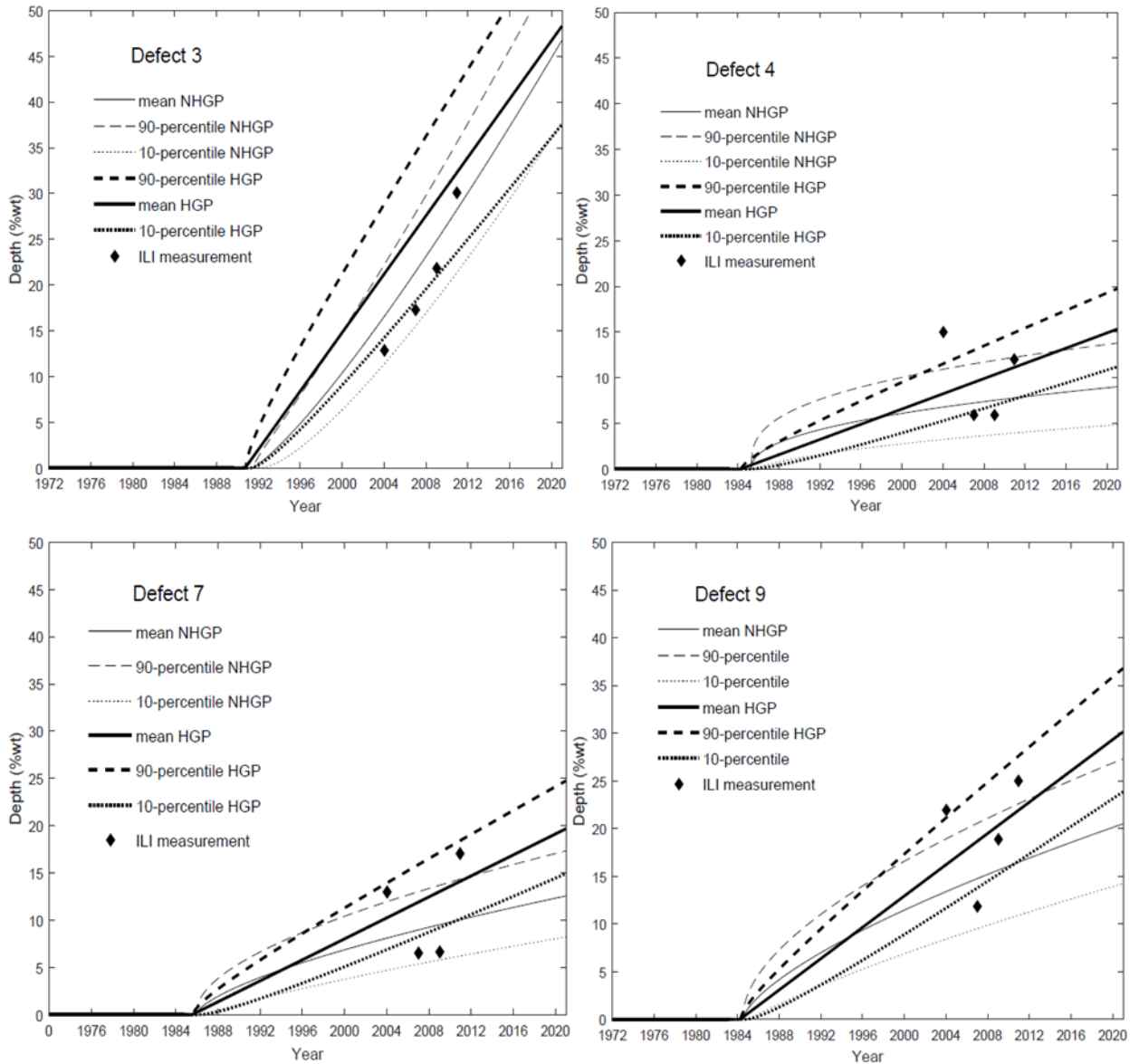


Figure 5.10 Comparisons of the growth path predictions of the NHGP- and HGP-based models for four random defects

The growth trend suggested by the ILI data, seems to be the determinant factor, as this might be closer to either a linear or a non-linear shape of the growth path. In the four randomly selected defects of Fig. 5.10, the predictions of the HGP-based model are more conservative, especially during the early years after initiation. In defect 3, where the ILI measurements appear to have the lowest measurement errors compared to the other three defects, both the NHGP and HGP come up with a similar growth path and an almost identical prediction for the defect depth in 2021. Furthermore, even though the ILI measurements for that same defect, suggest a path more akin to the NHGP model, the depth prediction in 2021, after a reasonably long period of time, i.e. 10 years, since last inspection, verifies the credibility of the HGP-based model, as well.

The initiation times in all four defects are almost the same for both models, with only the case of defect 4 differing marginally, in that the NHGP model indicates defect growth initiation 1-2 years later than the HGP model. However, such a clear trend, i.e. NHGP-based initiation times larger than HGP-based ones, cannot be claimed to exist, given these four defects. It is also noticed that defect 3, has the latest initiation time among the four. This is attributed to the fact that the ILI reported depths for this defect, indicate a higher growth rate compared to the rest of the defects. The BUS-SuS identifies it as a newer defect, compared to the other three and thus, indicates a succeeding initiation time. This observation is in accord with experimental results reported in the literature in the past, which suggest that metal-loss corrosion tends to grow faster during the early stages of development (Rodriguez and Provan, 1989).

In Fig. 5.11 next, the probability density functions (PDF) of the same four defects are presented for the years 2011, 2016 and 2021. The PDF curves are based on kernel density approximations, for the depth predictions of both the NHGP and HGP stochastic models, based on the posterior distribution derived from the proposed Bayesian methodology. It is illustrated that for both NHGP and HGP, the PDF curves move towards higher depths over time and also a tendency is revealed, for increased uncertainty in the predicted depth with time, since the spread of the curves tends to increase over time, as well.

The means of the predicted depths from the HGP model are generally higher compared to the NHGP predictions. This difference is less significant for defect 3, something expected given the increased proximity among the NHGP and HGP growth paths for this defect, as indicated in Fig. 5.10. However, there is a slight tendency towards reduction of the difference between the means of the predicted depths from the two growth models, over time. The standard deviation of the predicted depths, from the NHGP model, is generally

higher in all cases (except maybe defect 4). This is attributed to the fact that the shape parameter is a power law function with time and thus, the depth values usually entail more uncertainty.

The time-dependent system reliability is evaluated next for this pipe segment. In specific, the probability of failure is estimated separately against small leak, large leak and rupture, based on BUS-SuS with 20,000 samples. Then, the results are compared with respective evaluations, by means of a crude Monte Carlo (MC) simulation.

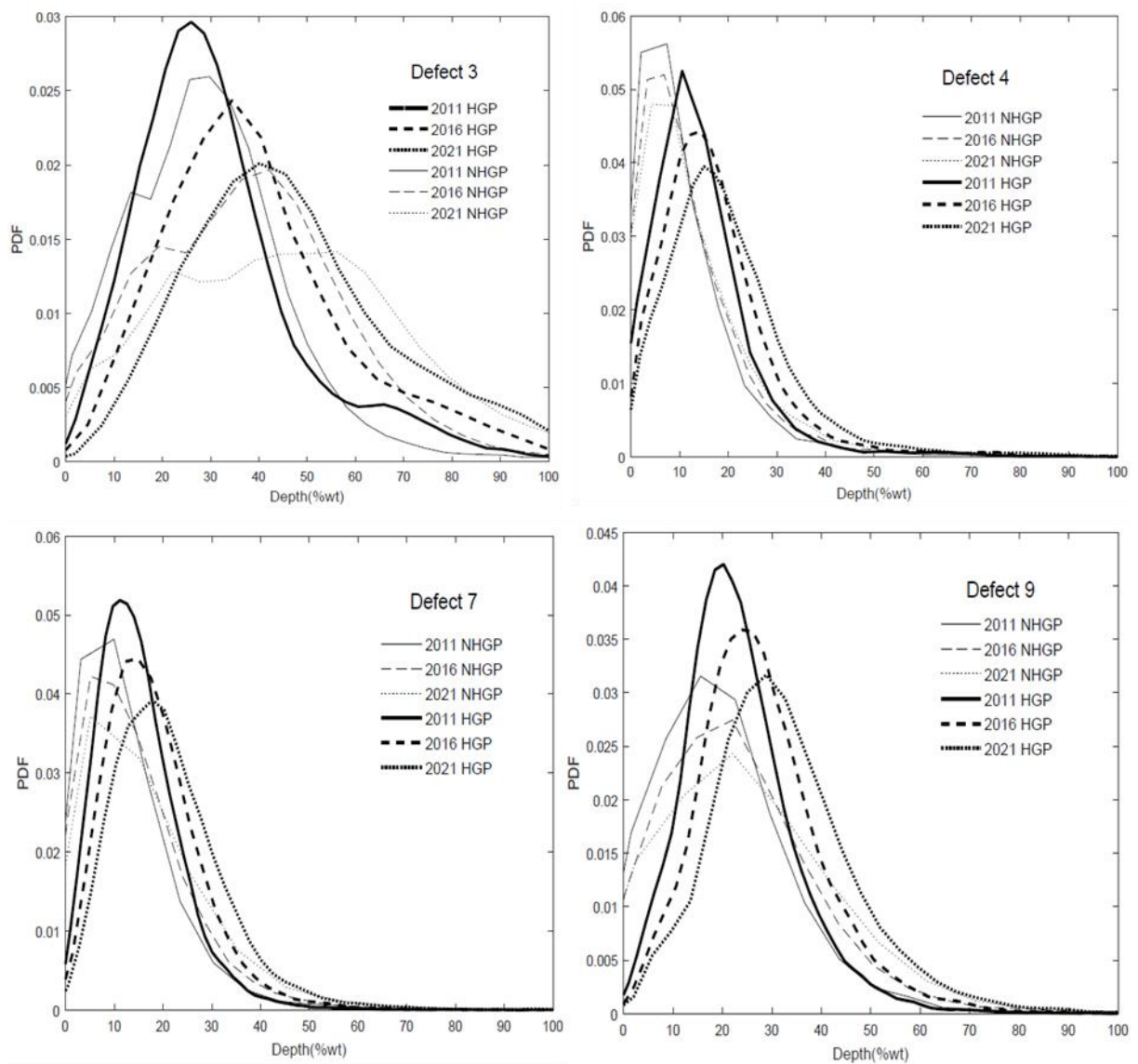
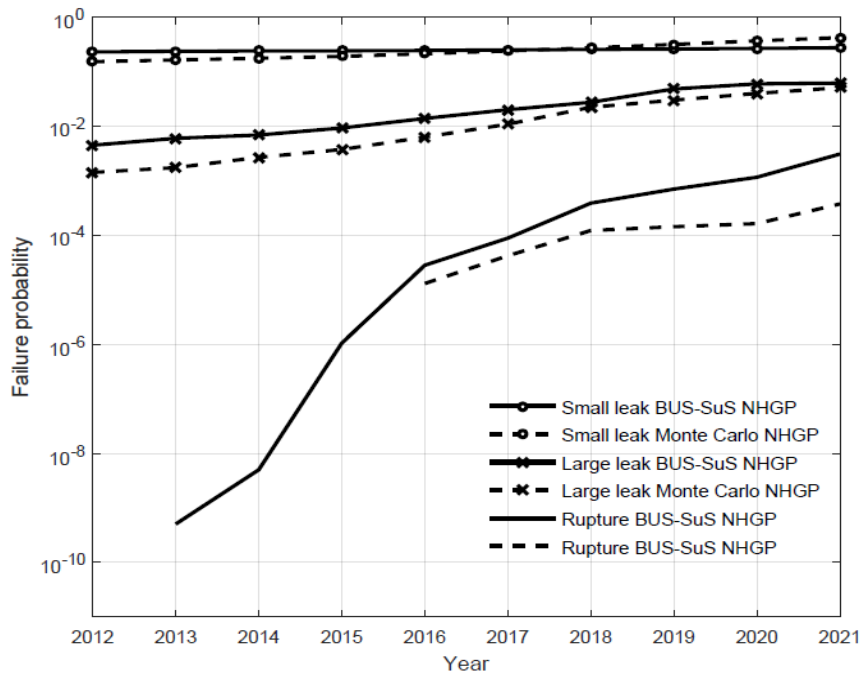
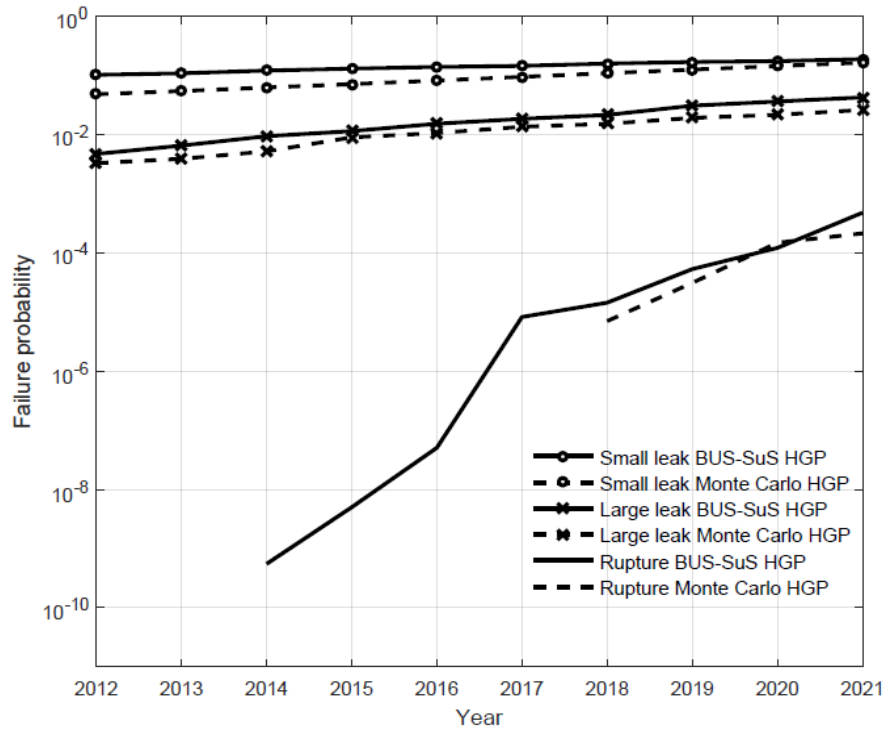


Figure 5.11 Marginal posterior PDFs of depth predictions of four defects in years 2011, 2016 and 2021

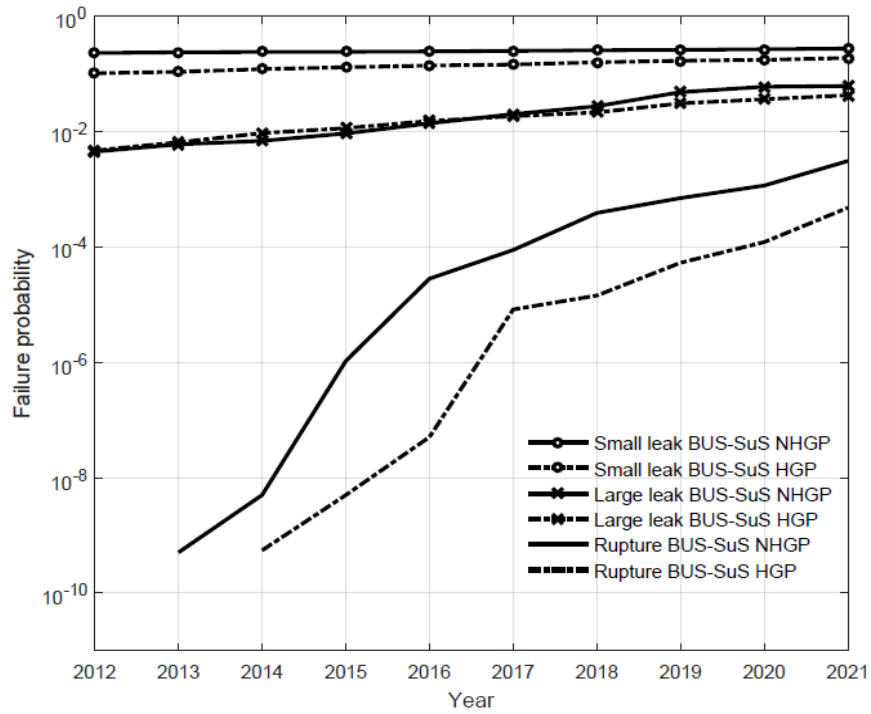
The aforementioned 20,000 samples from the posterior distribution, obtained for the comparisons among the NHGP and HGP depth predictions, are employed in the MC simulation. From these 20,000 samples, a total 4,000 sets of samples are arbitrarily selected and are used to further generate 250 random samples of the growth path for a each defect, which lead to a total 10^6 samples for the MC simulation. Employing samples of the posterior directly, has the advantage of taking the uncertainties in the growth parameters and their correlations into account, as opposed to the case of entirely approximating the posterior PDF. The probabilities of small leak, large leak and rupture, corresponding to either a NHGP or a HGP corrosion growth model and evaluated either directly with BUS-SuS or with a crude MC over a 10-year forecasting period, are presented in Fig. 5.12a-c. Fig. 5.12 indicates that small leak has the highest probability of occurrence over the entire forecasting period, with large leak having the second highest out of the three failure modes. Rupture presents very low failure probabilities consistently throughout the 10-year period and the competence of BUS-SuS with small failure probabilities is apparent in this case. It is noted that for relatively high probabilities (i.e. $<10^{-3}$), the BUS-SuS methodology and the typically adopted in literature MC, provide considerably proximate results. This is the case for both small leak and large leak and for both assumptions with respect to the corrosion growth model (i.e. NHGP and HGP).



(a)



(b)



(c)

Figure 5.12 (a-c) Comparison of small leak, large leak and rupture probabilities associated with different corrosion growth (NHGP, HGP) and different simulation methods for reliability evaluations (BUS-SuS, MC)

Furthermore, Fig. 5.12a indicates that in the case of NHGP, small leak probability when evaluated from BUS-SuS, is marginally higher in the first six years, i.e. 2012-2017, while afterwards it is slightly less than the respective MC estimation. For large leak, BUS-SuS consistently provides a more conservative estimation compared to MC, except for the last year of the forecast, where the values seem to match. The same underestimation from the MC is apparent in the rupture failure mode as well.

The discrepancies among the MC and BUS-SuS method are attributed to the approximate nature of the MC simulation method. This specific above-described MC method, accounts for the uncertainties of the growth parameters and their correlations only to certain extent, since the additionally generated samples equate to an approximate posterior distribution. On the other hand, in BUS-SuS such an approximation is not necessary. Next, the capacity of BUS-SuS for small probabilities (i.e. $<10^{-6}$), can also be observed in Fig. 5.12a. In specific, the MC estimation can be realised only beyond 2016, since before that the probability is too small for MC to produce credible (if any) results. On the contrary, BUS-SuS can provide the complete picture of the failure probabilities. Its evaluations initiate from the second year of the forecast period, i.e. 2013, and are in the order of 10^{-10} . The same features appear in Fig. 5.12b, which concern the HGP growth model. Minor differences with the aforementioned are identified in specific aspects, as for example the fact that the small leak probability curve from BUS-SuS, appears consistently higher than the respective MC one and also that the large leak curves are coherently more akin. When it comes to rupture, MC again presents limited capacity, in that it provides evaluations only in the last 4 years, i.e. from 2018 onwards, in contrast to BUS-SuS that provides predictions from the third year, starting again from a magnitude of 10^{-10} .

The HGP probabilities are lower than the respective NHGP ones over the entire 10-year period, especially the small ones, i.e. $<10^{-3}$. This is evident in Fig. 5.12c, where the NHGP rupture probability evaluations appear to be significantly more conservative compared to the HGP ones, almost one order of magnitude higher. The same is the case for small leak probabilities, but at a much smaller degree (almost one and half times higher), whereas large leak probability curves, intersect twice and differ marginally overall. The discrepancy is mainly attributed to the higher level of uncertainty involved in the NHGP model, as discussed previously for Fig. 5.11. In other words, the larger spread in the depth values generated from the NHGP model, due to the shape parameter being a power law function with time, is thought to produce more failure events in the reliability analysis.

This is overemphasized in the order of small probabilities, i.e. $<10^{-3}$, where a single failure event can create a significant difference in the overall system reliability.

5.7 High-pH SCC Case Study

5.7.1 Model Feasibility Study

According to the four-stage model of Parkins (1987) illustrated in Fig. 5.13, there is a threshold stress intensity factor (SIF) for crack growth in high-pH SCC (K_{ISCC}). Typically, when the stress intensity factor K is, $K \leq K_{ISCC}$, the crack growth rate (CGR) can be considered to be approximately zero (Song et al., 2011). The ILI tools have a resolution limit in detecting crack depths, which generally initiates from 1 mm in depth (Foreman et al., 2016; Hryciuk et al., 2016; Skow and LeBlanc, 2014). At such a depth, the growth follows deep-crack growing behavior and the methodology proposed in this study, for high-pH SCC under constant loading, is broadly applicable (Malyukova et al., 2004; Jaske and Beavers, 1998). The magnitude of K_{ISCC} for a given crack can depend on the surrounding environmental conditions (Song et al., 2011). Using pre-cracked specimens, Parkins (1987) measured K_{ISCC} in 1N-1N carbonate-bicarbonate solution at 75 °C to be 21 MPa·m^{0.5}. This threshold SIF is equivalent to a crack penetration of 1.1 mm into the pipe wall for an X52 pipe, with a 20 inch outer diameter and 0.32 inch wall thickness, operating at 72% of specified minimum yield strength (SMYS) (Song et al., 2011; Parkins, 1987). Generally, under the threshold K_{ISCC} at 21 MPa·m^{0.5}, the crack depth exceeds 1mm.

The characteristic form of SCC features is the presence in patches, of up to hundreds of longitudinal cracks, on the outside surface of the pipe. These small cracks typically coalesce, to form long shallow defects that can lead to failure (Wenk, 1974). ILI data may define either a detailed profile of the crack depth, as a function of its length or it may provide only an indication of the maximum crack depth and length. When a detailed depth profile is available, an effective surface crack feature can be obtained, using the procedures described in detail in Jaske et al. (1996), Jaske and Beavers (1998) and Kiefner and Veith (1989). The effective area is defined by its length and actual cross-sectional depth. The depth of an elliptical crack feature, of the same length and area as the effective feature, is then used to determine the crack's effective depth. If a detailed profile is not available, the

effective surface crack feature can be defined as a semi-elliptically shaped feature, with the measured maximum depth and length.

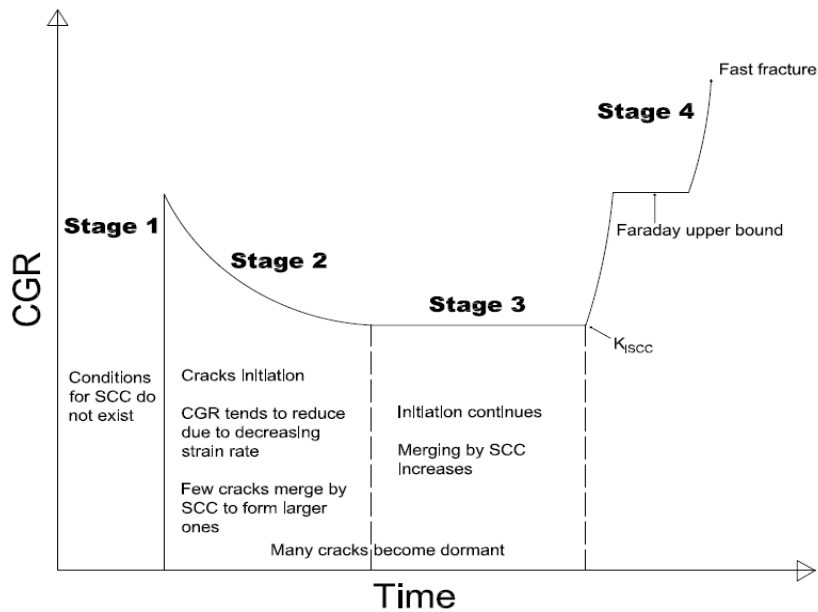


Figure 5.13 Four stages of high-pH SCC

Moreover, SCC are typically longitudinal surface cracks that connect to form long shallow defects, with length to depth (L/d) ratios that are usually in the range of 50 to 200 (Jaske and Beavers, 1998). In fact, for long and deep surface high-pH SCC features under static high gas pressure with such a high (L/d) ratio, the length can be considered to practically remain unchanged (Jaske et al., 1996; Jaske and Beavers, 1998; Timashev and Bushinskaya, 2016).

5.7.2 Numerical Application

The methodology is illustrated and validated based on hypothetical, i.e. simulated, inspection data, with respect to an existing pipe segment, which suffered an in-service failure in 2002 due to high-pH SCC (Hryciuk et al., 2016). This segment is part of a pipeline system built in 1960 with 609 mm diameter and 7.9 mm wall thickness, from pipe material conforming to API 5L grade X52 and external asphalt enamel coating. After the failure, extensive hydrostatic tests in the whole pipeline system followed in 2002 and also numerous soil samples were collected at selected locations. However, the aforementioned SCC mitigation measures are considered temporary (Hryciuk et al., 2016; CEPA, 2007).

On pipeline material samples removed from lines that were hydrostatically tested, further tests on SCC cracks that survived the pressure developed during the test (typically 110% of SMYS), indicated growth rates of 0.29 mm/year to 0.5 mm/year. Furthermore, it was decided to extensively perform remediation works of more permanent nature, i.e. the replacement of the original degraded coating by a new one.

SCC is a particular class of corrosion, the development process of which stops, when the contact between the steel surface and the ground is prevented. Thus, by replacing the coating, the growth of existing cracks is also arrested. Accordingly, a 100% solids liquid epoxy coating was applied to the pipeline system in 2003, including the susceptible part nearby the rupture location of 2002. An ILI inspection in 2014 revealed the remanence of five sub-critical SCC features in the susceptible part, whose growth had been arrested by the recoating and thus, were considered fit for service. Subsequently, the part containing verified SCC was cut out, in order to perform a full scale burst test. Material tests showed a minimum tensile strength of 428 MPa and minimum Charpy Energy at 0 C of 18 J, in a subsize specimen of 5 x 10 x 55 mm, equivalent to 36 J full size specimen (Hryciuk et al., 2016). These values are above the API X52 minimum requirements of 460 Mpa tensile strength and 27 J Charpy absorbed energy and actually met the requirements of API 5L X52 (Hryciuk et al., 2016; API Standard, 2007).

Based on the above-described information, a hypothetical case study was considered in an attempt to illustrate and validate the proposed methodology of this chapter. In specific, five future ILIs are assumed to take place after 2014. It is assumed that due to local degradation of the coating applied in 2003, SCC features start to generate and grow after 2014 and are detected in the five future ILIs. To that end, SCC features are assumed to initiate based on the NHHP model, by deterministically setting the parameters $\lambda_o=0.5$ and $\delta=1.0$. In addition, these are assumed to grow with a unique random rate that follows a uniform distribution, with a lower bound of 0.29 mm/year and an upper bound of 0.50 mm/year, as per the previously gathered actual data from the same pipeline system.

The results of the extensive study, presented in Foreman et al. (2016), were adopted to quantify the measurement error and PoD for the five future inspections considered. The study in Foreman et al. (2016), is based on significant populations of infield inspection results from a variety of pipeline sections of different diameters. The aim of their study, was to develop an absolute depth size specification, for ILI-based crack integrity management of pipelines. A depth detection threshold of >1mm is defined herein, along with a PoD of 98.3%, as per the aforementioned study. Furthermore, the measurement

error is assumed to fall within the bounds of $\pm 1\text{mm}$ with 90% probability, as per the respective absolute sizing model for cracks, from Foreman et al. (2016). Therefore, it is estimated that $q=4.0785$ in Eq. (5.5) and also that the measurement error follows a multivariate normal distribution, with mean zero and standard deviation $\sigma=7.29\%w_t$. For simplicity, the constant and non-constant biases included in the measurement errors given by Eq. (5.1), are assumed to be equal to zero and unity for all inspections respectively. Finally, the random scattering errors associated with different inspections are defined as mutually independent, with the same standard deviation of unity.

Individual crack features, are assumed to result from the coalescence of multiple longitudinal surface cracks that have already merged, to form the final detected length to depth (L/d) profile that follows a deep-crack growing behaviour. Their spatial dependence due to similar manufacture and operation environment is accounted for, through the correlation of their growths, based on the Copula method. Furthermore, it is considered that during the deep crack growing stage, individual features cannot further merge. Deep crack growing behaviour, apart from the studies already mentioned (i.e. Song et al., 2011; Malyukova et al., 2004; Jaske and Beavers, 1998; Wenk, 1974), is supported by the actual infield SCC cracks detected in 2014 on this very pipeline system (Hryciuk et al., 2016). For the inspection data, only the critical dimension, i.e. depth, was generated in the simulation and the length was evaluated according to the assumed ratio $L/d = 50/1$, throughout the time interval under examination (Jaske et al., 1996; Jaske and Beavers, 1998; Timashev and Bushinskaya, 2016). This is also above the absolute detection threshold, reported in Foreman et al. (2016) for crack lengths. The simulated inspection data are illustrated in Table 5.2.

5.7.3 Validation of Bayesian Formulation

The Bayesian updating was carried out for both the NHPP and NHGP models, based on the inspection data. The shape and scale parameters of the gamma prior distributions, for the parameters of the models α , κ , β_i and λ_o , δ , were all set to unity, and the newly detected cracks in the j th inspection were assumed to initiate between the $(j-1)$ th and j th inspections.

Table 5.2 Summary of the input simulated inspection data (newly detected crack features in brackets)

Time of inspection	Year 4	Year 7	Year 9	Year 11	Year 15
Number of detected cracks	0	1	4 (3)	10 (6)	27 (17)
Measured depth (mm) (Mean)	0	1.26	1.87	1.95	2.71
(Standard deviation)	0	0	0.29	0.80	1.35

A total of 20,000 samples were generated to evaluate the probabilistic characteristics of the model parameters. The means, medians and standard deviations of the posterior marginal distributions of the parameters λ_o , δ of the NHPP model, along with the average PoD, denoted by $\overline{\text{PoD}}_1, \overline{\text{PoD}}_2, \overline{\text{PoD}}_3, \overline{\text{PoD}}_4$ and $\overline{\text{PoD}}_5$, for the crack features generated prior to the first inspection year and among the rest of inspection years respectively, are summarised in Table 5.3. Furthermore, the same information for the NHGP parameters α , κ that are common for all crack features, is presented in Table 5.3. When compared with the actual values, the posterior mean and median values of λ_o and δ are considered to be in satisfactory agreement, which validates the Bayesian formulation described in Section 5.4. This is further illustrated in Fig. 5.14 and Fig. 5.15 for the NHPP and NHGP models, respectively.

Table 5.3 Posterior data of the methodology parameters

Parameter	NHPP		NHGP						
	$\lambda_o(0.5)$	$\delta(1.0)$	α	κ	$\overline{\text{PoD}}_1$	$\overline{\text{PoD}}_2$	$\overline{\text{PoD}}_3$	$\overline{\text{PoD}}_4$	$\overline{\text{PoD}}_5$
Mean	0.8955	0.7631	1.1369	0.8156	0.0334	0.3730	0.4211	0.4628	0.5717
Median	0.8955	0.7630	1.1522	0.8878	0	0.3479	0.3930	0.4684	0.6194
Standard deviation	0.0234	0.0066	0.1653	0.1845	0.0791	0.3693	0.2988	0.2704	0.2429

In Fig. 5.14, the simulation results are presented for the period between initiation of degradation of the coating, i.e. 2014, and the last inspection, 15 years later. The mean values of the number of generated features, i.e. $\Lambda(t) = \int_0^t \lambda_o \tau^\delta d\tau$, were calculated for the 15-year period, with the values λ_o , δ set to their corresponding posterior medians. For comparison, $\Lambda(t)$ evaluated by the actual values of λ_o and δ , the simulated total number

(detected and undetected) of cracks, as well as the simulated number of crack features detected in each of the five ILIs, are also illustrated in Fig. 5.14. $\Lambda(t)$ agrees with the actual mean very satisfactorily, which proves the validity of the Bayesian model.

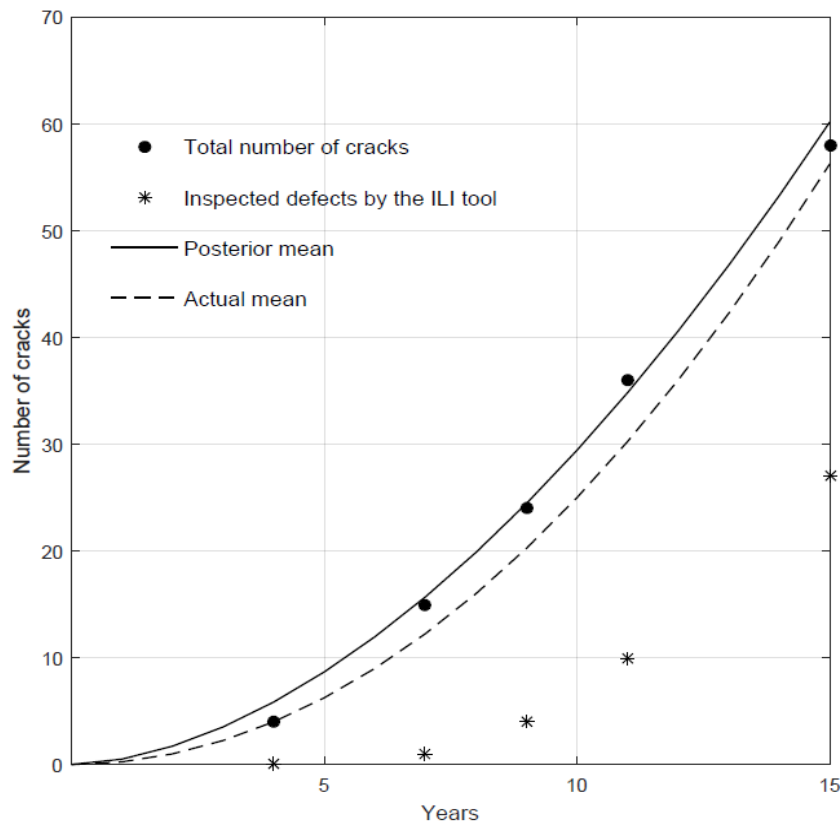


Figure 5.14 Comparison of predicted and actual number of crack features

For the same case, the depths of the detected crack features at year 15, were next evaluated and compared with the corresponding actual crack depths. The predicted depth for each crack was set equal to the mean depth derived from the NHGP growth model, with the parameters of the model, i.e. α , κ , β_i and t_{i0} , set equal to the respective posterior medians. In the Bayesian updating, constant c of Eq. (5.27) was evaluated at each inspection year, based on the procedure described in Section 5.4.3. The values of c are shown in Table 5.4. The results are illustrated in Fig. 5.15 and it can be deduced that the model predictions are in good agreement with reality. In specific, the predicted depths for 23 out of 27 crack features, i.e. 85% of the total, fall within the range of $\pm 10\% w_i$ of the corresponding actual depths, which is the typical confidence interval for inspection tool accuracy used in the pipeline industrial practice (Zhang and Zhou, 2013).

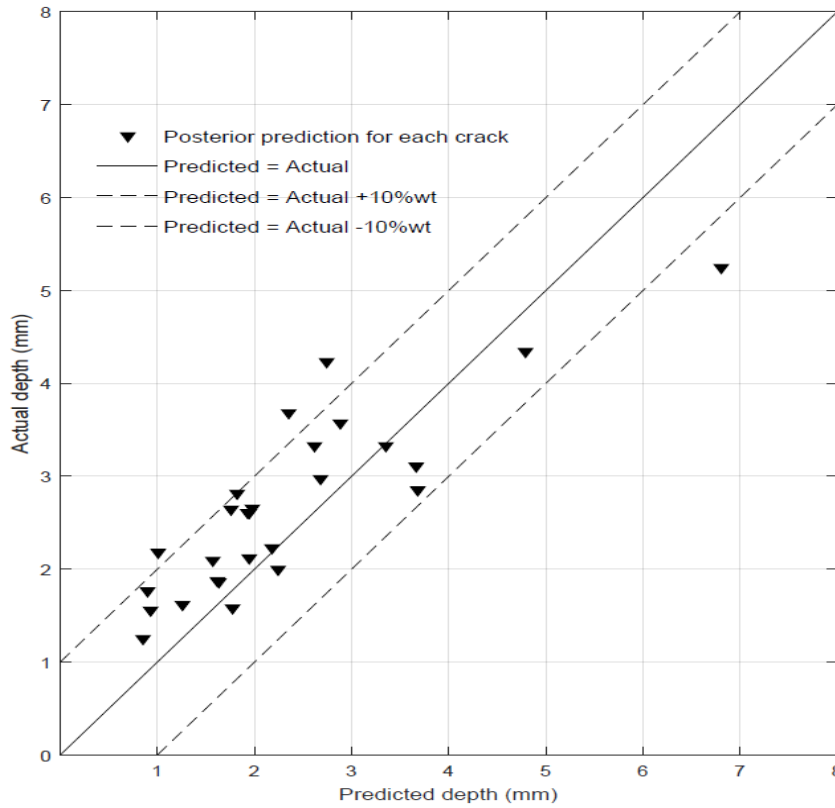


Figure 5.15 Comparison of predicted and actual depths of crack features at year 15

For the four crack features that predictions deviate significantly from the corresponding actual depths, i.e. more than $10\% w_t$, the maximum absolute deviation is $20\% w_t$. As a result, the methodology as a whole, including both the generation model NHPP and growth model NHGP as parts of the Bayesian formulation with DA, is validated against the corresponding actual data and its accuracy and suitability for relevant cases is verified.

Table 5.4 Constant c values for different inspection years

Time of inspection	Year 4	Year 7	Year 9	Year 11	Year 15
Constant c	0	6.2796	4.3460	3.0084	2.0840

5.7.4 Parametric and Reliability Analyses

To investigate the effect of correlations of the marginal growth processes, on the growth model and system reliability, different Gaussian copula-based dependence structures were considered. The posterior system reliability was estimated by the method described in

Section 5.5.3 and validated against results from a crude Monte Carlo (MC) simulation. For the MC simulation, a total of 10^6 simulation iterations were realised in a similar manner to the procedure described in Section 5.6.3. In both methods employed to carry out the time-dependent system reliability analysis, i.e. integrated SuS and MC, the internal pressure was set equal to the maximum allowed operating pressure (MAOP), which was assumed time-independent, herein. The pipe geometry, i.e. wall thickness w , and external diameter D , and material property, i.e. specified minimum tensile strength, were represented by a single random variable for each of these parameters at different crack features, as illustrated in Table 5.5. It was assumed that d_{ij} ($i=1, 2, \dots, s$ and $j=1, 2, \dots, l$) are identically distributed and equicorrelated, with the corresponding coefficient ρ set equal to 0.2, 0.5, 0.8 and 0.0, where 0.0 corresponds to independent and identically distributed samples. The stochastic dependence among d_{ij} was modelled by generating dependent samples of increments of d_{ij} and Δd_{ij} , on the prescribed inspection times. Δd_{ij} was generated as described in Section 5.3.3, with the i th element, i.e. marginal function, being part of a vector of a total of n random samples, i.e. multivariate function.

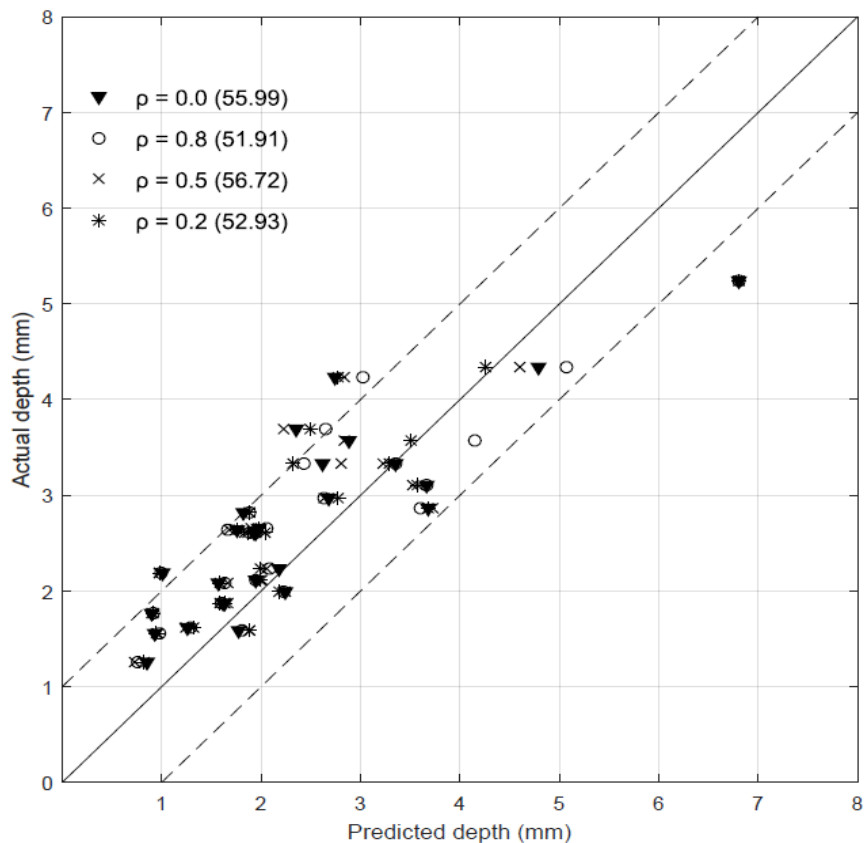


Figure 5.16 Comparison of the predicted and actual depths of crack features at year 15 for different correlation coefficients between stochastic growths

Fig. 5.16 compares the predictions of the growth model, i.e. NHGP, at year 15, with respect to different scenarios about the coefficient ρ and thus, illustrates the impact of different dependence structures. The mean squared error of prediction (MSEP), defined as $1/s \sum_{i=1}^s (d_{pi} - d_{ai})^2$, quantitatively evaluated the predicting accuracy of the growth model, where d_{pi} and d_{ai} denote the predicted and actual depths of the i th crack feature and s is the number of total detected features. The MSEP values are illustrated in brackets in Fig. 5.16 (the higher the accuracy the lower the corresponding MSEP value). It is therefore observed that the most accurate correlation scenario is the $\rho = 0.8$ one. However, there is not a clear trend indicated, by neither the depth predictions nor the MSEP results, with respect to different correlation scenarios. In fact, for the vast majority of crack features, i.e. 22 out of total 27, the depth predictions have negligible discrepancy among different correlation structures. Nevertheless, for all correlation scenarios the methodology is validated against the actual data. Thus, the results suggest that the correlation structure does not impact the Bayesian updating significantly, but the selection of a specific correlation structure is possible to affect the accuracy of the growth model, post updating.

Table 5.5 Random variables included in the reliability analysis

Random Variable	Nominal value	Unit	Mean/Nominal	COV	Distribution type	Source
Diameter	609	mm	1.0	0.06%	Normal	Zhang and Zhou, 2013
Wall thickness	7.90	mm	1.0	0.25/mean	Normal	Zhang and Zhou, 2013
Tensile strength	428	MPa	1.08	3%	Normal	Zhang and Zhou, 2013

Next, the posterior time-dependent reliability was evaluated on year 15 and all inspection years before that. The results are presented in Fig. 5.17, based on both the method of Section 5.5.3 and a Monte Carlo simulation. It is observed that the direct estimation of reliability, based on the combination of BUS-SuS and DA, is in very good agreement with the MC estimations. The marginal difference spotted in the 4th inspection, i.e. year 11, is attributed to the approximate nature of the MC simulation method. In both simulation methods, the reliability estimations that correspond to different correlation scenarios have negligible difference. This finding is in line with the study of Zhou et al. (2012) for metal-

loss corrosion defects that have independent initial depths and grow dependently, based on stochastic gamma processes. The results, therefore, suggest that correlations between stochastic growths of individual crack features, have a negligible impact on the posterior system reliability.

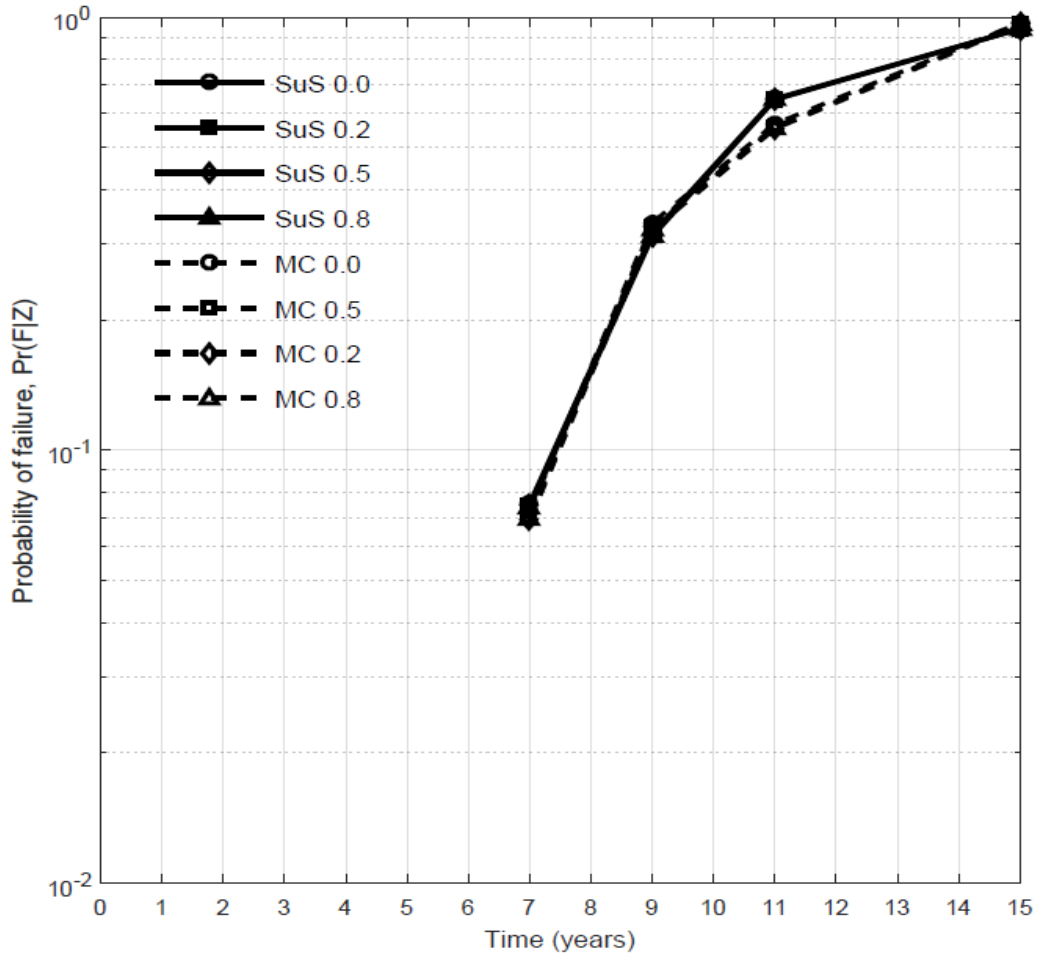


Figure 5.17 Posterior system reliability at inspection times, based on the proposed methodology and Monte Carlo, for different correlation scenarios among stochastic growths of the crack features

5.8 Conclusions

A stochastic process-based Bayesian methodology was proposed that is adequate for integrity management programs in gas pipelines. The proposed methodology (BUS-SuS) was illustrated and validated through two case studies involving existing gas pipelines, with metal-loss corrosion and stress corrosion cracking (SCC) respectively. In the first case study, the metal-loss corrosion data were readily available from multiple ILIs and the growth of each corrosion defect was modelled by nonhomogeneous gamma process

(NHGP)- and homogeneous gamma process (HGP)- based models. The numerical application consisted of initially applying the growth models on 17 external corrosion defects, based on three ILIs that took place before a subsequent field measurement in 2010, while considering the measurement errors of inspections. The model predictions were compared with the corresponding actual field measurements. The validation of the model was satisfactory for 14 of the 17 defects in the range of $\pm 10\% w_t$, for the absolute differences among the proposed methodology's predictions and field measurements. Further analysis of the results, indicated that the underestimations of the proposed methodology, are due to large measurement errors in ILIs. Therefore, it proves to be a reliable method in the setting of a real pipeline application, demonstrating at the same time additional efficiency compared to MCMC techniques, which are typically adopted in literature.

Furthermore, the time-dependent system reliability analysis was evaluated for a pipe segment that contains 10 corrosion defects. Internal pressure was modelled by a Ferry Borges stochastic process. Both the NHGP and HGP models were employed. It was shown that the proposed methodology facilitates the estimation of small posterior failure probabilities directly, without the requirement of either explicit knowledge or approximation of the posterior joint probability distribution of the random variables. The estimations were compared with results from crude Monte Carlo (MC) simulations and the aforementioned assumptions were verified. Reliability estimations from the proposed methodology, but also from MC at a lower extent, appear to give more conservative results when the NHGP growth model is employed. This is mainly attributed to the higher uncertainty contained in the NHGP model, due to the fact that the shape parameter is a power law function and, thus, it produces corrosion depth values of higher uncertainty.

In the second case study, Bayesian updating was conducted by using BUS-SuS in conjunction with the data augmentation (DA) technique. Simulated data were used, corresponding to an existing gas pipeline with high-pH SCC defects, to illustrate and validate the proposed methodology. The crack generation was characterised by the non-homogeneous Poisson process (NHPP) and the growth, in terms of the crack depth, by the non-homogeneous gamma process (NHGP), with a time-dependent shape parameter and a time-independent scale parameter. Furthermore, the Gaussian copula method was adopted to model the dependence among the stochastic growths of individual crack features. The model parameters were all uncertain variables evaluated from the proposed updating

methodology, based on imperfect data from multiple ILIs. The Bayesian framework accounted for the imperfect detectability of the ILI tool, as defined by the PoD, and also for the measurement errors associated with the ILI data. The Bayesian updating was performed together with the data augmentation algorithm, to account for undetected crack features. The posterior time-dependent system reliability was evaluated through coupling the updated crack growth model, with a probabilistic structural reliability model. The underlying high-dimensional issues, were solved using subset simulation, in a similar fashion to the first case study.

Different scenarios were considered with respect to the correlations of stochastic growths of crack features, in an effort to examine their impact on the posterior growth model and the system reliability. Stochastic growths of individual crack features were assumed identically distributed and equicorrelated, with the coefficient ρ equal to 0.2, 0.5, 0.8 and 0.0. The results from the Bayesian updating of the generation and growth models, indicate that the predicted overall crack population corresponding to the base case, i.e. $\rho = 0.0$, is in satisfactory agreement with the actual crack population, which validates the proposed methodology. The other three correlation scenarios also lead to predictions in good agreement with the actual data and therefore the Bayesian methodology is validated as a whole, irrespective of the correlation scenario. However, there were some discrepancies, identified through the MSE, in the accuracy of predictions among the different scenarios. The most accurate was the one with ρ equal to 0.8. The evaluations of the posterior time-dependent system reliability, based on both the direct coupled SuS methodology and the crude Monte Carlo simulation, led to similar results, which verify the correctness of the proposed methodology. Finally, for different dependence structures, the results from both simulation models were found to have a negligible impact on the posterior system reliability. Overall, the Bayesian framework proposed in this chapter, proves to be particularly advantageous for energy pipelines, which typically involve multiple random variables and particularly rare failure probabilities, which are often in the order of 10^{-6} or less.

6. Conclusions, Research Achievements and Future Works

6.1 General Conclusions

The work reported in this thesis focused on certain critical aspects of the engineering challenges included in reliability-based integrity management of energy pipelines. In specific, stochastic modelling within a structural reliability framework was carried out, along with statistical modelling for reliability predictions based on historical failures and the results were cross-verified. In addition, robust methodologies for estimation of small posterior failure probabilities were proposed, based on in-line inspection data. Conclusions obtained from the research, along with contributions to knowledge and future works are presented in the following.

6.1.1 Structural Reliability Analyses for Predictions in Energy Pipelines

Two probabilistic methodologies were proposed for onshore gas transmission pipelines subjected to external metal-loss corrosion, based on a robust integration of stochastic processes within a structural reliability analysis (SRA) framework. They were illustrated through two realistic case studies and were based on two different inspection and maintenance plans, i.e. DA and ILI inspections and repairs. The first methodology investigated a predominant failure mechanism, i.e. external metal-loss corrosion, and evaluated rupture probabilities regarding a reference pipe segment. The latter was constructed by employing the average characteristics of ruptured pipes, from PHMSA database of the United States Department of Transportation, for the period 2002-2014. The uncertainties were modelled comprehensively, through stochastic modelling of the segment-based loading and capacity. The non-homogeneous Poisson process was employed for the generation of new defects and the Poisson square wave process to model the growth of the defects. The internal pressure load was modelled through a discrete Ferry-Borges stochastic process. An implicit ILI inspection and maintenance plan was incorporated subsequently, based on standardised codes of practice, along with the corresponding uncertainties of the inspection procedure. Considering the use of realistic characteristics from the PHMSA database, it can be inferred that this model provides

additional knowledge on the state of the PHMSA onshore gas transmission network among 2002-2014, a representative period of the up-to-date techniques and strategies for operation and rehabilitation in the industry, amplifying the relevance of the results to reliability analyses for new or existing pipelines.

The second probabilistic methodology provided an accurate prediction of the time-dependent reliability for unpiggable pipeline systems, subjected to external metal-loss corrosion. The application of the proposed methodology on an example pipeline system was realised by considering a preventive direct excavation, assessment and repair strategy. The non-homogeneous Poisson process was employed for the generation of corrosion defects over time and a parameterized stochastic process, i.e. non-linear function of two random variables, for the defect growth, with respect to a single pipe segment of 12m. A Poisson square wave process model was adopted for the internal pressure loading. The reliability of the corroding pipe segment was evaluated by means of a Monte Carlo simulation, against the failure mode of burst. Next, a heuristic method, i.e. SSA, was employed, in order to update the corresponding reliability of a linear pipeline system, composed of a series of segments. The estimated reliability of the single segment, which is directly associated with the failure mode of burst, was used in the SSA analysis, instead of the hazard function associated with the time to failure. The pipeline system was assumed to be imperfectly repaired in every PM action, which is industry-consistent, due to human and financial constraints. The SSA method accurately quantified changes in reliability, due to the imperfect repairs. The results demonstrated the efficiency of the methodology in accurately quantifying pipeline system reliability, by incorporating the effects of failure probabilities of both repaired and unrepaired segments over time.

The probabilistic methodologies proposed in this chapter can assist operators in selecting efficient preventive ECDA and repair strategies for unpiggable pipelines, as well as ILI and repair strategies for piggable ones. In fact, for piggable pipelines, the two methodologies can be compared and the optimal one can be identified, from an analysis that conjointly considers failure probabilities and maintenance costs. The methodologies of this chapter can therefore assist operators in making informed maintenance decisions, based on reliability and risk.

6.1.2 Statistical Analyses for Reliability Predictions in Energy Pipelines

In the first case study of this chapter, the NPI established approach was employed, in an attempt to derive inductive inferences from the lifetimes of a set of ruptured onshore gas transmission pipelines, as reported in the PHMSA database in the period 2002-2014. The NPI method analysed the rupture incidents from a non-repairable systems perspective, based on the time to failure of the ruptured pipe segments. The analysis showed that NPI is an advantageous method for derivation of inferences for a future pipe segment that ruptures due to a specific failure cause, by providing imprecise probabilities and survival functions for this event, based on historical failure data. The results, among others, indicated external corrosion as the predominant rupture cause for the aforementioned period under consideration in the USA, with ruptures taking place mainly after 30 years of pipeline operation. The second case study was based on historical incident data from the PHMSA database, for the period 2002-2014 as well. An empirical discrete hazard model was adopted, in conjunction with a non-subjective parameter estimation technique, i.e. non-linear quantile regression, to evaluate hazard and reliability functions. The model provided inferences on the reliability of a region's reference pipe segment for its complete lifecycle, even in case of scarce, incomplete and censored data, as opposed to ROCOF methods that only account for the limited time period under study. Furthermore, non-linear quantile regression depicted accurately the hazard dataset. Thus, it is considered that the generic nature of the historical data was sufficiently accounted for and that the resulting reliability lies within a credible expectation range. The numerical application of the second case study on the PHMSA database for the period 2002-2014, concerned rupture incidents of onshore gas transmission pipelines.

The results of the second statistical methodology were compared with these of the first case study of the previous chapter (Section 3.5), which was based on the same PHMSA 2002-2014 set of data. The results demonstrated reasonable proximity, which constitutes an inherent validation of the soundness of both methodologies and their estimations. The second statistical methodology therefore, can help pipeline operators to derive plausible expectations for the performance of either new or existing pipelines. Those evaluations can also correspond separately to specific parameters, like defect growth rates or defect density or other pipeline attributes that define risk, by means of parametric studies. Furthermore, the numerical application results of the second case study, are thought to provide further

information about the PHMSA onshore gas transmission network among 2002-2014 with respect to rupture, which is more advantageous compared to the ROCOF-based approaches typically employed in literature. The methodologies of this chapter can therefore assist operators in making informed maintenance decisions based on reliability and risk.

6.1.3 Bayesian Analysis of Pipeline Reliability based on Imperfect Inspection Data

A stochastic process-based Bayesian methodology was proposed in this chapter, adequate for corrosion management programs regarding gas pipelines. The proposed methodology (BUS-SuS) was illustrated and validated through two case studies, involving existing gas pipelines with metal-loss corrosion and stress corrosion cracking (SCC), respectively. In the first case study, metal-loss corrosion data were available from multiple in-line inspections (ILIs) and the growth of each corrosion defect was modelled by both nonhomogeneous gamma process (NHGP)- and homogeneous gamma process (HGP)-based models. The numerical application consisted of initially applying the growth models on 17 external corrosion defects, based on three ILIs that took place before a subsequent field measurement in 2010, while considering the measurement errors of inspections. The model predictions were compared with the corresponding actual measurements from the field. The validation of the model was satisfactory for 14 out of 17 defects, in the range of $\pm 10\% w_t$ for the absolute differences among the methodology predictions and field measurements. Further analysis of the results, indicated that the reasons for the underestimations from the proposed methodology, were large measurement errors in ILIs. Therefore, it proved to be a reliable method in the setting of a real pipeline application, demonstrating at the same time additional efficiency compared to MCMC techniques, which are typically adopted in literature.

Furthermore, the time-dependent system reliability analysis was evaluated for a pipe segment that contains 10 corrosion defects. Internal pressure was modelled by a Ferry-Borges stochastic process. Both NHGP and HGP models were employed. It was shown that the proposed methodology facilitates the estimation of small posterior failure probabilities directly, without the requirement of either explicit knowledge or approximation of the posterior joint probability distribution of the random variables. The estimations were compared with results from crude Monte Carlo (MC) simulations and the

aforementioned assumptions were verified. Reliability estimations from the proposed methodology, but also from MC at a lower extent, gave more conservative results when the NHGP growth model was employed. This is mainly attributed to the higher uncertainty contained in the NHGP model, due to the fact that the shape parameter is a power law function with time and, thus, more uncertain corrosion depth values are produced.

In the second case study, Bayesian updating was carried out by using BUS-SuS, in conjunction with a data augmentation (DA) technique. Simulated data corresponding to an existing gas pipeline with high-pH SCC defects were used to illustrate and validate the proposed methodology. The crack generation was characterised by the non-homogeneous Poisson process and the growth, in terms of the crack depth, by the non-homogeneous gamma process, with a time-dependent shape parameter and a time-independent scale parameter. Furthermore, the Gaussian copula method was used to model the dependence among stochastic growths of individual crack features. The model parameters were all uncertain variables and were evaluated based on imperfect data obtained from multiple ILIs. The Bayesian framework accounted for the imperfect detectability of the ILI tool, as defined by the PoD, and also for the measurement errors associated with the ILI data. The Bayesian updating was performed together with the data augmentation algorithm for the undetected crack features, in order to obtain the posterior distributions of the model parameters. The updated time-dependent system reliability was subsequently evaluated, through coupling the updated crack growth model with a probabilistic structural model. The underlying high-dimensional structural reliability problems were solved using SuS, in a similar fashion to the first case study for small failure probabilities ($< 10^{-6}$).

Different scenarios were considered with respect to correlations of the stochastic growths of crack features, in an effort to examine their impact on the posterior growth model and the system reliability. Stochastic growths of individual crack features were assumed identically distributed and equicorrelated, with the coefficient ρ equal to 0.2, 0.5, 0.8 and 0.0. The results from the Bayesian updating of the generation and growth models, indicated that the predicted overall crack population corresponding to the base case, i.e. $\rho = 0.0$, was in satisfactory agreement with the actual crack population, which validates the proposed Bayesian methodology. The other three correlation scenarios also led to predictions of acceptable agreement with the actual data and therefore the Bayesian methodology was validated, for all correlation scenarios. However, there were some discrepancies in the accuracy of predictions among different scenarios, which were

identified through the mean squared error of prediction (MSEP). The most accurate among all four scenarios, was the one with ρ equal to 0.8. The evaluations of the posterior time-dependent system reliability on every inspection year, based on the direct BUS-SuS methodology and the crude Monte Carlo, led to almost identical results, which verifies the soundness of the proposed methodology. The results for different dependence structures, based on both reliability models, i.e. BUS-SuS and Monte Carlo, was found to have a negligible impact on the posterior system reliability. Overall, BUS-SuS proved to be particularly advantageous for underground energy pipelines, which contain many random variables and involve rare failure probabilities, especially rupture probabilities, which are often in the order of 10^{-6} and less.

6.2 Research Achievements

The main contributions to knowledge from the research presented in this thesis, can be summarized in the following. To begin with, in Chapter 3 a novel SRA methodology was proposed that can predict time-dependent reliability for unpiggable corroding energy pipelines on the system level, while taking into consideration imperfect repairs. This was accomplished by linking the results of structural reliability analysis (SRA) to long-term preventive maintenance (PM) planning, for multi-segment pipeline systems. The Split System Approach (SSA) was adopted to achieve this. To the author's best knowledge, SSA had never been applied to a corroding energy pipeline system before with the reliability estimated by a SRA, as opposed to the hazard function associated with the time to failure (lifetime distribution) employed in previous SSA studies. Furthermore, the results can be conveniently updated in the presence of new inspection and health monitoring information. The model was proposed in the context of a realistic maintenance strategy that is consistent with typical industry practice, namely External Corrosion Direct Assessment. Therefore the developed methodology is directly applicable in real industry practice. The optimal strategy can be subsequently determined, from a straightforward incorporation of maintenance costs.

The contributions to knowledge derived from the research presented in Chapter 4, is first the application of the theory of competing risks on energy pipelines. Competing risks arise when a failure can result from one of several causes and one cause precludes the others. As a result, the occurrence of one failure affects the probability of failure of the rest and

should be taken into account in reliability studies. This theory has been widely applied in many fields like engineering and medical science, with applications in reliability, public health and demography among others. To the best of the author's knowledge, this was an existing gap in reliability studies concerning energy pipelines. Next, a robust combination of an empirical hazard model, with the non-linear quantile regression technique was proposed, which can provide a credible range of expected lifecycle performance for gas transmission pipelines on the segment level, even in the case of scarce and censored data. This statistical method was validated against the SRA methodology proposed in the first case study of Chapter 3. The cross-verification of SRA and statistical analyses has always been a practical challenge in pipeline studies, due to the failure data being scarce and generic. However, this was dealt with efficiently herein, by properly taking into account the uncertainties associated with both methodologies. The numerical applications of the aforementioned methodologies (including the SRA methodology proposed in the first case study of Chapter 3) on the PHMSA database for onshore gas transmission pipeline rupture incidents during the period 2002-2014, provide novel insights on the reliability against rupture of pipes of this network, by considering the time to rupture of pipe segments, instead of the RCOF failure rate which is typically examined in literature.

The contributions from Chapter 5 include first the validation of BUS-SuS against an industry application, with subsequent insights on its efficiency and second the computation of small ($<10^{-6}$) posterior failure probabilities conditional on inspection data, for the first time in pipeline studies. Second, another novelty is the development of a probabilistic model for high-pH SCC in gas pipelines, based on imperfect ILI data. A robust hybrid Bayesian framework was proposed, based on BUS-SuS and a DA technique, which eliminates the uncertainty regarding ensuring that the final samples have reached the posterior distribution. Finally, the spatial correlation among the growth of different crack features was quantified based on inspection data and was readily available for both the development of the growth model and the evaluation of the system reliability, something covered for the first time in the reliability-based corrosion management literature, to the best of the author's knowledge.

6.3 Recommendations for future study

Although the research has reached its aims, there are some unavoidable limitations, mainly due to time and data constraints, which are listed below in the form of recommendations for future research.

First, the spatial variability at different defects across the pipeline, can be exhaustively taken into consideration. That is, local covariates such as pipe material, coating type, soil condition, if known, can be accurately depicted in the growth model, to yield the complete picture of the pipeline degradation, due to corrosion.

Second, multiple integrity threats can be considered in the structural reliability analysis methodologies, for comparison with the respective reliability results from statistical analyses. In specific, along with gradual deterioration models due to metal-loss corrosion or stress corrosion cracking, external shocks due to mechanical damage from external third party interference, can be modelled as well.

Third, multi-objective optimal maintenance management strategies for energy pipelines facing multiple integrity threats can be developed and implemented, because an integrity plan that minimizes the maintenance cost and maximizes the pipeline reliability, while accounting for multiple potential failure causes, would be comprehensive and advantageous to decision making.

Finally, the outcome, i.e. defect information, of any planned inspection can be used to update the various parameters (e.g. probability of detection, inspection tool errors, defect generation and growth models) employed in the analysis when conducting a multi-objective optimization approach. The updated parameters can be subsequently used to re-evaluate the optimal inspection interval in the subsequent years.

REFERENCES

- Abdalla Filho, J.E., Machado, R.D., Bertin, R.J. and Valentini, M.D., 2014. On the failure pressure of pipelines containing wall reduction and isolated pit corrosion defects. *Computers & Structures*, 132, pp.22–33.
- AER, 2013. *Report 2013-B: Pipeline Performance in Alberta, 1990–2012*. Alberta Energy Regulator.
- Ahammed, M., 1998. Probabilistic estimation of remaining life of a pipeline in the presence of active corrosion defects. *International Journal of Pressure Vessels and Piping*, 75(4), pp.321–329.
- Al-Amin, M., Zhou, W., Zhang S., Kariyawasam, S. and Wang, H., 2012. Bayesian model for calibration of ILI tools. In: *2012 9th International Pipeline Conference*. American Society of Mechanical Engineers, pp.201–208.
- Al-Amin, M. and Zhou, W., 2014. Evaluating the system reliability of corroding pipelines based on inspection data. *Structure and Infrastructure Engineering*, 10(9), pp.1161–1175.
- Allaoui, H. and Artiba, A., 2004. Integrating simulation and optimization to schedule a hybrid flow shop with maintenance constraints, *Computers & Industrial Engineering*, 47(4), pp. 431–450.
- Alrabghi, A. and Tiwari, A., 2015. State of the art in simulation-based optimisation for maintenance systems, *Computers & Industrial Engineering*, 82, pp. 167–182.
- Andersen, P.K., Geskus, R.B., de Witte, T., and Putter, H., 2012. Competing risks in epidemiology: possibilities and pitfalls. *International journal of epidemiology*, 41(3), pp.861–870.
- Animah, I., Shafiee, M., Simms, N., Erkoyuncu, J. A. and Maiti, J., 2018. Selection of the most suitable life extension strategy for ageing offshore assets using a life-cycle cost-benefit analysis approach. *Journal of Quality in Maintenance Engineering*, 24(3), 311-330.
- API Standard, 2007. 579-1/ASME FFS-1 Fitness for Service. *Houston, TX: American Petroleum Institute*.
- Asadi, Z.S. and Melchers, R.E., 2017. Extreme value statistics for pitting corrosion of old underground cast iron pipes. *Reliability Engineering & System Safety*, 162, pp.64-71.

Ascher, H. and Feingold, H., 1984. *Repairable systems reliability: modeling, inference, misconceptions and their causes* (p. 232). New York: M. Dekker.

ASME, 2012. *ASME B31.8S-2004 - Managing System Integrity of Gas Pipelines: Supplemental to ASME B31.8*, New York.

Au, S.-K. and Beck, J.L., 2001. Estimation of small failure probabilities in high dimensions by subset simulation. *Probabilistic Engineering Mechanics*, 16(4), pp.263–277.

Baker Jr, M., 2004. Stress corrosion cracking study. *Michael Baker Jr., Inc, OPS TT08*.

Baker, M., 2008. Pipeline corrosion. Final report submitted to the US department of transportation pipeline and hazardous materials safety administration. *Washington, DC, USA*.

Banczek, E. P., Zarpelon, L. M. C., Faria, R. N. and Costa, I., 2009. Corrosion resistance and microstructure characterization of rare-earth-transition metal–aluminum–magnesium alloys, *Journal of Alloys and Compounds*, 479(1), pp. 342–347.

Barone, G. and Frangopol, D.M., 2014. Reliability, risk and lifetime distributions as performance indicators for life-cycle maintenance of deteriorating structures. *Reliability Engineering & System Safety*, 123, pp.21–37.

Basile, O., Dehombreux, P. and Riane, F., 2004. Identification of reliability models for non repairable and repairable systems with small samples. In: *Proceedings of IMS2004 Conference on Advances in maintenance and modeling, simulation and intelligent monitoring of degradation, Arles* (pp.1–8).

Bazán, F.A.V. and Beck, A.T., 2013. Stochastic process corrosion growth models for pipeline reliability. *Corrosion Science*, 74, pp.50–58.

Beck, A. T. and de Santana Gomes, W. J., 2012. A comparison of deterministic, reliability-based and risk-based structural optimization under uncertainty, *Probabilistic Engineering Mechanics*, 28, pp. 18–29.

Beck, A. T. and Verzenhassi, C. C., 2008. Risk optimization of a steel frame communications tower subject to tornado winds, *Latin American Journal of Solids and Structures*, 5(3), pp. 187–203.

- Benjamin, A.C. and Andrade, E.Q., 2003. Modified method for the assessment of the remaining strength of corroded pipelines. In: *Rio Pipeline Conference*.
- Betz, W., Beck, J. L., Papaioannou, I. and Straub, D. 2018. Bayesian inference with reliability methods without knowing the maximum of the likelihood function. *Probabilistic Engineering Mechanics*, 53, 14-22.
- Betz, W., Papaioannou I. and Straub, D., 2014. Adaptive variant of the BUS approach to Bayesian updating. In *Proceedings of the 9th international conference on structural dynamics (EURODYN)*. Porto, Portugal (pp. 3021-3028).
- Betz, W., Papaioannou, I., Beck, J. L. and Straub D., 2018. Bayesian inference with subset simulation: strategies and improvements. *Computer Methods in Applied Mechanics and Engineering*, 331, 72-93.
- Bolt, R., Hilgenstock, G.A., Ruhrgas, E.O.N., Vega, D.V., ENAGAS, S.A.A., Gas, S.R., Rasmussen, O. and Gassco, A.S., 2006. Using or Creating Incident Databases for Natural Gas Transmission pipelines. In: *23rd World Gas Conference June*. pp.1–5.
- Briš, R., 2008. Parallel simulation algorithm for maintenance optimization based on directed Acyclic Graph, *Reliability Engineering & System Safety*, 93(6), pp. 874–884.
- Brongers, M. P. H., Beavers, J. A., Jaske, C. E. and Delanty, B. S., 2000. Effect of hydrostatic testing on ductile tearing of X-65 line pipe steel with stress corrosion cracks, *Corrosion*, 56(10), pp. 1050–1058.
- Bucher, C. and Frangopol, D. M., 2006. Optimization of lifetime maintenance strategies for deteriorating structures considering probabilities of violating safety, condition, and cost thresholds, *Probabilistic Engineering Mechanics*, 21(1), pp. 1–8.
- Cade, B.S. and Noon, B.R., 2003. A gentle introduction to quantile regression for ecologists. *Frontiers in Ecology and the Environment*, 1(8), pp.412–420.
- Caleyo, F., Alfonso, L., Alcántara, J., and Hallen, J.M., 2008. On the estimation of failure rates of multiple pipeline systems. *Journal of Pressure Vessel Technology*, 130(2), p.21704.
- Caleyo, F., Gonzalez, J.L., and Hallen, J.M., 2002. A study on the reliability assessment methodology for pipelines with active corrosion defects. *International Journal of Pressure Vessels and Piping*, 79(1), pp.77–86.

- Caleyo, F., Valor, A., Alfonso, L., Vidal, J., Perez-Baruch, E. and Hallen, J.M., 2015. Bayesian analysis of external corrosion data of non-piggable underground pipelines. *Corrosion Science*, 90, pp.33–45.
- Caleyo, F., Velázquez, J.C., Valor, A., and Hallen, J.M., 2009. Markov chain modelling of pitting corrosion in underground pipelines. *Corrosion Science*, 51(9), pp.2197–2207.
- Cao, Q.V. and Dean, T.J., 2015. Using non-linear quantile regression to estimate the self-thinning boundary curve. In *Southern Silvicultural Research Conference* (p. 349).
- Cao, Q.V. and Wang, J., 2015. Evaluation of methods for calibrating a tree taper equation. *Forest Science*, 61(2), pp.213-219.
- CEPA, 2007. Stress corrosion cracking recommended practices. *Canadian Energy Pipeline Association, Alberta*.
- Chang, C.-H., Tung, Y.K. and Yang, J.C., 1994. Monte Carlo simulation for correlated variables with marginal distributions. *Journal of Hydraulic Engineering*, 120(3), pp.313–331.
- Chaves, I. A., Melchers, R. E., Peng, L., and Stewart, M. G., 2016. Probabilistic remaining life estimation for deteriorating steel marine infrastructure under global warming and nutrient pollution. *Ocean Engineering*, 126, 129-137.
- Chebaro, M.R. and Zhou, W., 2010, January. A limit state function for pipelines containing long corrosion defects. In *2010 8th International Pipeline Conference* (pp. 511-517). American Society of Mechanical Engineers.
- Chen, C., 2005. An introduction to quantile regression and the QUANTREG procedure. In *Proceedings of the Thirtieth Annual SAS Users Group International Conference*. Cary, NC: SAS Institute Inc.
- Cheng, G., Xu, L. and Jiang, L., 2006. A sequential approximate programming strategy for reliability-based structural optimization, *Computers & structures*, 84(21), pp. 1353–1367.
- Ching, J. and Hsu, W.-C., 2008. Transforming reliability limit-state constraints into deterministic limit-state constraints, *Structural Safety*, 30(1), pp. 11–33.

- Choi, Y.-S., Shim, J.-J. and Kim, J.-G., 2005. Effects of Cr, Cu, Ni and Ca on the corrosion behavior of low carbon steel in synthetic tap water, *Journal of alloys and compounds*, 391(1), pp. 162–169.
- CONCAWE, 2015. Performance of European cross-country oil pipelines: statistical summary of reported spillages in 2013 and since 1971. *Brussels, Belgium: Report no 4/15*.
- Corder, I., 1995. The application of risk techniques to the design and operation of pipelines, In *IMECHE Conference Transactions, Mechanical Engineering Publications*, pp. 113–126.
- Corder, I. and Chatain, P., 1995. EPRG Recommendations for the Assessment of the Resistance of Pipelines to External Damage, In *Proceedings of the EPRG/PRC 10th Biennial Joint Technical Meeting On Line Pipe Research*, Cambridge, UK.
- Cosham, A. and Hopkins, P., 2001. A New Industry Document Detailing Best Practices In Pipeline Defect Assessment, In *Fifth International Onshore Pipeline Conference Amsterdam*, The Netherlands.
- Coolen, F.P.A., 1996. Comparing two populations based on low stochastic structure assumptions. *Statistics & Probability Letters*, 29(4), pp.297–305.
- Coolen, F.P.A., Coolen-Schrijner, P. and Yan, K.J., 2002. Nonparametric predictive inference in reliability. *Reliability Engineering & System Safety*, 78(2), pp.185–193.
- Coolen, F.P.A. and Yan, K.J., 2004. Nonparametric predictive inference with right-censored data. *Journal of Statistical Planning and Inference*, 126(1), pp.25–54.
- Coolen-Schrijner, P. and Coolen, F.P.A., 2004. Non-parametric Predictive Inference for Age Replacement with a Renewal Argument. *Quality and Reliability Engineering International*, 20(3), pp.203–215.
- Cox, D.R. and Oakes, D., 1984. *Analysis of survival data*. CRC Press.
- Dann, M. R. and Huyse, L., 2018. The effect of inspection sizing uncertainty on the maximum corrosion growth in pipelines. *Structural Safety*, 70, 71-81.
- Dann, M. R. and Maes, M. A., 2018. Stochastic corrosion growth modeling for pipelines using mass inspection data. *Reliability Engineering & System Safety*, 180, 245-254.

De Leon, D., and Macías, O.F., 2005. Effect of spatial correlation on the failure probability of pipelines under corrosion. *International journal of pressure vessels and piping*, 82(2), pp.123–128.

DiazDelaO, F. A., Garbuno-Inigo, A., Au, S. K. and Yoshida, I., 2017. Bayesian updating and model class selection with Subset Simulation. *Computer Methods in Applied Mechanics and Engineering*, 317, pp. 1102-1121.

Dong, C. F., Li, X. G., Liu, Z. Y. and Zhang, Y. R., 2009. Hydrogen-induced cracking and healing behaviour of X70 steel, *Journal of alloys and compounds*, 484(1), pp. 966–972.

Ebeling, C.E., 2004. *An introduction to reliability and maintainability engineering*. Tata McGraw-Hill Education.

EGIG, 2015. 9th EGIG report 1970-2013: gas pipeline incidents, Groningen, MA, Netherlands: *European Gas Pipeline Incident Data Group*.

El-Abbasy, M.S., Senouci, A., Zayed, T., Mirahadi, F., and Parvizsedghy, L., 2014. Condition prediction models for oil and gas pipelines using regression analysis. *Journal of Construction Engineering and Management*, 140(6), p.4014013.

Engelhardt, G. R., Macdonald, D. D. and Urquidi-Macdonald, M., 1999. Development of fast algorithms for estimating stress corrosion crack growth rate, *Corrosion Science*, 41(12), pp. 2267–2302.

Fan, L., Liu, Z.-Y., Guo, W.-M., Hou, J., Du, C.-W., and Li, X.-G., 2015. A New Understanding of Stress Corrosion Cracking Mechanism of X80 Pipeline Steel at Passive Potential in High-pH Solutions. *Acta Metallurgica Sinica (English Letters)*, 28(7), pp.866–875.

Fang, Y., Xiong, J., and Tee, K.F., 2015. Time-variant structural fuzzy reliability analysis under stochastic loads applied several times. *Structural Engineering and Mechanics*, 55(3), pp.525-534.

Finkelstein, M. and Shafiee, M., 2017. Preventive maintenance for systems with repairable minor failures. *Proceedings of the Institution of Mechanical Engineers, Part O: Journal of Risk and Reliability*, 231(2), pp.101-108.

Foreman, G., Bott, S., Sutherland, J. and Tappert, S., 2016. The Development and Use of an Absolute Depth Size Specification in ILI-Based Crack Integrity Management of

Pipelines. In: *2016 11th International Pipeline Conference*. American Society of Mechanical Engineers.

Francis, A., McCallum, M., Van Os, M.T., and Van Mastrigt, P., 2006. A New Probabilistic Methodology for Undertaking External Corrosion Direct Assessment. In: *2006 International Pipeline Conference*. American Society of Mechanical Engineers, pp.937–950.

Francis, A., McCallum, M., and Jandu, C., 2009. Pipeline life extension and integrity management based on optimized use of above ground survey data and inline inspection results. *Strength of materials*, 41(5), pp.478–492.

Frangopol, D.M. and Soliman, M., 2016. Life-cycle of structural systems: recent achievements and future directions. *Structure and Infrastructure Engineering*, 12(1), pp.1–20.

Fu, B., Stephens, D., Ritchie, D. and Jones, C.L., 2000. Methods for assessing corroded pipeline—review, validation and recommendations. *Report GRTC*, 3281.

Goodfellow, G. D., Haswell, J. V, McConnell, R. and Jackson, N. W., 2008. Development of risk assessment code supplements for the UK pipeline codes IGE/TD/1 and PD 8010, In *2008 7th International Pipeline Conference*, American Society of Mechanical Engineers, pp. 461–471.

Gomes, W.J.S., Beck, A.T. and Haukaas, T., 2013. Optimal inspection planning for onshore pipelines subject to external corrosion. *Reliability Engineering & System Safety*, 118, pp.18–27.

Golub, E., Dresnack, R., FH (Bud) Griffis and Pignataro, L.J., 1996. *Pipeline accident effects for natural gas transmission pipelines*. Institute of Transportation, New Jersey Institute of Technology.

Gong, C. and Zhou, W., 2018. Multi-objective maintenance strategy for in-service corroding pipelines using genetic algorithms. *Structure and Infrastructure Engineering*, 1-11.

Guo, B., Song, S. and Ghalambor, A., 2013. *Offshore pipelines: design, installation, and maintenance*. Gulf Professional Publishing.

- Gupta, A. and Lawsirirat, C., 2006. Strategically optimum maintenance of monitoring-enabled multi-component systems using continuous-time jump deterioration models, *Journal of Quality in Maintenance Engineering*, 12(3), pp. 306–329.
- Haladuick, S. and Dann, M. R., 2018. Decision Making for Long-Term Pipeline System Repair or Replacement. *ASCE-ASME Journal of Risk and Uncertainty in Engineering Systems, Part A: Civil Engineering*, 4(2), 04018009.
- Haladuick, S. and Dann, M. R., 2018. Value of information-based decision analysis of the optimal next inspection type for deteriorating structural systems. *Structure and Infrastructure Engineering*, 1-10.
- Hill, B.M., 1988. De Finetti's Theorem, Induction, and A (n) or Bayesian nonparametric predictive inference (with discussion). *Bayesian statistics*, 3, pp.211–241.
- Hill, B.M., 1993. Parametric models for A sub n: splitting processes and mixtures. *Journal of the Royal Statistical Society. Series B (Methodological)*, pp.423–433.
- Hinchliffe, S.R. and Lambert, P.C., 2013. Flexible parametric modelling of cause-specific hazards to estimate cumulative incidence functions. *BMC medical research methodology*, 13(1), pp.1-13.
- Hohenbichler M. and Rackwitz R., 1983. First-order concepts in system reliability. *Structural Safety*, 1(3), pp.177–88.
- Hohl, G. and Knauf, G., 1999. Field Hydrotesting and its Significance to Modern Pipelines, *Proceedings EPRG/PRCI*, 12.
- Hong, H.P., 1999. Inspection and maintenance planning of pipeline under external corrosion considering generation of new defects. *Structural Safety*, 21(3), pp.203–222.
- Hong, H.P., Zhou, W., Zhang, S., and Ye, W., 2014. Optimal condition-based maintenance decisions for systems with dependent stochastic degradation of components. *Reliability Engineering & System Safety*, 121, pp.276–288.
- Hryciuk, P.M., Carzoglio, E., Minellono, J.A., Martinetto, L., Guillen, P.M. and Grillenberger, J., 2016. The Use of Hydrotesting and EMAT Inline Inspection Technology for the Integrity Management of Stress Corrosion Cracking (SCC) in Gas Pipelines. In: *2016 11th International Pipeline Conference*. American Society of Mechanical Engineers.

- Hu, J., Tian, Y., Teng, H., Yu, L. and Zheng, M., 2014. The probabilistic life time prediction model of oil pipeline due to local corrosion crack, *Theoretical and applied fracture mechanics*, 70, pp. 10–18.
- IGEM, 2008. IGEM/TD/1 Edition 5: Steel pipelines for high pressure gas transmission. *Loughborough: The Institution of Gas Engineers and Managers*.
- Jaske, C.E. and Beavers, J.A., 1998. Review and proposed improvement of a failure model for SCC of pipelines. In *1998 2nd International Pipeline Conference* (pp. 439-445). American Society of Mechanical Engineers.
- Jaske, C.E. and Beavers, J.A., 1998. Predicting the failure and remaining life of gas pipelines subject to stress corrosion cracking. In: *International Gas Research Conference. Government Institutes Inc*, pp.281–290.
- Jaske, C.E., Beavers, J.A. and Harle, B.A., 1996. *Effect of stress corrosion cracking on integrity and remaining life of natural gas pipelines* (No. CONF-960389--). NACE International, Houston, TX (United States).
- Kiefner, J.F. and Vieth, P.H., 1989. *A modified criterion for evaluating the remaining strength of corroded pipe* (No. PR-3-805). Battelle Columbus Div., OH (USA).
- Kiefner, J.F., Mesloh, R.E. and Kiefner, B.A., 2001. Analysis of DOT Reportable incidents for gas transmission and gathering system pipelines, 1985 through 1997. *Pipeline Research Council International, Inc., Catalogue*, (L51830e).
- Kiefner, J.F. and Rosenfeld, M.J., 2012. The role of pipeline age in pipeline safety. *INGAA*, Oct.
- Kishawy, H.A., and Gabbar, H.A., 2010. Review of pipeline integrity management practices. *International Journal of Pressure Vessels and Piping*, 87(7), pp.373–380.
- Klaassen, K.B. and Van Peppen, J.C.L., 1989. *System reliability*. Edward Arnold.
- Koenker, R. and Machado, J.A.F., 1999. Goodness of fit and related inference processes for quantile regression. *Journal of the American Statistical Association*, 94(448), pp.1296–1310.
- Koenker, R. and Park, B.J., 1996. An interior point algorithm for non-linear quantile regression. *Journal of Econometrics*, 71(1), pp.265–283.

- Koenker, R., 2012. *quantreg: Quantile Regression*. R package version 4.98. Available at <http://CRAN.R-project.org/package=quantreg> (accessed 10 February 2016).
- Kulkarni, V.G., 1995. *Modeling and analysis of stochastic systems*. Chapman & Hall, Ltd., London, UK, UK.
- Kulkarni, V.G., 2009. *Modeling and analysis of stochastic systems*. CRC Press.
- Kuniewski, S.P., Van der Weide, J.A.M. and Van Noortwijk, J.M., 2009. Sampling inspection for the evaluation of time-dependent reliability of deteriorating systems under imperfect defect detection. *Reliability Engineering & System Safety*, 94(9), pp.1480–1490.
- Lam, C. and Zhou, W., 2016. Statistical analyses of incidents on onshore gas transmission pipelines based on PHMSA database, *International Journal of Pressure Vessels and Piping*, 145, pp.29-40.
- Lau, B., Cole, S.R., and Gange, S.J., 2009. Competing risk regression models for epidemiologic data. *American journal of epidemiology*, 170, pp.244-256.
- Lawless, J.F. and Fredette M., 2005. Frequentist prediction intervals and predictive distributions, *Biometrika*, 92, pp. 529–542.
- Lecchi, M., 2011. Evaluation of predictive assessment reliability on corroded transmission pipelines. *Journal of Natural Gas Science and Engineering*, 3(5), pp.633–641.
- Leemis, L.M., 1995. *Reliability: probabilistic models and statistical methods*. Prentice-Hall, Inc.
- Leewis, K., 2012. *The Australian Pipeliner*. [Online] [Accessed September 2015].
- Leis, B.N., and Stephens, D.R., 1997. An alternative approach to assess the integrity of corroded line pipe-part I: current status. In: *The Seventh International Offshore and Polar Engineering Conference*. International Society of Offshore and Polar Engineers.
- Lewis, E., 1996. *Reliability Engineering*, 2nd edition. New York.
- Li, S.-X., Yu, S.-R., Zeng, H.-L., Li, J.-H., and Liang, R., 2009. Predicting corrosion remaining life of underground pipelines with a mechanically-based probabilistic model. *Journal of Petroleum Science and Engineering*, 65(3), pp.162–166.
- Little, R.J.A. and Rubin, D.B., 2014. *Statistical analysis with missing data*. John Wiley & Sons.

- Macdonald, K. A. and Cosham, A., 2005. Best practice for the assessment of defects in pipelines—gouges and dents, *Engineering Failure Analysis*, Elsevier, 12(5), pp. 720–745.
- Maes, M.A., Faber, M.H. and Dann, M.R., 2009. Hierarchical modeling of pipeline defect growth subject to ILI uncertainty. In: *ASME 2009 28th International Conference on Ocean, Offshore and Arctic Engineering*. American Society of Mechanical Engineers, pp.375–384.
- Malyukova, M.G., Timashev, S.A. and Maltsev, I.L., 2004, January. Practical Method of Updating Stochastic Remaining Life of Pipelines Using ILI Data. In *2004 International Pipeline Conference* (pp. 2487-2492). American Society of Mechanical Engineers.
- Manfredi, C., and Otegui, J.L., 2002. Failures by SCC in buried pipelines. *Engineering Failure Analysis*, 9(5), pp.495–509.
- Maturi, T.A., Coolen-Schrijner, P. and Coolen, F.P.A., 2010. Nonparametric predictive inference for competing risks. *Proceedings of the Institution of Mechanical Engineers, Part O: Journal of Risk and Reliability*, 224(1), pp.11–26.
- Maturi, T., 2010. *Nonparametric predictive inference for multiple comparisons* (Doctoral dissertation, Durham University).
- Melchers, R., 2004. *Structural Reliability Analysis and Prediction*, 2nd Edition. Wiley.
- Melchers, R.E., 2016. Developing realistic deterioration models. In *Life-Cycle of Engineering Systems: Emphasis on Sustainable Civil Infrastructure: Proceedings of the Fifth International Symposium on Life-Cycle Civil Engineering (IALCCE 2016)*, 16-19 October 2016, Delft, The Netherlands (p. 28). CRC Press.
- Melchers, R. E., and Ahammed, M., 2016. Pitting corrosion of offshore water injection steel pipelines. In *The 26th International Ocean and Polar Engineering Conference*. International Society of Offshore and Polar Engineers.
- Morrison, T. and Spencer, P., 2014. Quantile Regression-A Statisticians Approach to the Local Ice Pressure-Area Relationship. In: *OTC Arctic Technology Conference*. Offshore Technology Conference.
- Morrison, T. B. and Worthingham, R. G., 1992. Reliability of high pressure line pipe under external corrosion, In *Proceedings of the International Conference on Offshore Mechanics and Arctic Engineering*, American Society of Mechanical Engineers, p. 401.

- NACE International, 2010. *Standard Recommended Practice: Pipeline External Corrosion Direct Assessment Methodology*. NACE International.
- Nelsen, R.B., 2006. *An introduction to copulas, ser. Lecture Notes in Statistics*. New York: Springer.
- Nessim, M., Zhou, W., Zhou, J. and Rothwell, B., 2009. Target reliability levels for design and assessment of onshore natural gas pipelines. *Journal of Pressure Vessel Technology*, 131(6), p.61701.
- Nessim, M. and Zhou, W., 2011. Guidelines for Reliability Based Design and Assessment of Onshore Natural Gas Pipelines. Submitted to Pipeline Research Council International. *Inc. CFER Report L, 177*.
- NTSB, 2015. *Integrity Management of Gas Transmission Pipelines in High Consequence Areas*, NTSB SS-15/01.
- Okasha, N.M. and Frangopol, D.M., 2010. Redundancy of structural systems with and without maintenance: An approach based on lifetime functions. *Reliability Engineering & System Safety*, 95(5), pp.520–533.
- Opeyemi, D.A., Patelli, E., Beer, M. and Timashev, S.A., 2015. Comparative studies on assessment of corrosion rates in pipelines as semi-probabilistic and fully stochastic values. In *12th International Conference on Applications of Statistics and Probability in Civil Engineering*, ICASP12, July 12-15, Vancouver, Canada.
- Pandey, M.D., 1998. Probabilistic models for condition assessment of oil and gas pipelines. *NDT & E International*, 31(5), pp.349–358.
- Pandey, M.D., and Lu, D., 2013. Estimation of parameters of degradation growth rate distribution from noisy measurement data. *Structural Safety*, 43, pp.60–69.
- Papaoiannou, I., Betz, W., Zwirgmaier, K. and Straub, D., 2015. MCMC algorithms for subset simulation. *Probabilistic Engineering Mechanics*, 41, 89-103.
- Parkins, R.N., 1987. Factors Influencing Stress Corrosion Crack Growth Kinetics. *Corrosion. Vol. 43*. pp. 130-138.

- Payten, W. M., Wei, T., Snowden, K. U., Bendeich, P., Law, M. and Charman, D., 2011. Crack initiation and crack growth assessment of a high pressure steam chest, *International Journal of Pressure Vessels and Piping*, 88(1), pp. 34–44.
- Peabody, A.W., 2001. Control of Pipeline Corrosion, ed. R. Bianchetti (Houston, TX: NACE International, 2001).
- Peng, X., Hang, P. and Chen, L., 2009. Long-distance oil/gas pipeline failure rate prediction based on fuzzy neural network model. In: *Computer Science and Information Engineering*, 2009 WRI World Congress on. IEEE, pp.651–655.
- PHMSA, 2015. phmsa.dot.gov. [Online] Available at: <http://phmsa.dot.gov>[Accessed September 2015].
- Qian, G., Niffenegger, M., Zhou, W. and Li, S., 2013. Effect of correlated input parameters on the failure probability of pipelines with corrosion defects by using FITNET FFS procedure. *International Journal of Pressure Vessels and Piping*, 105, pp.19–27.
- Qin, H., Zhou, W. and Zhang, S., 2015. Bayesian inferences of generation and growth of corrosion defects on energy pipelines based on imperfect inspection data. *Reliability Engineering & System Safety*, 144, pp.334–342.
- Papadakis, G. A., 2000. Assessment of requirements on safety management systems in EU regulations for the control of major hazard pipelines. *Journal of hazardous materials*, 78(1-3), 63-89.
- Rigdon, S.E. and Basu, A.P., 2000. *Statistical methods for the reliability of repairable systems*. Wiley New York.
- Rodriguez, E. S., and Provan, J. W., 1989. Part II: development of a general failure control system for estimating the reliability of deteriorating structures, *Corrosion*, 45(3), pp. 193–206.
- Rubin, D.B., 2004. *Multiple imputation for nonresponse in surveys*. John Wiley & Sons.
- Schneider, R., Thöns, S. and Straub, D., 2017. Reliability analysis and updating of deteriorating systems with subset simulation. *Structural Safety*, 64, pp.20–36.

- Senouci, A., Elabbasy, M., Elwakil, E., Abdrabou, B., and Zayed, T., 2014. A model for predicting failure of oil pipelines. *Structure and Infrastructure Engineering*, 10(3), 375-387.
- Shafiee, M. and Ayudiani, P.S., 2015. Development of a risk-based integrity model for offshore energy infrastructures-application to oil and gas pipelines. *International Journal of Process Systems Engineering*, 3(4), pp.211-231.
- Shafiee, M., Finkelstein, M. and Chukova, S., 2011. Burn-in and imperfect preventive maintenance strategies for warranted products. *Proceedings of the Institution of Mechanical Engineers, Part O: Journal of Risk and Reliability*, 225(2), pp.211-218.
- Shafiee, M. and Finkelstein, M., 2015. An optimal age-based group maintenance policy for multi-unit degrading systems. *Reliability Engineering & System Safety*, 134, pp.230-238.
- Shafiee, M., Finkelstein, M. and Bérenguer, C., 2015. An opportunistic condition-based maintenance policy for offshore wind turbine blades subjected to degradation and environmental shocks. *Reliability Engineering & System Safety*, 142, pp.463-471.
- Skow, J. and LeBlanc, L., 2014. In-line inspection tool performance evaluation using field excavation data. In: *Proceedings of the ASME 2014 10th international pipeline conference, IPC*.
- Song, F. M., 2009. Predicting the mechanisms and crack growth rates of pipelines undergoing stress corrosion cracking at high pH, *Corrosion science*, 51(11), pp. 2657–2674.
- Song, F., Lu, B., Gao, M. and Elboudjaini, M., 2011. *Development of a commercial model to predict stress corrosion cracking growth rates in operating pipelines* (No. 20.14080).
- Stephens, D.R. and Leis, B.N., 2000, October. Development of an alternative criterion for residual strength of corrosion defects in moderate-to high-toughness pipe. In *2000 3rd International Pipeline Conference* (pp. 012-021). American Society of Mechanical Engineers.
- Stephens, M. and Nessim, M., 2006. A comprehensive approach to corrosion management based on structural reliability methods. In: *2006 International Pipeline Conference*. American Society of Mechanical Engineers, pp.695–704.

- Straub, D. and Faber, M.H., 2005. Risk based inspection planning for structural systems. *Structural Safety*, 27(4), pp.335–355.
- Straub, D. and Papaioannou, I., 2014a. Bayesian updating with structural reliability methods. *Journal of Engineering Mechanics*, 141(3), p.4014134.
- Straub, D. and Papaioannou, I., 2014b. *Bayesian analysis for learning and updating geotechnical parameters and models with measurements*. Chapter 5, pp.221–264.
- Straub, D., Papaioannou, I. and Betz, W., 2016. Bayesian analysis of rare events. *Journal of Computational Physics*, 314, pp.538–556.
- Streicher, H., and Rackwitz, R., 2004. Time-variant reliability-oriented structural optimization and a renewal model for life-cycle costing, *Probabilistic Engineering Mechanics*, 19(1), pp. 171–183.
- Sun, Y., Fidge, C. and Ma, L., 2014. Optimizing Preventive Maintenance Strategies for Linear Assets. In *Engineering Asset Management 2011: Proceedings of the Sixth World Congress on Engineering Asset Management*. London: Springer-Verlag London.
- Sun, Y., Fidge, C. and Ma, L., 2011. Reliability prediction of long-lived linear assets with incomplete failure data. In: *Quality, Reliability, Risk, Maintenance, and Safety Engineering (ICQR2MSE)*, 2011 International Conference on. IEEE, pp.143–147.
- Sun, Y., Ma, L. and Mathew, J., 2007. Prediction of system reliability for multiple component repairs. In: *Industrial Engineering and Engineering Management, 2007 IEEE International Conference on*. IEEE, pp.1186–1190.
- Sun, Y., Ma, L. and Morris, J., 2009. A practical approach for reliability prediction of pipeline systems. *European Journal of Operational Research*, 198(1), pp.210–214.
- Taflanidis, A. A. and Beck, J. L., 2008. Stochastic subset optimization for optimal reliability problems, *Probabilistic Engineering Mechanics*, 23(2), pp. 324–338.
- Tanner, M.A. and Wong, W.H., 1987. The calculation of posterior distributions by data augmentation. *Journal of the American statistical Association*, 82(398), pp.528–540.
- Tee, K.F., Cai, Y. and Chen, H.-P., 2013. Structural damage detection using quantile regression. *Journal of Civil Structural Health Monitoring*, 3(1), pp.19–31.

- Tee, K.F., Khan, L.R. and Li, H.S., 2014. Application of subset simulation in reliability estimation for underground pipelines. *Reliability Engineering and System Safety*, 130, pp.125-131.
- Teixeira, A.P., Soares, C.G., Netto, T.A. and Estefen, S.F., 2008. Reliability of pipelines with corrosion defects. *International Journal of Pressure Vessels and Piping*, 85(4), pp.228–237.
- Timashev, S.A., Malyukova, M.G., Poluian, L.V. and Bushinskaya, A.V., 2008, January. Markov description of corrosion defects growth and its application to reliability based inspection and maintenance of pipelines. In *2008 7th International Pipeline Conference* (pp. 525-533). American Society of Mechanical Engineers.
- Timashev, S.A. and Bushinskaya, A.V., 2016. *Diagnostics and Reliability of Pipeline Systems*. Springer.
- UKOPA, 2014. *Pipeline Product Loss Incidents and Faults Report (1962-2013)*, Ambergate, UK: UKOPA.
- Valdebenito, M.A. and Schuëller, G.I., 2010. A survey on approaches for reliability-based optimization. *Structural and Multidisciplinary Optimization*, 42(5), pp.645-663.
- Valentin, T., Andrei, I., Tarean, C. and Toma, N., 2014. Maintenance of the Romanian National Transportation System of Crude Oil and Natural Gas, *Procedia Engineering*, 69, pp. 980–985.
- Valor, A., Caleyó, F., Alfonso, L., Rivas, D. and Hallen, J.M., 2007. Stochastic modeling of pitting corrosion: a new model for initiation and growth of multiple corrosion pits. *Corrosion science*, 49(2), pp.559–579.
- Valor, A., Caleyó, F., Alfonso, L., Vidal, J. and Hallen, J.M., 2014. Statistical analysis of pitting corrosion field data and their use for realistic reliability estimations in non-piggable pipeline systems. *Corrosion*, 70(11), pp.1090–1100.
- Valor, A., Caleyó, F., Hallen, J.M. and Velázquez, J.C., 2013. Reliability assessment of buried pipelines based on different corrosion rate models. *Corrosion Science*, 66, pp.78–87.

- Van Burgel, M., De Wacht, M. and Van Os, M.T., 2011. A complete and integrated approach for the assessment of non-piggable pipelines. In: *Proc. of the International Gas Union Research Conference* pp.1689–1703.
- Van Noortwijk, J.M., 2009. A survey of the application of gamma processes in maintenance. *Reliability Engineering & System Safety*, 94(1), pp.2–21.
- Van Os, M.T. and Van Mastrigt, P., 2006. A direct assessment module for pipeline integrity management at Gasunie. In: *23rd World Gas Conference*.
- Velázquez, J.C., Caleyó, F., Valor, A. and Hallen, J.M., 2009. Predictive model for pitting corrosion in buried oil and gas pipelines. *Corrosion*, 65(5), pp.332–342.
- Walley, P., 1991. *Statistical reasoning with imprecise probabilities*. Peter Walley.
- Weichselberger, K., 2000. The theory of interval-probability as a unifying concept for uncertainty. *International Journal of Approximate Reasoning*, 24(2), pp.149–170.
- Wenk, R.L., 1974. Field investigation of stress corrosion cracking. In: *5th Symposium on Line Pipe Research*, American Gas Association, Inc., Catalog. No L30174.
- Witek, M., 2018. Validation of in-line inspection data quality and impact on steel pipeline diagnostic intervals. *Journal of Natural Gas Science and Engineering*.
- Witek, M., Batura, A., Orynyak, I. and Borodii, M., 2018. An integrated risk assessment of onshore gas transmission pipelines based on defect population. *Engineering Structures*, 173, 150-165.
- Yan, Z., Zhang, S. and Zhou, W., 2014. Model error assessment of burst capacity models for energy pipelines containing surface cracks. *International Journal of Pressure Vessels and Piping*, 120, pp.80–92.
- Zhang, S., 2014. *Development of Probabilistic Corrosion Growth Models with Applications in Integrity Management of Pipelines*. Doctoral dissertation, The University of Western Ontario.
- Zhang, S. and Zhou, W., 2013. System reliability of corroding pipelines considering stochastic process-based models for defect growth and internal pressure. *International Journal of Pressure Vessels and Piping*, 111, pp.120–130.

- Zhang, S. and Zhou, W., 2014. Cost-based optimal maintenance decisions for corroding natural gas pipelines based on stochastic degradation models. *Engineering Structures*, 74, pp.74–85.
- Zhang, S., Zhou, W., Al-Amin, M., Kariyawasam, S. and Wang, H., 2012. Time-dependent corrosion growth modeling using multiple ILI data. In *2012 9th International Pipeline Conference* (pp. 693-702). American Society of Mechanical Engineers.
- Zhou, W., 2010. System reliability of corroding pipelines. *International Journal of Pressure Vessels and Piping*, 87(10), pp.587–595.
- Zhou, W., 2011. Reliability evaluation of corroding pipelines considering multiple failure modes and time-dependent internal pressure. *Journal of Infrastructure Systems, ASCE*, 17(4), pp.216–224.
- Zhou, W., Hong, H.P. and Zhang, S., 2012. Impact of dependent stochastic defect growth on system reliability of corroding pipelines. *International Journal of Pressure Vessels and Piping, Vol. 96-97*, pp. 68-77.
- Zhou, W., Xiang, W. and Hong, H.P., 2017. Sensitivity of system reliability of corroding pipelines to modeling of stochastic growth of corrosion defects. *Reliability Engineering & System Safety*, 167, pp.428–438.
- Zhou, W. and Zhang, S., 2015. Impact of model errors of burst capacity models on the reliability evaluation of corroding pipelines. *Journal of Pipeline Systems Engineering and Practice*, 7(1), p.4015011.

Appendix A: Step-by-Step Procedure for Estimating the Posterior Failure Probabilities Conditional on the ILI Data

For each one of the s defects:

1) Sample from the prior distributions:

- Generate a defect-specific rate parameter β_i and t_{i0} initiation time from the gamma distribution and the truncated normal distribution, respectively.
- Generate one common parameter α for the HGP-based model and an additional κ for the NHGP-based one, from the respective prior gamma distribution.

2) Generate the defect depths based on the stochastic growth model (either HGP or NHGP):

- Generate the depth increment Δd_{ij} from the gamma distribution between the $(j-1)^{\text{th}}$ and j^{th} inspections with the rate and shape parameters equal to β_i and $\alpha(t_j - t_{j-1})^\kappa$ respectively.
- Calculate $A\Delta d_{ij} = \sum_{j=1}^l \Delta d_{ij}$ for $j = 1, 2, \dots, l$ inspections.

3) Under the common assumption that the inspections are statistically independent given the model predictions Δd_{ij} , estimate the combined likelihood function of all inspections:

$$L(\mathbf{y}_i | A\Delta \mathbf{d}_i) = \prod_{j=1}^l L_{ij}(y_{ij} | A\Delta d_{ij})$$

4) Define the observation event $Z = \{P \leq cL(\boldsymbol{\theta})\}$.

5) Transform the limit state function of Step 4 in the standard Normal space based on Eq. (5.22).

6) Run a new SuS for each year t for a forecasting period of 10 years

- Estimate d_i from the stochastic growth model (either HGP or NHGP) with a shape parameter $\alpha(t - t_{i0})^\kappa$ and a rate parameter β_i at every year of the forecasting period.
- Estimate P_{Sf_i} and P_{SR} from Eq. (3.8) and (3.9a-b).

- Estimate the transformed limit state function $G_{fm}(\mathbf{V})$ according to Eq. (5.42).
- Define each intermediate event $F'_\chi = F_\chi \cap Z = \max(G_{fm}(\mathbf{v}), R_A(\mathbf{v})) \leq 0$.
- For each year estimate the probability $\Pr(F_{f_m} | Z)$ with intermediate events $F'_0 \supset F'_1 \supset \dots \supset F'_{M_D}$, where $F'_0 = F_0 \cap Z = Z$.
- Estimate $\Pr(F_{f_m} | Z)$ for the respective failure mode:

* when $d_i \geq w_i$:

- Small leak: $\Pr(F_1 | Z)$ for the joint event $(P_{Sfi} \geq P_{Sop}) \cap Z$.
- Large leak: $\Pr(F_2 | Z)$ for the joint event $(P_{Sfi} < P_{Sop}) \cap (P_{Sfi} < P_{S_R}) \cap Z$.
- Rupture: $\Pr(F_3 | Z)$ for the joint event $(P_{Sfi} < P_{Sop}) \cap (P_{S_R} < P_{Sfi}) \cap Z$.

* when $d_i < w_i$:

- Large leak: $\Pr(F_2 | Z)$ for the joint event $(P_{Sfi} < P_{Sop}) \cap (P_{Sfi} < P_{S_R}) \cap Z$.
- Rupture: $\Pr(F_3 | Z)$ for the joint event $(P_{Sfi} < P_{Sop}) \cap (P_{S_R} < P_{Sfi}) \cap Z$.

9) Estimate $\Pr(F_{f_{m_i}} | Z)$ for each year for each defect.

10) Estimate $\Pr(F_{f_m} | Z)$ for each year for the pipeline segment according to Eq. (5.44).

Appendix B: List of Publications

Conference papers

Pesinis, K., Tee, K.F., 2016. *Reliability-based Long-term Maintenance Activities for A Gas Transmission Pipeline System*. Proceedings of the 16th Structural Faults and Repair Conference and Exhibition, Edinburgh, United kingdom, May 17-19, paper 1678.

Pesinis, K., Tee, K.F., 2017. *A hazard-based predictive approach for onshore gas transmission pipelines using historical failures*. Risk, Reliability and Safety: Innovating Theory and Practice. Proceedings of the 26th European Safety and Reliability Conference, ESREL 2016, p. 332.

Pesinis, K., Tee, K.F., 2017. *Bayesian Analysis for Corroding Energy Pipelines*. Proceedings of the 12th International Conference on Structural Safety & Reliability (ICOSSAR 2017): Vienna, 8130.

Pesinis, K., Tee, K.F., 2018. *Bayesian Updating of Stochastic Process-based Models for Corroding Gas Pipelines based on Imperfect Inspection Information*. Risk, Reliability and Safety: Innovating Theory and Practice. Proceedings of the 28th European Safety and Reliability Conference, ESREL 2018.

Articles

Tee, K.F., and Pesinis, K., 2017. Reliability prediction for corroding natural gas pipelines. *Tunnelling and Underground Space Technology*, 65, pp.91-105.

Pesinis, K., and Tee, K.F., 2017. Statistical model and structural reliability analysis for onshore gas transmission pipelines. *Engineering Failure Analysis*, 82, pp.1–15.

Pesinis, K., and Tee, K.F., 2018. Bayesian Analysis of Small Probability Incidents for Corroding Energy Pipelines. *Engineering Structures*, 165, pp. 264–277.

Tee, K.F., Pesinis, K., Coolen-Maturi, T., 2018. Competing Risks Survival Analysis of Ruptured Gas Pipelines: A Nonparametric Predictive Approach. *International Journal of Pressure Vessels and Piping* (under review, submitted November 2016).

Pesinis, K., and Tee, K.F., 2018. : Bayesian Updating and Reliability Analysis for High-pH Stress Corrosion Cracking in Gas Pipelines. *Journal of Engineering Mechanics ASCE* (under review, submitted in May 2018).